Università degli studi di Napoli
Federico II

Facoltà di Scienze Matematiche Fisiche
e Naturali

Tesi di Dottorato in Fisica Fondamentale e Applicata

# *Topological States of Matter*

**Coordinatore**

**Prof. R. Velotta**

**Candidato**

**Vincenzo Parente**

Anno Accademico 2011/2012

# Contents

# Chapter 1

# Introduction: Topological Insulators

*Beauty is the first test:*
*there is no permanent place*
*in the world for ugly mathematics.*

*G. H. Hardy*

## 1.1 Topological aspects of energy bands

The possible existence of topologically non trivial phases relies on the topological structure of the first Brillouin zone (FBZ). The identification of points of the reciprocal lattice connected by a lattice vector leads to the identification of opposite edges in the first Brillouin zone, giving a non trivial structure to it. Take for example a two-dimensional square lattice, the first Brillouin zone then is a square whose opposite edges are identified as shown in fig. 1.1, i.e. an ordinary torus $T^2$. In the three-dimensional case the topological structure of the Brillouin zone is a little more complicated and could be built from the two-dimensional case giving to the torus a finite thickness and identifying the internal and the external surface so obtained. The band structure, then, could be seen as an application from the FBZ to the space of periodic Hamiltonians $\mathcal{H}(\mathbf{k})$ having eigenvalues $E_n(\mathbf{k})$. Quantum Hamiltonians $\mathcal{H}(\boldsymbol{k})$ could be classified in equivalence classes, where the equivalence relation is defined so that two Hamiltonians are equivalent if their band structures are topologically equivalent. Two manifolds[1] $M$ and $N$ are topologically equiv-

[1] In general the manifold structure is not needed to talk about topological equivalence. Topological spaces are the most general structures that could be classified using topological equivalence. Here we are interested in manifolds.

alent if an application $f : M \to N$ exists such that it is continuous and it admits a continuous inverse too. Such an application is said to be an *homeomorphism*, and it is an equivalence relation since it's symmetric, reflexive and transitive. Thus, two band structures $\{E_n(\mathbf{k})\}$ and $\{E'_n(\mathbf{k})\}$ are topologically equivalent if an homeomorphism exists mapping each band $E_n(\mathbf{k})$ to one $E'_n(\mathbf{k})$. It is clear that only band structures with the same number of bands could be topologically equivalent, and that the mapping must connect bands with the same band index $n$. That's why it is usually said that two band structures are equivalent if their bands could be deformed continuously one in the other without closing any gap. This relation of equivalence is too restrictive for physical purposes, since it's not possible put all the ordinary insulators in one class, and the topological ones in another one. However, it's possible to apply a coarser classification criterion having a deep physical root. Core bands do not contribute to physical observables, and thus they can be ignored somehow. Thus, insulators with different numbers of core bands could be seen as equivalent even if they have a different number of bands. In this this minimal model for an insulator, only the conduction and the valence bands will be considered. In the next sections it will be shown a well established example of non trivial insulator, the Quantum Hall system, and then topological insulators will be analyzed.

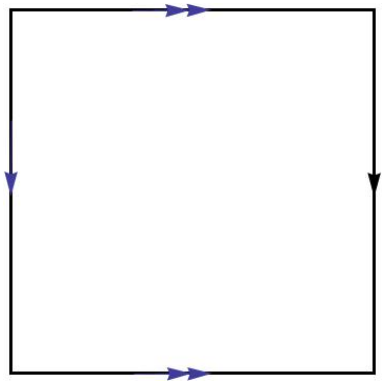

**Figure 1.1:** First Brillouin zone for the square lattice

## 1.2 Quantum Hall Effect

Quantum Hall states are the main example of non trivial insulators. Since the topological root of Integer Quantum Hall Effect (IQHE) has been pointed out [129] the concepts of differential geometry have gained a great importance

in the investigation of the states of matter. The conductivity tensor for the Hall system could be written using the Kubo formula, and the result could be interpreted using the notion of Chern numbers. The topological meaning of the Hall conductance makes clear the stability of the result to small perturbations. Given the Bloch function $\Psi = e^{i\vec{k}\cdot\vec{r}}u(\vec{r})$, the Hamiltonian for the periodic function $u(\vec{r})$ is

$$H = \frac{\hbar^2}{2m}\left(-i\partial_x + k_1\right)^2 + \frac{\hbar^2}{2m}\left(-i\partial_x + k_2 - \frac{eBx}{\hbar}\right)^2 + eEx \tag{1.2.1}$$

The sample averaged Hall conductivity from the Kubo formula is

$$\sigma_H = -\frac{e^2}{A}\sum_{mn} f(\varepsilon_n)\left[\frac{(v_\mu)_{nm}(x_\nu)_{mn}}{\varepsilon_m - \varepsilon_n + i\eta} + \frac{(x_\nu)_{nm}(v_\mu)_{mn}}{\varepsilon_m - \varepsilon_n - i\eta}\right] \tag{1.2.2}$$

The matrix element of the operator $(x_\mu)_{mn}$ could be related to $(v_\mu)_{mn}$, considering that the position and velocity operators are linked through the Heisenberg equation

$$v_\mu = \frac{dx_\mu}{dt} = \frac{1}{i\hbar}[x_\mu, H] \tag{1.2.3}$$

Projecting equation (1.2.3) on states $m$ and $n$ then

$$(v_\mu)_{mn} = \frac{1}{i\hbar}(\varepsilon_n - \varepsilon_m)(x_\mu)_{mn} \tag{1.2.4}$$

Equation (1.2.2) could be written, therefore, using only matrix elements of the velocity operator

$$\sigma_H = \frac{ie^2\hbar}{A}\sum_{mn} f(\varepsilon_n)\left[\frac{(v_\mu)_{nm}(v_\nu)_{mn}}{(\varepsilon_m - \varepsilon_n)(\varepsilon_m - \varepsilon_n + i\eta)} - \frac{(v_\nu)_{nm}(v_\mu)_{mn}}{(\varepsilon_m - \varepsilon_n)(\varepsilon_m - \varepsilon_n - i\eta)}\right] \tag{1.2.5}$$

In the limit $\eta \to 0^+$ there will be a $\delta$-like contribution and a second contribution coming from the principle value

$$\lim_{\eta\to 0^+}\frac{1}{\varepsilon_m - \varepsilon_n \pm i\eta} = \mathcal{P}\frac{1}{\varepsilon_m - \varepsilon_n} \mp i\delta(\varepsilon_m - \varepsilon_n) \tag{1.2.6}$$

the conductivity has two contributions. The total on shell contribution coming from the two parts of equation(1.2.2)

$$\tilde{\sigma}_H = -\frac{\pi e^2\hbar}{A}\sum_{m\neq n} v_{nm}v_{mn}\left[\frac{f(\varepsilon_m) - f(\varepsilon_n)}{\varepsilon_m - \varepsilon_n}\right]\delta(\varepsilon_m - \varepsilon_n) \tag{1.2.7}$$

At $T = 0$ the main contribution to $\tilde{\sigma}$ comes from the Fermi level. If the Fermi level lies in a gap between two Landau levels then $\tilde{\sigma}_H = 0$, since the matrix elements of the velocity operators between localized states are null. Only the principal value contribution then remains in (1.2.2)

$$\sigma_H = \frac{ie^2\hbar}{A} \sum_{mn} f(\varepsilon_n) \left[ \frac{(v_\mu)_{nm}(v_\nu)_{mn}}{(\varepsilon_m - \varepsilon_n)^2} - \frac{(v_\nu)_{nm}(v_\mu)_{mn}}{(\varepsilon_m - \varepsilon_n)^2} \right] \tag{1.2.8}$$

The velocity operator could be written as a derivative of the Hamiltonian with respect to the momentum components

$$v_\mu = \frac{1}{\hbar} \frac{\partial H}{\partial k_\mu}. \tag{1.2.9}$$

Using this relation the contribution to the conductivity (1.2.8) coming from the $n$th level is

$$\sigma_{H,n} = \frac{2\pi i}{A} \frac{e^2}{h} \sum_{m \neq n} \frac{1}{(\varepsilon_m - \varepsilon_n)^2} \left[ \left\langle \frac{\partial H}{\partial k_\mu} \right\rangle_{nm} \left\langle \frac{\partial H}{\partial k_\nu} \right\rangle_{mn} - \left\langle \frac{\partial H}{\partial k_\nu} \right\rangle_{nm} \left\langle \frac{\partial H}{\partial k_\mu} \right\rangle_{mn} \right]. \tag{1.2.10}$$

The derivatives of the Hamiltonian with respect to the momentum are related to derivatives of the wave functions

$$\left\langle \frac{\partial H}{\partial k_\mu} \right\rangle_{nm} \left\langle \frac{\partial H}{\partial k_\nu} \right\rangle_{mn} = (\varepsilon_m - \varepsilon_n)^2 \left\langle \frac{\partial u_n}{\partial k_\mu} \middle| \frac{\partial u_n}{\partial k_\nu} \right\rangle \tag{1.2.11}$$

With this result the conductivity (1.2.8) finally reads

$$\begin{aligned} \sigma_{H,n} &= \frac{2\pi i}{A} \frac{e^2}{h} \sum_{m \neq n} \left[ \left\langle \frac{\partial u_n}{\partial k_\mu} \middle| \frac{\partial u_n}{\partial k_\nu} \right\rangle - \left\langle \frac{\partial u_n}{\partial k_\nu} \middle| \frac{\partial u_n}{\partial k_\mu} \right\rangle \right] = \\ &= \frac{i}{2\pi} \frac{e^2}{h} \int d^2k \int d^2r \left[ \frac{\partial u_n^*}{\partial k_\mu} \frac{\partial u_n}{\partial k_\nu} - \frac{\partial u_n^*}{\partial k_\nu} \frac{\partial u_n}{\partial k_\mu} \right] = \\ &= \frac{1}{2\pi i} \frac{e^2}{h} \int d^2k \ \vec{\nabla} \times \vec{\mathcal{A}} \cdot \hat{z} \end{aligned} \tag{1.2.12}$$

Here the vector potential

$$\vec{\mathcal{A}} = \left\langle u_n \middle| \vec{\nabla} u_n \right\rangle \tag{1.2.13}$$

has been introduced, and the integral in $k$ space runs on the whole FBZ. The integral in reals space covers the unit cell of the lattice. By virtue of the Stoke's theorem the conductivity finally becomes

$$\sigma_{H,n} = \frac{1}{2\pi i} \frac{e^2}{h} \int_{\partial FBZ} d\vec{k} \cdot \vec{\mathcal{A}} \tag{1.2.14}$$

since $\vec{\mathcal{A}}$ is nothing but the gradient of the phase of the wave function $u_n$ then the integral is a integer $\nu$, since the wave function is always single valued and the absence of degeneracy is supposed

$$\sigma_{H,n} = \frac{e^2}{h}\nu \tag{1.2.15}$$

As pointed out at the beginning of the chapter, the FBZ is a torus $T^2$ and the absence of its boundary would imply Hall conductivity to be always null. This is true only if the gauge potential $\vec{\mathcal{A}}$ is uniquely defined inside the FBZ, i.e. only if the wave function is uniquely defined on $T^2$. Due to the non trivial topological structure of the FBZ it is possible to have a non- unique definition of the wave functions $u_n$ [73]. These topological aspects will be analyzed in the following subsection.

### 1.2.1 Topological Aspects of QHE

A remarkable property of wave functions in a magnetic field is that its number of zeros is determined by the magnetic flux threatening the unit cell. Given a rational magnetic flux $\phi = p/q$ per unit cell, the boundary conditions for the periodic function $u_{\vec{k}}(x, y)$ in the unit cell of edges $a$ and $b$ are

$$\begin{aligned} u_{\vec{k}}(x + qa, y) &= e^{-i\pi p\frac{y}{b}} u_{\vec{k}}(x, y) \\ u_{\vec{k}}(x, y + b) &= e^{i\pi p\frac{x}{qa}} u_{\vec{k}}(x, y) \end{aligned} \tag{1.2.16}$$

Thus the phase change around the boundary is $2\pi p$, and it's a topological invariant i.e. invariant respect to gauge trasformation. This phase change is related to the number of zeros of the wave function. Indeed, in general the total phase accumulated in the transport around the boundary of the unit cell is

$$\begin{aligned} \frac{1}{i}\int d\vec{l}\cdot\vec{\nabla}\theta_{\vec{k}}(x, y) &= \frac{1}{i}\int d\vec{l}\cdot\vec{\nabla}\log\frac{u_{\vec{k}}(x, y)}{|u_{\vec{k}}(x, y)|} = \\ &= \frac{1}{i}\left[\log\frac{u_{\vec{k}}(x, y)}{|u_{\vec{k}}(x, y)|}\bigg|_{2\pi} - \log\frac{u_{\vec{k}}(x, y)}{|u_{\vec{k}}(x, y)|}\bigg|_{0}\right] \end{aligned} \tag{1.2.17}$$

In the next it will be supposed that the wave function has just one zero in the unit cell. The result of the above integral could be different from zero if the logarithm has some branch cut. If the wave function has a zero in the interior of the unit cell then its the phase is not defined in that point and it appears as a branch point for the logarithm. The circle integral (1.2.17) then is equal to $2\pi$ if and only if the wave function has a zero in the interior of the

unit cell. Note that the number of zeros is bounded by the flux for each $u_{\vec{k}}$, but since the vector $\vec{k}$ is a continuous index the subset of zeros of the wave function for all the vectors in the FBZ is dense in the unit cell. This implies that fixing a point in the unit cell $(x_0, y_0)$ the wave function $u_{\vec{k}}(x_0, y_0)$ has zeros for some vectors $\vec{k}$ in the FBZ, a remarkable result from which QHE originates. Indeed, as in real space, in those points the phase of the wave function is not defined, and this reflects on the transition functions defined in the atlas on the FBZ. In general the atlas on $T^2$ is made up of 4 charts $H_i$, containing each one the four regions

$$\begin{aligned} H_1' &= \{(k_1, k_2) : 0 < k_1 < \pi/qa, 0 < k_2 < \pi/b\} \\ H_2' &= \{(k_1, k_2) : \pi/qa < k_1 < 2\pi/qa, 0 < k_2 < \pi/b\} \\ H_1' &= \{(k_1, k_2) : \pi/qa < k_1 < 2\pi/qa, \pi/b < k_2 < 2\pi/b\} \\ H_1' &= \{(k_1, k_2) : 0 < k_1 < \pi/qa, \pi/b < k_2 < 2\pi/b\} \end{aligned} \tag{1.2.18}$$

In the overlap between two regions $H_i$ and $H_j$ a transition function is defined

$$\Phi_{ij} = \exp i \left[\theta_i(k_1, k_2) - \theta_j(k_1, k_2)\right] = \exp i f_{ij}(k_1, k_2) \tag{1.2.19}$$

These functions could be defined considering the existence of zeros of the wave function. Indeed, supposing that $u_{\vec{k}}(x_0, y_0)$ admits a single zero in the chart $H_i$, then in all the other charts $H_j$ the phase of $u_{\vec{k}}$ could be fixed imposing that the value of the wave function in the point $(x_0, y_0)$ is real. In the chart $H_i$, a different convention must be applied, since it's not possible to define smoothly the phase of $u_{\vec{k}}(x_0, y_0)$ everywhere in $H_i$ due to the presence of the zero. However, another component $u_{\vec{k}}(x_1, y_1)$ could be used to define the phase there, thus defining the argument of the transition function $f(k_1, k_2)$. In this way, the principal bundle $P(T^2, U(1))$ for a spinless particle in a magnetic field is defined. Now it's possible to unveil the real nature of what has been called vector potential in the previous paragraph. The quantity $\vec{\mathcal{A}} = \left\langle u_n \middle| \vec{\nabla} u_n \right\rangle$ is a connection one form defined in the principal bundle $P(T^2, U(1))$, locally defined in each chart and whose property of transformation in the overlap between two charts is

$$\begin{aligned} \mathcal{A}_j &= e^{-if_{ij}(k_1,k_2)} \mathcal{A}_i e^{if_{ij}(k_1,k_2)} + e^{-if_{ij}(k_1,k_2)} \nabla_{\vec{k}} e^{if_{ij}(k_1,k_2)} = \\ &= \mathcal{A}_i + i \nabla_{\vec{k}} f_{i,j}(k_1, k_2) \end{aligned} \tag{1.2.20}$$

This connection one form has also a deep physical meaning, as analyzed in the paragraph 1.5 in a simple one dimensional case. The quantum Hall conductivity in (1.2.12) then involves the integral of the curvature $\mathcal{F} = d\mathcal{A} + \mathcal{A} \wedge \mathcal{A}$ associated with this connection

$$\mathcal{F} = \frac{\partial \mathcal{A}_i}{\partial k_j} dk_i \wedge dk_j = \frac{\partial u_{n,k}^*}{\partial k_i} \frac{\partial u_{n,k}}{\partial k_j} dk_i \wedge dk_j. \tag{1.2.21}$$

The integral of the curvature over the base space is an integer, the first Chern number $c_1$, and it is an invariant, since it only depends on the base space of the principal bundle but not on the gauge. A non zero quantum Hall conductivity originates from non triviality of the transition functions $f_{ij}(k_1, k_2)$. Indeed, considering a wave function with a single zero, Stoke' s theorem in (1.2.14) could be properly applied considering the boundary between the chart $H_i$ and the others

$$\begin{aligned}\sigma_{H,n} &= \frac{1}{2\pi i}\frac{e^2}{h}\int d^2k \;\; \vec{\nabla}\times\vec{\mathcal{A}}\cdot\hat{z} = \\ &= \frac{1}{2\pi i}\frac{e^2}{h}\left[\int_{H_I} d^2k \;\; \vec{\nabla}\times\vec{\mathcal{A}}_I\cdot\hat{z} + \int_{H_{II}} d^2k \;\; \vec{\nabla}\times\vec{\mathcal{A}}_{II}\cdot\hat{z}\right] = \\ &= \frac{1}{2\pi i}\frac{e^2}{h}\int_{\partial H_I} d\vec{k}\cdot[\mathcal{A}_I(\vec{k}) - \mathcal{A}_{II}(\vec{k})] = \frac{1}{2\pi}\frac{e^2}{h}\int_{\partial H_I} d\vec{k}\nabla_{\vec{k}} f(\vec{k})\end{aligned} \tag{1.2.22}$$

Here the region $H_i$ has been recalled $H_I$ while $H_{II} = \bigcup_{j\neq i} H_j$. The integral above is an integer, since the wave function has to be uniquely defined. Note that the absence of zeros would imply a trivially defined wave function, and thus a null quantum Hall conductance.

## 1.3 Connections on Principal Bundles

There are many ways to introduce connections on fiber bundles. Here it will shown the *Ehersmann connection*, defined trough the separation of the tangent space of a principal bundle in its horizontal and vertical subspaces. Let $P(M, G)$ be a principal bundle over the manifold $M$ with structure group $G$. Given a point $u \in P(M, G)$ so that $\pi u = p$ and $T_u P$, the space of vectors tangent to the fiber bundle in the point $u$ . The vertical subspace $V_u P \subset T_u P$ is defined as the space of vectors tangent to the fiber $G_p$ in $u$. Let $A$ be an element of the Lie algebra of the structure group, then though the right action of the gruop $G$ the element define a curve in $P$

$$R_{e^{tA}} u = ue^{tA},$$

note that the projection of each point of this curve is $\pi(ue^{tA}) = p$, i.e. the curve defined above is completely contained into the fiber $G_p$. Thus a vector that is tangent to this curve is tangent to the fiber. Explicitly, given a function $f : P \to \mathbb{R}$, the tangent vector to the curve $A^{\#}$ is

$$A^{\#}(f(u)) = \frac{due^{tA}}{dt}\Big|_{t=0}.$$

In this way, given $A$ then in each point of the principal bundle $P$ is has been built a vector contained into the vertical subspace. The vectorial field $A^{\#}$ is defined as the fundamental vector field generated from $A$, and the map $A \to A^{\#}$ results to be an isomorphism between the Lie algebra of the structure group and $V_uP$. Note that $\pi_* A^{\#} = 0$ and that the operation $\#$ preserves the Lie algebra structure, i.e. $[A^{\#}, B^{\#}] = [A, B]^{\#}$. The horizontal subspace is then defined as the complement of the vertical subspace. A connection on the bundle $P$ is then defined as the separation of the tangent space in $u$ in its vertical and horizontal subspace so that

- $T_uP = H_uP \oplus V_uP$
- a smooth vectorial field on $P$ can be written as the sum of its vertical and horizontal components

$$X = X^V + X^H, \text{ con } X^V \in V_uP \text{ e } X^H \in H_uP$$

- $H_{ug}P = R_{g*}H_uP$

In order to make concrete this abstract definition it is necessary to find a systematic way to decompose a vector field in its vertical and horizontal subspace. The mathematical tool projecting a generic vectorial field on its vertical component must be a 1-form, since it has to act on vectorial fields, and its values must be into the Lie algebra. The properties of the connection 1-form $\omega$, so defined, are

- $\omega(A^{\#}) = A$,
- $R_g^* \omega = Ad_{g^{-1}} \omega$

The horizontal subspace is defined as the kernel of $\omega$, i.e. the set of vectors $X \in T_uP$ such that $\omega(X) = 0$. The local expression of this 1-form is obtained considering the codifferential of a section on the principal bundle

$$\mathcal{A}_i = \sigma_i^* \omega \in \mathfrak{g} \otimes \Omega^1(U_i)$$

in order to have a 1-form uniquely defined on the fuber bundle, the local connection must satisfy some compatibility conditions. Let $X$ be a vector in $T_pM$, with $p \in U_i \cap U_j$ and $\sigma_i$ e $\sigma_j$ the sections on the bundle defined respectively in $U_i$ e $U_j$, then the vectors $\sigma_{i*}X$ and $\sigma_{j*}$ are connected through the transition function $t_{ij}$

$$\sigma_{j*}X = R_{t_{ij}*}(\sigma_{i*}X) + (t_{ij}^{-1} dt_{ij})^{\#} \tag{1.3.23}$$

Indeed, defining $\gamma : [0,1] \to M$, so that $\gamma(t) \in U_i \cap U_j,\ \forall t$ and $\dot{\gamma}(0) = X$, then

$$\sigma_{j*}X = \frac{d}{dt}\sigma_j(\gamma(t))\Big|_{t=0} = \frac{d}{dt}\sigma_i(t)t_{ij}(t)\Big|_{t=0} = \\ = \frac{d}{dt}\sigma_i(t)t_{ij}(p) + \sigma_i(p)\frac{d}{dt}t_{ij}(t)\Big|_{t=0}$$

In the following we are interested in the case of $G$ being a group of matrices. The first term is the result of the transport of the vector $X$ from $M$ to $P$, to which it is applied the by right action the element $t_{ij}$

$$\frac{d}{dt}\sigma_i(t)\Big|_{t=0} t_{ij}(p) = \frac{\partial\sigma_i(\gamma(t))}{\partial\gamma^\mu(t)}\frac{\partial\gamma^\mu(t)}{dt}\Big|_{t=0} t_{ij}(p) = (\sigma_{i*}X)t_{ij}(p) = R_{t_{ij}*}(\sigma_{i*}X)$$

The second term is

$$\sigma_i(p)\frac{d}{dt}t_{ij}(t)\Big|_{t=0} = \sigma_j(p)t_{ij}^{-1}(p)\frac{d}{dt}t_{ij}(t)\Big|_{t=0}$$

In the limit $t \to 0$ it follows that $t_{ij}^{-1}(p)t_{ij}(t) \in T_eG$. The term above is then a fundamental vector in $\sigma_j(p)$. Applying $\omega$ to both sides of (1.3.23) it follows that

$$\sigma_j^*\omega(X) = t_{ij}^{-1}\omega(\sigma_{i*}X)t_{ij} + t_{ij}^{-1}dt_{ij}(X) \Rightarrow \mathcal{A}_j = t_{ij}^{-1}\mathcal{A}_i t_{ij} + t_{ij}^{-1}dt_{ij}. \quad (1.3.24)$$

The curvature 2-form is defined as the covariant derivative of the connection 1-form

$$\Omega = D\omega \in \Omega^2(P) \otimes \mathfrak{g}$$

The derivative $D$ acts on Lie algebra valued 1-forms $\beta = \beta_\alpha \otimes e^\alpha$, where $\{e^\alpha\}$ is a basis in $\mathfrak{g}$ and $\beta_\alpha \in \Omega^r(m)$, then using the decomposition of a vector in its horizontal and vertical components

$$D\beta(X,Y) = (d_P\beta_\alpha) \otimes e^\alpha(X_H, Y_H)$$

This definition could be generalized to the case of $r$-forms acting on a generic vector space. The connection $\omega$ is said to be flat if $\Omega = 0$ and it satisfies the Cartan structure equation

$$\Omega(X,Y) = d_P\omega(X,Y) + [\omega(X), \omega(Y)] \quad (1.3.25)$$

The dimostration of this equation clarifies its meaning and proceeds step by step considering three different cases

- $X$ and $Y$ are both horizontal. By definition $\omega(X) = \omega(Y) = 0$, so the structure equation reduces to the definition of curvature,
- $X$ is horizontal and $Y$ is vertical. Since$Y_H = 0$, then $\Omega(X, Y) = 0$ and $\omega(X) = 0$. Only $d_P\omega(X, Y) = 0$ is left to be demostrated

$$\begin{aligned} d_P\omega(X,Y) &= X(\omega(Y)) - Y(\omega(X)) - [\omega(X), \omega(Y)] = \\ &= X(\omega(Y)) - [\omega(X), \omega(Y)] \end{aligned} \tag{1.3.26}$$

  Since $\omega(Y) \in \mathfrak{g}$ is constrant then the first term is null. The Lie parentesis of two vectorial fields is an horizontal field and then $d_P\omega(X, Y) = 0$
- $X$ and $Y$ are both vertical. In this case $\Omega(X, Y) = 0$. the external derivative of $\omega$ is $d_P\omega(X, Y) = -[\omega(x), \omega(Y)]$, making null the second term of the structure equation.

These three cases demostrate the structure equation in general. The curvature induces a 2-form on $M$

$$\mathcal{F} = \sigma_i^* \Omega \in \mathfrak{g} \otimes \Omega^2(U_i)$$

## 1.4 Caracteristic classes

A k-multilinear map $f : \underbrace{\mathfrak{g} \times \mathfrak{g} \times \cdots \times \mathfrak{g}}_{k\ times} \to \mathbb{R}$ is said to be $Ad\ G$ invariant if

$$f(Ad\, g\, V_1, \ldots, Ad\, g\, V_k) = f(V_1, \ldots, V_k) \quad \forall g \in G,\ V_1, \ldots, V_k \in \mathfrak{g}$$

If all the arguments are taken equal, the function above is called an *invariant polynomial* of grade $k$. The Chern-Weil theorem establish some important properties of $Ad\ G$ invariant function. Let $P(M, G)$ a principal bundle, $\omega$ a connection defined on it and $\Omega$ its curvature. A differential form of degree $2k$ could be defined composing $f$ and $\Omega$

$$f(\Omega)(V_1, \ldots, V_{2k}) = \frac{1}{2k!} \sum_P \sigma(P)\ f(\Omega(V_{P(1)}, V_{P(2)}), \ldots, \Omega(V_{P(2k-1)}, V_{P(2k)}))$$

where $V_1, \ldots, V_{2k} \in T_pP$ and the sum goes on all the possible permutations $P$. There is a unique closed differential form $\overline{f} \in \Omega^1(M)$ such that

$$f = \pi^* \overline{f}.$$

The map $f \to \overline{f}$ between the algebra $I(G)$ of the invariant polynomials on the Lie group $G$ and $H^*(M)$ is an homomorphism called *Weyl Homomorphism.*

The exactness of the differential form result lies on the Bianchi identity $D\Omega = 0$ and on the linearity of the polynomial. The demonstration of $df(\Omega) = Df(\Omega) = 0$ is done in full details in Nakahara. The cohomology class of $f(\Omega)$ is independent of the connection $\omega$. This class, called *characteristic class* $\chi_P(f)$, depends only on the principal bundle and on $f$, thus different choices of $f$ give rise to different classes. In the following one type of class, the Chern class, will be of particular interest. Let $E \to M$ a fiber bundle with fiber $\mathbb{C}^k$, with structure group $GL(k, \mathbb{C})$, $\mathcal{A}$ and $\mathcal{F}$ are respectively the local form of the connection and of the curvature. The total Chern class is the invariant polynomial

$$c(\mathcal{F}) = \det\left(\mathbb{I} + \frac{i\mathcal{F}}{2\pi}\right)$$

The determinant above could be expressed as the sum of even degrees forms

$$c(\mathcal{F}) = 1 + c_1(\mathcal{F}) + c_2(\mathcal{F}) + \dots$$

where $c_j(\mathcal{F}) \in \Omega^{2j}(M)$ is the $j$-th Chern class. Trivially, if $2j > m$ with $m = dim\ M$ then $c_j = 0$. Above all, the maximum degree of the Chern classes is $k$ such that

$$c_k(\mathcal{F}) = \det\left(\frac{i\mathcal{F}}{2\pi}\right).$$

Note that all the matrix operations are intended to act on the Lie group structure. For example, take a fiber bundle $(E, \pi, M, \mathbb{C}^2, SU(2))$, with $\dim M = 4$. The curvature $\mathcal{F}$ of a certain connection $\omega$

$$\mathcal{F} = \frac{i}{2}\mathcal{F}^\alpha \sigma_\alpha, \text{ with } \mathcal{F}^\alpha = \frac{1}{2}\mathcal{F}^\alpha_{\ \mu\nu} dx^\mu \wedge dx^\nu$$

The total Chern class is

$$\begin{aligned} c(\mathcal{F}) &= \det\begin{pmatrix} 1 + \frac{1}{4\pi}\mathcal{F}^3 & \frac{1}{4\pi}(\mathcal{F}^1 - i\mathcal{F}^2) \\ \frac{1}{4\pi}(\mathcal{F}^1 + i\mathcal{F}^2) & 1 - \frac{1}{4\pi}\mathcal{F}^3 \end{pmatrix} = \\ &= 1 - \left(\frac{1}{4\pi}\right)^2 (\mathcal{F}^1 \wedge \mathcal{F}^1 + \mathcal{F}^2 \wedge \mathcal{F}^2 + \mathcal{F}^3 \wedge \mathcal{F}^3) \end{aligned}$$

The single Chern classes explicitly are

$$\begin{aligned} c_0(\mathcal{F}) &= 1 \\ c_1(\mathcal{F}) &= 0 \\ c_2(\mathcal{F}) &= \left(\frac{i}{2\pi}\right)^2 \sum \frac{\mathcal{F}^\alpha \wedge \mathcal{F}^\alpha}{4} = \det\left(\frac{i\mathcal{F}}{2\pi}\right) \end{aligned}$$

In general it is not so easy to calculate the determinant above. Chern classes could be calculated in general using the trace of the curvature form

$$\begin{aligned} c_0(\mathcal{F}) &= 1 \\ c_1(\mathcal{F}) &= \frac{i}{2\pi}\mathrm{tr}\mathcal{F} \\ c_2(\mathcal{F}) &= \frac{i}{2\pi}[(\mathrm{tr}\mathcal{F})^2 - \mathrm{tr}\mathcal{F}^2] \\ &\vdots \end{aligned}$$

### 1.4.1 Bott-Chern connection

An interesting case of connection is the Bott-Chern connection, wich is essentially the Berry phase. Let $H(\boldsymbol{R})$ an Hamiltonian depending on some parameter $\boldsymbol{R} = (R_1, R_2, \ldots, R_n)$. In Berry phase the parameter is adiabatically changing in time, here will be considered constant at least for the moment. The parameter $\boldsymbol{R}$ will identify a point on a differential manifold M. Since the phase of a state $|n, \boldsymbol{R}\rangle$ is undetermined, we can consider the ray represented by this state as a fiber. Indeed a "point" is identified by a couple of data made up of a point in the base space parameter space, $\boldsymbol{R}$, and the phase of the wave function that is an element of $U(1)$. Thus, we are facing a principal bundle $P(M, U(1))$. A section is determined by fixing the phase of the wave function, and the projection is simply $\pi(e^{i\phi}|n, \boldsymbol{R}\rangle) = \boldsymbol{R}$. The canonical local trivialization is

$$\phi^{-1}(|n, \boldsymbol{R}\rangle) = (\boldsymbol{R}, e)$$

All the other elements in a fiber could be obtained using the right action of the group. The Berry connection is defined as

$$\mathcal{A} = \mathcal{A}_\mu dR^\mu = \langle \boldsymbol{R}|(d|\boldsymbol{R}\rangle)$$

This is effectively the local form of a connection on the principal bundle, since it satisfies the equation (1.3.24). Indeed, given two charts on M, $U_i$ and $U_j$, and the sections $\sigma_i(\boldsymbol{R}) = |\boldsymbol{R}\rangle_i$ and $\sigma_j(\boldsymbol{R}) = |\boldsymbol{R}\rangle_j$ are linked by transition function $t_{ij}$

$$|\boldsymbol{R}\rangle_j = |\boldsymbol{R}\rangle_i t_{ij}$$

Applying this relation to the definition of connection we obtain

$$\begin{aligned} \mathcal{A}_j = {}_j\langle \boldsymbol{R}|(d|\boldsymbol{R}\rangle_j) &= t_{ij}^{-1}(\boldsymbol{R})\ {}_i\langle \boldsymbol{R}|[d|\boldsymbol{R}\rangle_i t_{ij}(\boldsymbol{R}) + |\boldsymbol{R}\rangle_i dt_{ij}(\boldsymbol{R})] = \\ &= \mathcal{A}_i + t_{ij}^{-1}(\boldsymbol{R})dt_{ij}(\boldsymbol{R}) \end{aligned}$$

The local form of the curvature is

$$\mathcal{F} = d\mathcal{A} = (d\langle \boldsymbol{R}|) \wedge (d|\boldsymbol{R}\rangle) = \left(\frac{\partial \langle \boldsymbol{R}|}{\partial R^\mu}\right)\left(\frac{\partial |\boldsymbol{R}\rangle}{\partial R^\nu}\right) dR^\mu \wedge dR^\nu$$

The curvature enables us to interpret the result of Kubo formula for the Integer Hall Effect. Some important implications of Bott Chern connection are found in the theory of topological insulator and in IQHE.

## 1.5 Charge Polarization

The connection (1.2.13) plays an important role in the description of electrons in solids. Indeed, solids have been pointed out as systems naturally exhibiting Berry phase [145]. Here the space of parameters is the Brillouin zone, having a non trivial topological structure as pointed out previously. In the case of 1-dimensional solids this is particularly simple to be viewed, since a closed path in the first Brillouin zone is obtained making the wave vector $k$ varying in the whole FBZ, i.e. from $-\pi/a$ to $\pi/a$. This could be achieved through a time dependent perturbation to be included into the Shrödinger equation through the gauge potential $A(t)$

$$\left[\frac{1}{2m}\left(\boldsymbol{p} - \frac{e}{c}\boldsymbol{A}\right)^2 + V(x)\right]\Psi = i\hbar\partial_t\Psi \tag{1.5.27}$$

where the potential $V(x)$ is the periodic crystal field, i.e. $V(x+a) = V(x)$. Here I consider a linear chain with number of cell $N_c$, with one atom per cell whose position is specified by the vector $R$. The Bloch functions are defined as usual

$$|\Psi_{n,k}\rangle = \frac{1}{\sqrt{N_c}} e^{ikx} |u_{n,k}\rangle . \tag{1.5.28}$$

The periodic functions $|u_{n,k}\rangle$ satisfy the normalization

$$\langle u_{n,k}|u_{n,k}\rangle = \frac{1}{N_c}\int u^*_{n,k} u_{n,k}\, dx = 1. \tag{1.5.29}$$

If the frequencies of the external perturbation are small compared with the interlevel spacing then it's possible to write the wave function for the $n$-th level as

$$\Psi_n(t,x) = \exp\left[i\left(kx - \frac{1}{\hbar}\int_0^t dt'\, \epsilon_n(t')\right)\right] u_{k(t)}(x) \tag{1.5.30}$$

where it is assumed that $k$ in the exponential is time independent, while the periodic function $u_{k(t)}(x)$ depends on $k(t) = k - e/c\ \ A(t)$ and so the energy

eigenvalues $\epsilon(t) = \epsilon(k(t))$. A solution of the type (1.5.30) exists if the phase $\gamma_n(t)$ is added

$$\Psi_n(t,x) = \exp\left[i\left(\gamma_n(t) + kx - \frac{1}{\hbar}\int_0^t dt'\ \epsilon_n(t')\right)\right] u_{k(t)}(x). \tag{1.5.31}$$

Following [145] the normalization of the periodic function $u_{nk}(x)$ is

$$\frac{2\pi}{a}\int_0^a |u_{nk}(x)|^2 dx = 1. \tag{1.5.32}$$

The explicit expression for the adiabatic phase, linking it to derivatives of the periodic function $|u_{nk}\rangle$, is found introducing the wave function (1.5.31) in the Schrödinger equation (1.5.27)

$$\dot{\gamma}_n(t) = \frac{2\pi}{a}\int_0^a \left\langle u_{nk(t)}\right| i\partial_t \left|u_{nk(t)}\right\rangle\ dx \Rightarrow \gamma_n = \frac{2\pi}{a}\int_{-\pi/a}^{\pi/a} \langle u_{nk}|\, i\partial_k\, |u_{nk}\rangle\ dk \tag{1.5.33}$$

where it has been assumed that the potential makes $k$ varying over the whole Brillouin zone. This nothing but the connection (1.2.13), and this shows its connection with the Berry phase for electrons in solids under a time dependent perturbation. Introducing the Wannier functions

$$a_n(x - ma) = \left(\frac{a}{2\pi}\right)^{-1/2} \frac{1}{\sqrt{N_c}} \int e^{-ik(x-ma)}\, |u_{n,k}\rangle\ dk \tag{1.5.34}$$

the origin of the name *charge polarization* is clear[2]

$$P_{\rho,n} = \frac{2\pi}{a}\int_{-\pi/a}^{\pi/a} \langle u_{nk}|\, i\partial_k\, |u_{nk}\rangle\ dk = \frac{2\pi}{a}\int_{-\infty}^{\infty} x|a_n(x)|^2 dx \tag{1.5.35}$$

where $a_n(x)$ is the Wannier function for the $n$-th level. The total charge polarization is obtained trivially summing on all the occupied bands

$$P_{\rho,n} = \frac{1}{2\pi}\sum_n \int_{-\pi}^{\pi} \langle u_{nk}|\, i\partial_k\, |u_{nk}\rangle\ dk \tag{1.5.36}$$

The charge polarization (1.5.35) is not gauge independent. Indeed, considering a gauge transformation $u_{n,k}(x) \to e^{if(k)}u_{nk}(x)$, then the charge polarization takes a term dependent of the gauge function $f(k)$

$$P_{\rho,n} \to P_{\rho,n} + \frac{2\pi}{a}\left[f(\pi) - f(-\pi)\right] \tag{1.5.37}$$

[2]The symmetry properties of the Wannier functions have been used to derive the following equation. In particular the translation invariance by lattice vectors gives $N_c$ equal contributions. This is the reason why only the contribution at $m = 0$ appears.

the last term must be an integer, since the wave function must be uniquely defined everywhere. This expresses the fact that charge polarization is defined up to multiple integers of the lattice constant and, thus, that it is not a physically meaningful quantity in itself. On the contrary variations of the polarization are gauge independent, and thus well defined quantities as it will be analyzed below. On a general ground (1.5.35) could acquire every real value. The symmetry of the system, if present, makes it discrete. Indeed, if the system has inversion symmetry the value of the Berry phase could be 0 or $\pi$. This happens because the Wannier functions can have definite symmetry properties around 0 (i.e. $a(x) = \pm a(-x)$) or $a/2$, giving the two possible values of the polarization.

## 1.6 Topological Insulators

It has been shown in the previous section that magnetic field is necessary in order to have a non null Chern number, i.e. a non trivial insulator. This also implies that a time reversal invariant Hamiltonian $\mathcal{H}(\vec{k})$, i.e. an Hamiltonian respecting the identity

$$H(-k) = \Theta H(k)\Theta^{-1} \tag{1.6.38}$$

(where $\Theta = e^{i\pi\frac{S_y}{\hbar}}K$ is the time reversal operator) is always characterized by a null Chern number. Indeed, considering the definition of the first Chern number and (1.2.21)

$$c_1 = \frac{1}{2\pi}\int_{FBZ} d\vec{k}\ \ \mathcal{F}(\vec{k}) \tag{1.6.39}$$

it follows that $\mathcal{F}(-\vec{k}) = -\mathcal{F}(\vec{k})$ in the case of a time reversal invariant Hamiltonian. At a first glance this would imply that all insulating systems respecting (1.6.38) must be topologically trivial. However a deeper analysis of topological invariants of the principle bundle $P(T^2, U(1))$ describing electrons in solids shows that this is not true, since the Chern numbers are only a subset of all the possible invariants characterizing the manifold. As it will be show in the following, a different kind of invariant, relying on Kramers degeneracy, exists that characterizes a different class of insulators, the *topological insulators*. In the next subsection the 1D case will be analyzed and the expression for this invariant will be worked out. Then, it will be shown how this kind of invariant could be defined for higher dimensional system, and how it could be calculated in the 3D case starting from the knowledge of some characteristics of the bulk bands in a symmetric case.

### 1.6.1 1D Topological Insulators

In this subsection it will be analyzed in full details the existence of non trivial 1D insulators. In this case, the FBZ is a circle, and the two points $k = 0, \pi$ are such that $H(-k) = H(k)$ and thus are called *time reversal invariant points* (TRIPs). In these points Kramers theorem ensures that energy bands must have a double degeneracy while, if there are not other symmetries, they are non-degenerate outside the TRIPs as shown in fig. 1.2. The $2N$ energy

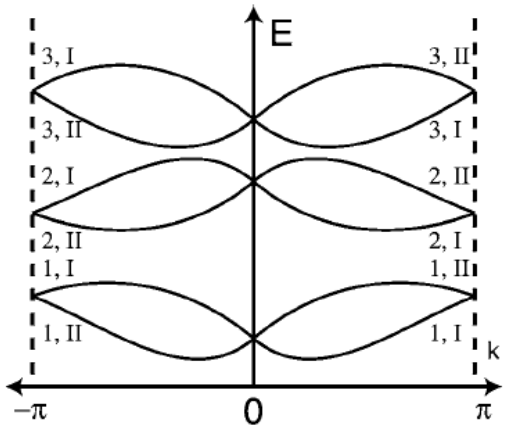


**Figure 1.2:** Sketcth of the energy bands of a linear chain with time reversal symmetry. Bands are organized in couples, with degeneracy at the TRIPs.

bands of the linear chain are grouped in $N$ pairs of bands that are degenerate in $k = 0, \pi$ and whose wave functions are connected by time reversal

$$\begin{aligned} \left|u^I_{-k,\alpha}\right\rangle &= -e^{i\chi_{k\alpha}}\Theta\left|u^{II}_{k,\alpha}\right\rangle \\ \left|u^{II}_{-k,\alpha}\right\rangle &= e^{i\chi_{-k\alpha}}\Theta\left|u^{I}_{k,\alpha}\right\rangle \end{aligned} \tag{1.6.40}$$

For each element of this pair a connection (1.2.13) can be defined

$$\mathcal{A}^i(k) = i\sum_\alpha \left\langle u^i_{k\alpha}\right| \nabla_k \left|u^i_{k\alpha}\right\rangle . \tag{1.6.41}$$

The sum of the connection of every band having the same label $I$or $II$ makes us the partial polarizations

$$\mathcal{P}^i = \frac{1}{2\pi}\int_{-\pi}^{\pi} dk\ \mathcal{A}^i(k) = \frac{1}{2\pi}\int_0^{\pi} dk\ [\mathcal{A}^i(k) + \mathcal{A}^i(-k)]. \tag{1.6.42}$$

The sum of the two partial polarizations in nothing but the total charge polarization (1.5.36) $P_\rho = P^I + P^{II}$ and it vanishes when time reversal symmetry holds, as discussed previously. However, starting from $P^I$ and $P^{II}$

another polarization could be defined, the *time reversal polarization*, that is the difference of the two partial polarization

$$P_\theta = P^I - P^{II}. \tag{1.6.43}$$

The physical meaning of this quantity could be analyzed introducing Wannier functions, as done for $P_\rho$ in the previous section. As the charge polarization expresses the mean position of the electron in the unit cell, $P_\theta$ then expresses the difference between the mean value of the position of electrons in the two bands related by time reversal. In the following subsection a tight binding model having a non trivial topological phase will be analyzed, and the meaning of $P_\theta$ described here will be seen. All these definitions seem to depend on the choice of the label $I$ and $II$, but it's possible to cast the time reversal polarization in a way that it is manifestly $U(2N)$ invariant. The term $\mathcal{A}^i(-k)$ in (1.6.42) could be written as

$$\begin{aligned}
\mathcal{A}^I(-k) &= -i \sum_\alpha \left\langle u^I_{-k\alpha} \right| \nabla_k \left| u^I_{-k\alpha} \right\rangle = \\
&= -i \sum_\alpha \left\langle u^{II}_{k,\alpha} \right| \Theta e^{-i\chi_{k\alpha}} \nabla_k e^{i\chi_{k\alpha}} \Theta \left| u^{II}_{k,\alpha} \right\rangle = \\
&= -\sum_\alpha \nabla_k \chi_{k\alpha} - i \sum_\alpha \left\langle u^{II}_{k,\alpha} \right| \Theta \nabla_k \Theta \left| u^{II}_{k,\alpha} \right\rangle = \\
&= \mathcal{A}^{II}(k) - \sum_\alpha \nabla_k \chi_{k\alpha}
\end{aligned} \tag{1.6.44}$$

and the same relation could be written for $\mathcal{A}^{II}(-k)$. The partial polarization then is

$$\mathcal{P}^I = \frac{1}{2\pi} \left[ \int_0^\pi dk \; \mathcal{A}(k) + i \log \frac{\mathrm{Pf}(w(\pi))}{\mathrm{Pf}(w(0))} \right] \tag{1.6.45}$$

The matrix $w_{\alpha\beta}$ is

$$w_{\alpha\beta} = \left\langle u_{-k\alpha} \right| \Theta \left| u_{k\beta} \right\rangle \tag{1.6.46}$$

written explicitly the matrix $w_{\alpha\beta}$ is block-diagonal

$$w = \begin{pmatrix} \ddots & 0 & 0 & 0 & \cdots \\ \cdots & w_\alpha & 0 & 0 & \cdots \\ \cdots & 0 & w_\beta & 0 & \cdots \\ \cdots & 0 & 0 & w_\gamma & \cdots \\ \cdots & 0 & 0 & 0 & \ddots \end{pmatrix} \tag{1.6.47}$$

where each one of the blocks $w_\alpha$ us built using the relations (1.6.40)

$$w_\alpha = \begin{pmatrix} 0 & e^{i\chi_{k\alpha}} \\ -e^{i\chi_{-k\alpha}} & 0 \end{pmatrix} \tag{1.6.48}$$

The important feature of the matrix $w$ relies on its symmetry properties, the matrix being antisymmetric in the TRIPs and thus it makes sense the Pfaffian in (1.6.45). The time reversal polarization could be conveniently re-expressed using the charge polarization

$$P_\theta = P^I - P^{II} = 2P^I - P_\rho. \tag{1.6.49}$$

written explicitly this definition is

$$\begin{aligned} P_\theta &= \frac{1}{2\pi}\left[2\int_0^\pi dk\ \mathcal{A}(k) + 2i\log\frac{\mathrm{Pf}[w(\pi)]}{\mathrm{Pf}[w(0)]} - \int_{-\pi}^{\pi} dk\ \mathcal{A}(k)\right] = \\ &= \frac{1}{2\pi}\left[\int_0^\pi dk\ \mathcal{A}(k) - \int_{-\pi}^{0} dk\ \mathcal{A}(k) + 2i\log\frac{\mathrm{Pf}[w(\pi)]}{\mathrm{Pf}[w(0)]}\right] \end{aligned} \tag{1.6.50}$$

As done in (1.6.44), the second term of the previous equation could be expressed using the phase $\chi_{k\alpha}$

$$\int_{-\pi}^{0} dk\ \mathcal{A}(k) = \int_0^\pi \mathcal{A}(-k) = \int_0^\pi \mathcal{A}(k) - \sum_\alpha \int_0^\pi dk(\nabla_k\chi_{k\alpha} + \nabla\chi_{-k\alpha}) \tag{1.6.51}$$

Thus the time reversal polarization is

$$P_\theta = \frac{1}{2\pi}\left[\sum_\alpha \int_0^\pi dk(\nabla_k\chi_{k\alpha} + \nabla_k\chi_{-k\alpha}) + 2i\log\frac{\mathrm{Pf}[w(\pi)]}{\mathrm{Pf}[w(0)]}\right] \tag{1.6.52}$$

By virtue of (1.6.48) the quantity $w^\dagger\nabla_k w$ is

$$\begin{aligned} w^\dagger\nabla_k w &= \begin{pmatrix} 0 & -e^{-i\chi_{-k\alpha}} \\ e^{-i\chi_{k\alpha}} & 0 \end{pmatrix}\begin{pmatrix} 0 & i\nabla_k\chi_{k,\alpha}e^{i\chi_{k\alpha}} \\ -i\nabla_k\chi_{-k\alpha}e^{i\chi_{-k\alpha}} & 0 \end{pmatrix} = \\ &= \begin{pmatrix} i\nabla_k\chi_{k\alpha} & 0 \\ 0 & i\nabla_k\chi_{-k\alpha} \end{pmatrix} \end{aligned} \tag{1.6.53}$$

Thus the time reversal polarization is

$$P_\theta = \frac{1}{2\pi i}\left[\sum_\alpha \int_0^\pi dk\ \ \mathrm{tr}(w^\dagger\nabla_k w) - 2\log\frac{\mathrm{Pf}[w(\pi)]}{\mathrm{Pf}[w(0)]}\right] \tag{1.6.54}$$

Moreover the determinant of $w$ is

$$\det\ w = e^{i\sum_\alpha \chi_{k\alpha}+\chi_{-k\alpha}} \tag{1.6.55}$$

thus $\mathrm{tr} w^\dagger \nabla_k w = \nabla_k \log\det w(k)$. With this last consideration the time reversal polarization is expressed as the product of the ratios of the Pfaffian and the square root of the determinant of the matrix $w$ in the TRIPs

$$P_\theta = \frac{1}{i\pi}\log\frac{\sqrt{\det w(\pi)}}{\mathrm{Pf}[w(\pi)]}\frac{\mathrm{Pf}[w(0)]}{\sqrt{\det w(0)}} \tag{1.6.56}$$

This makes clear that $P_\theta$ is an integer, since for definition $\det w = \mathrm{Pf}[w]^2$, and that it is defined only modulus 2 due to the ambiguity of the logarithm. The brach of $\sqrt{\det w}$ could be defined in the whole FBZ, since there is not a topological obstruction in defining continuously the wave function everywhere in the sense specified in the previous section. An odd value of $P_\theta$ arises from the Pfaffian being not in the same brach of $\sqrt{\det w}$ in 0 or $\pi$. Using these properties it is possible to express time reversal polarization in an alternative way, commonly found in literature [37]

$$(-1)^{P_\theta} = \frac{\sqrt{\det w(\pi)}}{\mathrm{Pf}[w(\pi)]}\frac{\sqrt{\det w(0)}}{\mathrm{Pf}[w(0)]} \tag{1.6.57}$$

From equations (1.6.56) and (1.6.57) it is clear that $P_\theta$ is $U(2N)$ invariant. Indeed, since $\mathrm{Pf}[XAX^T] = \det[X]\mathrm{Pf}[A]$, the ratio between the Pfaffian and the square root of a matrix is invariant under a unitary transformation up to a sign. The product of two of such ratios is then totally invariant. The transformation matrix is supposed to be functions of $k$, and thus a change of the sign of the determinant is possible in principle. Since the transformation is supposed to be smooth as a function of $k$, this change is not possible since $SU(2N)$ is disconnected from its complement.
However time reversal polarization is still *gauge dependent*, since the sign of the Pfaffian can be changed in one of the TRIPs. Indeed, the $\mathrm{Pf}[w(\Gamma_i)]$ is the product of the phases included in the definition of time reversal, due to the simple structure of (1.6.47)

$$\mathrm{Pf}[w(\Gamma_i)] = e^{i\chi_{\Gamma_i,\alpha}} e^{i\chi_{\Gamma_i,\beta}} e^{i\chi_{\Gamma_i,\gamma}} \dots \tag{1.6.58}$$

A change in the sign of the Pfaffian can then arise if one (or any odd number) of the phases is shifted by $\pi$ due to a phase choice

$$|u_{\alpha,k}\rangle \to e^{if_\alpha(k)}|u_{\alpha,k}\rangle \tag{1.6.59}$$

If the function $f_\alpha(k)$ is such that $f_\alpha(\Gamma_i) = \pi$ then the charge polarization change sign. Thus, as in the case of charge polarization, only changes of $P_\theta$ are well defined. Even and odd values of the time reversal polarization

are topologically distinct in the sense that a smooth perturbation in the Hamiltonian preserving time reversal symmetry cannot change the value of $P_\theta$. However, a perturbation having only a numerable set of points where time reversal symmetry holds, and not in between, can make $P_\theta$ change its value. The perturbation is taken periodic, with period $T$ i.e. such that $H(t,k) = H(t+T,k)$. Time reversal symmetry (1.6.38) with the additional dependence of the Hamiltonian the a parameter $t$ becomes

$$H(-t,-k) = \Theta H(t,k)\Theta^{-1}. \tag{1.6.60}$$

The space of parameters $(t,k)$ is again a torus depicted in fig.1.3. As found for the dependence on $k$, two values of the parameter exists $t = 0$ and $t = T/2$ such that the Hamiltonian is time reversal invariant, doubling the number of TRIPs. The important feature of topological insulators is the existence of boundary states protected by time reversal symmetry. In both normal and topological insulators midgap states corresponding to wave functions located at the boundary could be present. The difference between a trivial insulator and a topological insulator could be seen in fig. 1.4. At the TRIPs Kramers

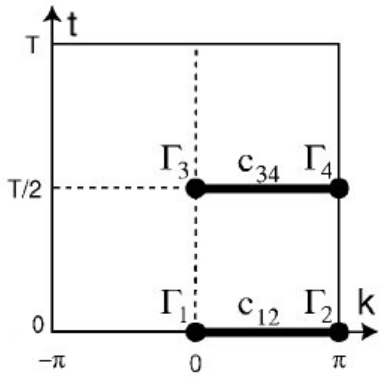


**Figure 1.3:** Space of parameters (t,k), for the Hamiltonian $H(k,t)$. Due to periodic boundary conditions the edges are identified, giving a torus as in the two dimensional case.

theorem ensures a double degeneracy, and this feature is common to both trivial and topological insulators. The difference between these two classes of materials comes in the behavior of midgap states when passing from one TRIP to another. In an ordinary insulars the wave functions making a pair in the TRIP $\Lambda_a$ make again a pair in $\Lambda_b$. In a topological insulator, instead, the partners in $\Lambda_a$ switch in $\Lambda_b$. This could be equivalently stated saying that in a normal insulator the midgap states cross the fermi level an even number of

times, while in a topological insulators they cross it an odd number of times. Note that in a normal insulator the midgap states could be continuously deformed pushing them in the conduction or valence band. In the case of a topological insulator this cannot be done, making the states topologically protected. In the next section a one dimensional model will be studied using tight binding method. This simple model contains all the important features highlighted in this section such as the switching of partners between TRIPs.

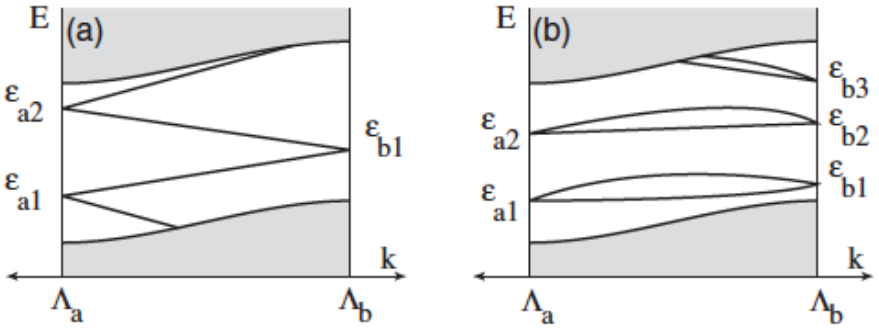


**Figure 1.4:** Behavior of boundary states in (a) a topological insulator and (b) a normal insulator.

#### 1.6.1.1 An example of 1D topological insulator.

Here a model proposed in [37] is analyzed. The system is made up of a linear chain, in which in addition to the hopping term $H_0$

$$H_0 = t_0 \sum_{i,\alpha} c^\dagger_{i,\alpha} c_{i+1,\alpha} + c^\dagger_{i+1,\alpha} c_{i,\alpha} \tag{1.6.61}$$

a staggered magnetic field $V_h$ and a dimerization term $V_t$ is considered

$$\begin{aligned} V_h &= h_{st} \sum_{i,\alpha\beta} (-1)^i \sigma^z_{\alpha\beta} c^\dagger_{i,\alpha} c_{i\beta} \\ V_t &= \Delta t_{st} \sum_{i,\alpha} (-1)^i (c^\dagger_{i,\alpha} c_{i+1,\alpha} + c^\dagger_{i+1,\alpha} c_{i,\alpha}) \end{aligned} \tag{1.6.62}$$

These two terms are necessary in order to obtain a topologically non trivial insulator. Indeed, it is possible to obtain an periodic Hamiltonian satisfying

the time reversal constraint (1.6.38) with a suitable choice of the dependence of the parameters $h_{st}$ and $\Delta t_{st}$

$$(\Delta t_{st}, h_{st}) = \left( \Delta t^0_{st} \cos 2\pi \frac{t}{T}, h^0_{st} \sin 2\pi \frac{t}{T} \right) \tag{1.6.63}$$

Spin orbit is added in order to analyze what happens when spin degeneracy is lifted

$$V_{so} = \sum_{i,\alpha} \vec{e} \cdot \vec{\sigma}_{\alpha\beta} (c^\dagger_{i,\alpha} c_{i+1,\alpha} - c^\dagger_{i+1,\alpha} c_{i,\alpha}) \tag{1.6.64}$$

The Hamiltonian is then periodic with period $T$ and it is time reversal invariant at $t = T/2$ and $t = T$. In these two values of the adiabatic parameter $t$ the staggered magnetic field is not present, and only the dimerization term survives. Kramer's theorem ensures the existence of a double degeneracy in these two TRIPs as seen in 1.5(a). In contrast, at $t = T/4$ and $3T/4$ only magnetic field survives, putting the system in an ordered Neel-like state. The dimerization term is responsible for the sliding effect represented in the left panel of fig.1.3. In 1.5(b) the spin orbit term has been suppressed, and the spin degeneracy arising in this way makes the bands linked through time reversal overlap for each value of $t$. Thus it is clear by comparison of 1.5(a) and 1.5(b) that spin-orbit interaction thus not lift the degeneracy at the TRIPs as any other interaction preserving time reversal. As it can be seen,

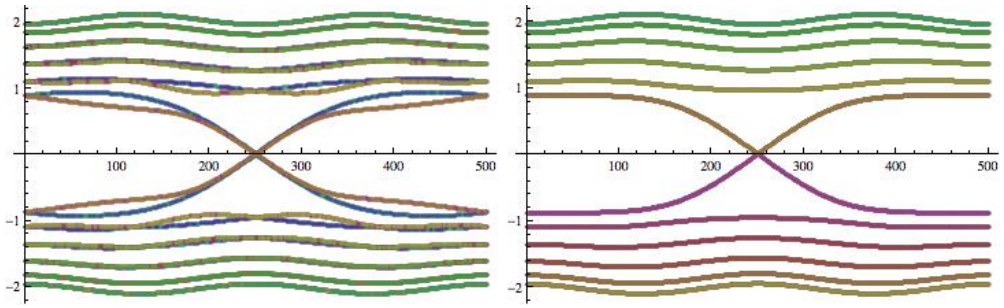


(a) (b)

**Figure 1.5:** Levels' dependence on the parameter t: a) with dimerization, magnetic field and spin orbit, b) the same without spin orbit. The system represented is made up of a linear chain with 12 sites, and the parameters are chosen as in [37] with $\Delta t^0_{st}/t_{st} = 0.4$, $h^0_{st}/t_{st} = 0.8$ and $\vec{e}/t_{st} = 0.1\hat{y}$.

at $t = T/2$ there are 4 levels crossing in the middle of the gap. These levels correspond to boundary states, i.e. states localized at the end of the chain

if open boundary conditions are applied. Since the gap closes, the system at $t = T$ is different from the one at $t = 0$, i.e. it will be in an excited state. It has been shown in [37] that the state of the system at $t = 2T$ will be in the same state as in $t = 0$. This is a consequence of the $\mathbb{Z}_2$ nature of the topological invariant associated to the non trivial structure of the energy levels.

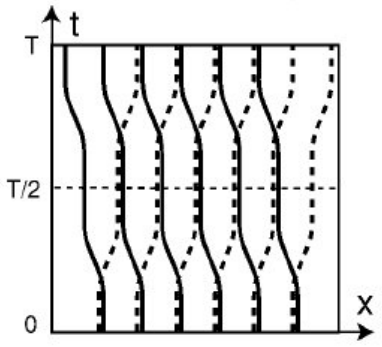


**Figure 1.6:** Centers of the Wannier functions for the 1D system depicted for different values of the parameter $t$. In a non trivial insulator the state of the system at $t = 0$ is different for the one at $t = T$, accumulating electrons at the end of the chain.

### 1.6.2 2D Topological Insulators

In this section it will be considered the case of a 2D solid, respecting time reversal symmetry i.e. $H(-k_x, -k_y) = \Theta H(k_x, k_y)\Theta^{-1}$ in a similar way as (1.6.60). It follows that all the consideration done in the end of section 1.6.1 apply to this case too. The four TRIPs defined in the FBZ as shown in figure 1.3 are identified through the vectors $\Gamma_{n_1 n_2}$

$$\Gamma_{n_1 n_2} = \frac{1}{2}(n_1 \boldsymbol{b}_1 + n_2 \boldsymbol{b}_2) \tag{1.6.65}$$

where $\boldsymbol{b}_a$ are the two vectors making a base in the reciprocal lattice. Given an edge of the FBZ orthogonal to a reciprocal lattice vector $\boldsymbol{G}$, the four $\Gamma_{n_1 n_2}$ are organized in two couples $\Lambda_a$ with $a = 1, 2$. The two $\Gamma$'s in a couple $\Lambda_a$ are the ones satisfying $\Gamma_{a1} - \Gamma_{a2} = \boldsymbol{G}/2$ in direction perpendicular to $\boldsymbol{G}$. In each TRIP the matrix (1.6.47) is antisymmetric and then the ratio $\delta_i$ is then

defined

$$\delta_i = \frac{\sqrt{\det(\Gamma_i)}}{\mathrm{Pf}[\Gamma_i]} \tag{1.6.66}$$

As discussed before, $P_\theta$ in (1.6.57) depends on the gauge but the product of all the four $\delta_i$ it is independent on the gauge and thus physically significative

$$(-1)^{\nu_0} = \prod_{n_i=0,1} \delta_{n_1 n_2} \tag{1.6.67}$$

The integer $\nu_0$ then distinguish the two topologically inequivalent 2D insulators. Commonly 2D topological insulators are known as Quantum Spin Hall Insulators (QSHI), in the following subsection the boundary states and the experimental realization of this kind of systems is briefly reviewed.

### 1.6.3 Quantum Spin Hall Effect

The QSHI exhibits an odd number of spin polarized edge states, and thus it is of central importance in the development of spintronics. The first candidate to be an intrinsic QSHI was graphene. Spin-orbit is, indeed, a possible interaction term compatible with all the symmetries of the system and capable to open a gap at the Dirac points. Unfortunately this gap is of the order of $10^{-3}$meV, and thus experimentally useless. After graphene, quantum wells based on type III semiconductors have been proposed as QSHI and experimentally realized. In particular HgTe-CdTe wells have a quantum transition as a function of the thickness $d$ of the well material HgTe. When $d$ is bigger than a threshold value $d_c$ the bands of the material invert their order, and surface states bands arise in the gap of the material. Indeed, the barrier material Cd-Te has a normal ordering of the bands, having the s-type band $\Gamma_6$ above the p-type band $\Gamma_8$, as shown in fig. 1.7. The description of the well in the $k\dot{p}$ scheme then involves the 6 bands $(|\Gamma_6, 1/2\rangle, |\Gamma_6, -1/2\rangle, |\Gamma_8, 3/2\rangle, |\Gamma_8, 1/2\rangle, |\Gamma_8, -1/2\rangle, |\Gamma_8, -3/2\rangle)$. These bands combine to make the spin up and spin down states of three subbands for the quantum well named $E1$, $H1$ and $L1$. The last one is separated from the others, and thus can be neglected leading to a 4 subbands model. At the $\Gamma$ point the $|\Gamma_6, \pm 1/2\rangle$ and $|\Gamma_8, \pm 1/2\rangle$ mix to make the $E1$ bands, while the $|\Gamma_8, \pm 3/2\rangle$ make the $H1$ bands. Away from the $\Gamma$ point time reversal and inversion symmetry determine the Hamiltonian, in the spirit of the $k \cdot p$ approximation and an additional constraint comes from the two subbands having opposite parities thus leading a paring done through an odd function of $k$. The effective Hamiltonian in the 4 subbands model at the lowest order

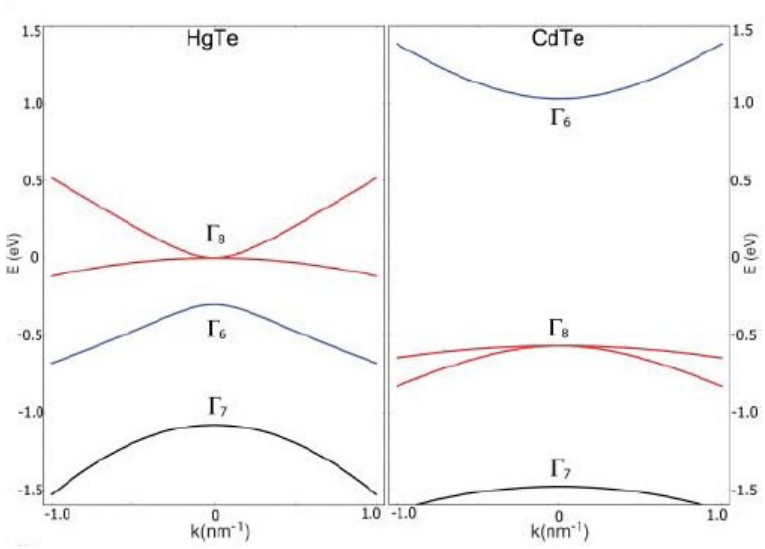


**Figure 1.7:** Band structure at the Γ point of CdTe (on the right) and HgTe (on the left)

finally can be written as

$$H_{eff}(\vec{k}) = \begin{pmatrix} H(\vec{k}) & 0 \\ 0 & H^*(-\vec{k}) \end{pmatrix} \tag{1.6.68}$$

where each $2 \times 2$ block is

$$H(\vec{k}) = \epsilon(\vec{k})\mathbb{I} + d_i(\vec{k})\sigma_i \tag{1.6.69}$$

Due to the symmetry consideration made above the functions $\epsilon(\vec{k})$ and $d_3(\vec{k})$ are even function of $k$, and thus at the lowest order are

$$\epsilon(\vec{k}) = C - D(k_x^2 + k_y^2), \quad d_3(\vec{k}) = M - B(k_x^2 + k_y^2) \tag{1.6.70}$$

while the functions $d_1(\vec{k})$ and $d_2(\vec{k})$ are odd functions of $k$, approximated to the linear order for the long wavelength limit

$$d_1 + id_2 = A(k_x + ik_y). \tag{1.6.71}$$

In all the formulas above the parameters $A, B, C, D, M$ are expansion coefficients that can be determined through experimental data or first principle calculations. The mass term $M$ plays the role of order parameter in the quantum transition from the trivial insulator and a topological insulator having

inverted gap. When the thickness of the well is below the critical value $d_c$ the subbands are in the same order of CdTe, and thus the gap is positive $M > 0$. When $d > d_c$, on the other hand, the subbands invert their order following the band structure of the well material HgTe, and the gap becomes negative $M < 0$. The threshold value is $d_c \approx 64$ Å, as shown in fig. 1.8

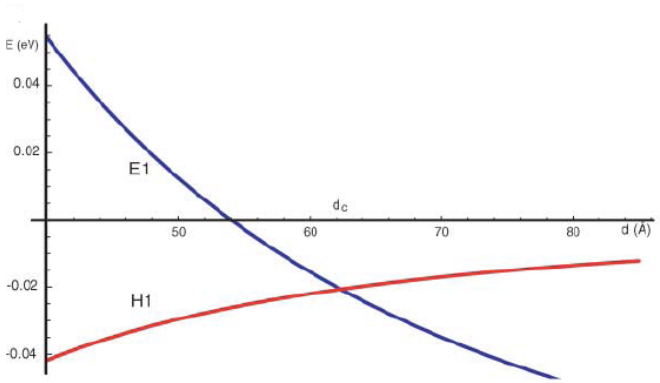


**Figure 1.8:** Energy of the subbands $E1$ and $H1$ as a function of the well-thickness $d$.

### 1.6.4 3D Topological Insulators

As shown in the previous sections, in 2D systems the existence of 4 TRIPs leads to the definition of a unique topological invariant characterizing non trivial phase of an insulator. In a 3D material there are 8 TRIPs $\Gamma_i$, analogous of (1.6.65)

$$\Gamma_{i=(n_1,n_2,n_3)} = \frac{1}{2}(n_1\mathbf{b}_1 + n_2\mathbf{b}_2 + n_3\mathbf{b}_3), \tag{1.6.72}$$

where $\mathbf{b}_i$ are basis vectors of the reciprocal lattice. In a 3D material 4 $\mathbb{Z}_2$ topological invariants $(\nu_0; \nu_1, \nu_2, \nu_3)$ can be defined. The invariant $\nu_0$ is the product of all the 8 $\delta_i$ in (1.6.66)

$$(-1)^{\nu_0} = \prod_{i=1}^{8} \delta_i. \tag{1.6.73}$$

The other three invariants are the products of the $\delta_i$ of TRIPs living in the same plane

$$(-1)^{\nu_k} = \prod_{n_k=1, n_{j\neq k}=0} \delta_{i=(n_1,n_2,n_3)} \tag{1.6.74}$$

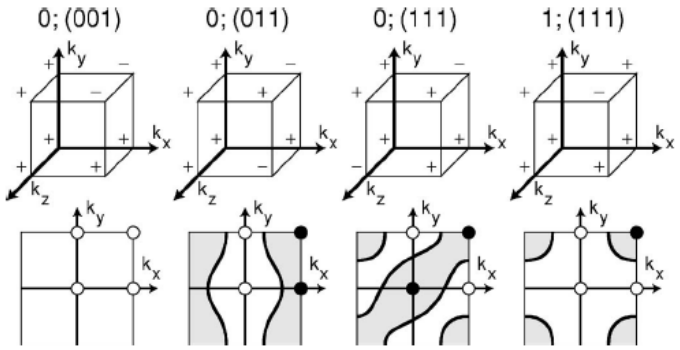


**Figure 1.9:** Fermi circles in the surface Brillouin zone for a) a weak topological insulator and b) a strong topological insulator. c) In the simplest strong topological insulator the Fermi circle encloses a single Dirac point.

The invariant $\nu_0$ distinguishes material having an odd or an even number of Dirac points where $\delta_i$ is negative. Materials having an even number of Dirac points The physical interpretation of these quantities can be given in terms of bulk-boundary correspondence. The surface Brillouin zone has 4 TRIPs, and the topological invariants describe the way in which these points are connected through surface states. A non-null topological invariant means that the TRIPs are connected in a non trivial way, i.e. the Fermi surface intersects a line connecting two given $\Gamma_a$ and $\Gamma_b$ intersects an odd number of times. In the case of weakly coupled 2D QSHI stacked around the $y$ direction, two possibilities can occur as depicted in fig. 1.9:

- the Fermi surface contains an even number of TRIPs as in fig. 1.9 a). The invariant $\nu_0$ is null and surface states can be localized through disorder. This state is called *weak topological insulators*,
- the Fermi surface contains an odd number of them (1 being the simplest case) as in fig. 1.9 b). The material in this case is called *strong TI*, since surface states are topologically protected by time-reversal symmetry, avoiding localizations phenomena.

### 1.6.5 Effective Theory for boundary states in 3D Topological Insulators

The prototype of 3D TI with single Dirac point is $Bi_2Se_3$: this material was predicted to be have Dirac-like surface states [146], and it has been confirmed experimentally [141]. Crystal structure of this material is represented in fig.

1.10. The material consists of 5 atom layers that are strongly coupled, making the so called quintuple layer. The coupling between two quintuple layers is much wakes, predominantly of the Van der Waals type. In fig. 1.11 a

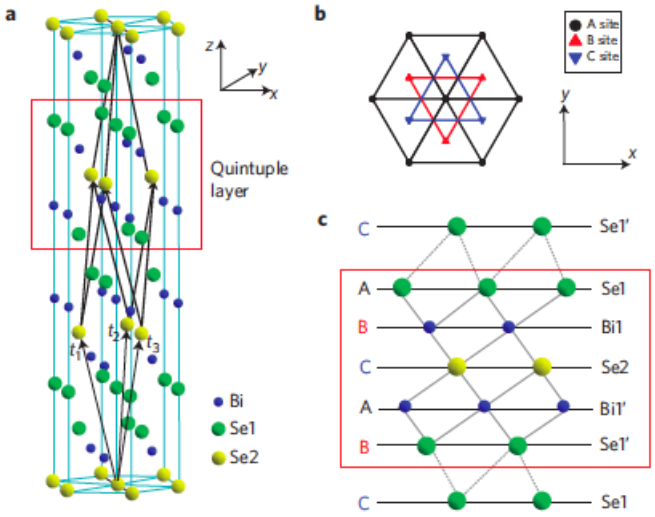


**Figure 1.10:** Unit cell of $Bi_2Se_3$.

scheme of the evolution of the atomic orbitals into electronic bands of $Bi_2Se_3$ is reported. Regions labeled with I, II and III corresponds to the introduction of the chemical bonding, crystal field and spin orbit interaction (SO) respectively. In the last stage it is seen that SO inverts the bands coming from $p_z$ orbitals of Se and Bi (having opposite parity) at the $\Gamma$ point. This produces the non trivial behavior of the material, with the birth of surface states. The effective Hamiltonian for these states can be calculated in $k \cdot p$ approximation, using the crystal symmetries. From this brief exposition, the minimal model that can be used is a 4 bands model, considering the spin and the layer degree of freedom, and thus the basis $\Psi^T = (|p1_z \uparrow\rangle, |p2_z \uparrow\rangle, |p1_z \downarrow\rangle, |p2_z \downarrow\rangle)$ will be used in the following. The symmetries of the crystal are

- time reversal symmetry $\mathcal{T}$

$$\mathcal{T} = i\sigma_y \otimes \mathbb{I}\mathcal{K} \tag{1.6.75}$$

  where $\mathcal{K}$ is the complex conjugation and $\sigma_i$ are the Pauli matrices in the spin space. In the following the matrices acting in the orbital space will be denoted with $\tau_i$.

- Inversion symmetry

$$\mathcal{I} = \mathbb{I} \otimes \tau_3 \tag{1.6.76}$$

- 3-fold rotational symmetry around the $z$-axis

$$C_3 = \exp\left(i\frac{\pi}{3}\sigma_z \otimes \mathbb{I}\right) \tag{1.6.77}$$

The general shape of the Hamiltonian $\mathcal{H}(\mathbf{k})$ is

$$\mathcal{H}(\mathbf{k}) = \begin{pmatrix} H_{11}(\mathbf{k}) & H_{12}(\mathbf{k}) \\ H_{21}(\mathbf{k}) & H_{22}(\mathbf{k}) \end{pmatrix} \tag{1.6.78}$$

where each block $H_{ij}(\mathbf{k})$ is a $2 \times 2$ block such that $H_{ii}(\mathbf{k}) = H_{ii}^{\dagger}(\mathbf{k})$ and $H_{ij}(\mathbf{k}) = H_{ji}(\mathbf{k})^{\dagger}$ $(i, j = 1, 2)$ to ensure hermicity. The commutation of the Hamiltonian with time reversal symmetry $\mathcal{T}\mathcal{H}(\mathbf{k})\mathcal{T} = \mathcal{H}(-\mathbf{k})$ implies that

$$\begin{aligned} H_{11}(-\mathbf{k}) &= H_{22}^{*}(\mathbf{k}) \\ H_{12}(-\mathbf{k}) &= -H_{21}^{*}(\mathbf{k}) \end{aligned} \tag{1.6.79}$$

Imposing the invariance of the Hamiltonian for the inversion operation $\mathcal{I}\mathcal{H}(\mathbf{k})\mathcal{I}^{\dagger} = \mathcal{H}(-\mathbf{k})$ implies that for each block $\tau_3 H_{ij}(\mathbf{k})\tau_3 = H_{ij}(-\mathbf{k})$, thus quadratic functions of the components $k_i$ of the wave vector are multiply the identity matrix or $\sigma_3$, while linear functions of $k_i$ will multiply $\sigma_x$ and $\sigma_y$. The last symmetry to be imposed is the rotational symmetry $C_3\mathcal{H}(\mathbf{k})C_3^{\dagger} = \mathcal{H}(C_3\mathbf{k})$ that imposes the following relations between the blocks of the Hamiltonian $\mathcal{H}(\mathbf{k})$

$$\begin{aligned} H_{ii}(\mathbf{k}) &= H_{ii}(C_3\mathbf{k}) \\ e^{i\frac{2\pi}{3}} H_{ij}(\mathbf{k}) &= H_{ij}(C_3\mathbf{k}). \end{aligned} \tag{1.6.80}$$

In order to have an Hamiltonian invariant for the symmetry $C_3$ the diagonal blocks have to contain only functions that are invariant for rotations around the $z$-axis, i.e. $k_z$ and quadratic functions of the type $k_x^2 + k_y^2$ and $k_z^2$, while the off-diagonal blocks must be of the type $\sigma_i k_i = \sigma_x k_x + \sigma_y k_y$. Considering the relations (1.6.79) the final form of the most general Hamiltonian respecting the symmetries is

$$\mathcal{H}(\mathbf{k}) = \epsilon(\mathbf{k})\mathbb{I}_{4\times 4} + \begin{pmatrix} M(\mathbf{k}) & A_1 k_z & 0 & k_- \\ A_1 k_z & -M(\mathbf{k}) & k_- & 0 \\ 0 & k_+ & M(\mathbf{k}) & -A_1 k_z \\ k_+ & 0 & -A_1 k_z & -M(\mathbf{k}) \end{pmatrix} \tag{1.6.81}$$

where $\epsilon(\mathbf{k}) = C + D_1 k_z^2 + D_2(k_x^2 + k_y^2)$ and $M(\mathbf{k}) = M - B_1 k_z^2 - B_2(k_x^2 + k_y^2)$. A simplified version of this model will be considered in the following: the sum of the diagonal quadratic terms

$$\epsilon(\boldsymbol{k})\mathbb{I}_{4\times 4} + M(\boldsymbol{k})\mathbb{I}_{2\times 2} \otimes \sigma_z$$

will be approximated with $\mathcal{M} = M + C_1 k_z^2 + C_2 \left(k_x^2 + k_y^2\right)$.

$$\mathcal{H}_0(\mathbf{k}) = \begin{pmatrix} \mathcal{M}(\mathbf{k}) & A_1 k_z & 0 & k_- \\ A_1 k_z & -\mathcal{M}(\mathbf{k}) & k_- & 0 \\ 0 & k_+ & \mathcal{M}(\mathbf{k}) & -A_1 k_z \\ k_+ & 0 & -A_1 k_z & -\mathcal{M}(\mathbf{k}) \end{pmatrix} \tag{1.6.82}$$

In addition it will be considered the case $C_2 = 0$, in order to have a analytically solvable model. In Chapter 2 the choice $M, C_1 = 0$, in order to have a non-trivial phase, while in Chapter 3 an additional simplification will be introduced: the dependence of the diagonal terms on $k$ will be neglected, and $\mathcal{M} \equiv \Delta$ i.e. the bulk gap of the material. This last simplification allows the analytical treatment done in Chapter 3 of curved boundaries, the results exposed are consistent with calculations done later results *citazione dei giapponesi.*

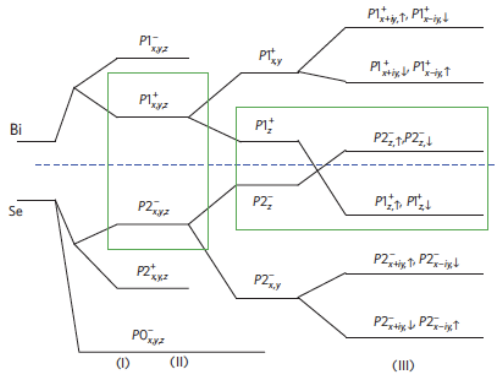


**Figure 1.11:** Schematic diagram of the evolution of the orbitals of Bi and Se into the conduction and valence band of $Bi_2Se_3$ at the $\Gamma$ point.

# Chapter 2

# Topological defects in graphene and 3D Topological Insulators

*Our hopes and expectations,*
*black holes and revelations.*

*Muse, "Starlight"*

In the previous chapter it has been shown that the surface states of a 3D topological insulator obey Dirac equation in 2+1 dimensions. Similarly, electrons in graphene satisfy the same relativistic equation. This is strictly true if the surface is clean, i.e. perfectly flat. It is clear that experimental sample will show local deformations of the boundary, and in the case of graphene the presence of a substrate or of flexural phonons will have the same effect. The problem of describing relativistic particles of arbitrary spin on curved space time has been solved during the 30's of the last century by Weyl [139] with the introduction of the tetrads formalism. In the next section this theory will be reviewed following the treatment done by Weinberg. Thus, after showing the procedure needed to write Dirac equation on a curved space time, a type of solution for this equation will be illustrated following Stodolsky. In conclusion of the chapter, Green function theory will be rewieved in flat space time since it will be used in later developments.

## 2.1 Dirac Spinors on curved Space Time

Given a N-dimensional space-time with general coordinates $x_\mu$ endowed with metric $g_{\mu\nu}(x^\eta)$, the equivalence principle guarantees the existence at each point $x^\mu$ of a system of coordinates $y^\alpha(x^\mu)$ in which the metric is the Minkowski

metric $\eta_{\alpha\beta} = \text{diag}(-1, 1, 1, \ldots)$. The coefficients of the Jacobian matrix characterizing the change of coordinates from the general $x^\mu$ to the $y^\alpha$, are called tetrads or vierbeins $e^\alpha{}_\mu$

$$e^\alpha{}_\mu = \frac{\partial y^\alpha}{\partial x^\mu}. \tag{2.1.1}$$

Since the local frame $y^\alpha$ is an inertial system the metric could be written using transformation rules for second rank tensors

$$g_{\mu\nu}(x) = \eta_{\alpha\beta} e^\alpha{}_\mu e^\beta{}_\nu \tag{2.1.2}$$

Tetrads have a definite tensorial character that can be identified following their definition. A change from the general coordinates $x^\mu$ to another system $\overline{x}^\mu$ leads the tetrads $e^\alpha{}_\mu$ to a new set $\overline{e}^\alpha{}_\mu$

$$\overline{e}^\alpha{}_\mu = \frac{\partial y^\alpha}{\partial \overline{x}^\mu} = \frac{\partial x^\nu}{\partial \overline{x}^\mu}\frac{\partial y^\alpha}{\partial x^\nu} = \frac{\partial x^\nu}{\partial \overline{x}^\mu} e^\alpha{}_\nu \tag{2.1.3}$$

These quantities, thus, form four covariant vector fields by definition. Tetrads have a definite property for change in the local frame $y^\alpha$. The principle of equivalence, indeed, ensures the existence of a local inertial frame but does not say that it is unique. Local Lorentz transformation $\Lambda^\beta_\alpha(x)$ The local inertial frame $y^\alpha$ is arbitrary chosen, and the tetrads transform like vectors under this transformation

$$e^\beta{}_\mu \to \Lambda^\alpha{}_\beta e^\beta{}_\mu \tag{2.1.4}$$

Given a contravariant tensor field $A^\mu(x)$ it can be contracted with the tetrads given four scalars $A^\alpha$ defined in the local inertial frame $y^\alpha$

$$A^\alpha = e^\alpha{}_\mu A^\mu \tag{2.1.5}$$

To refer the components of a covariant tensor field $A_\mu$ to the inertial frame it's necessary the quantities $e^\mu_\alpha$, obtained lowering the $\alpha$ index of tetrads using the Minkowski metric $\eta_{\alpha\beta}$ and raising their $\mu$ index through the inverse metric $g^{\mu\nu}$. The $e_\alpha{}^\mu$ satisfy both completeness and orthogonality relations, i.e. they are the inverse of the $e^\alpha{}_\mu$

$$\begin{aligned} e^\alpha{}_\mu e_\alpha{}^\nu &= \delta_\mu{}^\nu \\ e^\alpha{}_\mu e_\beta{}^\mu &= \delta^\alpha{}_\beta \end{aligned} \tag{2.1.6}$$

Similarly, the components of a tensor field defined in the inertial frame $y^\alpha$ could be referred to the general coordinates $x^\mu$ through the tetrads and their inverse. Tetrads show to be useful for the introduction of a covariant derivative for spinorial fields, since using these fields it is possible to define a covariant derivative for physical fields with half integer spin. The absence of

spinorial representation of $GL(4)$, indeed, implies that it is not possible to define a connection making the derivative behaving like a tensor for general changes of coordinates. However, the introduction of the local inertial coordinates $y^\alpha$ implies that the physical action for an half integer field must be covariant for Lorentz transformations dependent on position. Contracting the gradient with the inverse of the tetrads ${e_a}^\mu \partial_\mu$ gives a scalar under general transformation rules, but this quantity has not simple rules for local transformations in the inertial frame $\Lambda(x^\mu)$

$$\begin{aligned} {e_\alpha}^\mu \partial_\mu \Psi(x) &\longrightarrow {\Lambda_\alpha}^\beta(x)\, {e_\beta}^\mu \partial_\mu \left\{ D(\Lambda(x))\, \Psi(x) \right\} = \\ &= {\Lambda_\alpha}^\beta(x)\, {e_\beta}^\mu \left\{ D(\Lambda(x))\, \partial_\mu \Psi(x) + \left[ \partial_\mu D(\Lambda(x)) \right] \Psi(x) \right\} \end{aligned} \tag{2.1.7}$$

where $D(\Lambda)$ is the representation of Lorentz transformations followed by the field $\Psi$. A covariant derivative $\nabla_\mu$ must be introduced, then, so that its rule of transformation is

$$\nabla_\mu \Psi(x) \longrightarrow {\Lambda_\mu}^\alpha(x)\, D(\Lambda(x))\, {e_\alpha}^\mu \nabla_\mu \Psi(x) \tag{2.1.8}$$

where for definition are introduced the connection coefficients $\Gamma_\mu$

$$\nabla_\mu = \partial_\mu + \Gamma_\mu \tag{2.1.9}$$

Transformation rule (2.1.8) implies that the connection coefficients must transform in a non-tensorial way

$$\Gamma_\mu(x) \longrightarrow D(\Lambda(x))\, \Gamma_\mu(x)\, D^{-1}(\Lambda(x)) - \left[ \frac{\partial}{\partial x^\mu} D(\Lambda(x)) \right] D^{-1}(\Lambda(x)). \tag{2.1.10}$$

The explicit shape of the connection $\Gamma_\mu$ is determined starting from an infinitesimal Lorentz transformation

$${\Lambda^\alpha}_\beta(x) = {\delta^\alpha}_\beta + {\omega^\alpha}_\beta(x) \tag{2.1.11}$$

where the quantities ${\omega^\alpha}_\beta(x)$ are antisymmetric

$$\omega_{\alpha\beta}(x) = -\omega_{\beta\alpha}(x) \tag{2.1.12}$$

In general the representation $D(\Lambda(x))$ for such an infinitesimal Lorentz transformation is

$$D(1 + \omega(x)) = \mathbb{I} + \frac{1}{2} \omega^{\alpha\beta}(x)\, \Sigma_{\alpha\beta} \tag{2.1.13}$$

here the matrices $\Sigma_{\alpha\beta}$ are the generators of the spinorial representation of the Lorentz group, that can be written as commutators of the $\gamma^\alpha$ matrices

$$\Sigma_{\alpha\beta} = \frac{i}{4} [\gamma_\alpha, \gamma_\beta]. \tag{2.1.14}$$

These generators satisfy the well known algebra

$$[\Sigma_{\alpha\beta}, \Sigma_{\gamma\delta}] = \eta_{\gamma\beta}\Sigma_{\alpha\delta} - \eta_{\gamma\alpha}\Sigma_{\beta\delta} + \eta_{\delta\beta}\Sigma_{\gamma\alpha} - \eta_{\delta\alpha}\Sigma_{\gamma\beta}. \tag{2.1.15}$$

With $D(\Lambda)$ given in (2.1.13) the transformation rule (2.1.10) becomes

$$\Gamma_\mu(x) \longrightarrow \Gamma_\mu(x) + \frac{1}{2}\omega^{\alpha\beta}(x)[\Sigma_{\alpha\beta}, \Gamma_\mu(x)] - \frac{1}{2}\Sigma_{\alpha\beta}\frac{\partial}{\partial x^\mu}\omega^{\alpha\beta}(x) \tag{2.1.16}$$

Considering that the tetrads transform like vectors for Lorentz transformation

$$e^\alpha{}_\mu(x) \longrightarrow e^\alpha{}_\mu + \omega^\alpha{}_\beta e^\beta{}_\mu. \tag{2.1.17}$$

and using the relation $\delta^\mu{}_\nu = e_\alpha{}^\mu e^\alpha{}_\nu$ then it follow that

$$\begin{aligned} e^\alpha{}_\nu \nabla_\mu e^{\beta\nu} \longrightarrow & e^\alpha{}_\nu \nabla_\mu e^{\beta\nu} + \omega^\alpha{}_\gamma(x) e^\gamma{}_\nu \nabla_\mu e^{\beta\nu} \\ & + \omega^\beta{}_\gamma e^\alpha{}_\nu \nabla_\mu e^{\gamma\nu} + \nabla_\mu \omega^{\alpha\beta}(x) \end{aligned} \tag{2.1.18}$$

multiplying the above equation with $-\frac{1}{2}\Sigma^{\alpha\beta}$ and considering (2.1.15) and (2.1.16) finally the explicit form of the connection $\Gamma_\mu$ is obtained

$$\Gamma_\mu(x) = \frac{i}{2}\Sigma_{\alpha\beta} e^\alpha{}_\nu \nabla_\mu e^{\beta\nu} = \frac{i}{2}\Gamma^\alpha{}_\mu{}^\beta \Sigma_{\alpha\beta}. \tag{2.1.19}$$

Now it is possible to write the action for a tensorial field

$$\begin{aligned} S &= \int d^{n+1}x det\ e \left\{ \frac{1}{2} i \left[ \overline{\Psi}\gamma^\alpha e_\alpha{}^\mu \nabla_\mu \Psi - e_\alpha{}^\mu \nabla_\mu \overline{\Psi}\gamma^\alpha \Psi \right] - m\overline{\Psi}\Psi \right\} \\ &= \int d^{n+1}x det\ e \left\{ \frac{1}{2} i \left[ \overline{\Psi}\widetilde{\gamma^\mu} \nabla_\mu \Psi - \nabla_\mu \overline{\Psi}\widetilde{\gamma^\mu}\Psi \right] - m\overline{\Psi}\Psi \right\} \end{aligned} \tag{2.1.20}$$

the matrices $\widetilde{\gamma^\mu} = \gamma^\beta e_\beta{}^\mu$ have been defined and they satisfy the algebra

$$\left\{ \widetilde{\gamma^\mu}, \widetilde{\gamma^\nu} \right\} = g^{\mu\nu}. \tag{2.1.21}$$

Finally, Dirac equation on curved space time is obtained by a variation of (2.1.20) with respect to $\overline{\Psi}$

$$-i\gamma^\mu(\partial_\mu + \Gamma_\mu)\Psi + m\Psi = 0 \tag{2.1.22}$$

### 2.1.1 Stodolski phase

In the following chapters equation (2.1.22) will be solved in some cases where the spin connection $\Gamma_\mu$ is either null or can be readsorbed on the wave function through a suitable exponential, leaving as only effect of non trivial structure of space time the rotation of Dirac matrices

$$\gamma^\alpha e_\alpha{}^\mu \partial_\mu \Psi = 0 \tag{2.1.23}$$

This is in general a system of non linear partial differential equations of the fourth degree. Thus the solution of (2.1.23) is non trivial, and it could be usually achieved using perturbative methods i.e. in the limit of small curvature. This kind of procedure could be performed if the curvature tensor is a smooth tensorial field but in some cases, like topological defects, this assumption fails. A non perturbative approach to the solution of (2.1.23) was proposed by Stodolski [123] and it really based on the nature of tetrads. Let's start from a spinless particle on flat space time, whose wave functions will be a plane wave $e^{ik_\alpha x^\alpha}$. This could be interpreted as the exponential of the line integral

$$\int dx^\alpha p_\alpha \tag{2.1.24}$$

where in the above integral the components of the 4-momentum $p_\alpha$ are constant. It follows that (4.3.29) is the integral of an exact differential form, and thus it is not necessary to specify the path of integration. Following the spirit that has has led to the introduction of spic connection, on curved space time it could be assumed that (4.3.29) holds in the local inertial frame, and its translation to the generalized coordinates $x^\mu$ is achieved through tetrads

$$\int dx^\mu e^\alpha{}_\mu p_\alpha \tag{2.1.25}$$

here, in contrast to (4.3.29) the coefficients of the differential form $p_\mu$ depends on position, and in general they will not make an exact differential form. Thus, the path of integration should be defined when (2.1.25) is introduced. The most intuitive choice of the path is a gedesics arc, i. e. the classical path followed by the particle on curved space time. This is clearly an approximation, as it could be understood from the very basics of quantum mechanics. This is the limit of the method introduced by Stodolski. However, there are cases such as the topological defects, in which the differential form $p_\mu$ is exact, and then all these difficulties disapper giving a clean solution to relativistic equations on curved space time. In the case of a spinor the general solution of (2.1.23) is

$$\Psi = \Psi_0 \exp \int dx^\mu e^\alpha{}_\mu p_\alpha \tag{2.1.26}$$

where $\Psi_0$ is a constant spinor, that is a solution of Dirac equation on flat space time in $k$ space.

## 2.2 Topological Defects and their Geometrical Description

In the following chapters topological defects will be analyzed in both topological insulators and and graphene. Topological line defects are created through the Volterra process: given a three dimensional solid a wedge is cut with amplitude $\Omega$, and the free edges are glued together as shown in figure 2.1(a). If the edges match perfectly the crystal structure is locally reconstructed, and this happens if the $\Omega$ is a multiple of the angle characterizing the symmetry of the crystal. For example, in the case of a square lattice $\Omega$ is a multiple of $\pi/2$ as shown in fig. 2.1(b) where they are depicted the defects for $\Omega = \pi/2$, obtained removing a wedge of amplitude $\pi/2$ and the one with $\Omega = -\pi/2$ where the wedge with the same is introduced into the lattice. The crystal structure is altered only along the singular line $L$ in fig.

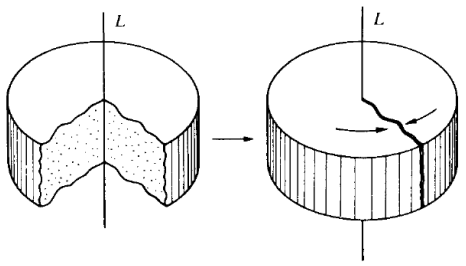


(a)

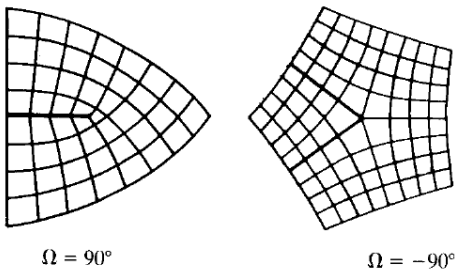


(b)

**Figure 2.1:** a)Volterra process creating a topological line defect. b) Disclinations for the square lattice with $\Omega = \pi/2$ and $\Omega = -\pi/2$.

2.1(a), in general defined as the line passing through the vertex of the wedge along which the rotation of the material is done in order to glue the free surfaces. This defect is called *wedge disclination* and can be characterized with the Frank vector, defined as the vector of modulus $\Omega$ and directed along the line $L$. The creation of a disclination implies the failure of local rotational symmetry of the lattice along the line $L$ and another kind of defect exists, affecting the other typical symmetry of solid i.e. the translational invariance. These defects, the *edge dislocations* are obtained through a Volterra-like process as shown in fig. 2.2(a): a wedge of amplitude $\Omega$ is cutted but it is not totally removed, instead it is re-introduced into the material but shifted of a vector $\vec{b}$, called the *Burgers vector*. As for the Frank vector in the case of

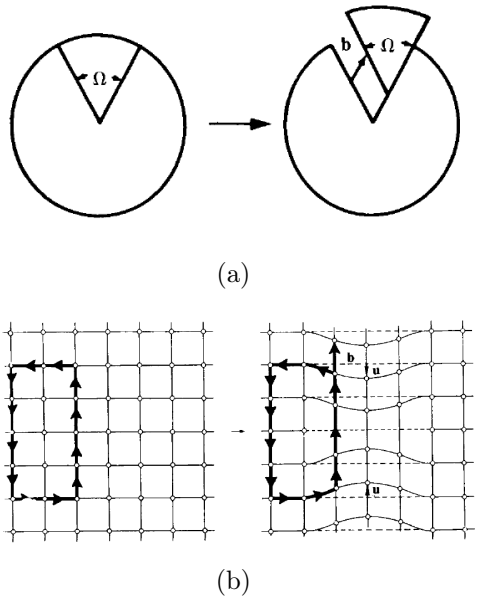


**Figure 2.2:** Edge dislocations from Volterra process.

disclinations, the vector $\vec{b}$ is important in the mathematical descriptions of dislocations. A closed path in the crystal before the creation of the dislocation, as the one shown in the left of fig. 2.2(b), could be mapped into a path in the crystal after the creation of the dislocation. Calling $x_n$ the original positions of the atoms, the positions of the atoms when the dislocation is introduced are $x_n + u_n$ where $u_n$ is the displacement field created by the defect. Then the closed path shown on the left of fig. 2.2(b) is mapped into the path on the right of the same figure step by step. The resulting path is not closed and the failure of closure is mathematical expressed by the Burger vector $\vec{b} = \sum_n \Delta u_n$, where $\Delta u_n$ is the amount of displacement introduce by

the defect in each step.
From a mathematical point of view Volterra process can be interpreted as a change of coordinates from the perfect lattice coordinates $x^\mu$ to the perturbed lattice coordinates $x^{'\mu}$. This simple consideration is at the base of the geometric formulation of the physics of topological defects, i.e. the effects of geometry of disclinations and dislocations on transport properties. In the continuum approximation a medium is modeled by Minkowski spacetime, and a regular (i.e. invertible and differentiable) change of coordinates cannot create neither curvature nor torsion. Indeed, the curvature tensor in term of the tetrads (2.1.1) is

$$R_{\mu\nu\lambda}{}^{\kappa} = e^{a\kappa}(\partial_\mu\partial_\nu - \partial_\nu\partial_\mu)e_{a\lambda}. \tag{2.2.27}$$

Due to Riemann theorem the curvature tensor is null if the tetrads are regular, i.e. if $x^\mu(x^a)$ are only change of coordinates of the flat space. As a consequence, the coordinates $x^{'\mu}$ of a topological defects must be singular, otherwise no new phenomena would be introduced with the defects in contrast to physical evidence[72]. In addition to curvature, a defect can also introduce torsion, i.e. the connection coefficients $\Gamma_{\mu\nu}{}^{\lambda}$ are not symmetric in the lower indexes so that the torsion tensor $T_{\mu\nu}{}^{\lambda}$ is different from zero

$$T_{\mu\nu}{}^{\lambda} = \frac{1}{2}(\Gamma_{\mu\nu}{}^{\lambda} - \Gamma_{\nu\mu}{}^{\lambda}) = \frac{1}{2}e_a{}^{\lambda}(\partial_\mu e^a{}_\nu - \partial_\nu e^a{}_\mu) \tag{2.2.28}$$

Torsion and curvature are linked through Cartan's structure equations [100]

$$\begin{aligned} d\hat{\theta}^\alpha + \omega^\alpha{}_\beta \wedge \hat{\theta}^\beta &= T^\alpha \\ d\omega^\alpha{}_\beta + \omega^\alpha{}_\gamma \wedge \omega^\gamma{}_\beta &= R^\alpha{}_\beta \end{aligned} \tag{2.2.29}$$

hold for the torsion two-form $T^\alpha = \frac{1}{2}T^\alpha{}_{\beta\gamma}\hat{\theta}^\beta \wedge \hat{\theta}^\gamma$ ( $\hat{\theta}^\alpha$ is the dual basis of the tetrads basis) and for the curvature two-form $R^\alpha{}_\delta = \frac{1}{2}R^\alpha{}_{\delta\beta\gamma}\hat{\theta}^\beta \wedge \hat{\theta}^\gamma$. In the following sections the effect of the torsion introduced by the edge disclinations and the curvature introduced by a wedge dislocation in a graphene monolayer will be studied using Boltzmann theory.

## 2.3 The edge dislocation

The Volterra process used to produce an edge dislocation that has been described above can be equivalently understood as cutting or inserting an half line of atoms in the perfect lattice. In the case of an hexagonal lattice a "line" of atoms can be identified with a zigzag-like arrangement of atoms,

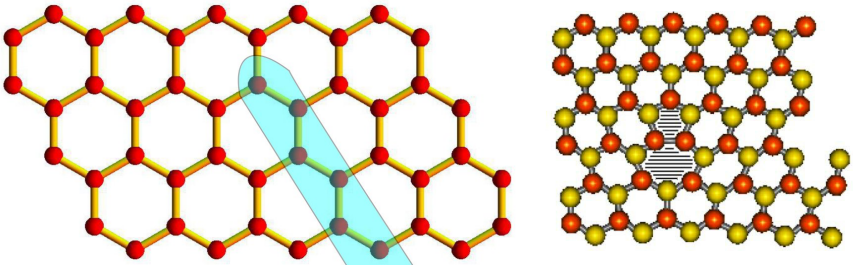

(a) (b)

**Figure 2.3:** Edge dislocation appearing as a pentagon-eptagon pair in the perfect lattice of a graphene monolayer.

as shown in fig. 2.3(a). In fig. 2.3(b) the edge dislocation then appears as a pentagon-eptagon pair, the rest of the lattice is still made by hexagons whose distortion is significant close to the defect. In the following the case of an edge disclocation oriented along the negative $x$ axis will be considered In the continuum limit the perfect lattice coordinates $x^a$ (in the following indicated using overlined indexes, in order to avoid confusion) is expressed through a multivalued change of coordinates as a function of the perturbed coordinates $x^\mu$

$$x^{\overline{1}} = x^1, \qquad x^{\overline{2}} = x^2 - \frac{b}{2\pi} \arctan \frac{y}{x} \tag{2.3.30}$$

where the branch of $\arctan(y/x)$ is defined so to that the function has a $2\pi$ along the negative $x$ semi-axis, and $b$ is the modulus of the Burger vector. The tetrads are easily found considering that $dx^a = e^a{}_\mu dx^\mu$ obtaining

$$e^a{}_\mu = \begin{pmatrix} 1 & 0 \\ \frac{b}{2\pi}\frac{y}{x^2+y^2} & 1 - \frac{b}{2\pi}\frac{x}{x^2+y^2} \end{pmatrix} \tag{2.3.31}$$

The inverse of these quantities are

$$e_a{}^\mu = \begin{pmatrix} 1 & 0 \\ -\frac{b}{2\pi}\frac{y}{x^2+y^2}\frac{1}{1-\frac{b}{2\pi}\frac{x}{x^2+y^2}} & \frac{1}{1-\frac{b}{2\pi}\frac{x}{x^2+y^2}} \end{pmatrix} \tag{2.3.32}$$

The tetrads are regular functions, thus (2.3.31) give a null Riemann tensor following (2.2.27). On the contrary the torsion is delta-like

$$T_{12}{}^{\overline{1}} = -b\delta(\vec{r}), \qquad T_{12}{}^{\overline{2}} = 0 \tag{2.3.33}$$

Indeed, in the case of an edge dislocation, since the Riemann tensor is null, the second equation in (2.2.29) is trivially satisfied if $\boldsymbol{\omega} = 0$, while the first

equation gives a $\delta$-like torsion due to the non holonomy of the $\theta$ coordinate in the origin

$$d(d\theta) = \delta(\vec{r})dr \wedge d\theta.$$

As a consequence of the geometrical features of an edge dislocation, the spin connection can be put to zero and the perturbation arising from only the rotation of Dirac matrices $\gamma^\mu = e_a{}^\mu \gamma^a$ is left

$$\begin{aligned} \gamma^1 &= \sigma_x \\ \gamma^2 &= \alpha(x,y)(-\beta(x,y)\sigma_x + \sigma_y) \end{aligned} \tag{2.3.34}$$

where the functions $\alpha(x,y)$ and $\beta(x,y)$

$$\begin{aligned} \alpha(x,y) &= \frac{1}{1 - \frac{b}{2\pi}\frac{x}{x^2+y^2}} \\ \beta(x,y) &= \frac{b}{2\pi}\frac{y}{x^2+y^2} \end{aligned} \tag{2.3.35}$$

The stationary part of the Dirac equation then becomes

$$-i\left[\sigma_x\partial_x + \alpha(x,y)(-\beta(x,y)\sigma_x + \sigma_y)\partial_y\right]\Psi = E\Psi \tag{2.3.36}$$

As discussed in subsection 2.1.1 a solution of this equation is given in terms of a solution of Dirac equation in flat space-time $\Psi_0$ using was Stodolsky phase

$$\Psi(\vec{r};\vec{r}_0) = \Psi_0 \exp i\int_{\vec{r}_0}^{\vec{r}} \mathbf{p}(\mathbf{r})d\mathbf{r} - iEt \equiv \Psi_0 \exp i\int_{\vec{r}_0}^{\vec{r}} p_\mu(x)dx^\mu \tag{2.3.37}$$

where the differential form $p(\mathbf{r})$ whose component I call $p_\mu(\mathbf{r})$ is nothing but the expression of the momentum $p_a$, defined in the local inertial frame, in the frame $x^\mu$ of the manifold

$$e^a{}_\mu p_a = p_\mu \tag{2.3.38}$$

From the tetrads (2.3.31) it follows that the components of (2.3.38) are

$$\begin{aligned} p_1(x,y) &= p_{\overline{1}} + \frac{b}{2\pi}\frac{y}{x^2+y^2}p_{\overline{2}} \\ p_2(x,y) &= \left(1 - \frac{b}{2\pi}\frac{x}{x^2+y^2}\right)p_{\overline{2}} \ . \end{aligned} \tag{2.3.39}$$

This differential form is curl-free, therefore it is the differential of the following potential $V(\vec{r})$

$$V(\vec{r}) = \vec{p}\cdot\vec{r} - \frac{p_{\overline{2}}\,b}{2\pi}\arctan\frac{y}{x} \ . \tag{2.3.40}$$

Thus, in the case of an edge dislocation it is possible to write Stodolsky phase avoiding any ambiguity on the integration path defining it. The first part of (2.3.40) is the flat contribution. The second part is the contribution of the defect, which is discontinuous on the branch cut line. The spinor solving (2.3.36) is

$$\Psi_{\vec{p},s}(\vec{r}) = \frac{1}{\sqrt{2}} \begin{pmatrix} 1 \\ s\, e^{i\theta_p} \end{pmatrix} e^{-i(\vec{p}+\vec{K})\cdot\frac{\vec{b}}{2\pi}\theta_r} e^{i\vec{p}\cdot\vec{r}} \ . \tag{2.3.41}$$

Here $s = +(-)$ identifies particles (holes), $\theta_r$ is the angle of the position vector in the $(x, y)$ plane, $\vec{p}$ is the wave vector of the electron making an angle $\theta_p$ with the positive $x$-axis and $\vec{K}$ is the position in the first Brillouin zone of the Dirac cone. This shows that the circulation around the defect increases the quantum phase by an amount $\vec{p}\cdot\vec{b}$. The edge dislocation thus reproduces the effects of a vortex singularity in a solid, where the flux of the vortex is fixed by the Burgers vector and the valley wave vector $\vec{K}$. This last contribution to the total phase accumulated by the particle comes from the holonomy generated by the edge dislocation in the lattice [92]. In the following section the scattering of a particle on an edge dislocation will be studied, and its contribution to resistivity will be calculated.

### 2.3.1 Scattering: phase shifts and cross section

Even if the dislocation is classified as a line defect, the edge dislocation acts on the electrons like an effective Ahronov-Bohm flux located in the brach point of the defect. The component with angular momentum $m$ of the exact wave function (2.3.41) is

$$\Psi_{m,s}(\vec{r}) = \frac{i^m}{\sqrt{2}} \begin{pmatrix} J_{m+f}(pr) \\ isJ_{m+1+f}(pr)e^{i\theta_r} \end{pmatrix} e^{-i(\vec{p}+\vec{K})\cdot\frac{\vec{b}}{2\pi}\theta_r} e^{im\theta_r} \tag{2.3.42}$$

where $f$ is the effective flux generated by the edge dislocation and $\theta_r$. In the following only those values of the angular momentum $m$ will be taken such that $m + f$ and $m + f + 1$ are positive. This because Bessel functions with negative index would give normalization problem [49; 50]. The outgoing wave function from the scattering center is in general the sum of the incoming unperturbed part and a scattered part with amplitude $f(\theta)$

$$\psi_{out}\,(\vec{r}) \ \sim \begin{pmatrix} 1 \\ se^{i\theta_k} \end{pmatrix} \left[ e^{i\vec{k}\cdot\vec{r}} + f(\theta)\, \frac{e^{ikr}}{\sqrt{r}} \right] \ . \tag{2.3.43}$$

The scattering amplitude is related to the sum of the phase shifts of each $m$ component of the incoming wave function

$$f(\theta) = \sqrt{\frac{1}{2\pi k}} \sum_{m=-\infty}^{\infty} (-1)^m \left[e^{2i\delta_m} - 1\right] e^{im\theta} \tag{2.3.44}$$

The phase shifts $\delta_m$ of the process are identified matching the incoming and the outgoing wave function[49; 50]

$$\delta_m(\vec{p}) = -\frac{\pi}{2}\left(\left|m + (\vec{p}+\vec{K})\cdot\frac{\vec{b}}{2\pi}\right| - |m|\right) \tag{2.3.45}$$

The $t-$matrix element describing the probability amplitude that an outgoing circular wave, of incoming wavevector $\vec{k}$ at the Fermi circle, is scattered into a plane wave of wavevector $\vec{p}$ ( with $|\vec{p}| = k$ ) is

$$\begin{aligned}
\langle p|t(\vec{k})|k\rangle &= \frac{1}{\pi R^2}\int r dr \int d\phi\, f(\phi) \begin{pmatrix} 1 & s e^{-i\theta_p} \end{pmatrix} \begin{pmatrix} 1 \\ s e^{i\theta_k} \end{pmatrix} e^{-i\vec{p}\cdot\vec{r}}\,\frac{e^{ikr}}{\sqrt{r}} = \\
&= \left[1 + e^{-i(\theta_p-\theta_k)}\right]\,\frac{1}{\pi R^2}\int_0^R r dr\,\frac{e^{ikr}}{\sqrt{r}} \times \\
&\times \sum_m (-1)^m [e^{2i\delta_m} - 1] \times \int_0^{2\pi} d\phi\, e^{im\phi}\, e^{-ipr\cos[\phi-(\theta_p-\theta_k)]}\ .
\end{aligned} \tag{2.3.46}$$

The factor $1/\pi R^2$ in front of the above integral comes from normalization of wave functions, since both waves are normalized to the square root of the area $\pi R^2$. The factor $\left[1 + e^{-i(\theta_p-\theta_k)}\right]$ arises from chiral nature of wave function and provides the cancellation of the backward scattering. The integration over $\phi$ gives a Bessel function $J_m$ and the integration on $r$ can be approximated as :

$$\frac{1}{R}\, e^{im(\theta_p-\theta_k)} \int_0^R r dr\,\frac{e^{ikr}}{\sqrt{r}}\, 2\pi i^m\, J_m(kr) \approx \sqrt{\frac{2\pi}{k}}\, e^{im(\theta_p-\theta_k)} e^{i\frac{\pi}{4}}\,(-1)^m\,\frac{1}{R}\int_0^R dr\ .$$

Finally:

$$\langle p|t(\vec{k})|k\rangle = \left[1 + e^{-i(\theta_p-\theta_k)}\right]\,\sqrt{\frac{2}{\pi k R^2}}\, e^{i\pi/4}\sum_m [e^{2i\delta_m} - 1]\, e^{im(\theta_p-\theta_k)} \tag{2.3.47}$$

Now the sum can be performed. Defining $\alpha$ as the non-integer part of the flux: $(\vec{p}+\vec{K})\cdot\vec{b}/2\pi = N + \alpha$, with $\alpha < 1$, we obtain ( $\Theta \equiv (\theta_p - \theta_k)$):

$$\begin{aligned}
\langle p|t(\vec{k})|k\rangle &= \left[1 + e^{-i\Theta}\right]\,\sqrt{\frac{2}{\pi k R}}\, e^{i\pi/4}\times \\
&\times \left[-2\pi\delta(\Theta)\,(1 - \cos\pi\alpha)\, + \sin\pi\alpha\frac{e^{-i(N+1/2)\Theta}}{\sin\Theta/2}\right]
\end{aligned} \tag{2.3.48}$$

Now the relaxation time of Eq.(3.3.26) can be estimated. The prefactor of Eq.(3.3.26), $\left(1-\hat{k}\cdot\hat{k}'\right) \equiv 1-\cos\Theta$ makes the first term in Eq.(2.3.48) disappear, which is likely to be spurious anyway[49]. It also compensates the divergency at $\Theta = 0$ of the second term. The final result is:

$$\frac{1}{\tau\left(\vec{k}_F\right)} = v_F \frac{4\sin^2\pi\alpha}{\pi k_F R^2} \int_0^{2\pi} d\theta_p \ (1-\cos\Theta) \ \frac{(1+\cos\Theta)}{\sin^2\Theta/2} = v_F \frac{16\sin^2\pi\alpha}{\pi k_F R^2} \ . \tag{2.3.49}$$

Hence, according to Eq.(3.3.25), the resistivity due to the elastic scattering on the edge dislocation is:

$$\overline{\rho}\left(\vec{k}_F\right) = 32\,\frac{\pi\hbar}{e^2}\,\frac{\overline{\sin^2\pi\alpha}}{\left(k_F R\right)^2} = 32\,\frac{\pi\hbar}{e^2}\,\frac{\sin^2\pi/3}{\left(k_F R\right)^2} \tag{2.3.50}$$

Prior to the averaging, this depends on the incoming direction due to the orientation of the Burgers vector, but is independent of the modulus of $k$ close to the neutrality point. When multiplying this result by the number of dislocations and after averaging over their random distribution, the full resistivity would be proportional to the density of the defects and inversely proportional to the density of carriers $n \propto k_F^2$. It is remarkable that close to the charge neutrality point $k_F \to 0$ the calculated resistivity tends to the finite limit $e^2\rho/\hbar \sim 8\pi^2 b^2/R^2$. Lattice relaxation, around the branch point, provided it is not too strong, would contribute to the resistivity with a term that is an higher positive power of $k_F$[44] and would not change this result qualitatively. The total cross section with $f(\phi)$ given by Eq. (2.3.44) is

$$\sigma_{tot} = \int d\phi \ |f(\phi)|^2 = \frac{4}{k} \sum_{m=-\infty}^{\infty} \sin^2\delta_m \tag{2.3.51}$$

## 2.4 Cross Section and resistivity from stress of an edge dislocation

A general elastic deformation $\vec{u}$ in solids is analyzed through the strain tensor

$$u_{ij} = \frac{1}{2}(\partial_i u_j + \partial_j u_i)$$

In graphene a gauge field can be built using $u_{ij}$, describing the interaction of electrons with stress [7; 124; 20]

$$\begin{aligned} V_x &= \frac{3}{4}\beta\kappa(u_{xx} - u_{yy}) \\ V_y &= \frac{3}{4}\beta\kappa u_{xy} \end{aligned} \tag{2.4.52}$$

where $\kappa$ is the bending rigidity of the graphene membrane and $\beta$ is a parameter that takes into account the variation on the hopping parameter due to the strain induced by the deformation. The deformation vector generated from an edge dislocation can be calculated from (2.3.30)

$$\begin{aligned} u_1 &= 0 \\ u_2 &= \frac{b}{2\pi} \arctan \frac{y}{x} \end{aligned} \tag{2.4.53}$$

The potential (2.4.52) with this deformation vector is

$$\begin{aligned} V_x &= -4\beta tbD \frac{x^2 y}{(x^2+y^2)^2} = -2\beta tbD \frac{\cos\theta \sin 2\theta}{r} \\ V_y &= -2\beta tbD \frac{x(x^2-y^2)}{(x^2+y^2)^2} = -2\beta tbD \frac{\cos\theta \cos 2\theta}{r}, \end{aligned} \tag{2.4.54}$$

giving a perturbation to the Hamiltonian of pristine graphene of the type

$$V = \sigma_i V_i = \frac{A}{r} \begin{pmatrix} 0 & -i\cos\theta e^{2i\theta} \\ i\cos\theta e^{-2i\theta} & 0 \end{pmatrix}. \tag{2.4.55}$$

This potential will be used in the following to evaluate the scattering cross section of electrons on stress generated by the edge dislocation. To do this, the scattered part will be evaluated as

$$\Psi_{sc} = \int d\vec{r}\,' G(\vec{r}, \vec{r}\,', \omega) V(\vec{r}\,') \Psi_{in}(\vec{r}\,'). \tag{2.4.56}$$

In the above formula $\Psi_{in}$ is the $m$-component of an unperturbed plane wave, $V$ is the potential (2.4.55), and $G(\vec{r}, \vec{r}\,', \omega)$ is the Green function for the equation (2.3.36). In the next subsection this Green function will be evaluated using spectral decomposition, and in the following subsection the cross section for the scattering on $V$ is derived.

### 2.4.1 Green function for an edge dislocation.

The Green function of an edge dislocation analyzed in term of angular momentum eigenfunctions is

$$G(\vec{r},\vec{r}\,',\omega) = i\int pdp\sum_{m,s}\frac{e^{im(\theta_r-\theta_{r'})}}{\omega-sp}\times$$
$$\times\frac{1}{2}\begin{pmatrix} J_{m+f}(pr)\,J^*_m(pr') & -is\,J_{m+f}(pr)\,J^*_{m+1}(pr')\,e^{-i\theta_{r'}} \\ -is\,J_{m+1+f}(pr)J^*_m(pr')\,e^{i\theta_r} & -J_{m+1+f}(pr)\,J^*_{m+1}(pr')\,e^{i(\theta_r-\theta_{r'})}\end{pmatrix} =$$

$$= \frac{i}{2\pi\hbar^2 v_F^2}\sum_m\int_{-\infty}^{\infty}EdE\,\frac{e^{im(\theta_r-\theta_{r'})}}{\omega-E}\times$$
$$\times\frac{1}{2}\begin{pmatrix} J_{m+f}(x)\,J^*_m(x') & -is\,J_{m+f}(x)\,J^*_{m+1}(x')\,e^{-i\theta_{r'}} \\ -is\,J_{m+1+f}(x)J^*_m(x')\,e^{i\theta_r} & -J_{m+1+f}(x)\,J^*_{m+1}(x')\,e^{i(\theta_r-\theta_{r'})}\end{pmatrix} \tag{2.4.57}$$

where the dimensionless variables $x = |E|r/\hbar v_F$ and $x' = |E|r'/\hbar v_F$ have been introduced. The integration path can be closed through a circumference at infinity, whose contribution can be neglected as in the free case (see Appendix C). In addition, some care should be done close to the origin: Bessel functions of arbitrary index have a branch cut along the negative real axis. Counting the power of $E$ of the integrand function, it can been seen that the branch point in the origin does not contribute. Indeed, Bessel functions $J_\nu(z)$ when expanded close to $z = 0$ go like $z^\nu$ and the integral defining the Green function close to the origin can be evaluated as

$$\int dE E^{2m+f} \xrightarrow{E\to 0} 0 \tag{2.4.58}$$

Using Cauchy theorem the integral then evaluates as

$$G(\vec{r},\vec{r}\,',\omega) = \pi\rho(\omega)\sum_m e^{im(\theta_r-\theta_{r'})}\times$$
$$\times\begin{pmatrix} J_{m+f}(x)\,J^*_m(x') & -is\,J_{m+f}(x)\,J^*_{m+1}(x')\,e^{-i\theta_{r'}} \\ -is\,J_{m+1+f}(x)J^*_m(x')\,e^{i\theta_r} & -J_{m+1+f}(x)\,J^*_{m+1}(x')\,e^{i(\theta_r-\theta_{r'})}\end{pmatrix} \tag{2.4.59}$$

where in the formula above $x = |\omega|r/\hbar v_F$ and $x' = |\omega|r'/\hbar v_F$ and the density of states for a linearly dispersive band, $\rho(\omega) = \omega/2\pi\hbar v_F$, has been introduced.

### 2.4.2 Cross section and resistivity

Using only the contribution of the pole Eq.(2.4.59),and the zero order wave-function Eq.(2.3.42), the integral giving the scattered part of the wave function is

$$\Psi_{sc} = \int d\vec{r}' G\left(\vec{r}, \vec{r}\,', \omega\right) V(\vec{r}\,')\Psi(\vec{r}') = (-i)^f Ak(S_1 + S_2) \tag{2.4.60}$$

where the two contributions to the integral above explicitly are

$$\begin{aligned} S_1 &= \sum_m \begin{pmatrix} sJ_{m+f}(kr) \\ -iJ_{m+1+f}(kr)e^{i\theta_r} \end{pmatrix} e^{im\theta_r} \times \\ &\times \int dr' d\theta_{r'} J_m(kr') J_{n+1}(kr') \cos\theta_{r'} e^{3i\theta_{r'}} e^{i(n-m)\theta_{r'}} \\ S_2 &= \sum_m \begin{pmatrix} sJ_{m+f}(kr) \\ -iJ_{m+1+f}(kr)e^{i\theta_r} \end{pmatrix} e^{im\theta_r} \times \\ &\times \int dr' d\theta_{r'} J_n(kr') J_{m+1}(kr') \cos\theta_{r'} e^{-3i\theta_{r'}} e^{i(n-m)\theta_{r'}} \end{aligned} \tag{2.4.61}$$

Let' s analyze the two contribution to the integral above. The first part gives

$$\begin{aligned} S_1 &= \sum_m \begin{pmatrix} sJ_{m+f}(kr) \\ -iJ_{m+1+f}(kr)e^{i\theta_r} \end{pmatrix} e^{im\theta_r} \int dr' d\theta_{r'} J_m(kr') J_{n+1}(kr') \cos\theta_{r'} e^{3i\theta_{r'}} e^{i(n-m)\theta_{r'}} \\ &= \begin{pmatrix} sJ_{n+4+f}(kr) \\ -iJ_{n+5+f}(kr)e^{i\theta_r} \end{pmatrix} e^{i(n+4)\theta_r} \int dr' J_{n+4}(kr') J_{n+1}(kr') + \\ &+ \begin{pmatrix} sJ_{n+2+f}(kr) \\ -iJ_{n+3+f}(kr)e^{i\theta_r} \end{pmatrix} e^{i(n+2)\theta_r} \int dr' J_{n+2}(kr') J_{n+1}(kr') \end{aligned} \tag{2.4.62}$$

These integrals are special cases of the critical case of the Weber-Schafheitlin integral [136]

$$\int_0^\infty dt J_{\alpha+p}(at) J_{\alpha-p-1}(bt) = \begin{cases} \frac{b^{\alpha-p-1}\Gamma(\alpha)}{a^{\alpha-p}\Gamma(\alpha-p)p!} \; {}_2F_1\left(\alpha, -p; \alpha-p; \frac{b^2}{a^2}\right) & \text{if} \quad b < a \\ \frac{(-1)^p}{2a} & \text{if} \quad b = a \\ 0 & \text{if} \quad b > a \end{cases} \tag{2.4.63}$$

In this case $(\alpha, p) = (n+3, 1)$ and $(n+2, 0)$ respectively, thus the first integral is equal to $-1/2k$ while the other is $1/2k$

$$\begin{aligned} S_1 = &-\frac{1}{2k} \begin{pmatrix} sJ_{n+4+f}(kr) \\ -iJ_{n+5+f}(kr)e^{i\theta_r} \end{pmatrix} e^{i(n+4)\theta_r} + \\ &+ \frac{1}{2k} \begin{pmatrix} sJ_{n+2+f}(kr) \\ -iJ_{n+3+f}(kr)e^{i\theta_r} \end{pmatrix} e^{i(n+2)\theta_r} \end{aligned} \tag{2.4.64}$$

Similarly the $S_2$ in (2.4.61) evaluates as

$$\begin{aligned} S_2 &= \sum_m \begin{pmatrix} sJ_{m+f}(kr) \\ -iJ_{m+1+f}(kr)e^{i\theta_r} \end{pmatrix} e^{im\theta_r} \int dr' d\theta_{r'} J_n(kr') J_{m+1}(kr') \cos\theta_{r'} e^{-3i\theta_{r'}} e^{i(n-m)\theta_{r'}} \\ &= \begin{pmatrix} sJ_{n-4+f}(kr) \\ -iJ_{n-3+f}(kr)e^{i\theta_r} \end{pmatrix} e^{i(n-4)\theta_r} \int dr' J_{n-4}(kr') J_{n+1}(kr') \\ &+ \begin{pmatrix} sJ_{n-2+f}(kr) \\ -iJ_{n-1+f}(kr)\, e^{i\theta_r} \end{pmatrix} e^{i(n-2)\theta_r} \int dr' J_{n-2}(kr') J_{n+1}(kr') \end{aligned} \tag{2.4.65}$$

This integral is evaluated using again results in eq. (2.4.63) with $(\alpha, p) = (n-1, -3)$ and $(n, -2)$ so that the first integral is equal to $-1/2k$ while the other is $1/2k$, as for $S_1$, giving the final result

$$\begin{aligned} \Psi_{sc} &= (-i)^f \frac{A}{2} e^{in\theta_r} \left\{ - \begin{pmatrix} J_{n+4+f}(kr) \\ iJ_{n+5+f}(kr)e^{i\theta_r} \end{pmatrix} e^{i4\theta_r} + \begin{pmatrix} J_{n+2+f}(kr) \\ iJ_{n+3+f}(kr)e^{i\theta_r} \end{pmatrix} e^{i2\theta_r} \right. \\ &- \left. \begin{pmatrix} J_{n-4+f}(kr) \\ iJ_{n-3+f}(kr)e^{i\theta_r} \end{pmatrix} e^{-i4\theta_r} + \begin{pmatrix} J_{n-2+f}(kr) \\ iJ_{n-1+f}(kr)e^{i\theta_r} \end{pmatrix} e^{-i2\theta_r} \right\} \end{aligned} \tag{2.4.66}$$

The dominant scattering amplitudes $f_{mn}$, to keep the order of the Bessel functions the lowest possible, are $\langle \Psi_0 | GV \Psi_{\pm 4} \rangle$ or $\langle \Psi_0 | GV \Psi_{\pm 2} \rangle$. Apart from the consideration that they imply incoming waves of relatively high order (i.e. $|n| = 2, 4$) , all of them lead to integrals of the kind

$$\begin{aligned} &\lim_{k\to 0} \frac{1}{\ell^2} \int_0^\infty r dr\, J_0(kr)\, J_f(kr) \approx \\ &\approx \frac{1}{k^2 \ell^2 \Gamma(1+1/3)} \int_0^{k\ell} t dt \left(\frac{1}{2}t\right)^{1/3} J_0(t) \sim (k\ell)^{1/3} \end{aligned} \tag{2.4.67}$$

Cross section should go as

$$\sigma_{tot} = \sum_{mn} |f_{mn}|^2 \sim (k\ell)^{2/3} \tag{2.4.68}$$

## 2.5 The wedge disclination

A wedge disclination is made by the Volterra process, i.e. cutting a wedge of angle amplitude $\alpha$ and pasting the edges. As in the case of an edge dislocation we define the angular variable $\theta = \arctan \frac{y}{x}$ with a branch cut on the negative $x$ axis. It follows that the tangent vectors are rotated, depending on the

azimuthal angle, even far from the defect. However, there is no rotation at the positive $x$ axis. All of this is encoded in the tetrad set

$$\begin{aligned} e^{\overline{1}}{}_1 &= \cos\frac{\theta}{n} \\ e^{\overline{1}}{}_2 &= -\sin\frac{\theta}{n} \\ e^{\overline{2}}{}_1 &= \sin\frac{\theta}{n} \\ e^{\overline{2}}{}_2 &= \cos\frac{\theta}{n} \ . \end{aligned} \tag{2.5.69}$$

Their inverses are

$$\begin{aligned} e_{\overline{1}}{}^1 &= \cos\frac{\theta}{n} \\ e_{\overline{1}}{}^2 &= -\sin\frac{\theta}{n} \\ e_{\overline{2}}{}^1 &= \sin\frac{\theta}{n} \\ e_{\overline{2}}{}^2 &= \cos\frac{\theta}{n} \end{aligned} \tag{2.5.70}$$

In the case of the formation of a pentagon defect, $\alpha = \pi/3$. As the tangent vectors at the edge are rotated by $\pi/6$ above the branch cut and by $\pi/6$ below it, $n \equiv 2\pi/\alpha = 6$. The overline on the labels has been introduced in order to distinguish the flat coordinates from the coordinates in the distorted lattice, i.e. $x^{\overline{a}} \equiv x^a$. The metric $g_{\mu\nu} = \eta_{ab} e^a{}_\mu e^b{}_\nu$ geerated by these tetrads is just the identity matrix. The connection coefficients $\Gamma_{\mu\nu}{}^\lambda = e_a{}^\lambda \partial_\mu e^a{}_\nu$ are:

$$\begin{aligned} \Gamma_{11}{}^1 &= 0 \\ \Gamma_{12}{}^1 &= -\frac{1}{n}\partial_x\theta \\ \Gamma_{21}{}^1 &= 0 \\ \Gamma_{22}{}^1 &= -\frac{1}{n}\partial_y\theta \\ \Gamma_{11}{}^2 &= \frac{1}{n}\partial_x\theta \\ \Gamma_{12}{}^2 &= 0 \\ \Gamma_{21}{}^2 &= \frac{1}{n}\partial_y\theta \\ \Gamma_{22}{}^2 &= 0 \end{aligned} \tag{2.5.71}$$

The torsion $S_{\mu\nu}{}^{\lambda} = \frac{1}{2}(\Gamma_{\mu\nu}{}^{\lambda} - \Gamma_{\nu\mu}{}^{\lambda})$ is

$$\begin{aligned} S_{12}{}^{1} &= -\frac{1}{2n}\partial_x\theta = -\frac{1}{2n}\frac{\sin\theta}{r} \\ S_{12}{}^{2} &= -\frac{1}{2n}\partial_y\theta = -\frac{1}{2n}\frac{\cos\theta}{r} \end{aligned} \tag{2.5.72}$$

The components of this tensor are singular at the origin. The only independent component of the curvature tensor is a Dirac delta, as shown by Kleinert in his book:

$$R_{121}{}^{1} = -\alpha\delta(\vec{r}) \tag{2.5.73}$$

### 2.5.1 Dirac equation on a wedge disclination

The spin connection

$$\Gamma_{\mu} = \frac{1}{4}\Gamma^{\alpha}{}_{\mu}{}^{\beta}\Sigma_{\alpha\beta} \tag{2.5.74}$$

is zero since the tetrads are regular functions. Thus, the wedge disclination affects Dirac equation only through the rotation of Dirac matrices

$$\begin{aligned} \gamma^1 = \gamma^a e_a{}^{1} &= \sigma_x\cos\frac{\theta}{n} + \sigma_y\sin\frac{\theta}{n} = \begin{pmatrix} 0 & e^{-i\frac{\theta}{n}} \\ e^{i\frac{\theta}{n}} & 0 \end{pmatrix} \\ \gamma^2 = \gamma^a e_a{}^{2} &= -\sigma_x\sin\frac{\theta}{n} + \sigma_y\cos\frac{\theta}{n} = \begin{pmatrix} 0 & -ie^{-i\frac{\theta}{n}} \\ ie^{i\frac{\theta}{n}} & 0 \end{pmatrix} \end{aligned} \tag{2.5.75}$$

Then the Dirac equation for a wedge dislocation is

$$-i\left[\begin{pmatrix} 0 & e^{-i\frac{\theta}{n}} \\ e^{i\frac{\theta}{n}} & 0 \end{pmatrix}\partial_x + \begin{pmatrix} 0 & -ie^{-i\frac{\theta}{n}} \\ ie^{i\frac{\theta}{n}} & 0 \end{pmatrix}\partial_y\right]\Psi = \epsilon\Psi \tag{2.5.76}$$

To solve this equation is helpful to introduce the unitary transformation

$$U = \begin{pmatrix} e^{i\frac{\theta}{2n}} & 0 \\ 0 & e^{-i\frac{\theta}{2n}} \end{pmatrix}. \tag{2.5.77}$$

Applying this transformation to the Dirac equation

$$-i\,U[\gamma^1\partial_x + \gamma^2\partial_y]U^{\dagger}U\Psi = \epsilon\,U\Psi\ . \tag{2.5.78}$$

By defining $\Phi = U\Psi$ we have

$$-i\left[\overrightarrow{\sigma}\cdot\overrightarrow{\partial} + \frac{\sigma\cdot\hat{r}}{2nr}\right]\Phi = \epsilon\Phi \tag{2.5.79}$$

Writing the free Dirac operator in cylindrical polar coordinates this equation becomes

$$-i\left[\sigma\cdot\hat{r}\left(\partial_r+\frac{1}{2nr}\right)+\frac{\sigma\cdot\hat{\theta}}{r}\partial_\theta\right]\Phi=\epsilon\Phi \tag{2.5.80}$$

In (2.5.80), similarly to what happens in [41], the electrons encircling the defect feel the flux of an effective gauge field. For the $K'$ valley the Dirac matrices on flat space time are

$$\begin{aligned}\gamma^1&=\sigma_x\\ \gamma^2&=-\sigma_y\end{aligned} \tag{2.5.81}$$

So Dirac equation becomes

$$[\sigma_x\partial_x-\sigma_y\partial_y]\Psi=i\epsilon\Psi \tag{2.5.82}$$

The above equation for the $K'$ valley could be obtained from teh one for the $K$ valley making a complex conjugation, but you have also to change the sign of energy to map the equations, i.e. you have to change particles with antiparticles. Let's pass to the case of the edge dislocation. The rotated Dirac matrices are

$$\begin{aligned}\gamma^{\overline{1}}&=\begin{pmatrix}0 & e^{i\frac{\theta}{n}}\\ e^{-i\frac{\theta}{n}} & 0\end{pmatrix}\\ \gamma^{\overline{2}}&=\begin{pmatrix}0 & ie^{i\frac{\theta}{n}}\\ -ie^{-i\frac{\theta}{n}} & 0\end{pmatrix}\end{aligned} \tag{2.5.83}$$

Note that these matrices are the complex conjugate of the one for the $K$ valley. Then Dirac equation for the wedge dislocation for the $K'$ valley is

$$\left[\begin{pmatrix}0 & e^{i\frac{\theta}{n}}\\ e^{-i\frac{\theta}{n}} & 0\end{pmatrix}\partial_x+\begin{pmatrix}0 & ie^{i\frac{\theta}{n}}\\ -ie^{-i\frac{\theta}{n}} & 0\end{pmatrix}\partial_y\right]\Psi=i\epsilon\Psi \tag{2.5.84}$$

A unitary transformation could be introduced so that the equation reduces to the flat one with a non abelian potential

$$U'=\begin{pmatrix}e^{-i\frac{\theta}{2n}} & 0\\ 0 & e^{i\frac{\theta}{2n}}\end{pmatrix}. \tag{2.5.85}$$

Note that $U'=U^\dagger$. Applying this unitary transformation than Dirac equation becomes

$$\left[\sigma\cdot\hat{r}^*\partial_r+\frac{\sigma\cdot\hat{\theta}^*}{r}\left(\partial_\theta+\frac{i\sigma_z}{2n}\right)\right]\Phi=i\epsilon\Phi \tag{2.5.86}$$

In the above equation the matrices $\sigma \cdot \hat{r}^*$ and $\sigma \cdot \hat{\theta}^*$ are the complex conjugate of the corrispondent one in the case of the $K$ valley. it should be stressed that the vector potential appears with the opposite sign. So, the Dirac equation in the $4 \times 4$ formalism is

$$\left[\alpha \cdot \hat{r}\partial_r + \frac{\alpha \cdot \hat{\theta}}{r}\left(\partial_\theta - \frac{i\sigma_z}{2n}\tau_z\right)\right]\Phi = i\epsilon\Phi \tag{2.5.87}$$

where the following representation of the spinor has been used

$$\Phi = \begin{pmatrix} \Phi_{AK} \\ \Phi_{BK} \\ \Phi_{AK'} \\ \Phi_{BK'} \end{pmatrix} \tag{2.5.88}$$

and the Dirac matrices in the $4 \times 4$ formalism are

$$\alpha^r = \begin{pmatrix} \sigma \cdot \hat{r} & 0 \\ 0 & \sigma \cdot \hat{r}^* \end{pmatrix} = \sigma^1 \otimes \mathbb{I}, \qquad \alpha^\theta = \begin{pmatrix} \sigma \cdot \hat{\theta} & 0 \\ 0 & \sigma \cdot \hat{\theta}^* \end{pmatrix} = \sigma^2 \otimes \tau^3 \tag{2.5.89}$$

In addition to this field another gauge field should be added in order to consider the non trivial boundary condition involving both the valleys. This gauge field is another $SU(2)$ gauge field

$$A_\theta = \frac{1}{4}\tau_2 \otimes \mathbb{I}_{2\times 2} \tag{2.5.90}$$

The gauge field coming from a wedge disclination seems to give an intrinsic Aharonov-Bohm effect, but in general $SU(2)$ could not give such an effect since it' s a simply connected group.

## 2.6 Screw dislocations in topological insulators

In a 3D material another kind of dislocation can be created: the material is cut along an half plane and the two free surfaces so created are glued back after a relative displacement along the direction of the plane, i.e. the right side is displaced upward and the left side is displaced downward as shown in fig. 2.4. In the case of the screw dislocation the Burger vector is oriented along the the defect line, differing from the edge dislocation in which the Burgers vector is orthogonal to the defect. The change of coordinates describing a screw dislocation is very similar to the edge dislocation one

$$\begin{aligned} x^{\bar{1}} &= x^1 \\ x^{\bar{2}} &= x^2 \\ x^{\bar{3}} &= x^3 - \frac{b}{2\pi}\arctan\frac{x^2}{x^1} \end{aligned} \tag{2.6.91}$$

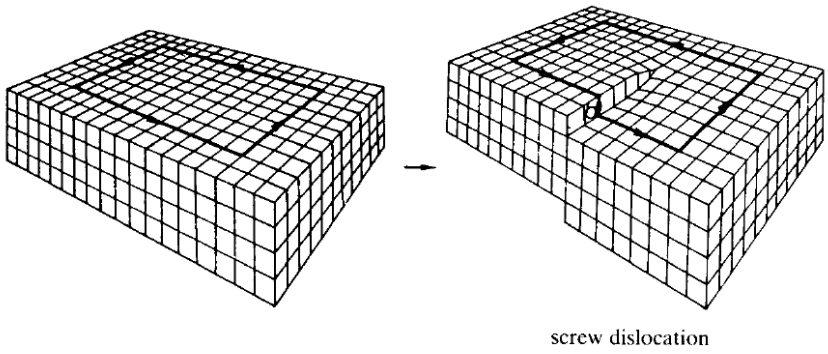


**Figure 2.4:** Volterra process for the screw dislocation

In this way, when circling around the vertical axis the $x^3$ coordinates jumps of $b$. Thus the tetrads are

$$e^a{}_\mu = \begin{pmatrix} 1 & 0 & 0 \\ 0 & 1 & 0 \\ \frac{b}{2\pi}\frac{y}{x^2+y^2} & -\frac{b}{2\pi}\frac{x}{x^2+y^2} & 1 \end{pmatrix} \tag{2.6.92}$$

The inverse tetrads are

$$e_a{}^\mu = \begin{pmatrix} 1 & 0 & 0 \\ 0 & 1 & 0 \\ -\frac{b}{2\pi}\frac{y}{(x^2+y^2)} & \frac{b}{2\pi}\frac{x}{(x^2+y^2)} & 1 \end{pmatrix} \tag{2.6.93}$$

The coordinates with overlined indexes make up the local inertial set of coordinates needed to use the tetrads machinery. In the case of the screw dislocation, and for topological defects in general, they have a straightforward interpretation trough the Volterra process, since the $x^{\overline{a}}$ can be interpreted as the coordinates before the Volterra process takes place. This could be understood considering how a $x^{\overline{3}} = const$ plane (existing before defect's creation) changes after the creation of the defect. The Volterra process consists in cutting the plane along the $x^{\overline{1}} > 0$ half-axis and pushing one side upward and the other downward. The surface created from the considered plane in this way is $x^3 = x^{\overline{3}} + \frac{b}{2\pi}\theta$, i.e. the third relation of (2.6.91). The torsion expressed in function of the tetrads is

$$S_{ab}{}^\mu = -\frac{1}{2}(\partial_a e_b{}^\mu - \partial_b e_a{}^\mu) \tag{2.6.94}$$

The only non vanishing component of the torsion for the screw dislocation is $S_{12}{}^{\overline{3}} = -b\delta(\vec{r})$, while the curvature is vanishing as in the case of the edge

dislocation. The rotation of Dirac matrices gives

$$\mathcal{H}_S(\vec{k}) = \mathcal{H}_0 - i\frac{b}{2\pi}\frac{\vec{\gamma}\cdot\hat{\theta}}{r}\partial_z \tag{2.6.95}$$

Later I will analyze the possible existence of spin connection. The Dirac equation could be solved using the Stodolsky phase, if the line integral defining it is path independent. In the following $\vec{r} = (x, y)$ is the position vector in a plane orthogonal to the $z$-axis and $\vec{R} = (x, y, z)$ is the whole position vector, $\vec{\mathfrak{K}} = (k_1, k_2, k_3) = (\vec{k}, k_3)$ is the wave vector for bulk states. The Stodolsky phase explicitly is

$$\int k_\mu dx^\mu = \int k_a e^a{}_\mu dx^\mu = \vec{\mathfrak{K}}\cdot\vec{R} - k_{\overline{3}}\frac{b}{2\pi}\theta \equiv \vec{\mathfrak{K}}\cdot\vec{R} + \frac{\vec{\mathfrak{K}}\cdot\vec{b}}{2\pi}\theta \tag{2.6.96}$$

This is the same result as in the case of the edge dislocation in graphene (2.3.40), where the phase accumulated by a particle moving around the screw dislocation is

$$\Omega = -\frac{k_{\overline{3}}b}{2\pi} = \frac{\vec{\mathfrak{K}}\cdot\vec{b}}{2\pi} \tag{2.6.97}$$

since the Burgers vector in the case of the screw dislocation is $\vec{b} = (0, 0, -b)$. Inserting a wave function of the type

$$\Psi(r, \theta, z) = \Phi(r, \theta)e^{ik_{\overline{3}}z} \tag{2.6.98}$$

in (2.6.95) the Dirac equation reduces to the one in flat space time with a magnetic flux given by $-\Omega$

$$\left\{-i\left[\vec{\gamma}\cdot\hat{r}\partial_r + \frac{\vec{\gamma}\cdot\hat{\theta}}{r}\left(\partial_\theta + i\frac{k_{\overline{3}}b}{2\pi}\right)\right] + \vec{\gamma}\cdot\hat{z}k_{\overline{3}} + \Delta\gamma_0\right\}\Phi(r, \theta) = E\Phi(r, \theta) \tag{2.6.99}$$

This is Dirac equation in cylindrical coordinates with a flux give by $-\Omega$ and its solution is

$$\Psi(r, \theta, z) = \begin{pmatrix} (E+\Delta)J_{m-\Omega}(kr) \\ k_3 J_{m-\Omega}(kr) \\ 0 \\ -ikJ_{m-\Omega+1}(kr)e^{i\theta} \end{pmatrix} e^{im\theta}e^{ik_3 z} \tag{2.6.100}$$

with the usual boundary condition

$$\Psi(r, \theta, z) = \Psi(r, \theta + 2\pi, z). \tag{2.6.101}$$

### 2.6.1 Possible bound states for the screw dislocation

In ref. [115] it has been shown that given the vector $\boldsymbol{K}$, that identifies the position of the Dirac cone in the FBZ, a screw dislocation with Burgers vector $\boldsymbol{b}$ hosts a Dirac-like mode if

$$\boldsymbol{K} \cdot \boldsymbol{b} = \pm\pi \mod 2\pi. \tag{2.6.102}$$

In this section it will be shown how these states arise starting from Hamiltonian (2.6.95)

$$\mathcal{H}_S = \mathcal{H}_0 + \frac{\vec{\gamma} \cdot \hat{\theta}}{r} \frac{\boldsymbol{b} \cdot \boldsymbol{k}}{2\pi} \tag{2.6.103}$$

where the unperturbed Hamiltonian $\mathcal{H}_0$ is in (1.6.81)

$$\mathcal{H}_0(\mathbf{k}) = \epsilon(\mathbf{k})\mathbb{I}_{4\times4} + \begin{pmatrix} M(\mathbf{k}) & A_1 k_z & 0 & k_- \\ A_1 k_z & -M(\mathbf{k}) & k_- & 0 \\ k_+ & 0 & -A_1 k_z & -M(\mathbf{k}) \end{pmatrix} \tag{2.6.104}$$

where $\epsilon(\mathbf{k}) = C + D_1 k_z^2 + D_2(k_x^2 + k_y^2)$ and $M(\mathbf{k}) = M - B_1 k_z^2 - B_2(k_x^2 + k_y^2)$. A simplified version of this model will be considered in the following: the sum of the diagonal quadratic terms

$$\epsilon(\boldsymbol{k})\mathbb{I}_{4\times4} + M(\boldsymbol{k})\mathbb{I}_{2\times2} \otimes \sigma_z$$

will be approximated with $\mathcal{M} = M + C_1 k_z^2 + C_2 \left(k_x^2 + k_y^2\right)$.

$$\mathcal{H}_0(\mathbf{k}) = \begin{pmatrix} \mathcal{M}(\mathbf{k}) & A_1 k_z & 0 & k_- \\ A_1 k_z & -\mathcal{M}(\mathbf{k}) & k_- & 0 \\ 0 & k_+ & \mathcal{M}(\mathbf{k}) & -A_1 k_z \\ k_+ & 0 & -A_1 k_z & -\mathcal{M}(\mathbf{k}) \end{pmatrix} \tag{2.6.105}$$

In addition it will be considered the case $C_2 = 0$, in order to have a analytically solvable model, and $M, C_1, C_2 > 0$, in order to have a non-trivial phase. In the spirit of $k \cdot p$ the wave function of an electron whose wave vector lies close to $\boldsymbol{K}$ is $e^{i\boldsymbol{K}\cdot\boldsymbol{r}}\Psi(\boldsymbol{r})$, where $\Psi(\boldsymbol{r})$ is a slowly varying function over the unit cell. The Hamiltonian (2.6.95) will be then written as

$$\mathcal{H}_S = \mathcal{H}_0 + \frac{\vec{\gamma} \cdot \hat{\theta}}{r} \frac{\boldsymbol{b} \cdot \boldsymbol{K}}{2\pi} = \mathcal{H}_0 + \frac{\vec{\gamma} \cdot \hat{\theta}}{2r} \tag{2.6.106}$$

where in the last equality (2.6.102) is supposed to hold. As the added flux is $\pi$ ( i.e. $hc/2e$ ) Time Reversal is not broken. Hence an odd gapless Dirac

cone of chiral states exists. In cylindrical coordinates (2.6.106) explicitly is

$$\begin{aligned}
(E-\Delta)\frac{1}{v_F}\Psi_A(\vec{\mathbf{r}}) &= i\frac{\partial}{\partial z}\Psi_B(\vec{\mathbf{r}}) + i\,e^{i\theta}\left[\frac{\partial}{\partial r}+\frac{i}{r}\frac{\partial}{\partial\theta}+\frac{1}{2r}\right]\Psi_D(\vec{\mathbf{r}})\\
(E+\Delta)\frac{1}{v_F}\Psi_B(\vec{\mathbf{r}}) &= i\frac{\partial}{\partial z}\Psi_A(\vec{\mathbf{r}}) + i\,e^{i\theta}\left[\frac{\partial}{\partial r}+\frac{i}{r}\frac{\partial}{\partial\theta}+\frac{1}{2r}\right]\Psi_C(\vec{\mathbf{r}})\\
(E-\Delta)\frac{1}{v_F}\Psi_C(\vec{\mathbf{r}}) &= i\,e^{-i\theta}\left[\frac{\partial}{\partial r}-\frac{i}{r}\frac{\partial}{\partial\theta}-\frac{1}{2r}\right]\Psi_B(\vec{\mathbf{r}}) - i\frac{\partial}{\partial z}\Psi_D(\vec{\mathbf{r}})\\
(E+\Delta)\frac{1}{v_F}\Psi_D(\vec{\mathbf{r}}) &= i\,e^{-i\theta}\left[\frac{\partial}{\partial r}-\frac{i}{r}\frac{\partial}{\partial\theta}-\frac{1}{2r}\right]\Psi_A(\vec{\mathbf{r}}) - i\frac{\partial}{\partial z}\Psi_C(\vec{\mathbf{r}})
\end{aligned} \tag{2.6.107}$$

A possible solution of the system above with angular momentum $n-1$ is

$$|E;b\rangle = \frac{1}{N}\begin{pmatrix}(E+\Delta)\,K_{n-1/2}(\kappa r)\\ k\,K_{n-1/2}(\kappa r)\\ 0\\ -i\kappa\,K_{n+1/2}(\kappa r)\,e^{-i\theta}\end{pmatrix} e^{-i(n-1)\theta}\,e^{-ikz}. \tag{2.6.108}$$

By direct substitution it can be seen that wave function with $n=0$ is a legitimate solution of (2.6.107)

$$\begin{aligned}
|E;1\rangle &= \frac{1}{N}\begin{pmatrix}(E+\Delta)\,K_{-1/2}(\kappa r)\\ k\,K_{-1/2}(\kappa r)\\ 0\\ -i\kappa\,K_{1/2}(\kappa r)\,e^{-i\theta}\end{pmatrix} e^{i\theta}\,e^{-ikz} =\\
&= \frac{1}{N}\begin{pmatrix}(E+\Delta)\\ k\\ 0\\ -i\Delta\,e^{-i\theta}\end{pmatrix} K_{-1/2}(\kappa r)\,e^{i\theta}\,e^{-ikz},
\end{aligned} \tag{2.6.109}$$

with the eigenvalue: $E^2-\Delta^2 = k^2-\kappa^2$. This yelds:

$$E^2 = (M-Ck^2)^2 + k^2 - \kappa^2 \tag{2.6.110}$$

We can choose $\kappa = |M-Ck^2| = \Delta$ and we have the Dirac cone dispersion in the $z-$direction. Note that in the case of the trivial insulator would be $\kappa = |M+Ck^2|$. This is unphysical because, increasing $k$, the energy increases and we expect that the state becomes less localized. Therefore $\kappa$ should decrease. To fix this physics correctly, $k$ should go imaginary at the boundary with a trivial insulator, so that the propagating states are confined to the non trivial insulator only. With a $\pi-$flux , time reversal (TR) is still

a good symmetry, and thus a second state resolving the equations (2.6.107) by applying time reversal symmetry to (2.6.109)

$$|E;\Theta 1\rangle \equiv |E;2\rangle = \frac{1}{N}\begin{pmatrix} 0 \\ i\Delta\, e^{i\theta} \\ -(E+\Delta) \\ -k \end{pmatrix} K_{1/2}(\kappa r)\, e^{-i\theta}\, e^{ikz}. \tag{2.6.111}$$

The couple of states found localized at the defect is consistent with the results of the Altland and Zirnbauer [6], who propose a generalization of the analysis made by Dyson [28; 29; 30] of condensed matter systems in term of the symmetries of the system. The symmetries that are useful to the classification are [127]

- Time Reversal Symmetry

$$\Theta = e^{i\pi S_y}\mathcal{C} \tag{2.6.112}$$

  where $S_y$ is the $y$ component of the spin operator and $\mathcal{C}$ is the complex conjugation. As discussed in previous chapters time reversal symmetry implies $H(k) = \Theta H(-k)\Theta^{-1}$.

- Particle-Hole symmetry $\Xi$, an antiunitary symmetry such that $H(k) = \Xi H(-k)\Xi^{-1}$. In the case of 3DTI the explicit form of Particle-Hole Symmetry is

$$\Xi = \begin{pmatrix} 0 & 0 & 0 & -1 \\ 0 & 0 & 1 & 0 \\ 0 & -1 & 0 & 0 \\ 1 & 0 & 0 & 0 \end{pmatrix} \mathcal{C}$$

- Chiral Symmetry $\Pi$, a unitary transformation that change the sign of the Hamiltonian without reversing the sign of $\boldsymbol{k}$ $H(k) = -\Pi H(k)\Pi^{-1}$, whose explicit form is

$$\Pi = i \cdot \Theta\Xi = i \cdot \begin{pmatrix} 0 & 1 & 0 & 0 \\ -1 & 0 & 0 & 0 \\ 0 & 0 & 0 & 1 \\ 0 & 0 & -1 & 0 \end{pmatrix}$$

Hamiltonian (2.6.95), in presence of a non zero chemical potential $\mu$ has niegther the Particle Hole symmetry $\Xi$ nor the Chiral Symmetry $\Gamma$, Indeed $\Xi^T H(\mu)\Xi = -H(-\mu)$ and $\Pi^\dagger H(\mu)\Pi = H(-\mu)$. As analyzed in [127] it belongs to the class AII, in 3D the Hamiltonian has a corresponding $\mathbb{Z}_2$

invariant and the protected gapless modes are chiral Dirac Fermions. From states (2.6.109) and (2.6.111) it's possible to obtain two chiral states. The projectors $L$ and $R$ on the left chiral and right chiral states, respectively, are

$$\begin{aligned} L &= \frac{1 - i\Pi}{2} \\ R &= \frac{1 + i\Pi}{2} \end{aligned} \tag{2.6.113}$$

and their action on the states is

$$\begin{aligned} L\,|1\rangle = L\,|2\rangle &= \frac{1}{2}(|1\rangle + |2\rangle) \\ R\,|1\rangle = R\,|2\rangle &= \frac{1}{2}(|1\rangle - |2\rangle) \end{aligned} \tag{2.6.114}$$

Thus, the sum $|1\rangle + |2\rangle$ is a left chiral state, while $|1\rangle - |2\rangle$ has right-wise chirality. The two states so built are one the time reversal of the other.

# Chapter 3

# Spin connection and Boundary states in 3D Topological Insulators

It has been in the previous Chapter Dirac equation in curved space time has been used to describe topological defects in graphene. In this Chapter it will be shown that the boundary states for a 3D TI obey the same equation, starting from the study of symmetric cases like a spherical and a cylindrical TI by using the $k \cdot p$ Hamiltonian (1.6.82). The more realistic case of a bump on the top of the surface will be then treated, and starting from Dirac equation and scattering theory the contribution to resistivity due to this defect is calculated.

## 3.1 Introduction.

As described in chapter 1, strong Topological Insulators (TI 's) are a new class of materials with a bulk gap but surface states defined on surfaces of all orientations[36; 35; 97; 58], making the boundaries gapless. The number of surface states at a flat surface with a given orientation is odd, and each of them shows a conical singularity, described by the two dimensional Dirac equation[58]. Localized states also exist at other lattice defects, such as screw dislocations[115; 126; 127]. The transport features of electrons at the surfaces of TI 's is being intensively studied. The wavefunctions have an internal spinorial structure made up of two slowly varying components related by time reversal invariance. Backscattering due to smooth perturbations which preserve the time reversal symmetry is forbidden, making the transport properties of these compounds similar to those of graphene in the

absence of intervalley scattering[20]. Surfaces with a finite curvature allow for scattering processes due to the existence of a non trivial metric, which has been studied in the classical limit[24], when wavepackets are well approximated by point particles following classical trajectories. An analysis of the electronic properties of curved surfaces of TI 's requires information about the way a non trivial metric changes the effective Dirac equation. It is well known that the Dirac equation could be written on a curved space time introducing the spin connection and the rotation of Dirac matrices[100]. The existence of the spin connection has been postulated in topological insulators[81]. The emergence of the spin connection from the combination of the three dimensional electronic structure of a TI and the two dimensional metric of a boundary with intrinsic curvature has not been studied so far. In the next section, we analyze the surface states for the simplest curved boundary with a non trivial metric, the sphere. The conservation of the angular momentum in this geometry allows us to calculate the entire spectrum of surface states, and to show that the spin connection term is induced in the effective surface hamiltonian. We use this information to analyze the effect of the curvature in the scattering by a bump in a flat surface, a process considered in the classical limit in[24]. Related processes can be defined in graphene with topological defects[22]. Technical details of the calculations are discussed in the appendices, including an analytical study of the boundary states in a cylinder, calculated numerically in[32]. The boundary of a cylinder can be considered a surface without intrinsic curvature and spin connection.

## 3.2 Model of a spherical topological insulator.

The surface states of model single particle hamiltonians for a TI have been studied particularly for a flat boundary [119] and for an infinite cylinder boundary surface [32]. A minimal model reproducing the band structure of a TI requires four orbitals, related in pairs by the time reversal symmetry[146]. A further simplification includes just the linear in-momentum contributions to the hamiltonian of Ref. [146]:

$$\mathcal{H} = \hat{\gamma}^0 \Delta + \hbar v_F \hat{\gamma}^i k_i \tag{3.2.1}$$

where $v_F$ is the Fermi velocity and the matrices $\hat{\gamma}^a$ are given in terms of Pauli matrices by $\hat{\gamma}^0 = \tau_0 \otimes \tau_z$, $\hat{\gamma}^1 = \sigma_x \otimes \tau_x$, $\hat{\gamma}^2 = -\sigma_y \otimes \tau_x$ $\hat{\gamma}^3 = \sigma_z \otimes \tau_x$. Here $\sigma_a$ and $\tau_b$ denote matrices in the spin and even-odd orbital parity spaces, respectively. This hamiltonian satisfies time reversal symmetry $T = \mathcal{K} i\sigma_y \otimes \mathbb{I}_{2\times 2}$ (here $\mathbb{I}_{2\times 2}$ the $2 \times 2$ identity and $\mathcal{K}$ the complex conjugation). Bulk eigenfunctions in

cartesian coordinates are:

$$|\Psi_{1,\pm}\rangle = \frac{1}{N_\pm}\begin{pmatrix}\epsilon_\pm(\vec{\mathbf{k}})+\Delta\\ \hbar v_F k_z\\ 0\\ \hbar v_F k_-\end{pmatrix} e^{i\vec{k}\cdot\vec{r}}, \quad |\Psi_{2,\pm}\rangle = \frac{1}{N_\pm}\begin{pmatrix}0\\ \hbar v_F k_+\\ \epsilon_\pm(\vec{\mathbf{k}})+\Delta\\ -\hbar v_F k_z\end{pmatrix} e^{i\vec{k}\cdot\vec{r}} \quad (3.2.2)$$

($k_\pm = k_x \pm ik_y$), where the band energies are

$$\epsilon_\pm(\vec{\mathbf{k}}) \equiv \pm\sqrt{\Delta^2 + \hbar^2 v_F^2\left(k_x^2+k_y^2+k_z^2\right)}$$

and $N_\pm$ is the norm of the states. Surface states appear in this model if the gap parameter, $\Delta$, changes its sign at the boundary, so that, e.g., $\Delta > 0$ in the inside, and $\Delta < 0$ in the vacuum. The model allows also for the analytical computation of the surface bands of a cylinder[32], as shown in section 3.2.2. Later we will include also quadratic corrections to the hamiltonian in Eq.4.1.1 and we will show that boundary conditions need to be chosen in a different way in that case.

### 3.2.1 Spherical Topological Insulator

In order to obtain the solution of the hamiltonian 4.1.1 onto a sphere we rephrase its eigenvalue equations into spherical coordinates. The eigenvector of energy $E$, $\Psi \equiv (\Psi_A, \Psi_B, \Psi_C, \Psi_D)$, satisfies the equations:

$$\begin{aligned}
(E-\Delta)\Psi_A &= i\left[\cos(\theta)\partial_r - \frac{\sin(\theta)}{r}\partial_\theta\right]\Psi_B - ie^{-i\phi}\left[\sin(\theta)\partial_r + \frac{\cos(\theta)}{r}\partial_\theta - i\frac{1}{r\sin(\theta)}\partial_\phi\right]\Psi_D\,,\\
(E+\Delta)\Psi_B &= i\left[\cos(\theta)\partial_r - \frac{\sin(\theta)}{r}\partial_\theta\right]\Psi_A - ie^{-i\phi}\left[\sin(\theta)\partial_r + \frac{\cos(\theta)}{r}\partial_\theta - i\frac{1}{r\sin(\theta)}\partial_\phi\right]\Psi_C\,,\\
(E-\Delta)\Psi_C &= -ie^{i\phi}\left[\sin(\theta)\partial_r + \frac{\cos(\theta)}{r}\partial_\theta + i\frac{1}{r\sin(\theta)}\partial_\phi\right]\Psi_B - i\left[\cos(\theta)\partial_r - \frac{\sin(\theta)}{r}\partial_\theta\right]\Psi_D\,,\\
(E+\Delta)\Psi_D &= -ie^{i\phi}\left[\sin(\theta)\partial_r + \frac{\cos(\theta)}{r}\partial_\theta + i\frac{1}{r\sin(\theta)}\partial_\phi\right]\Psi_A - i\left[\cos(\theta)\partial_r - \frac{\sin(\theta)}{r}\partial_\theta\right]\Psi_C\,,
\end{aligned} \quad (3.2.3)$$

(here $\hbar = v_F = 1$), with the boundary conditions

$$\Delta(r,\theta,\phi) = \begin{cases}\Delta_{in} & r < R\\ \Delta_{out} & r > R\end{cases} \quad (3.2.4)$$

We choose $\Delta_{in} = -\Delta_{out} = \Delta$ for simplicity, so that the exponential decay of the boundary states into the bulk near a flat surface is defined by the length

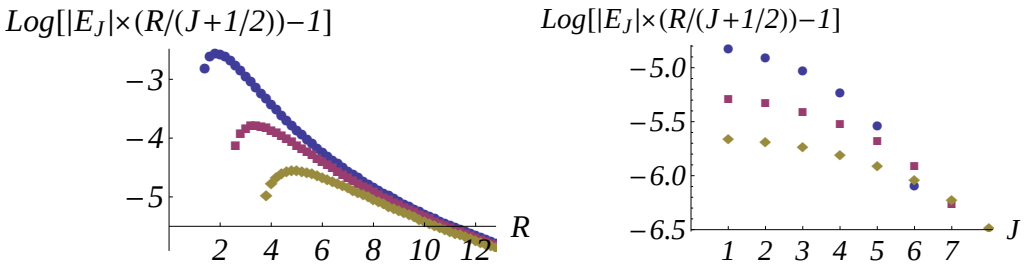


**Figure 3.1:** Dependence of the surface energy levels on angular momentum, $J$, and radius, $R$. The deviation from the result for the two dimensional Dirac equation on a sphere, see eq. 3.2.5 is plotted. Top: Dependence on $R$. From top to bottom, $J = 1, 2, 3$. Bottom: Dependence on $J$. From top to bottom, $R = 8, 10, 12$. In all cases, $v_F = 1$ and $\Delta = 1$ .

scale $\Lambda = \hbar v_F/\Delta$. The angular momentum is conserved and is quantized in half integer units (see, for instance Ref. [42]). Its eigenfunctions allow us to reduce the set of Eq.s(3.2.3) to two coupled differential equations for the radial coordinates, as discussed in subsection 3.2.1.2. It can be shown that the energy spectrum converges exponentially to the one of the two-dimensional Dirac equation onto a sphere:

$$E_J = \pm \frac{\hbar v_F (J+1/2)}{R} \times \left[1 + \mathcal{O}\left(e^{-R/\Lambda}\right)\right] \ ,$$
$$J = \frac{1}{2}, \frac{3}{2} \cdots J_{max} \ . \tag{3.2.5}$$

where $J_{max} \sim R/\Lambda$. The multiplicity of each level is $2J+1$. The exponential convergence of the energy levels to the asymptotic value in eq. 3.2.5 is shown in Fig. 3.1. This type of convergence implies that the effective hamiltonian describing the surface modes does not admit an expansion on higher order derivatives, of the type $\Delta(\Lambda\partial_i)^n$. The study of the hamiltonian in eq. 4.1.1 can be extended in a straightforward way to the case when $\Delta_{out} \neq \Delta_{in}$, although it becomes cumbersome to obtain analytical expansions in the limit $R \to \infty$. The numerical solution, shows an agreement with the spectrum in Eq. 3.2.5 of the same accuracy as those reported in Fig. 3.1.

As quadratic terms do not break the spherical symmetry, they can be safely added to Eq. 4.1.1, by the simple substitution $\Delta \to \Delta + \alpha(k_x^2 + k_y^2 + k_z^2)$, where $\alpha$ is a constant. Hence the angular part of the wavefunctions remains unchanged while its radial part satisfies second order coupled equations, in place of those in Eq. 3.2.3. For each value of the energy, $E$, we find evanescent waves with two different decay lengths, $\Lambda_1(E)$ and $\Lambda_2(E)$, which are given by

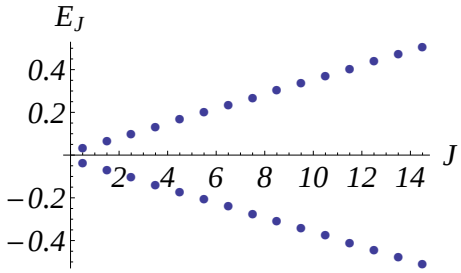


**Figure 3.2:** (Color online). Energy levels of a spherical topological insulator of radius $R = 30$ with a quadratic dispersion relation, obtained by the replacement $\Delta \to \Delta + \alpha(k_x^2 + k_y^2 + k_z^2)$ in eq. 4.1.1. Other parameters are $\Delta = 1$ and $v_F = 1$. The boundary conditions are $\Psi_A(R) = \Psi_B(R) = \Psi_C(R) = \Psi_D(R) = 0$.

the roots of a fourth order polynomial. The boundary conditions need to be replaced. The simplest boundary condition compatible with the new second order equations is $\Psi_A(R) = \Psi_B(R) = \Psi_C(R) = \Psi_D(R) = 0$[119]. By solving numerically these boundary conditions, we find again an agreement with eq. 3.2.5 similar to that shown in Fig. 3.1. Results are shown in Fig. 3.2. We conclude that the boundary states on a spherical TI satisfy the Dirac equation on the surface of the sphere. The spin connection, related to the intrinsic curvature of the metric, clearly emerges at the boundaries of a TI. More generally, the boundary states satisfy the Dirac equation on a curved space-time.

#### 3.2.1.1 Angular momentum eigenstates

Generalized angular momentum operators $J$ can be defined as usual as the sum of spin and orbital angular momentum. It can be shown that the Hamiltonian in eq. 3.2.3 commutes with $J^2, J_z$ therefore its eigenstates can be labeled by $|j, m\rangle$ with $\vec{\mathbf{J}}^2|j, m\rangle = j(j+1)|J, J_z\rangle$ and $J_z|j, m\rangle = m|J, J_z\rangle$. In order to obtain single valued eigenfunctions, the values of $J$ and $J_z$ must be half integers. As usual by using $J^+|j; j\rangle = 0$ and $J^-|j, m\rangle \propto |j, m-1\rangle$ we can explicitly construct the wavefunctions of the different states $|j, m\rangle$. The Hamiltonian eigenfunction can be thus expanded onto the the lowest angular momenta states:

$$\left|\frac{1}{2}\ ,\ \frac{1}{2}\right\rangle = A\begin{pmatrix} -\cos(\theta) \\ 0 \\ \sin(\theta)e^{i\phi} \\ 0 \end{pmatrix} + B\begin{pmatrix} 0 \\ -\cos(\theta) \\ 0 \\ \sin(\theta)e^{i\phi} \end{pmatrix} + C\begin{pmatrix} 1 \\ 0 \\ 0 \\ 0 \end{pmatrix} + D\begin{pmatrix} 0 \\ 1 \\ 0 \\ 0 \end{pmatrix}$$

$$\left|\frac{1}{2}\ ,\ -\frac{1}{2}\right\rangle = A\begin{pmatrix} \sin(\theta)e^{-i\phi} \\ 0 \\ \cos(\phi) \\ 0 \end{pmatrix} + B\begin{pmatrix} 0 \\ \sin(\theta)e^{-i\phi} \\ 0 \\ \cos(\phi) \end{pmatrix} + C\begin{pmatrix} 0 \\ 0 \\ 1 \\ 0 \end{pmatrix} + D\begin{pmatrix} 0 \\ 0 \\ 0 \\ 1 \end{pmatrix}$$

$$\left|\frac{3}{2}\ ,\ \frac{3}{2}\right\rangle = A\begin{pmatrix} -\sin(\theta)\cos(\theta)e^{i\phi} \\ 0 \\ \sin^2(\theta)e^{2i\phi} \\ 0 \end{pmatrix} + B\begin{pmatrix} 0 \\ -\sin(\theta)\cos(\theta)e^{i\phi} \\ 0 \\ \sin^2(\theta)e^{2i\phi} \end{pmatrix} +$$
$$+ C\begin{pmatrix} \sin(\theta)e^{i\phi} \\ 0 \\ 0 \\ 0 \end{pmatrix} + D\begin{pmatrix} 0 \\ \sin(\theta)e^{i\phi} \\ 0 \\ 0 \end{pmatrix}$$

$$\left|\frac{3}{2}\ ,\ \frac{1}{2}\right\rangle = A\begin{pmatrix} -2\cos^2(\theta)+\sin^2(\theta) \\ 0 \\ 3\sin(\theta)\cos(\theta)e^{i\phi} \\ 0 \end{pmatrix} + B\begin{pmatrix} 0 \\ -2\cos^2(\theta)+\sin^2(\theta) \\ 0 \\ 3\sin(\theta)\cos(\theta)e^{i\phi} \end{pmatrix} +$$
$$+ C\begin{pmatrix} 2\cos(\theta) \\ 0 \\ \sin(\theta)e^{i\phi} \\ 0 \end{pmatrix} + D\begin{pmatrix} 0 \\ 2\cos(\theta) \\ 0 \\ \sin(\theta)e^{i\phi} \end{pmatrix} \tag{3.2.6}$$

where the states $|3/2,-1/2\rangle, |3/2,-3/2\rangle$ are not explicitly exhibited, here.

#### 3.2.1.2 Spherical boundary states and energy spectrum

It can be snown that boundary states in the spherical case for $j = m = n-1/2$ $(n > 0)$ have the following form:

$$\left\langle r,\theta,\phi \left| J-\frac{1}{2}, J_z-\frac{1}{2}\right\rangle = f_1^{\mp}(r)\begin{pmatrix} 0 \\ -\cos\theta\sin^{n-1}\theta e^{i(n-1)\phi} \\ 0 \\ \sin^n\theta e^{in\phi} \end{pmatrix} + f_2^{\mp}(r)\begin{pmatrix} \sin^{n-1}\theta e^{i(n-1)\phi} \\ 0 \\ 0 \\ 0 \end{pmatrix}. \tag{3.2.7}$$

Here $f^-(r)$ and $f^+(r)$ are radial functions localized at the boundary for $r < R$ and $r > R$, respectively, and they satisfy the equations:

$$\begin{aligned}(E \mp \Delta) f_2^{\mp} &= -i\partial_r f_1^{\mp} - \frac{i}{r}(n+1) f_1^{\mp} \,, \\ (E \pm \Delta) f_1^{\mp} &= -i\partial_r f_2^{\mp} + \frac{i}{r}(n-1) f_2^{\mp} \,.\end{aligned} \tag{3.2.8}$$

The system can be decoupled in a pair of Bessel equations

$$\begin{aligned}\frac{d^2}{dr^2} f_1^{\pm} + \frac{2}{r}\frac{d}{dr} f_1^{\pm} - \left[(\Delta^2 - E^2) + \frac{n(n+1)}{r^2}\right] f_1^{\pm} = 0 \,, \\ \frac{d^2}{dr^2} f_2^{\pm} + \frac{2}{r}\frac{d}{dr} f_2^{\pm} - \left[(\Delta^2 - E^2) + \frac{n(n-1)}{r^2}\right] f_2^{\pm} = 0 \,,\end{aligned} \tag{3.2.9}$$

whose solutions are:

$$\begin{aligned} if\ r < R \qquad & \begin{cases} f_1^-(r) = -i\frac{\Delta - E}{\kappa}\, C^-\, i_n(\kappa r) \\ f_2^-(r) = C^-\, i_{n-1}(\kappa r) \end{cases} \\ if\ r > R \qquad & \begin{cases} f_1^+(r) = -iC^+\, \frac{\Delta + E}{\kappa} k_n(\kappa r) \\ f_2^+(r) = C^+\, k_{n-1}(\kappa r) \end{cases} \end{aligned} \tag{3.2.10}$$

where $i_n\,, k_n$ are the modified spherical Bessel functions:

$$i_n(x) \equiv \sqrt{\frac{\pi}{2x}} I_{n+\frac{1}{2}}(x) \ , \qquad k_n(x) \equiv \sqrt{\frac{\pi}{2x}} K_{n+\frac{1}{2}}(x) \,. \tag{3.2.11}$$

The matching conditions can be written written using Eq. (3.2.10)

$$\begin{cases} -iC^- \,(\Delta - E)\, i_n(\kappa R) = -iC^+ \,(\Delta + E)\, k_n(\kappa R) \,, \\ C^-\, i_{n-1}(\kappa R) = C^+\, k_{n-1}(\kappa R) \,, \end{cases} \tag{3.2.12}$$

which give rise to an implicit equation for the eigenenergies of the system:

$$\frac{\Delta - E}{\Delta + E} = -\frac{k_n(\kappa R)\, i_{n-1}(\kappa R)}{i_n(\kappa R)\, k_{n-1}(\kappa R)} \,. \tag{3.2.13}$$

This equation, in the limit $\Delta R \to \infty$, gives the admissible values of the energy:

$$E_n = \pm n \frac{\hbar v_F}{R} \ , \qquad n = 1,\, \ldots\,, n_{max}. \tag{3.2.14}$$

### 3.2.2 Boundary states at cylinder surface

In the following appendixes we will use $\hbar = v_F = 1$, except in main results. Let us start from the $\vec{k} \cdot \vec{p}$ model Hamiltonian of Eq.(4.1.1):

$$H\left[\vec{r}\right] = \begin{pmatrix} \Delta & i\partial_z & 0 & i(\partial_x + i\partial_y) \\ i\partial_z & -\Delta & i(\partial_x + i\partial_y) & 0 \\ 0 & i(\partial_x - i\partial_y) & \Delta & -i\partial_z \\ i(\partial_x - i\partial_y) & 0 & -i\partial_z & -\Delta \end{pmatrix}. \tag{3.2.15}$$

To find surface states in this approximation is enough to match the solutions of the Schrödinger equation at the surface of the cylinder. The gap $\Delta$ should change its sign between in and out of the surface. We rewrite the eigenvalue problem in cylindrical coordinates for the 4-component spinor $(\Psi_A, \Psi_B, \Psi_C, \Psi_D)$:

$$\begin{aligned}
(E-\Delta)\,\Psi_A(\vec{\mathbf{r}}) &= i\frac{\partial}{\partial_z}\Psi_B(\vec{\mathbf{r}}) + e^{i\theta}\left(i\frac{\partial}{\partial r} - \frac{1}{r}\frac{\partial}{\partial\theta}\right)\Psi_D(\vec{\mathbf{r}}) \\
(E+\Delta)\,\Psi_B(\vec{\mathbf{r}}) &= i\frac{\partial}{\partial_z}\Psi_A(\vec{\mathbf{r}}) + e^{i\theta}\left(i\frac{\partial}{\partial r} - \frac{1}{r}\frac{\partial}{\partial\theta}\right)\Psi_C(\vec{\mathbf{r}}) \\
(E-\Delta)\,\Psi_C(\vec{\mathbf{r}}) &= e^{-i\theta}\left(i\frac{\partial}{\partial r} + \frac{1}{r}\frac{\partial}{\partial\theta}\right)\Psi_B(\vec{\mathbf{r}}) - i\frac{\partial}{\partial_z}\Psi_D(\vec{\mathbf{r}}) \\
(E+\Delta)\,\Psi_D(\vec{\mathbf{r}}) &= e^{-i\theta}\left(i\frac{\partial}{\partial r} + \frac{1}{r}\frac{\partial}{\partial\theta}\right)\Psi_A(\vec{\mathbf{r}}) - i\frac{\partial}{\partial_z}\Psi_C(\vec{\mathbf{r}})
\end{aligned} \tag{3.2.16}$$

(in the following $k$ is in the $\hat{z}$ direction, which is the axis of the infinite cylinder. Inside the cylinder, the wavefunctions which are mostly localized close to the surface involve the modified Bessel functions $I_n(\kappa r)$ with integer $n$. They diverge exponentially at infinity but are finite for $r \to 0$. The two eigenfunctions at fixed energy $E$ are ($\kappa$ is unknown for the moment):

$$\begin{aligned}
|E, 1_<\rangle &= \frac{1}{N}\begin{pmatrix} (E+\Delta)\,I_n(\kappa r) \\ k\,I_n(\kappa r) \\ 0 \\ i\kappa\,I_{n+1}(\kappa r)\,e^{-i\theta} \end{pmatrix} e^{-in\theta}\,e^{-ikz}, \\
|E, 2_<\rangle &= \frac{1}{N}\begin{pmatrix} i\kappa\,I_n(\kappa r)e^{i\theta} \\ 0 \\ -k\,I_{n+1}(\kappa r) \\ (E-\Delta)\,I_{n+1}(\kappa r) \end{pmatrix} e^{-i(n+1)\theta}\,e^{-ikz}.
\end{aligned} \tag{3.2.17}$$

The energies of these states are $E = \pm\sqrt{\Delta^2 + k^2 - \kappa^2}$. Outside the cylinder, the functions $K_n(\kappa r)$ replace the $I_n(\kappa r)$, as the former decay exponentially

for $\kappa r \to \infty$ and $\Delta \to -\Delta$. The eigenfunctions are:

$$|E,1_>\rangle = \frac{1}{N}\begin{pmatrix}(E-\Delta)\,K_n(\kappa r)\\ k\,K_n(\kappa r)\\ 0\\ -i\kappa\,K_{n+1}(\kappa r)\,e^{-i\theta}\end{pmatrix} e^{-in\theta}\,e^{-ikz},$$
$$|E,2_>\rangle = \frac{1}{N}\begin{pmatrix}-i\kappa\,K_n(\kappa r)\,e^{i\theta}\\ 0\\ -k\,K_{n+1}(\kappa r)\\ (E+\Delta)\,K_{n+1}(\kappa r)\end{pmatrix} e^{-i(n+1)\theta}\,e^{-ikz}. \tag{3.2.18}$$

The eigenvalues are again those of Eq.(3.2.17). The two wavefunctions inside the cylinder should be matched to the two outside for each value of $n$. The matching conditions at $R$, the radius of the cylinder, lead to

$$\mathrm{Det}\begin{vmatrix} i\kappa I_n(\kappa R) & (E+\Delta)I_n(\kappa R) & -i\kappa K_n(\kappa R) & (E-\Delta)K_n(\kappa R)\\ 0 & kI_n(\kappa R) & 0 & kK_n(\kappa R)\\ -kI_{n+1}(\kappa R) & 0 & -kK_{n+1}(\kappa R) & 0\\ (E-\Delta)I_{n+1}(\kappa R) & i\kappa I_{n+1}(\kappa R) & (E+\Delta)K_{n+1}(\kappa R) & -i\kappa K_{n+1}(\kappa R)\end{vmatrix} = 0. \tag{3.2.19}$$

The vanishing of the determinant implies:

$$\left[I_n^2\,K_{n+1}^2 + K_n^2\,I_{n+1}^2\right]\,\kappa^2 + \left(2\kappa^2 - 4\Delta^2\right)\,I_n\,I_{n+1}K_n\,K_{n+1} = 0\,. \tag{3.2.20}$$

The presence of products of the Bessel functions $I_n$ and $K_n$ assures that, in the limit of $\kappa R >> 1$, there is just an inverse powerlaw dependence of the secular problem on $\kappa R$. and Eq.(3.2.20) becomes:

$$\kappa^2 = \Delta^2\,\left[1 - \frac{(n+1/2)^2}{\Delta^2 R^2}\right]\,. \tag{3.2.21}$$

Hence, the energy of the states is, according to Eq.(3.2.22)

$$E = \pm\hbar v_F\,\sqrt{k^2 + \frac{(n+1/2)^2}{R^2}} + \mathcal{O}\left(\frac{\hbar v_F^2}{\Delta^2 R^2}\right) \qquad R \gg \frac{\hbar v_F}{\Delta} \tag{3.2.22}$$

This result is in complete agreement with Eq.5 of Ref. [32]. Let us now consider the opposite limit $\kappa R << 1$. Expansion gives, up to second order in $1/\kappa R$:

$$\kappa^2\,\left\{2n(n+1)\left[1 + \frac{1}{16\,n^2(n+1)^2}\right] + \frac{1}{2}\right\} = \Delta^2\,. \tag{3.2.23}$$

The energy reads in this limit:

$$E_n(k) \approx \pm\Delta\sqrt{1 - 1/\left(2n(n+1)\left[1+\frac{1}{16\,n^2(n+1)^2}\right]+\frac{1}{2}\right)+\left(\frac{\hbar v_F k_z}{\Delta}\right)^2} + \mathcal{O}\left(\frac{\hbar\Delta R}{v_F}\right) \quad for \quad R \ll \hbar v_F/\Delta \ . \tag{3.2.24}$$

## 3.3 Scattering off a gaussian bump

We now derive the resistivity for electrons propagating at the flat boundary surface of a TI, when they are scattered off a gaussian bump of height $z\left(|\vec{r}|\right) = h\, e^{-r^2/\ell^2}$. Changes in the Dirac Equations are well localized in space close to the bump, hence a scattering picture can be fruitfully adopted in this kind of setting. The Boltzmann relaxation-time approximation can be used ($\nu(0) = k_F/(\pi\hbar v_F)$ is the density of states at the Fermi level for both spins):

$$\rho\left(k_F\right) = \frac{2}{e^2 v_F^2 \nu(0)}\,\frac{1}{\tau(k_F)} \ , \tag{3.3.25}$$

where the usual definition of the total relaxation rate is

$$\frac{1}{\tau(k_F)} = \frac{2\pi}{\hbar}\nu(0)\int_0^{2\pi} d\theta\left(1-\hat{k}\cdot\hat{k}'\right)\left|\left\langle k|t^{eff}|k'\right\rangle\right|^2 . \tag{3.3.26}$$

Here $\left\langle k|t^{eff}|k'\right\rangle$ is the matrix element of the $t-$matrix, which depends on the energy and on the scattering angle $\theta$ between the incoming and outgoing wave. Since the metric induced on the manifold by the bump is axially symmetric, it is convenient to rewrite the two dimensional Dirac equation in flat space time in cylindrical coordinates:

$$-i\hbar v_F\left(\sigma^r\partial_r + \sigma^\theta\,\frac{1}{r}\partial_\theta\right)\Psi = E\Psi \ . \tag{3.3.27}$$

Here the matrices $\sigma^{r,\theta}$ are $\sigma^r = \cos\theta\sigma^x + \sin\theta\sigma^y$ and $\sigma^\theta = -\sin\theta\sigma^x + \cos\theta\sigma^y$. Given the metric[26]

$$g_{\mu\nu} = \begin{pmatrix} -1 & 0 & 0 \\ 0 & 1+f(r) & 0 \\ 0 & 0 & r^2 \end{pmatrix} \ , \tag{3.3.28}$$

where $f(r) = (dz(r)/dr)^2$, we may read the tetrads

$$\begin{aligned} {e_x}^1 &= \frac{\cos\theta}{\sqrt{1+f(r)}}, \quad {e_y}^1 = \frac{\sin\theta}{\sqrt{1+f(r)}} \ , \\ {e_x}^2 &= -\frac{\sin\theta}{r} \ , \qquad {e_y}^2 = \frac{\cos\theta}{r} \ . \end{aligned} \tag{3.3.29}$$

The Dirac equation on a radially symmetric manifold is

$$\begin{aligned} - \quad & i\left[\frac{\sigma^r}{\sqrt{1+f(r)}}\partial_r + \sigma^\theta\left(\frac{1}{r}\partial_\theta + \frac{i}{2r}\left(1 - \frac{1}{\sqrt{1+f(r)}}\right)\sigma^z\right)\right]\Psi = \\ = \quad & E\Psi \ , \end{aligned} \tag{3.3.30}$$

The gauge potential in (3.3.30) is the spin connection

$$\Gamma_\mu = \frac{i}{2}\left(1 - \frac{1}{\sqrt{1+f(r)}}\right)\sigma^z\delta_{\mu 2}. \tag{3.3.31}$$

We pose $\Psi = \Phi \exp\int_r^{+\infty} dr'\, A_\theta(r')$ with $A_\theta$ is the spin connection above. This real prefactor can be interpreted as the origin of charge puddles accumulating at the bump. The $m$ component of the spinor $\Phi$ has the form ($m$ is the angular momentum integer):

$$\Phi_m(r,\theta|\vec{k},s) = \begin{pmatrix} u_{sm}(r) \\ is\, v_{sm}(r)\, e^{i\theta} \end{pmatrix} e^{im(\theta-\theta_k)} \tag{3.3.32}$$

where $\theta_k$ is the angle that the direction of the $\vec{k}$ vector of the incoming wave forms with the polar axis. Substituting (3.3.32) in the Dirac eq.(3.3.30) and dropping the labels $s, m$, we find that the functions $u(r), v(r)$ have to satisfy the following equations:

$$\begin{aligned} &\frac{1}{\sqrt{1+f}}\frac{d^2u(r)}{dr^2} + \frac{1}{r}\frac{du(r)}{dr} + \left(\frac{d}{dr}\frac{1}{\sqrt{1+f}}\right)\frac{du(r)}{dr} - \frac{m^2}{r^2}\sqrt{1+f}\,u(r) + k^2u(r) = 0, \\ &\frac{1}{\sqrt{1+f}}\frac{d^2v(r)}{dr^2} + \frac{1}{r}\frac{dv(r)}{dr} + \left(\frac{d}{dr}\frac{1}{\sqrt{1+f}}\right)\frac{dv(r)}{dr} - \frac{(m+1)^2}{r^2}\sqrt{1+f}\,v(r) + k^2v(r) = 0. \end{aligned} \tag{3.3.33}$$

Due to the symmetry of the problem is suitable to expand the Green's function for the flat space-time problem in polar coordinates

$$G(z,z') = \frac{1}{2\pi}\sum_{m=-\infty}^{+\infty} e^{im(\theta-\theta')}g_m(r,r'). \tag{3.3.34}$$

The Green function displaying the correct jump of the derivative at $r = r'$ is:

$$g_m(x, x') = 2\pi^2 \, J_m\left(x_<\right) Y_m\left(x_>\right) \quad . \tag{3.3.35}$$

Here $r_<(r_>)$ is the smaller (larger) of the two arguments $r, r'$. We now specialize the shape of the bump $h(r)$ to be the gaussian bump $z(|\vec{r}|)$.This implies that $f(r) = (4h^2r^2/\ell^4)e^{-2(r/\ell)^2}$. We assume that the ratio $h/\ell$ is small, so that we can expand Eq.s (3.3.33) by retaining just the lowest power of $h/\ell$. By comparison with the system for the flat space (i.e. $f(r) = 0$), we define the perturbative potential :

$$\frac{h^2}{\ell^2} V_m(r) = \frac{2h^2}{\ell^4} r^2 \, e^{-2r^2/\ell^2} \, \left[ \frac{d^2}{dr^2} + \left( \frac{4}{r} - \frac{8r}{\ell^2} \right) \frac{d}{dr} - \frac{m^2}{r^2} \right] \quad . \tag{3.3.36}$$

In the Born approximation, the Dyson equation for *e.g.* $u_{km}$ reads:

$$\begin{aligned} u_{km}(r) &= J_m(kr) + \frac{h^2}{\ell^2} \int_0^\infty dr' \, r' \, g_m(r, r') V_m(r') \, J_m(kr') \\ &= J_m(kr) + \frac{2h^2}{\ell^4} \int_0^\infty dr' \, g_m(r, r') \, r'^3 \, e^{-2r'^2/\ell^2} \times \\ &\qquad \times \left\{ k^2 + \left( \frac{3}{r'} - \frac{8r'}{\ell^2} \right) \frac{d}{dr'} \right\} \, J_m(kr') \end{aligned} \tag{3.3.37}$$

We have used the fact that $J_m$ solves the Bessel differential equation to simplify the action of $V_m$ on$J_m$ itself. By defining :

$$\tan \delta_m = \frac{4\pi^2 k^2 h^2}{\ell^4} \int_0^\infty dr' J_m(kr') r'^3 e^{-2r'^2/\ell^2} \left\{ 1 + \frac{1}{k^2} \left( \frac{3}{r'} - \frac{8r'}{\ell^2} \right) \frac{d}{dr'} \right\} J_m(kr'), \tag{3.3.38}$$

the scattering state for $r/\ell \to \infty$ takes the form $u_{km}(r) \sim J_m(kr) + \tan \delta_m Y_m(kr)$. By exploiting the symmetry of the Dirac massless equation with respect to replacements $u \leftrightarrow v$, $m \leftrightarrow -m - 1$, it is easy to see, that the sums which include $\delta_m$, for all $m$, are equal. Therefore, our result is valid for both components of the spinor solution given by Eq.(3.3.32). The integrals of Eq.(3.3.38) can be evaluated analytically. The asymptotic expansion of the Bessel functions implies that, far from the bump ( $r/\ell \to \infty$ ), the outgoing wave takes the form:

$$\begin{aligned} u_{km}(r) &\sim_{r/\ell \to \infty} \frac{1}{\sqrt{1 + \tan^2 \delta_m}} \cos \chi_m + \frac{\tan \delta_m}{\sqrt{1 + \tan^2 \delta_m}} \sin \chi_m \\ &\equiv \cos\left(\chi_m + \delta_m\right) \qquad \chi_m = kr - \frac{m\pi}{2} - \frac{\pi}{4} \; . \end{aligned}$$

We now evaluate the $t-$ matrix element for a scattering event, in which an incoming wave with wavevector $\vec{k}$ is scattered elastically by the gaussian bump and a plane wave of wavevector $\vec{p}$ emerges. The $t-$matrix element is:

$$\begin{aligned}\langle p|t(\vec{k})|k\rangle &= \left[1+e^{-i(\theta_p-\theta_k)}\right]\sqrt{\frac{2}{\pi k R^2}}\,e^{i\pi/4}\,\frac{1}{R}\times \\ &\times \int_0^R dr\, e^{\frac{\hbar^2}{\ell^4}\int_r^R dr'\, r'^2\, e^{-2(r'/\ell)^2}} \sum_m [e^{2i\delta_m}-1]\, e^{-im(\theta_p-\theta_k)}\ .\end{aligned} \tag{3.3.39}$$

The space integral arises from the exponential prefactor of $\Psi$ defined after Eq.(3.3.31). To evaluate the relaxation time formula of Eq.(3.3.40) we first perform the integral over the angle $\theta_p$ of the square modulus of the angle dependent exponentials in the sums. The integral is non vanishing only for $m-m'=\pm 2,0$. By rearranging the sums then eq. (3.3.40) is obtained.

Eq. (3.3.30) describes an unrelaxed lattice. Relaxation of the structure, besides adding an effective gauge potential, may further change the spin connection. As elastic deformations do not add any curvature, the change only implies a trivial holonomy on the wave function. This is a way of restating the Saint Venant conditions for the two-dimensional case. The inverse relaxation time (3.3.26) using the elements of the t-matrix (3.3.39) explicitly evaluates as

$$\frac{1}{\tau\left(\vec{k}_F\right)} = \frac{n_b v_F}{k_F}\times\sum_m \left[\sin^2\delta_m - \cos\left(\delta_{m+1}-\delta_{m-1}\right)\sin\delta_{m+1}\sin\delta_{m+1}\right]. \tag{3.3.40}$$

At low incoming electron energy, it turns out that the terms with $m=0,\pm 1,\pm 2$ are $\mathcal{O}[(k\ell)^4]$ and when choosing $4\pi^2h^2/\ell^2\sim 1$, they sum up to $\mathcal{S}\approx 0.733$. The terms with $m=\pm 3$ are $\mathcal{O}[(k\ell)^8]$, while the terms $m=\pm 4$ are $\mathcal{O}[(k\ell)^{12}]$.Eventually, the resistivity for independent point like defects, when the carrier density is low, (i.e. low incoming energy) is:

$$\rho\left(k_F\right)\sim\frac{2h}{e^2}\,n_b\pi\ell^2\left\{\mathcal{S}\left(\frac{h}{\ell}\right)\,(k_F\ell)^2+\mathcal{O}\left[(k_F\ell)^4\right]\right\}. \tag{3.3.41}$$

$\mathcal{S}\left(h/\ell\right)$ is a numerical prefactor which depends on the strength of the perturbation parametrized by $h/\ell$. The plot of the resistivity $vs$ energy in dimensionless units, $k_F\ell$, for various values of $h/\ell$ is shown in Fig. 3.3. The leading term is proportional to the density of carriers $n$. It has been proven recently that the classical limit for large incoming energy (i.e. relatively high densities

$n$) corresponds to an energy independent $v_F\,\tau(k_F)$ [24]. This implies that, according to Eq.(3.3.25), $\rho \propto h/(e^2 k_F) \sim 1/\sqrt{n}$, in this limit. We derive the same conclusion with a careful analysis of the sum in Eq.(3.3.40) at $k\ell >> 1$. Classically, angular momentum conservation in the scattering implies that $m \sim kb$. Here $b$ is the impact parameter measured from the center of the bump in the direction orthogonal to $\vec{k}$. By asymptotically expanding the Bessel functions appearing in the phase shifts, it turns out that there is a collection of terms contributing to the sum, which are roughly independent of $m$, as long as $k\ell >> m$. For these $m$ values, $\tan\delta_m$ is of the form:

$$\tan\delta_m \approx \pi \left(\frac{h}{\ell}\right)^2 \frac{k\ell}{2} \left[\sqrt{\frac{\pi}{2}} - (-1)^m \frac{2}{(k\ell)^3}\right] . \tag{3.3.42}$$

All other terms scale for $m >> k\ell$ as

$$\sqrt{\frac{m}{2}} \left(\frac{k\ell}{2}\right)^{2(m+1)} \frac{1}{(2m-1)!!} \tag{3.3.43}$$

and therefore they rapidly converge to zero.

We conclude that in the semiclassical limit $k\ell \gg 1$ a factor $k_F$ comes from the relevant terms in the sum of Eq.(3.3.40), which are all of the same order. This factor cancels with the $k_F$ appearing in the denominator, so that the result for $v_F\tau(k_F)$ is independent of $k_F$. This is in fact found numerically. In Fig. 3.3 we see that the conductivity $\sim \rho^{-1}$ grows linearly at large $k_F\ell$ and has a minimum in the neighborhood of $k_F\ell \sim 1$. In section 3.4 we report a simple argument based on a saddle point approximation of the $\sum_m$ which qualitatively recovers the classical limiting result for large $k_F\ell$, derived in Ref. [24]. In Fig. 3.3 it is shown a significant increase of the cross section of the bump for $k_F\ell \sim 1$ and $h/\ell \gtrsim 0.2$. This increase is due to quantum resonances induced by the non trivial spin connection.

## 3.4 Semiclassical approximation

In this Section we present a tasteful derivation of the classical high energy limit for the relaxation time. The latter can be obtained by assuming classical diffusion along the geodesic trajectories across the bump and yields[24]:

$$\frac{1}{\tau} \approx \frac{v_F}{2A} \int db\, \theta^2(b) . \tag{3.4.44}$$

Here $b$ is the impact parameter of the incoming particle, while $\theta$ is the scattering angle and $A$ is the area of the sample. The starting point is the usual

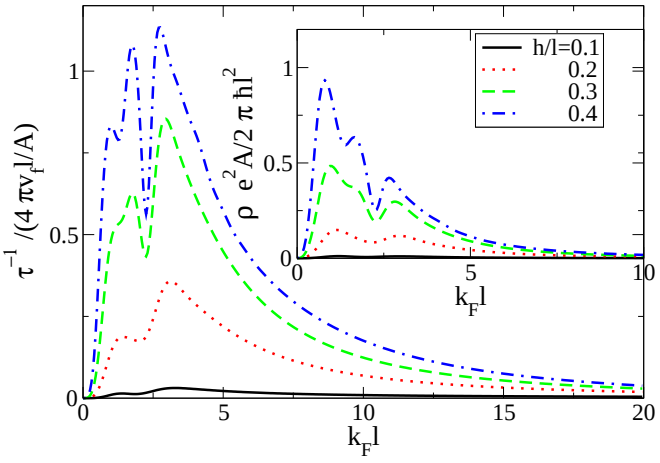


**Figure 3.3:** (Color on-line) Main Panel: inverse scattering time as a function of $k_F l$ for different values of the aspect ratio of the bump $h/l$. Inset: the resistivity due to scattering off a bump on the surface of a topological insulator, in units $\rho \cdot e^2 A/(2\pi\hbar\ell^2)$ vs. dimensionless energy $k\ell$, at different ratios $h/\ell$.

expression for the relaxation time of Eq.(3.3.40):

$$\frac{1}{\tau} = \frac{v_F}{kA}\int_0^\pi d\theta\,(1-\cos\theta)\left|\sum_m f_m(\theta)\right|^2 \tag{3.4.45}$$

given in terms of the scattering amplitudes $f_m(\theta) = \left[e^{i2\delta_m}-1\right]e^{im\theta}$. At high energy, many $m$ terms contribute to the sum, so that we take its continuum limit, which amounts to integrate over continuous values of the classical angular momentum $m = kb$. As forward scattering is excluded form Eq.(3.4.45), it is enough to apply the saddle point approximation to the resulting integral[79]:

$$\sum_m e^{i(2\delta_m+m\theta)} \approx e^{i(2\delta_{m_0}+m_0\theta)} \times \int dm\, e^{i\frac{d^2\delta}{dm^2}\Big|_0 (m-m_0)^2}. \tag{3.4.46}$$

Here $m_0$ is the stationary point, which solves the saddle point equation:

$$\left.\frac{d\delta_m}{dm}\right|_{m_0} - \frac{\theta}{2} = 0. \tag{3.4.47}$$

Derivation of this equation, once more, provides a relation between the second derivative of the phase shift $\delta_m$ and the the angle $\theta$

$$\frac{d^2\delta_m}{dm^2} - \frac{1}{2}\frac{d\theta}{dm} = 0. \tag{3.4.48}$$

An analytical continuation in the complex $m$ plane allows us to make the integral converge. Gaussian integration in Eq.(3.4.46) implies that

$$\left|\sum_m f_m(\theta)\right|^2 \approx \pi \left|\frac{dm}{d\theta}\right| , \tag{3.4.49}$$

thus yielding the expected result:

$$\begin{aligned} \frac{1}{\tau} &\sim \frac{v_F}{k}\frac{1}{A}\int d\theta(1-\cos\theta)\left|\frac{dm}{d\theta}\right| \\ &\sim \frac{v_F}{k}\frac{1}{A}\int dm\,\frac{\theta^2}{2} \sim \frac{v_F}{A}\int db\,\theta^2(b)\,. \end{aligned} \tag{3.4.50}$$

In the last equality the conservation of the angular momentum $m = kb$ has been exploited, together with the remark that the scattering angle only depends on $b$ in the classical diffusion. This reproduces the desired high energy behavior.

The analysis of Eq.(3.3.40) provides a similar conclusion. The quantity $\delta_{m+1} - \delta_{m-1}$, appearing as the argument of the cosine, is $\approx 2\ d\delta_m/dm$. At large incoming energies, $\delta_m \approx (2m+1)\pi/2$, which is consistent with the asymptotic form of the wavefunction given in Eq.(3.3). To lowest order we get, according to Eq.(3.4.47),

$$\sin^2\delta_m - \cos\left(\delta_{m+1} - \delta_{m-1}\right)\sin\delta_{m+1}\sin\delta_{m-1} \approx \frac{\theta^2}{2}\,, \tag{3.4.51}$$

so that we recover again

$$\frac{1}{\tau} \approx \frac{v_F}{kA}\int dm\,\frac{\theta^2}{2} \approx \frac{v_F}{A}\int db\,\theta(b)^2\,. \tag{3.4.52}$$

## 3.5 Conclusions

We have shown in Section II how the two dimensional Dirac equation in curved space emerges at the simplest boundary with non trivial metric, the surface of a sphere. The metric enters through the spin connection, which reflects the properties of the internal spin under parallel transport along the

surface[100]. The spin connection reflects a quantum feature of the electrons, and cannot be inferred from solely classical arguments. The spin connection leads to a finite Berry phase when the electron is transported around a closed geodesic. A manifestation of this effect is the quantization of the total angular momentum in half integer units.

The model that we have studied leads to simple analytical expressions of the energies and wavefunctions of the boundary states. They can be used as a zeroth approximation to situations close to spherical symmetry, or where an isotropic electronic structure can be obtained by rescaling a length. We find that the corrections to the two dimensional Dirac equation depend exponentially on $R/\Lambda \equiv R\Delta/\hbar v_F$[1].

The model describes external surfaces of mesoscopic crystals and internal voids in bulk systems. In the case of a small void, we find that two doublets at a finite distance of the Dirac energy appear for radii $R \gtrsim 2/\Lambda$. These voids will act as molecules embedded into the bulk material. The interaction energy of electrons localized inside the voids scales as the level separation, $E_{int} \approx e^2/(\epsilon R)$, where $\epsilon$ is the dielectric constant of the topological insulator. At temperatures below this scale, voids with an odd number of electrons will give rise to magnetic moments. The RKKY interaction between moments at different vacancies should decay exponentially, $J_{RKKY}(\vec{\mathbf{r}} - \vec{\mathbf{r}}') \sim e^{-|\vec{\mathbf{r}}-\vec{\mathbf{r}}'|/\Lambda}$. Hence, small vacancies might give rise to a paramagnetic susceptibility in topological insulators. If they are within a distance $d \sim \Lambda$ from the surface, these local moments will hybridize with the surface states, leading to the Kondo effect[34; 65].

We have analyzed the scattering of Dirac fermions by surface corrugations which induce a non trivial curvature in the quantum limit, $k_F\ell \lesssim 1$. We find that the resistivity due to a finite concentration of bumps, $n_b$, vanishes as $k_F^2$ for small $k_F$, due to a combination of a density of states factor, which goes as $k_F$, and a scattering time which increases as $k_F^{-3}$. By comparison, the scattering time in the classical regime[24] ($k_F\ell \to \infty$) is independent of $k_F$, and $\rho \sim k_F^{-1}$. The wave nature of the quasiparticles allow them to diffract around the bump, making it effectively transparent for long wavelengths, $k_F\ell \ll 1$. The non trivial curvature induces quantum reseonances for $k_F\ell \sim 1$ and an aspect ratio $h/\ell \gtrsim 0.2$.

# Chapter 4

# Electron-Phonon Interaction at the surface of a Topological Insulator

In this Chapter the interaction of surface states with Rayleigh phonons, i.e. surface phonons, for $Bi_2Te_3$ is treated by means of perturbation theory. Starting from the expression of the electron polarizator for a 2D Dirac gas [140], screening effects are treated in RPA approximation. The phonon dumping and the correction to frequency of surface phonons is calculated and the comparison with a non relativistic 2DEG is done. An analysis of surface plasmons and possible superconductive instability is done in the conclusion of the chapter. It is found that for physical values of the Fermi momentum such an instability can occurr, but the critical temperature is too small to be experimentally relevant.

## 4.1 Stress through minimal coupling

We will study the electron-phonon interaction on the surface of a 3D topological insulators with a single Dirac cone at the $\Gamma$ point. Low energy effective theory of electrons are described in $\boldsymbol{k} \cdot \boldsymbol{p}$ approximation using symmetries of the lattice [146; 58; 114]. A linearized version of this model, suitable for calculations, is the massive Dirac equation in 3+1 dimensions [107]

$$\mathcal{H}_0 = \hat{\gamma}^0 \Delta + \hbar v_F \hat{\gamma}^i k_i \tag{4.1.1}$$

where $v_F$ is the Fermi velocity and the matrices $\hat{\gamma}^a$ are given in terms of Pauli matrices by $\hat{\gamma}^0 = \mathbb{I}_{2\times 2} \otimes \tau_z$, $\hat{\gamma}^1 = \sigma_x \otimes \tau_x$, $\hat{\gamma}^2 = -\sigma_y \otimes \tau_x$ $\hat{\gamma}^3 = \sigma_z \otimes \tau_x$. Here $\sigma_a$ and $\tau_b$ denote matrices in the spin and even-odd orbital parity spaces,

respectively. The Hamiltonian (4.1.1) can describe both a 3D topological insulator, provided that the mass has a domain wall singularity where it changes sign, and also topological nodal semimetals[14]. The electron-phonon interaction is a linear combination of the components of the strain tensor, through generic $4 \times 4$ matrices $A_{ij}$, to be determined so that the interaction is compatible with the symmetries of the system as discussed in 4.2

$$\mathcal{H}_{el-ph} = A_{ij}\partial_i U_j \tag{4.1.2}$$

where $\boldsymbol{U}$ is the displacement field operator, to be determined through the equations of elasticity. The high symmetry of the $\Gamma$ point implies that the only possible coupling to the strain tensor is through the identity matrix (see appendix 4.2), i.e. $\mathcal{H}_{el-ph} = \mathbb{I}_{4\times4}\partial_i U_i$. At zero energy the quantum state is doubly degenerate, and the projection of the bulk Hamiltonian (4.1.1) on this subspace is the Hamiltonian for surface states

$$\mathcal{H} = \mathcal{H}_0 + \mathcal{H}_{el-ph} \tag{4.1.3}$$

where $\mathcal{H}_0 = -i\hbar v_F \boldsymbol{\sigma} \cdot \nabla$ is the free Hamiltonian in 2+1 dimensions, and $\mathcal{H}_{el-ph} = \mathbb{I}_{2\times2}\Lambda(q)\partial_i U_i$ where $q$ is the modulus of the phonon momentum. The constant $\Lambda(q)$ comes from the matrix element of the operator $\mathcal{H}_{el-ph}$ between the zero energy states

$$\Lambda(q) = \int_0^\infty dz e^{-2\Delta z}\phi_q(z) \tag{4.1.4}$$

here $\phi_q(z)$ takes into account the behavior of phonons in the direction orthogonal to the surface, and thus will be determined once the Rayleigh modes are analyzed. In second quantization[121; 40]

$$\mathcal{H}_{el-ph}(q,\omega) = \alpha\Lambda \sum_{\boldsymbol{q},\Lambda,\omega} \langle \mathbf{k}+\mathbf{q}|\nabla\cdot\boldsymbol{U}|\mathbf{k}\rangle\, c^\dagger_{\mathbf{k}+\mathbf{q}} c_{\mathbf{k}} + h.c. \tag{4.1.5}$$

here $\alpha = 35eV$ is a constant characterizing the electron-phonon interaction[40; 61], and $|\boldsymbol{k}, s\rangle$ is the surface state

$$|\boldsymbol{k}, s\rangle = \frac{1}{\sqrt{2}}\begin{pmatrix} 1 \\ se^{i\theta_k}\end{pmatrix} e^{i\boldsymbol{k}\cdot\boldsymbol{r}} \tag{4.1.6}$$

The displacement field operator is

$$\boldsymbol{U}(\boldsymbol{r},t) = \sqrt{\frac{\hbar}{2\rho_M\omega}} \sum_i \boldsymbol{u}_i(\boldsymbol{r}) b_i e^{-i\omega_i t} + h.c. \tag{4.1.7}$$

Here $\boldsymbol{u}_i(\boldsymbol{r})$ is the displacement vector and $i$ indicates the type of phonons: longitudinal, transverse or Rayileigh mode. In the following I will analyze the contribution of this last type of phonons, so this index will not appear anymore. The displacement field operator has dimensions of a length $[\boldsymbol{U}] = [L]$, thus the displacement vector $\boldsymbol{u}$ has the dimensions $[L]^{-3/2}$.

## 4.2 Symmetry Analysis in the Continuum limit

The electron-phonon interaction (4.1.2) is built contracting the strain tensor

$$u_{ij} = \frac{1}{2}(\partial_i u_j + \partial_j u_i)$$

with a $4 \times 4$ matrix $A_{ij}$. TI with surface states close to the $\Gamma$ point and graphene [88] are two remarkable examples where this approach is helpful. Indeed, the symmetry groups constraining the shape of $\mathcal{H}_{el-ph}$ are the little groups [86] preserving the wave vector of the electrons and phonons. Long-wavelength phonons have momenta close to the $\Gamma$ point and thus the little group for a generic $q$ is the space group of the crystal. Symmetries of the lattice then can simplify the shape of the dynamical matrix, but since electrons lying close to the Fermi level, on the other side, have usually a trivial little group it is not possible in general to simplify the electron-phonon interaction following the same principle. In the case treated in this chapter the Dirac cone is at the $\Gamma$ point and in the long wavelength limit the little group for surface states coincides with the space group of the lattice, as for the phonons. In the case of $Bi_2Se_3$ the space group $G = \{C_6, \mathcal{I}, \mathcal{T}\}$ has been described in (1.6.5). Starting from the Dirac matrices in the Hamiltonian (4.1.1)

$$\begin{aligned} \alpha_0 &= i\mathbb{I} \otimes \tau_z \\ \alpha_i &= \sigma_i \otimes \tau_x \end{aligned} \tag{4.2.8}$$

it's possible to write a basis in the whole space of $4 \times 4$ matrices. In the following combinations of these matrices will be studied so that they preserve all the operations of $G$. The matrix $\alpha_5$ is

$$\alpha_5 = i\alpha_0\alpha_1\alpha_2\alpha_3 = -\mathbb{I} \otimes \tau_y \tag{4.2.9}$$

The 4 matrices $\alpha_\mu\alpha_5$ are then

$$\begin{aligned} \alpha_0\alpha_5 &= \mathbb{I} \otimes \tau_x \\ \alpha_i\alpha_5 &= -i\sigma_i \otimes \tau_z \end{aligned} \tag{4.2.10}$$

The 6 matrices $\Sigma_{\mu\nu} = i/2[\alpha_\mu, \alpha_\nu]$ are (in the following $i < j$)

$$\begin{aligned} \Sigma_{0i} &= -i\sigma_i \otimes \tau_y \\ \Sigma_{ij} &= \epsilon_{ijk}\sigma_k \otimes \mathbb{I} \end{aligned} \tag{4.2.11}$$

These 15 matrices, plus the identity matrix, make a basis in the space of $4 \times 4$ matrices $\{\Gamma_i\}$ explicitly written in table 4.1. Note that immaginary units have been added to make all the matrices hermitian, for calculation convenience. It is possible to show that the only matrices built from this set

| | Matrix | $C_n$ | $\mathcal{T}$ |
|---|---|---|---|
| $\Gamma_1$ | $\mathbb{I}$ | Y | Y |
| $\Gamma_2$ | $i\gamma_0$ | Y | Y |
| $\Gamma_3$ | $\gamma_1$ | | |
| $\Gamma_4$ | $\gamma_2$ | | |
| $\Gamma_5$ | $\gamma_3$ | Y | |
| $\Gamma_6$ | $\gamma_5$ | Y | |
| $\Gamma_7$ | $\gamma_0\gamma_5$ | Y | Y |
| $\Gamma_8$ | $i\gamma_1\gamma_5$ | | |
| $\Gamma_9$ | $i\gamma_2\gamma_5$ | | |
| $\Gamma_{10}$ | $i\gamma_3\gamma_5$ | Y | |
| $\Gamma_{11}$ | $i\Sigma_{01}$ | | Y |
| $\Gamma_{12}$ | $i\Sigma_{02}$ | | Y |
| $\Gamma_{13}$ | $i\Sigma_{03}$ | Y | Y |
| $\Gamma_{14}$ | $\Sigma_{12}$ | Y | |
| $\Gamma_{15}$ | $\Sigma_{13}$ | | |
| $\Gamma_{16}$ | $\Sigma_{23}$ | | |

**Table 4.1:** Basis in the space of $4 \times 4$ matrices

that are hermitian and that do not break time reversal are only the following 4

$$\alpha_0\alpha_5, \quad i\Sigma_{0i}. \tag{4.2.12}$$

The most general constant perturbation, i.e. not depending on phonon and electron momenta that preserves time reversal, must be a linear combination of these 4 matrices. From table 4.1 it is possible to extract 4 vectors
From those 4 vectors it is possible to write 7 bilinears that are second rank

| | TR | I |
|---|---|---|
| $\boldsymbol{a} = (\gamma_1, \gamma_2, \gamma_3)$ | -1 | -1 |
| $\boldsymbol{b} = (\Sigma_{23}, \Sigma_{31}, \Sigma_{12})$ | -1 | +1 |
| $\boldsymbol{p} = (i\Sigma_{01}, i\Sigma_{02}, i\Sigma_{03})$ | +1 | -1 |
| $\boldsymbol{b}' = (i\gamma_1\gamma_5, i\gamma_2\gamma_5, i\gamma_3\gamma_5)$ | -1 | +1 |

tensors respecting time reversal

$$\begin{aligned} \boldsymbol{a}^2 &= a_i a_j \\ \boldsymbol{b}^2 &= b_i b_j \\ \boldsymbol{b}'^2 &= b'_i b'_j \\ \boldsymbol{p}^2 &= p_i p_j \\ \boldsymbol{a} \otimes \boldsymbol{b} &= a_i b_j \\ \boldsymbol{b} \otimes \boldsymbol{b}' &= b_i b'_j \\ \boldsymbol{a} \otimes \boldsymbol{b}' &= a_i b'_j \end{aligned} \tag{4.2.13}$$

of those the terms $\boldsymbol{a} \otimes \boldsymbol{b}$ and $\boldsymbol{a} \otimes \boldsymbol{b}'$ break inversion symmetry, so five bilinears remain

$$\begin{aligned} \boldsymbol{a}^2 &= a_i a_j \\ \boldsymbol{b}^2 &= b_i b_j \\ \boldsymbol{b}'^2 &= b'_i b'_j \\ \boldsymbol{p}^2 &= p_i p_j \\ \boldsymbol{b} \otimes \boldsymbol{b}' &= b_i b'_j \end{aligned} \tag{4.2.14}$$

The four squares are all the same, since

$$\begin{aligned} \Sigma_{\mu\nu}\Sigma_{\mu\eta} &= \gamma_\nu \gamma_\eta \\ (i\gamma_\mu\gamma_5)(i\gamma_\nu\gamma_5) &= \gamma_\mu\gamma_\nu \end{aligned} \tag{4.2.15}$$

so we are left only with two independent bilinears

$$\begin{aligned} \boldsymbol{a}^2 &= a_i a_j \\ \boldsymbol{b} \otimes \boldsymbol{b}' &= b_i b'_j \end{aligned} \tag{4.2.16}$$

Explicitly the components of these two tensors are

$$\begin{aligned} a_i a_j &= (\sigma_i \otimes \tau_x)(\sigma_j \otimes \tau_x) = \delta_{ij}\mathbb{I} \otimes \mathbb{I} + i\epsilon_{ijk}\sigma_k \otimes \mathbb{I} \\ b_i b'_j &= (\sigma_i \otimes \mathbb{I})(\sigma_j \otimes \tau_z) = \delta_{ij}\mathbb{I} \otimes \tau_z + i\epsilon_{ijk}\sigma_k \otimes \tau_z \end{aligned} \tag{4.2.17}$$

These tensors are made up of two pieces: the trace, that is respectively the identity matrix and the matrix for the mass term $i\gamma_0$, plus an antisymmetric-antihermitian part. Thus the strain tensor in the fully isotropical model will couple only to the traces of these two tensors. The coupling to the mass term could be neglected since it only provides corrections to the localization lengths of the boundary states.

## 4.3 Surface waves

The displacement vector in (4.1.7) in general is

$$\boldsymbol{u}(\boldsymbol{r}) = \boldsymbol{u}(z)\frac{e^{i(q\cdot r-\omega t)}}{\sqrt{\mathcal{A}}} \tag{4.3.18}$$

where $\mathcal{A}$ is the area of the sample. In the case of Rayleigh modes it can be shown that the displacement vector is in the plane though the direction of propagation perpendicular to the surface. Thus the index $t$ is really a part of the displacement vector that takes into account the out of plane part of the displacement. Note that only the longitudinal part of the Rayleigh wave enters into the definition of the electron-phonon coupling. This could be explained, considering that the longitudinal and transverse part of the wave could be written in term of a 4-potential $(\phi_l, \boldsymbol{\chi})$ as

$$\begin{aligned} \mathbf{u}_L(\mathbf{r}) &= \nabla\phi_l \\ \mathbf{u}_T(\mathbf{r}) &= \nabla\times\boldsymbol{\chi} \end{aligned} \tag{4.3.19}$$

Since the electtron-phonon coupling is proportional to the divergenge of $\mathbf{u} = \mathbf{u}_L + \mathbf{u}_T$, then it is clear that only $\mathbf{u}_L$ contributes to the coupling. In order to have a mode polarized in the plane identified but the normal to the plane and the direction of the motion, the transverse part is $\boldsymbol{\chi} = \hat{e}_t\phi_t$ (where $\hat{e}_t \perp \hat{e}_q$ & $\hat{e}_t \perp \hat{e}_z$). The vector $\boldsymbol{u}(z)$, expressed through two scalar fields $\phi_l(z)$ and $\phi_t(z)$, then is [60]

$$\boldsymbol{u}(z) = \left(iq\phi_l - \frac{d\phi_t}{dz}\right)\hat{e}_q + \left(\frac{d\phi_l}{dz} + iq\phi_t\right)\hat{e}_z \tag{4.3.20}$$

where the functions $\phi_{l,t}$ are

$$\phi_{l,t} = a_{l,t}e^{-iq_{l,t}z} + b_{l,t}e^{iq_{l,t}z}. \tag{4.3.21}$$

Here the dispersion relation is

$$q_{l,t} = \sqrt{\frac{\omega^2}{c_{l,t}^2} - q^2}. \tag{4.3.22}$$

The Rayleigh mode has a linear dispersion relation $\omega = c_R q$, with the velocity related to the transverse phonon velocity through a dimensionless constant $\xi < 1$ determined through the equation of elasticity $c_R = \xi c_t$. With these definitions the decay lengths for the longitudinal and the transverse modes could be defined in function of the phonon momentum $k$ as $q_{l,t} = i\lambda_{l,t} q$, where two dimensionless parameters have been introduced

$$\lambda_t = \sqrt{1-\xi^2}, \quad \lambda_l = \sqrt{1-\gamma_0^2\xi^2}. \tag{4.3.23}$$

Here $\gamma_0 = c_t/c_l$. With this choice the coefficients $a_{l,t} = 0$, and the only coefficients $b_{l,t}$ remain to be computed using the equation of propagation of elastic waves, as done in Landau Lifshitz. The solutions for the longitudinal and the transversal part are

$$\phi_l = \sqrt{\frac{C}{q}} e^{-\lambda_l q z}, \quad \phi_t = \sqrt{\frac{C}{q}} e^{-\lambda_t q z}. \tag{4.3.24}$$

$$\partial_i u_i = -\sqrt{\frac{C}{q}} q^2 (1-\lambda_l^2) e^{-\lambda_l q z} \tag{4.3.25}$$

The coefficient $C$ is

$$\frac{1}{C} = \lambda_l - \lambda_t + \frac{(\lambda_l - \lambda_t)^2}{2\lambda_l^2 \lambda_t} \tag{4.3.26}$$

Note that the matrix element between the potential (4.1.5) and the exponentially decaying electronic modes involves the gap too, since the matrix element is proportional to the integral ($\hbar = v_F = 1$), determining the constant $\Lambda$

$$\Lambda = 2\Delta \int_0^\infty dz e^{-2\Delta z - \lambda_{l,t} q z} = \frac{2\Delta}{2\Delta + \lambda_{l,t}|q|} \tag{4.3.27}$$

With this last observation the electron phonon coupling could written finally as

$$\nabla \cdot \boldsymbol{u} = -\sqrt{\frac{C}{q}} q^2 (1-\lambda_l^2) \frac{2\Delta}{2\Delta + \lambda_l |q|} \tag{4.3.28}$$

The values of the dimensionless constants are $\lambda_l = 0.85$ and $\lambda_t = 0.39$, and are fixed by the values of the velocities for longitudinal and transverse modes. Considering the definition of $\lambda_l$ then the above expression becomes

$$\mathcal{H}_{el-ph}(q,\omega) = \frac{\alpha}{\sqrt{\mathcal{A}}} \sqrt{\frac{C}{q}} \left( \frac{\omega_q^{(0)}}{c_l} \right)^2 \sqrt{\frac{\hbar}{2\rho_M \omega}} \Lambda(q) \sum_{\mathbf{k}} c^\dagger_{\mathbf{k}+\mathbf{q}} c_{\mathbf{k}} + h.c. \tag{4.3.29}$$

The constant $\alpha$ has the dimension of an energy, and it is introduced in [62], the factor $1/\sqrt{\mathcal{A}}$ comes from equation (4.3.18) and $\omega_q^{(0)} = c_R q$ is the dispersion for Rayleigh phonons with $c_R = \xi c_t$ being their velocity.

## 4.4 Electron polarizator

In the following the effects of the electron-phonon interaction on the phonon spectrum is considered. The central object to calculate the correction to the dispersion relation of phonons and their scattering is the polarization $P(k,\nu_n)$, whose expression at finite temperature is

$$P(q,\nu_n) = -2\int \frac{d^2k}{(2\pi)^2}\frac{n^0_{k+q}-n^0_k}{i\hbar\nu_n-(\epsilon_{k+q}-\epsilon_k)}\left[1-ss'\frac{k+q\sin\phi}{|\boldsymbol{k}+\boldsymbol{q}|}\right] \tag{4.4.30}$$

At zero temperature the polarization is written as a $P_0$ term, having $\mu=0$, and a term $\Delta P$ depending on the chemical potential [140]

$$P(k,\omega) = P_0 + \Delta P. \tag{4.4.31}$$

Introducing the density of states at the Fermi level

$$N_F = \frac{k_F}{2\pi\hbar v_F} \tag{4.4.32}$$

and the dimensionless variables $\tilde{\omega}=\omega/2v_Fk_F$, $\tilde{q}=q/2k_F$, the two terms in (4.4.31) can be written as

$$P_0 = -i\pi\frac{1}{16\pi\hbar}\frac{q^2}{\sqrt{\omega^2-v_F^2q^2}} = -i\frac{\pi}{4}N_F\frac{\tilde{q}^2}{\sqrt{\tilde{\omega}^2-\tilde{q}^2}} \tag{4.4.33}$$

and the term depending on the finite chemical ponential is

$$\begin{aligned}\Delta P = -N_F\Big\{1-\frac{1}{4}\frac{\tilde{q}^2}{\sqrt{\tilde{\omega}^2-\tilde{q}^2}}\times \\ \times\Big\{G\left(\frac{\tilde{\omega}+1}{\tilde{q}}\right)-\Theta\left(\frac{1-\tilde{\omega}}{\tilde{q}}-1\right)\left[G\left(\frac{1-\tilde{\omega}}{\tilde{q}}\right)-i\pi\right]+ \\ -\Theta\left(\frac{\tilde{\omega}-1}{\tilde{q}}-1\right)G\left(\frac{\tilde{\omega}-1}{\tilde{q}}\right)\Big\}\Big\}\end{aligned} \tag{4.4.34}$$

Here the function $G(x)$ is

$$G(x) = x\sqrt{x^2-1}-\ln(x+\sqrt{x^2-1}) \tag{4.4.35}$$

Note that in the static limit the polarization has no imaginary part. A better estimation of the phonon dump could be obtained through the imaginary part of the polarization in the RPA approximation

$$P_{RPA} = \frac{P(q,\omega)}{1-v_qP(q,\omega)} \tag{4.4.36}$$

where $v_q = e^2/\epsilon_0 q$ is the 2D Coulomb interaction. In the limit $\omega \to 0$ at the lowest non null order in $\omega$ the real and the imaginary part of the polarization are

$$\begin{aligned} ReP(q,\omega) &= -N_F \\ ImP(q,\omega) &= N_F \tilde{\omega}\sqrt{\frac{1}{\tilde{q}^2}-1} \end{aligned} \tag{4.4.37}$$

In the RPA approximation the imaginary part of the polarization then reads

$$Im(P_{RPA}) = \frac{Im[P(q,\omega)]}{(1-v_q Re[P(q,\omega)])^2 + Im[P(q,\omega)]^2} \tag{4.4.38}$$

where it has been assumed $k < 2k_F$. Thus in the limit $\omega \to 0$ with $q \ll 2k_F$ the imaginary part of polarization then is, considering that the limit $\hbar\omega \ll \hbar v_F q \ll \mu$ is considered

$$\mathrm{Im}[P_{RPA}](q,\omega) = \begin{cases} \frac{4\pi N_F}{\alpha_{FS}}\tilde{\omega}\tilde{q} \text{ for } q < \frac{\alpha_{FS}k_F}{2\pi} \\ \\ Im[P(q,\omega)] \text{ for } q > \frac{\alpha_{FS}k_F}{2\pi} \end{cases} \tag{4.4.39}$$

Here the effective fine structure constant $\alpha_{FS}$ has been introduced

$$\alpha_{FS} = \frac{e^2}{\epsilon_0 \hbar v_F} = 0.1. \tag{4.4.40}$$

In contrast with electrodynamics, in the definition of $\alpha_{FS}$ the Fermi velocity appears, and no the light velocity, and a reasonable estimation of the dielectric constant $\epsilon_0 \approx 50$ [133; 43]. This explains the difference in the order of magnitude of the two constants. The phonons decay rate $\Gamma_q$ is obtained multiplying the imaginary part of the polarization for the square of the matrix element of the electron- phonon interaction in (4.3.29) and multiplying per $\mathcal{A}$. In the limit $k \ll p_F$ thus the decay rate is obtained using (4.4.39)

$$\Gamma_q = \begin{cases} \frac{\alpha^2 C}{4\alpha_{FS}^2 \rho_M c_l^2}\frac{(\omega_q^{(0)})^4}{v_F^2 c_l^2 k_F}\Lambda(q)^2 \text{ for } q < \frac{\alpha_{FS}k_F}{2\pi}, \\ \\ \frac{1}{16}\frac{\mu}{\hbar^2 v_F^2}\frac{2\hbar\alpha^2 C c_R^2}{\rho_M c_l^4 v_F}(\omega_q^{(0)})^2\Lambda(q)^2 \text{ for } q > \frac{\alpha_{FS}k_F}{2\pi} \end{cases} \tag{4.4.41}$$

These linewidths vanish as $q \to 0$, so that the Rayleigh phonons are well defined at small wave vectors. The quality factor, measuring the broadening of the phonon energy, turns out to be

$$Q = \frac{\hbar\omega_q}{\Gamma_q} = \begin{cases} \frac{\alpha_{FS}^2}{\pi\gamma K(k_F)}\left(\frac{2k_F}{q}\right)^3\frac{1}{\Lambda^2(q)} \text{ for } q < \frac{\alpha_{FS}k_F}{2\pi}, \\ \\ 16\frac{\hbar v_F}{k_F}\frac{\rho_M c_l^4 v_F}{2\alpha^2 C c_R^3}\frac{1}{q}\frac{1}{\Lambda^2(q)} \text{ for } q > \frac{\alpha_{FS}k_F}{2\pi} \end{cases} \tag{4.4.42}$$

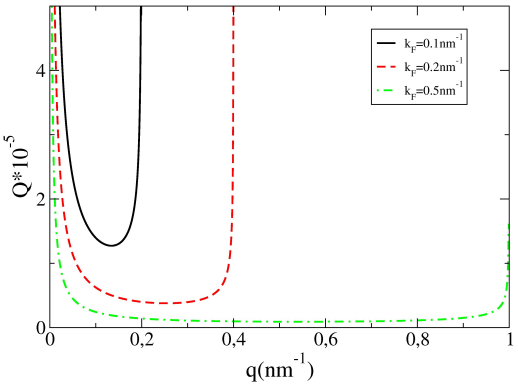


**Figure 4.1:** Quality factor $Q$ as a function of momentum $k$ for different values of the Fermi wave vector: in black $k_F = 0.1$ nm$^{-1}$, in dashed red $k_F = 0.2$ nm$^{-1}$, in dashed dotted green $k_F = 0.5$ nm$^{-1}$.

where $\gamma = c_R/v_F \approx 3 \times 10^{-3}$. Here the dimensionless quantity $K(k_F)$ has been introduced

$$K(k_F) = \frac{2\alpha^2 C \xi^2 c_t^2 k_F^2}{\hbar \rho_M c_l^4 \pi v_F} = 2.35 \text{ nm}^2 k_F^2 \tag{4.4.43}$$

The value of the constants used in the above equation for $Bi_2Te_3$ are[40]: $\alpha = 35eV$, $\rho_M = 7860Kg/m^3$, $p_F \approx 10^2$ nm$^{-1}$, $C = 1.20$, $c_l = 2800m/s$, $c_t = 1600m/s$, $v_F = 4.36 \times 10^5 m/s$ and $\xi = 0.89$. The quality factor then depends on the third power of $q$, through the constant $K(k_F)$ and the ratio $\gamma = \xi c_t/v_F \approx 3 \times 10^{-3}$ between $\xi c_t$, i.e. the velocity of Rayleigh waves, and the Fermi velocity $v_F$.

### 4.4.1 Static limit and renormalization of Rayleigh phonons frequency

In order to see effects originated from the Fermi surface such as Kohn anomaly a different limit should be analyzed, i.e. considering a finite wave vector in contrast with what done in the previous calculation. The real part of polarization in the static limit $\omega \to 0$ is

$$P(q,0) = -\frac{k_F}{2\pi\hbar v_F} + \Theta(q-2k_F)\frac{q}{8\pi\hbar v_F} G_< \left(\frac{2k_F}{q}\right) \tag{4.4.44}$$

where in this case it has not been performed the approximation $k \ll 2p_F$. In the RPA approximation the polarization in the static limit is

$$P_{RPA}(k,0) = \frac{P(q,0)}{1 - v_q P(q,0)} = -\frac{4k_F - k\Theta(q-2k_F)G_<\left(\frac{2k_F}{q}\right)}{8\hbar v_F + \frac{e^2}{2\kappa_0 q}\left\{4k_F - q\Theta(q-2k_F)G_<\left(\frac{2k_F}{q}\right)\right\}} \tag{4.4.45}$$

Thus Khon anomaly shows up in the quality factor as a change of its depen-

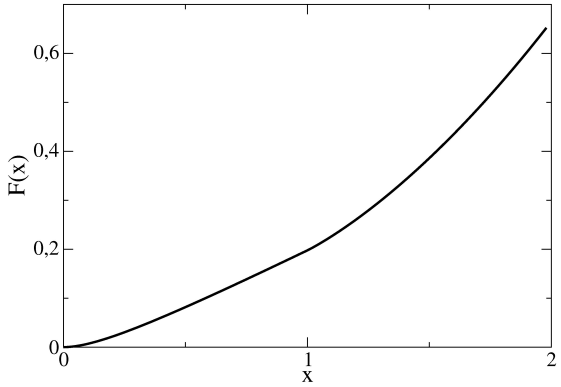


**Figure 4.2:** Plot of the function $F(x)$.

dence on the phonon momentum. The correction to the phonon frequency, $\Delta\omega_q = -|M(q)|^2 P(q,0)/\hbar$, is

$$\Delta\omega_q = -\omega_q^{(0)}\, K(k_F)\, \Lambda^2(q)\, F\left(\frac{q}{2k_F}\right). \tag{4.4.46}$$

The function $F(x)$ is

$$F(x) = x^2 \frac{\frac{2}{x} - \Theta(x-1)G_<\left(\frac{1}{x}\right)}{8 + 2\alpha_{FS}\left\{\frac{2}{x} - \Theta(x-1)G_<\left(\frac{1}{x}\right)\right\}} \tag{4.4.47}$$

and it is plotted in fig. 4.2. The function $F(x)$ goes like $x/4$ for $(\alpha_{FS}/4) < x < 1$ and it has the following limit for $x > 1$

$$F(x) \approx x^2 \frac{\pi}{16 + 2\alpha_{FS}\pi} \tag{4.4.48}$$

The correction to the phonon frequencies

$$\omega = \omega_q^{(0)}\left[1 - K(k_F)\Lambda^2(q)F(\tilde{q})\right] \tag{4.4.49}$$

is plotted in fig. 4.3(a). In narrow gap TIs, the decay of the electronic surface

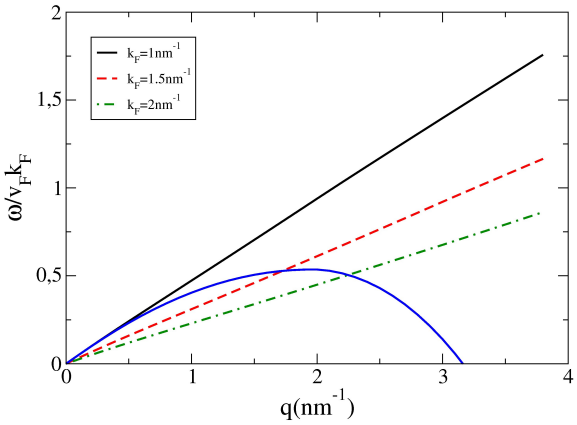


(a)

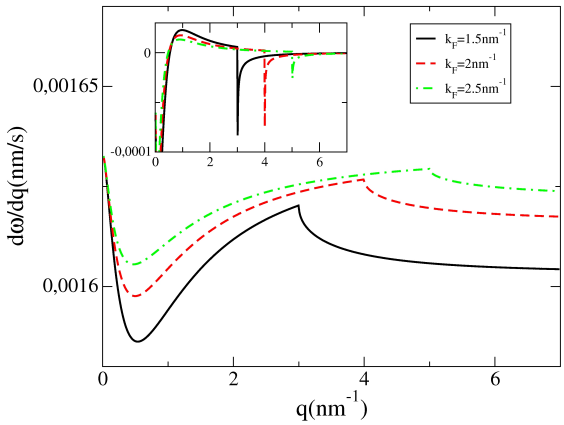


(b)

**Figure 4.3:** a)The dispersion relation eq.(4.4.49) as a function of wave vector $k$. The blue curve shows the phonon dispersion relation for $\Lambda(q) \approx 1$. b) Derivative of the dispersion relation .(4.4.49) showing a singularity in the second derivative.

states could be comparable to the decay of the Rayleigh modes, leading to $\Lambda(q) \approx 1$. In that case, the softening of the modes shown in Fig. 4.3(a) suggests a lattice instability at some finite wavevector, $q_c$. Nte that, for $q_c \approx k_F$ a scalar potential can strongly reduce the density of states at the Fermi energy, due to the formation of scalar potential superlattice (see refs. [108; 48; 144] for similar effects in graphene). The density of states determines the electronic polarizability. The reduction of the polarizability implies that the renormalization of the Rayleigh modes will be arrested. Hence we expect that in narrow gap TIs, the Rayleigh waves at momenta comparable to $k_F$

will be unstable, leading to the formation of a superlattice, and to a strong reduction of the density of states of surface electronic modes at the Fermi level. This effect should be measurable by STM experiments [144], and it will also modify the electronic transport properties.

## 4.5 Comparison with 2DEG

The real and imaginary part of the polarization $P(q,\omega)$ for a 2DEG are

$$\begin{aligned} Re[P(q,\omega)] &= -N_F\left[1+\frac{k_F}{q}\left(\text{sign}(\nu_-)\Theta(\nu_-^2-1)\sqrt{\nu_-^2-1}-\text{sign}(\nu_+)\Theta(\nu_+^2-1)\sqrt{\nu_+^2-1}\right)\right] \\ Im[P(q,\omega)] &= -N_F\frac{k_F}{q}\left[\Theta(1-\nu_-^2)\sqrt{1-\nu_-^2}-\Theta(1-\nu_+^2)\sqrt{1-\nu_+^2}\right] \end{aligned} \tag{4.5.50}$$

here the density of states at the Fermi level

$$N_F = \frac{m}{2\pi\hbar^2} = \frac{k_F}{2\pi\hbar v_F},\quad v_F = \frac{\hbar k_F}{m} \tag{4.5.51}$$

and the frequency dependent quantities $\nu_\pm$ are

$$\nu_\pm = \frac{\omega}{qv_F} \pm \frac{q}{2k_F}. \tag{4.5.52}$$

In the static limit $\omega \to 0$ the $\nu_\pm$ are both equal to $q = q/2k_F$, thus the imaginary part vanishes and the real part becomes

$$Re[P(q,0)] = -N_F\left[1-\frac{2k_F}{q}\Theta(q^2-4k_F^2)\sqrt{\left(\frac{q}{2k_F}\right)^2-1}\right] \tag{4.5.53}$$

The static polarization for the 2DEG is continuous at $2k_F$, as shown on fig. (4.4(a)), but its first derivative is not as shown in fig. (4.4(b)). The right limit of the derivative of the static polarization goes like

$$\lim_{q\to 2k_F^+}\frac{dP[q,0]}{dq} \propto \frac{1}{\sqrt{q^2-4k_F^2}} \tag{4.5.54}$$

In RPA approximation the static polarization (4.5.53) becomes

$$P_{RPA}[q,0] = \frac{P[q,0]}{1-v_qP[q,0]} = -N_F\frac{1}{\tilde{q}}\frac{\tilde{q}-\Theta(\tilde{q}^2-1)\sqrt{\tilde{q}^2-1}}{1+\frac{\alpha_{FS}}{\tilde{q}}\frac{1}{\tilde{q}}[\tilde{q}-\Theta(\tilde{q}^2-1)\sqrt{\tilde{q}^2-1}]}, \tag{4.5.55}$$

where as in the draft $\tilde{q} = q/2k_F$. The screening of Rayleigh phonons due to el-ph interaction has the same shape as for surface states of TI

$$\omega(q) = \omega^{(0)}(q)\left[1 - \frac{K(k_F)}{4}\Lambda(q)^2 F\left(\frac{q}{2k_F}\right)\right] \tag{4.5.56}$$

where $K(k_F) = 2.35\text{nm}\ k_F^2$ and $\Lambda(q)$ is the structure factor, both supposed to be valid for the 2DEG too. The explicit form of the function $F(x)$ is the only difference between the two cases

$$F(x) = \frac{x - \Theta(x^2-1)\sqrt{x^2-1}}{1 + \frac{\alpha_{FS}}{x^2}[x - \Theta(x^2-1)\sqrt{x^2-1}]} \tag{4.5.57}$$

The discontinuity in the first derivative of the polarization reflects in a discontinuity of the first derivative of the frequency as shown in fig. (4.5)

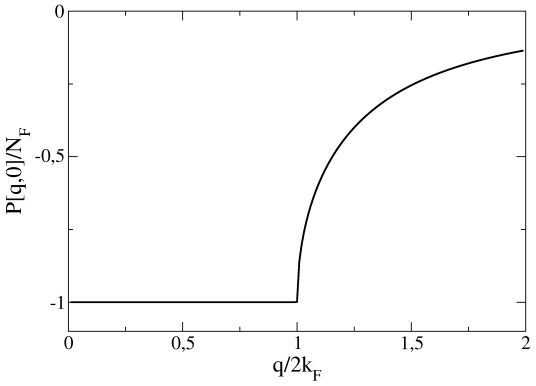


(a)

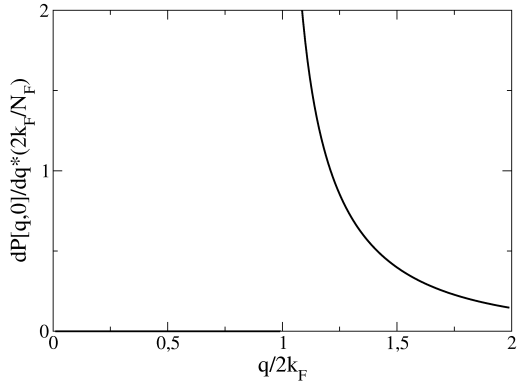


(b)

**Figure 4.4:** Static polarization of the 2DEG

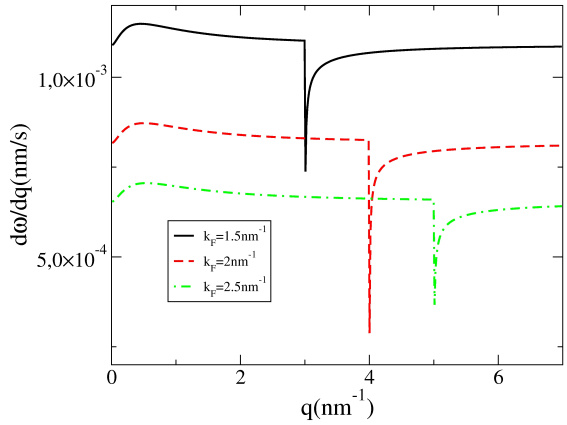


**Figure 4.5:** Derivative of the phonon frequency (4.5.56)

## 4.6 Electron-electron interaction

Both Coulomb interaction and phonon mediated interaction, obtained multiplying the square of the electron-phonon coupling $M(q)$ (vertex correction, where Migdal theorem is supposed to hold [87]) per the phonon propagator, contribute to the electron-electron interaction

$$V(q,\omega) = v_q + |M(k)|^2 \frac{1}{\hbar} D_0(\omega) \tag{4.6.58}$$

where the on-shell value of $\omega(k)$ has been used for Rayleigh modes, and the constant $K(p_F)$ is in (4.4.43). We finally analyze the effective electron-electron interaction mediated by Rayleigh waves. In Fig. 4.6 the static interaction $V(q/2k_F)$ multiplied for the density of states at the Fermi level $\rho(E_F) = k_F/2\pi\hbar v_F$ is depicted. In order to discuss superconductivity it is relevant the parameter $\lambda$

$$\lambda = \frac{2\rho(E_F)}{\pi} \int_0^\pi d\theta \;\; V\left(2k_F \sin\frac{\theta}{2}, 0\right) \cos^2\frac{\theta}{2}. \tag{4.6.59}$$

In Fig. 4.7 the values of $\lambda$ as a function of the Fermi level is reported. At a relatively small value of $k_F$ there is a cross over toward a possible superconductive state in which $\lambda < 0$. For these values of $k_F$ the Coulomb repulsion is smaller that the phonon mediated attractive interaction

$$\frac{e^2}{\epsilon_0 k_F} \ll \frac{\alpha^2 C (k_F a)^3}{M_{u.c.} c_s^2 k_F^2}. \tag{4.6.60}$$

In the above formula $a$ and $M_{u.c.}$ are respectively the lattice constant and the mass in the unit cell, $c_s$ is the velocity of sound. In this regime a rough

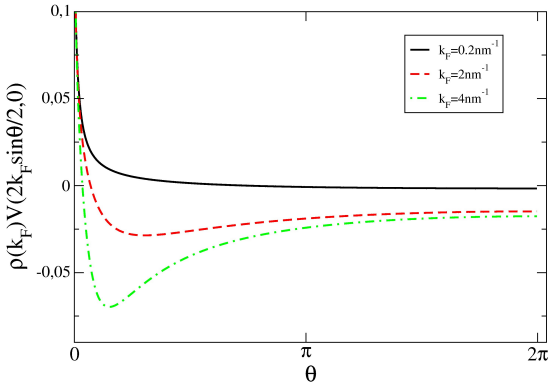


**Figure 4.6:** The effective interaction in static limit $V(q,\omega)$ for the static dielectric constant $\epsilon_0 \approx 50$ for different values of $k_F$

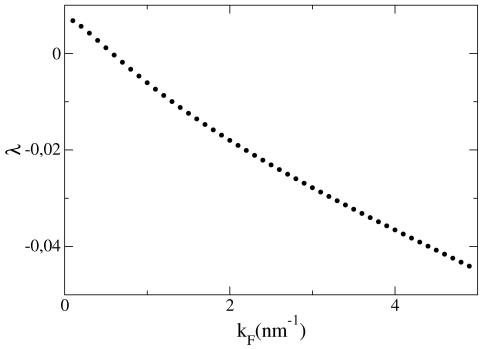


**Figure 4.7:** The coefficient $\lambda$ as a function of the Fermi mometnum $k_F$.

estimation of $\lambda$ is the product of $V_{ph}$ with the density of states

$$\lambda \approx \frac{\alpha^2 C (k_F a)^3}{M_{u.c.} c_s^2 \mu}. \tag{4.6.61}$$

This estimation is consistent with the data in fig. 4.7. Indeed, for $\mu \approx 0.1eV$ it follows that $k_F a \approx 0.1$ and the above formula gives $\lambda \approx 10^{-2}$.

### 4.6.1 Static dielectric function

In this section the polarization in RPA approximation (4.4.36) is considered when the interaction then reads in this case

$$P_{RPA}(q,\omega) = \frac{P(q,\omega)}{1 - V(q,\omega)P(q,\omega)} \tag{4.6.62}$$

The contribution of the last interaction is . I will now write explicitly the polarization in the static limit $\omega \to 0$, so to compare its expression with the

one used till now in our work. In the static limit $P(k,0)$ is

$$P(q,0) = -\frac{k_F}{2\pi\hbar v_F} + \Theta(q-2k_F)\frac{q}{8\pi\hbar v_F}G_<\left(\frac{2k_F}{q}\right) \tag{4.6.63}$$

substituting this expression in the RPA we have

$$P_{RPA}(q,0) = -4N_F\frac{2-\tilde{q}\theta(\tilde{q}-1)G_<\left(\frac{1}{\tilde{q}}\right)}{8+[2\alpha_{FS}+K(k_F)2\xi c_t k_F\tilde{q}^3D_0(0)]\left\{\frac{2}{\tilde{q}}-\theta(\tilde{q}-1)G_<\left(\frac{1}{\tilde{q}}\right)\right\}} \tag{4.6.64}$$

In the static limit $D_0(0) = -1/\omega_q^{(0)} = -1/\xi c_t q$, and thus the above expression simplifies as

$$P_{RPA}(q,0) = -4N_F\tilde{q}\frac{\frac{2}{\tilde{q}}-\theta(\tilde{q}-1)G_<\left(\frac{1}{\tilde{q}}\right)}{8+[2\alpha_{FS}-K(p_F)\pi\tilde{q}^2]\left\{\frac{2}{\tilde{q}}-\theta(\tilde{q}-1)G_<\left(\frac{1}{\tilde{q}}\right)\right\}} \tag{4.6.65}$$

This has been calculated considering the unperturbed dispersion for Rayleigh phonons $\omega_q^{(0)} = \xi c_t q$. We can also use our result for the dispersion relation (4.4.49). The polarization then gets a correction in the denominator

$$P_{RPA}(q,0) = -4N_F\tilde{q}\frac{\frac{2}{\tilde{q}}-\theta(\tilde{q}-1)G_<\left(\frac{1}{\tilde{q}}\right)}{8+[2\alpha_{FS}-K(k_F)\tilde{q}^2(1-K(k_F)F(\tilde{q}))^2]\left\{\frac{2}{\tilde{q}}-\theta(\tilde{q}-1)G_<\left(\frac{1}{\tilde{q}}\right)\right\}} \tag{4.6.66}$$

The full dielectric constant then could be calculated, in static limit

$$\begin{aligned}\epsilon(q,0) &= \epsilon_0 + V(q,0)P_{RPA}(q,0) = \\ &= \epsilon_0 - \frac{[2\alpha_{FS}-K(k_F)\tilde{q}^2(1-K(k_F)F(\tilde{q}))^2]\left\{\frac{2}{\tilde{q}}-\theta(\tilde{q}-1)G_<\left(\frac{1}{\tilde{q}}\right)\right\}}{8+[2\alpha_{FS}-K(k_F)\tilde{q}^2(1-K(k_F)F(\tilde{q}))^2]\left\{\frac{2}{\tilde{q}}-\theta(\tilde{q}-1)G_<\left(\frac{1}{\tilde{q}}\right)\right\}}\end{aligned} \tag{4.6.67}$$

## 4.7 Dynamic dielectric function and plasmons

To determine the plasmon frequency $\omega_p(k)$ a different approximation for the polarization could be used. A stable solution requires $\operatorname{Im} P(k,\omega) = 0$, and

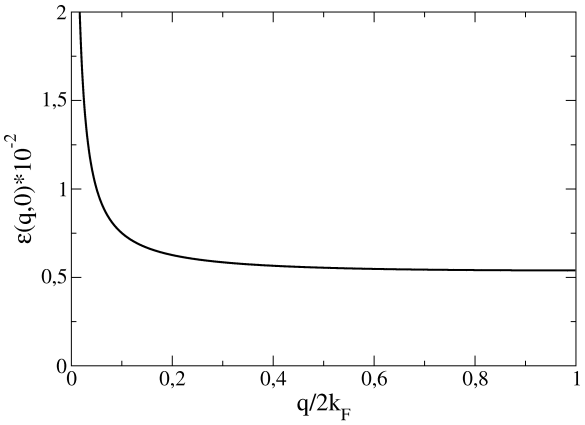


**Figure 4.8:** Correction to the dielectric function versus momentum $k$.

the limits $k \to 0$ and $\hbar\omega \ll \mu$ could be considered. In these approximations the polarization reduces to

$$P(k,\omega) = \frac{v_F p_F}{4\pi\hbar}\frac{k^2}{\omega^2} = \frac{p_F}{\pi\hbar v_F}\frac{x^2}{y^2} \tag{4.7.68}$$

where the adimensional variables $x = k/2p_F$ and $y = \omega/v_F p_F$ have been introduced. The plasmon frequency then is defined through the equation

$$\epsilon_0 = V(k,\omega_p)P(k,\omega_p) \tag{4.7.69}$$

where for later convenience the potential (4.6.58) is written synthetically as

$$V(k,\omega) = \frac{\hbar v_F \pi}{p_F}\frac{1}{x}g(x,y). \tag{4.7.70}$$

Here the function $g(x,y)$ has been introduced

$$g(x,y) = \alpha_{FS} + K(p_F)\xi\frac{c_t}{v_F}x^3(1 - K(p_F)F(x))D_0(y) \tag{4.7.71}$$

Introducing (4.7.68) and (4.7.70) in (4.7.69), the equation defining the adimensional variable $y$ is obtained

$$y^4 - (f_1^2(x) + y_0^2(x))y^2 + y_0^2(x)f_1^2(x)\left[1 - \frac{1}{4\alpha_{FS}\gamma^2}K(p_F)f_1^2(x)\right] = 0. \tag{4.7.72}$$

In above eqaution the frequency $y_0(x)$ has been defined, being the plasmon frequency in absence of electron-phonon interaction

$$y_0^2(x) = \frac{\alpha_{FS}}{\epsilon_0}x \tag{4.7.73}$$

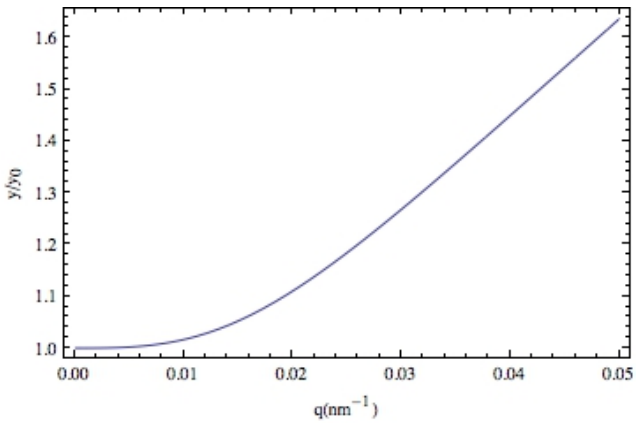


**Figure 4.9:** Ratio $y(x)/y_0(x)$ as a function of $k$.

and the function $f_1(x)$ has been introduced for simplicity

$$f_1(x) = 2\gamma x(1 - K(p_F)F(x)). \tag{4.7.74}$$

As in previous sections the parameter $\gamma$ is the ratio between the Rayleigh wave velocity and the Fermi velocity. Equation (4.7.72) has one real positive solution

$$y^2(x) = \frac{y_0^2(x)}{2}\left[1 + \frac{f_1^2(x)}{y_0^2(x)} + \sqrt{\left(1 - \frac{f_1^2(x)}{y_0^2(x)}\right)^2 + \frac{K(p_F)}{\alpha_{FS}\gamma^2}\frac{f_1^2(x)}{y_0^2(x)}}\right] \tag{4.7.75}$$

In figure 4.9 the ratio $y(x)/y_0(x)$ is reported. The plasmon frequency then takes a big correction till $k_0$, where the correction coming from phonons disappears and the phonon-free result is gained again. The correction to the plasmon frequency results to be dependent of the Fermi wave vector. Indeed, the ratio $f_1(x)/y_0(x)$ is independent of $p_F$, then the only possible dependence is contained in $K(p_F) \propto p_F^2$. Thus $y^2(x)/y_0^2(x)$ goes linearly in $p_F$, i.e. the plasmon frequency $\omega(k)$ goes linearly in $p_F$.

## 4.8 Existence of surface phonons in slab geometry

I will consider now the problem of a slab with elastic constants $\lambda_1, \mu_1$, with thickness $h$, rigidly attached to a seminfinite medium with constants $\lambda_2, \mu_2$ occupying the region $z < 0$. Boundary conditions are given by

- free surface condition at $z = h$

$$\sigma_1 \cdot n_z|_{z=h} = 0$$

- continuity of stress at $z = 0$

$$\sigma_1 \cdot n_z|_{z=0} = \sigma_2 \cdot n_z|_{z=0}$$

- continuity of displacement at $z = 0$

$$u_1|_{z=0} = u_2|_{z=0}$$

Both the slab and the bulk are considered homogeneous elastic media described by the stress tensor

$$\sigma_{ij} = \frac{E}{1+\sigma}\left(u_{ij} + \frac{\sigma}{1-2\sigma}u_{ll}\delta_{ij}\right) = 2\rho[c_t^2 u_{ij} + (c_l^2 - 2c_t^2)u_{ll}\delta_{ij}]. \quad (4.8.76)$$

In the geometry described above two different polarization are possible for surface phonons: Rayleigh modes, polarized in the $xz$ plane, and the Love waves, polarized in the $xy$ plane. The former mode is analyzed in the following subsection. A discussion on Love could be found for example in Ref.[113]

### 4.8.1 Rayleigh modes

To write the the general ansatz on the displacement vector i will introduce the function $\phi(\mathbf{r})$ and the vector function $\boldsymbol{\chi}(\mathbf{r})$ so that the longitudinal and the transverse part of $\mathbf{u}$ are

$$\begin{aligned} \mathbf{u}_L(\mathbf{r}) &= \nabla\phi \\ \mathbf{u}_T(\mathbf{r}) &= \nabla \times \boldsymbol{\chi} \end{aligned} \quad (4.8.77)$$

The function $\phi$ and each component of $\boldsymbol{\chi}$ satisfy the wave equation with velocity of propagation $c_l$ and $c_t$ respectively. In the slab the most general form of this functions giving surface waves polarized in the $xz$ plane are

$$\begin{aligned} \phi &= (A\sinh\lambda_l z + B\cosh\lambda_l z)e^{i(kx-\omega t)} \\ \boldsymbol{\chi} &= \hat{e}_y(C\sinh\lambda_t z + D\cosh\lambda_t z)e^{i(kx-\omega t)} \end{aligned} \quad (4.8.78)$$

The displacement vector then is

$$\begin{aligned} u_{Ix}(\mathbf{r}) &= \partial_x\phi - \partial_z\chi_y = [ik(A\sinh\lambda_l z + B\cosh\lambda_l z) - \lambda_t(C\cosh\lambda_t z + D\sinh\lambda_t z)]e^{i(kx-\omega t)} \\ u_{Iz}(\mathbf{r}) &= \partial_z\phi + \partial_x\chi_y = [\lambda_l(A\cosh\lambda_l z + B\sinh\lambda_l z) + ik(C\sinh\lambda_t z + D\cosh\lambda_t z)]e^{i(kx-\omega t)} \end{aligned} \quad (4.8.79)$$

The components of the strain tensor we need to write the boundary conditions are

$$\begin{aligned} u_{xz} &= \frac{1}{2}\{ik[\lambda_l(A\cosh\lambda_l z + B\sinh\lambda_l z) + ik(C\sinh\lambda_t z + D\cosh\lambda_t z)] + \\ &\quad [ik\lambda_l(A\cosh\lambda_l z + B\sinh\lambda_l z) - \lambda_t^2(C\sinh\lambda_t z + D\cosh\lambda_t z)]\}e^{i(kx-\omega t)} \\ u_{xx} &= ik[ik(A\sinh\lambda_l z + B\cosh\lambda_l z) - \lambda_t(C\cosh\lambda_t z + D\sinh\lambda_t z)]e^{i(kx-\omega t)} \\ u_{zz} &= [\lambda_l^2(A\sinh\lambda_l z + B\cosh\lambda_l z) + ik\lambda_t(C\cosh\lambda_t z + D\sinh\lambda_t z)]e^{i(kx-\omega t)} \end{aligned} \tag{4.8.80}$$

Similarly for the bulk the functions $\phi$ and $\boldsymbol{\chi}$ are

$$\begin{aligned} \phi &= Ee^{\lambda_l z}e^{i(kx-\omega t)} \\ \boldsymbol{\chi} &= \hat{e}_y Fe^{\lambda_t z}e^{i(kx-\omega t)} \end{aligned} \tag{4.8.81}$$

The displacement vector is

$$\begin{aligned} u_x &= (ikEe^{\lambda_l z} - \lambda_t Fe^{\lambda_t z})e^{i(kx-\omega t)} \\ u_z &= (\lambda_l Ee^{\lambda_l z} + ikFe^{\lambda_t z})e^{i(kx-\omega t)} \end{aligned} \tag{4.8.82}$$

and the strain tensor is

$$\begin{aligned} u_{xx} &= -(k^2Ee^{\lambda_l z} + ik\lambda_t Fe^{\lambda_t z})e^{i(kx-\omega t)} \\ u_{zz} &= (\lambda_l^2 Ee^{\lambda_l z} + ik\lambda_t\lambda_t Fe^{\lambda_t z})e^{i(kx-\omega t)} \\ u_{xz} &= \frac{1}{2}[ik(\lambda_l Ee^{\lambda_l z} + ikFe^{\lambda_t z}) + (ik\lambda_l Ee^{\lambda_l z} - \lambda_t^2 Fe^{\lambda_t z})] \end{aligned} \tag{4.8.83}$$

The boundary conditions written explicitly are

$$\begin{aligned} 2ik\lambda_{l1}(A\cosh\lambda_{l1}h + B\sinh\lambda_{l1}h) - (k^2+\lambda_t^2)(C\sinh\lambda_{t1}h + D\cosh\lambda_{t1}h) &= 0 \\ [c_{l1}^2\lambda_{l1}^2 - (c_{l1}^2 - 2c_{t1}^2)k^2](A\sinh\lambda_{l1}h + B\cosh\lambda_{l1}h) + 2ik\lambda_{t1}c_{t1}^2(C\cosh\lambda_{t1}h + D\sinh\lambda_{t1}h) &= 0 \\ \left(\frac{c_{t1}}{c_{t2}}\right)^2[2ik\lambda_{l1}A - (k^2+\lambda_{t1}^2)D] &= [2ik\lambda_{l2}E - (k^2+\lambda_{t2}^2)F] \\ [c_{l1}^2\lambda_{l1}^2 - (c_{l1}^2 - 2c_{t1}^2)k^2]B + 2ik\lambda_{t1}c_{t1}^2 C &= [c_{l2}^2\lambda_{l2}^2 - (c_{l2}^2 - 2c_{t2}^2)k^2]E + 2ik\lambda_{t1}c_{t1}^2 F \\ ikB - \lambda_{t1}C &= ikE - \lambda_{t2}F \\ \lambda_{l1}A + ikD &= \lambda_{l2}E + ikF \end{aligned} \tag{4.8.84}$$

The solution of this system of 6 equation in the six unknowns given by the coefficients contained in the definition of the displacement vector is possible, as usual, if the determinant of the coefficient matrix is null. In principle this

equation defines the dispersion relation for the surface waves. In this case, the equation will be of the 12th degree, and some simplification is needed to understand physics in a faster and clearer way. The first step is to consider a thin slab, whose thickness is negligible compared to the bulk material one. This limit i call "ultra-thin" since it consist in taking only the zero-th approximation for displacement vector in the slab (approximation possible since there is a combination of hyperbolic functions in the definition of $\mathbf{u}$ in the slab). In this approximation the system becomes

$$\begin{aligned}
2ik\lambda_{l1}A - (k^2+\lambda_t^2)D &= 0\\
[c_{l1}^2\lambda_{l1}^2 - (c_{l1}^2 - 2c_{t1}^2)k^2]B + 2ik\lambda_{t1}c_{t1}^2C &= 0\\
\left(\frac{c_{t1}}{c_{t2}}\right)^2 [2ik\lambda_{l1}A - (k^2+\lambda_{t1}^2)D] &= [2ik\lambda_{l2}E - (k^2+\lambda_{t2}^2)F]\\
[c_{l1}^2\lambda_{l1}^2 - (c_{l1}^2 - 2c_{t1}^2)k^2]B + 2ik\lambda_{t1}c_{t1}^2C &= [c_{l2}^2\lambda_{l2}^2 - (c_{l2}^2 - 2c_{t2}^2)k^2]E + 2ik\lambda_{t1}c_{t1}^2F\\
ikB - \lambda_{t1}C &= ikE - \lambda_{t2}F\\
\lambda_{l1}A + ikD &= \lambda_{l2}E + ikF
\end{aligned} \tag{4.8.85}$$

The first two equation coincide with the first member of the third and the fourth equation respectively, giving a further simplification to the system

$$\begin{aligned}
2ik\lambda_{l1}A - (k^2+\lambda_t^2)D &= 0\\
[c_{l1}^2\lambda_{l1}^2 - (c_{l1}^2 - 2c_{t1}^2)k^2]B + 2ik\lambda_{t1}c_{t1}^2C &= 0\\
[2ik\lambda_{l2}E - (k^2+\lambda_{t2}^2)F] &= 0\\
[c_{l2}^2\lambda_{l2}^2 - (c_{l2}^2 - 2c_{t2}^2)k^2]E + 2ik\lambda_{t1}c_{t1}^2F &= 0\\
ikB - \lambda_{t1}C &= ikE - \lambda_{t2}F\\
\lambda_{l1}A + ikD &= \lambda_{l2}E + ikF
\end{aligned} \tag{4.8.86}$$

Thus the third and third and the fourth equation make up an homogeneous system of two equations in the two unknowns $E, F$ that could be solved separately

$$\begin{aligned}
[2ik\lambda_{l2}E - (k^2+\lambda_{t2}^2)F] &= 0\\
[c_{l2}^2\lambda_{l2}^2 - (c_{l2}^2 - 2c_{t2}^2)k^2]E + 2ik\lambda_{t1}c_{t1}^2F &= 0
\end{aligned} \tag{4.8.87}$$

as it could be seen easily, these two equations coincide with the system defining Rayleigh waves in the previous section. Thus in the ultra-thin limit the bulk is unaffected by the slab. Note that since the system is homogeneous it is possible to fix the relation of one coefficient as a function of the other, thus leaving a free parameter. I will assume to fix this parameter too, through

normalization of the displacement vector. This is equivalent to say that the slab is so thin that it does not affect the normalization of the mode, and this seems consistent with the hypothesis of a really thin slab. Due to these considerations the system is reduced to an inhomogeneous system of 4 equations in 4 unknowns

$$\begin{aligned} 2ik\lambda_{l1}A - (k^2+\lambda_t^2)D &= 0 \\ [c_{l1}^2\lambda_{l1}^2 - (c_{l1}^2 - 2c_{t1}^2)k^2]B + 2ik\lambda_{t1}c_{t1}^2C &= 0 \\ ikB - \lambda_{t1}C &= M_1 \\ \lambda_{l1}A + ikD &= M_2 \end{aligned} \tag{4.8.88}$$

where $M_1$ and $M_2$ are assumed to be given quantities, fixed through the solution of the previous system for $E, F$. The solution of this system is possible if the determinant $\Delta$ of the coefficients matrix is different from zero

$$\Delta = c_{l1}^2\lambda_{l1}\lambda_{t1}(k^2 - \lambda_{t1}^2)(\lambda_{l1}^2 - k^2) \tag{4.8.89}$$

here

$$\begin{aligned} \lambda_l &= k\sqrt{1-\gamma^2\xi^2} \\ \lambda_t &= k\sqrt{1-\xi^2} \end{aligned} \tag{4.8.90}$$

and $\gamma = c_t/c_l$. With this definition the determinant above becomes

$$\Delta = -c_{l1}^2\sqrt{1-\gamma^2\xi^2}\sqrt{1-\xi^2}k^6\xi^4\gamma^2 \tag{4.8.91}$$

Note that here $xi \equiv \xi_1$, that is the parameter determining both the dispersion relation through the equation $\omega_R(k) = c_t\xi k$, as above and the decay length through the definitions above. This parameter is obviously related to the decay length calculated in the medium II through the system (4.8.87)

$$\xi_1 = \frac{c_R}{c_{t1}} = \frac{c_R}{c_{t2}}\frac{c_{t2}}{c_{t1}} = \xi_2\frac{c_{t2}}{c_{t1}}. \tag{4.8.92}$$

This shows that the determinant $\Delta$ could not be zero, and thus the system (4.8.88) has a non null solution. Indeed, to have a null $\Delta$ it should be $\xi_1 = 0$ or $\xi_1 \geqslant 1$. Note that in any case there are some restriction on the elastic parameters in the two materials. Since $\xi_1 < 1$ then

$$\xi_2\frac{c_{t2}}{c_{t1}} < 1 \Rightarrow \frac{c_{t2}}{c_{t1}} > 1$$

# Chapter 5

# A Study on Charged Neutron Star in $AdS_5$

The formalism used to study defects and scattering processes in the previous chapters is also at the base of the analysis of systems through AdS-CFT correspondence: it has been postulated a correspondence between the boundary theory of a $D+1$ general relativistic models and $D$ dimensional condensed matter systems. Motivated by an open question raised in recent times regarding the phase transition during the collapse of a neutron star to form a black hole and related stability issues, we have constructed charged neutron stars in $AdS_5$ and show that these stars become unstable at a particular value of their radius, regarded as the Chandrasekhar radius. We reproduced the calculations recently done in [54] in our $AdS_5$ charged star. The analysis shows that the non-Fermi liquid behavior found there in $AdS_4$ is still true in this higher dimensional case with the presence of Kosevich-Lifshitz oscillations.

## 5.1 Introduction

In recent times there has been a flurry of activity in the interplay between condensed matter physics and AdS/CFT trying to bridge the gulf that exists in between them giving rise to several interesting original ideas in this frontier (For an introduction to this field see for exmple [118; 52; 57; 90]). Recently in a series of papers [25; 9] the authors addressed the issue of a holographic description of an astrophysical phenomena i.e. the collapse of a neutron star toward the formation of a black hole beyond the so-called Oppenheimer-Volkoff (OV) limit [104]. Near the very end of their article [25], they have proposed an open question regarding the CFT meaning of

the OV limit under consideration.The Neutron Star to Black Hole formation gives a hunch of a second-order quantum phase transition from a condensed matter physicist's view point turning a high density baryonic state into a thermal QGP state and thus the issue needs proper investigation as suggested in [25; 9]. The main point of investigation is rather open ended and it would be really interesting to settle the issue whether a reliable realization of a degenerate fermionic star can indeed be achieved conclusively in the AdS/CFT duality framework. We have tried to formulate the very problem on our own way rendering hope to give a partial, if not complete, explanation of the underlying phenomena which of course needs further study.

In this note we study charged neutron stars in $AdS_5$ space and focus on their collapse toward the formation of a black hole. This process is particularly interesting and worth studying from the holographic point of view (see [25; 9] and references therein). This is because in terms of the boundary theory this process might as well symbolize a phase transition in $AdS$ space.

First we present a construction of a charged star in AdS space by adopting numerical methods. Then we find that such a star ceases to exist at a particular value of the mass, charge and radius. This fact implies that this star becomes unstable at this value of the mass and charge. This instability will trigger the formation of a new phase and (presumably) the star will collapse to form a black hole. Now the behavior of a test fermion in the black hole background has recently been analyzed in [83]. It is concluded from their analysis that in this black hole phase the boundary theory has excitations about the Fermi-surface which is unlike the Fermi liquid. Further research on this point [80] has shown that the Fermi vector depends exponentially on the scaling dimension if one uses the duality to extremal RN black holes while computing the non-Fermi liquid Green function. This proved the fact of violation of Luttinger theorem incase of non-Fermi liquids which is even true in case of the extremal $AdS_5$ RN Black Hole. All such computations reported in [83; 95; 56; 82] revealed the presence of a Fermi surface in the bulk of a non-Fermi liquid type. For a much better and clear understanding of their results and the underlying phenomena that occurs, we thought that it might be worthwhile to explore the boundary description of a simpler system, that of an ideal Fermi gas in AdS without the presence of a Black Hole. [1]

We perform a similar kind of analysis by putting in a test fermion in the bulk with the charged neutron star serving as the background. From the dynamics of such a bulk fermionic field one can compute the two point function of the boundary composite operator that corresponds to the bulk

[1]It is worth pointing out here that in [55] the authors evaluated the fermionic correlators on a background with fermions but without a Black Hole horizon.

fermion. Although, we have not written down the boundary correlation function explicitly in the star background, but we gave a possible direction how to do that in practice. [2] We hope that, from the pole structure of these two point function, it will be evident that in the hydrodynamic limit one gets either a Fermi liquid or a non-Fermi liquid type of behavior, nevertheless the explicit computation needs to be performed. Via the AdS/CFT dictionary for fermions [99] the conformal dimension of the dual operator in the boundary CFT can be controlled by the bulk fermionic mass. In [95], it has been already found that by tuning the mass one can match the conformal dimension of the boundary operator to that of the free fermion, and thus one obtains the spectral function exhibiting a peak which is consistent with a Fermi liquid behavior. It is quite clear from their analysis that one can deviate away from the Fermi liquid behavior by tuning the mass away from the free value as the mass was interpreted as the proxy for coupling in [95].

However, we recalled the fact that if one computes the fermionic correlation functions in charged $AdS_5$ black hole backgrounds using probe fermion and analyze the spectral peak as done in [80], one finds that the Fermi momentum depends exponentially on the probe fermion mass interpreted as a proxy for the coupling and thereby violates Luttinger theorem indicating a non-Fermi liquid behavior as was found in [83]. We then show, following [54], the presence of Kosevich-Lifshitz (KL) kind of oscillation in our $AdS_5$ charged neutron star setting. One must emphasize the fact that , we are working with "global AdS" i.e. the spatial sections are $S^3$ rather than planes which implies that the field theory under consideration is on $time \times S^3$ instead of being on Minkowski space. In [53; 55; 54] the authors studied electron stars working with a field theory defined on the Minkowski space whereas the authors of [25; 9] adopted our point of view.

## 5.2 Construction of charged neutron stars

In this section we present the construction of the charged neutron star in $AdS_5$. We will work with units in which the $AdS$ radius is set to unity. We consider the following metric ansatz

$$ds^2 = -A(r)dt^2 + B(r)dr^2 + r^2 d\omega_3^2. \tag{5.2.1}$$

[2]The computation is difficult in the sense that the boundary theory under consideration is strongly interacting, and the neutron star to black hole collapse process is time-dependent and hence the radial holographic dimension can't be easily constructed on the CFT side.

Besides the metric we have a dynamical gauge field ($H$) and a fermionic field ($\psi$) in this background. We will work in the gauge where the radial component of the gauge field is zero (i.e. $H_r = 0$). With this choice of gauge we write the gauge field as

$$H(r) = h(r)dt. \tag{5.2.2}$$

Further we consider fermionic species with mass $m$, charged under this gauge field with charge $q$. However, we shall treat the fermions in a hydrodynamic approximation. For this we will take the limit [3] that the number of particles per AdS radius is infinite with $\epsilon_F/m$ fixed, $\epsilon_F$ being the Fermi energy. The ideal degenerate Fermi gas formed by these particles can then be described by the following hydrodynamic stress tensor for ideal fluids

$$T_{\mu\nu} = (\rho + p)u_\mu u_\nu + p g_{\mu\nu}, \tag{5.2.3}$$

where the pressure $p$ and the density $\rho$ are related to each other by the flat space equation of state for the fermions i.e.

$$p + \rho = \mu n \tag{5.2.4}$$

The use of the flat space approximation is again justified as there are large number of fermions within a given $AdS$ radius and therefore the fermions do not see the curvature of the space time. In order to be consistent with this approximation, the mass and charge of the fermions must be greater than the $AdS$ radius (i.e. unity in our case). This equation of state is implicitly given by

$$p = \frac{(\mu - m)^3 \left(8m^2 + 3\mu(3m + \mu)\right)}{1920\pi^2}, \rho = \frac{2m^5 - 5m^2\mu^3 + 3\mu^5}{480\pi^2}, \tag{5.2.5}$$

where $\mu$ is the chemical potential for the fermions, which can be expressed in terms of the Fermi momentum ($k_F$) by the relation

$$\mu = \sqrt{k_F^2 + m^2}.$$

In this flat space approximation for the fermions the particle number density ($\tilde{n}$) is given in terms of the volume of the Fermi surface and we have

$$\tilde{n} = \frac{\left(\mu^2 - m^2\right)^2}{128\pi^2}. \tag{5.2.6}$$

[3] before taking this limit we must also ensure that the central charge of the boundary CFT is taken to infinity (something similar to the large N limit for $\mathcal{N} = 4$ Yang-Mills) with all other quantities keeping fixed. This is required to ensure that all the multi-trace operators are suppressed. One way to think of this limit in the bulk is to consider N species of fermions with the same mass and then take N to infinity keeping everything else fixed.

Then it immediately follows that the charge density ($n$) is given by

$$n = q\tilde{n} = q\frac{(\mu^2 - m^2)^2}{128\pi^2}. \tag{5.2.7}$$

Note that in our problem these relations are locally valid and generally $\mu, n, p$ and $\rho$ are functions of $r$-coordinate [4] which we ultimately solve for. Here we would like to draw attention of the reader to a subtle point. $u_\mu$ as defined in (5.2.3) is a static velocity field: $u_\mu dx^\mu = A(r)dt$ and the radial profiles of $p$ and $\rho$ are determined by imposing the stress energy conservation which leads to the following condition:

$$\frac{dp}{dr} + \frac{1}{A}\frac{dA}{dr}(\rho + p) = 0 \tag{5.2.8}$$

This equation is very easy to solve. By making use of (5.2.4) one easily verifies the fact that (5.2.8) is satisfied while the chemical potential obeys

$$\mu(r) = \frac{\epsilon_F}{A(r)} \tag{5.2.9}$$

where at this stage $\epsilon_F$ is an arbitrary constant. Thus the radial dependence of the chemical potential $\mu$ is simply due to the gravitational redshift.

### 5.2.1 The Equations to be solved

In the above set up we now write down the dynamical equations which we must solve in order to obtain the Neutron star numerically.

Firstly we have the Einstein equations. The two non-trivial Einstein equations are obtained from the rr-component and the tt-component and they are respectively given by

$$\begin{gathered} 3r\left(2A'(r) + rh'(r)^2\right) - 4A(r)\left(B(r)\left(r^2p(r) + 6r^2 + 3\right) - 3\right) = 0, \\ A(r)\left(6rB'(r) - 4B(r)^2\left(r^2\rho(r) - 6r^2 - 3\right) - 12B(r)\right) - 3r^2B(r)h'(r)^2 = 0, \end{gathered} \tag{5.2.10}$$

where as mentioned before we consider the pressure and the density as functions of the radial coordinate.

Then we consider the Maxwell equations. In this case the non-trivial equation stems out from the t-component (which is a mere generalization of Coulombs law). This equation is given by

$$\left(\frac{A'(r)}{A(r)} - \frac{6}{r}\right)h'(r) + \frac{B'(r)h'(r)}{B(r)} - 2B(r)n(r) - 2h''(r) = 0. \tag{5.2.11}$$

[4] the symmetries of AdS prevent these quantities from becoming functions of the other coordinates

Finally we have to consider the equation of motion for the fermions. However, since the fermions are treated in a hydrodynamic approximation this equation is the conservation of the stress tensor[5]. In this case the radial component yields the non-trivial equation and is given by

$$A(r)\left(2rB(r)^2A'(r)(p(r)+\rho(r))+3rB'(r)h'(r)^2+\right.$$
$$\left.-6B(r)h'(r)\left(rh''(r)+3h'(r)\right)\right)+3rB(r)A'(r)h'(r)^2+4rA(r)^2B(r)^2p'(r)=0. \tag{5.2.12}$$

In these equations both $p(r)$ as well as $\rho(r)$ are present explicitly. However, we will eliminate both $p(r)$ and $\rho(r)$ in terms of $\mu(r)$ with the help of the equation of state (5.2.5). Now these equations are extremely non-linear and we have to resort to numerical means in order to solve them.

### 5.2.2 Solving the equations

One obvious solution to these equations is the charged black hole in $AdS_5$ with the chemical potential being constant throughout the space. In terms of the above mentioned functions this solution may be written as [21],

$$\begin{aligned} A(r) &= \left(1+r^2\left(1-\frac{M}{r^4}+\frac{Q^2}{r^6}\right)\right), \\ B(r) &= \left(1+r^2\left(1-\frac{M}{r^4}+\frac{Q^2}{r^6}\right)\right)^{-1}, \\ \mu(r) &= m, \\ h(r) &= \mu_B-\frac{Q}{r^2}. \end{aligned} \tag{5.2.13}$$

where $m$ and $\mu_B$ are constants. The parameter $m$ is related to the ADM mass of the Hole as $M=\frac{3\omega_3}{16\pi G}m$ [21] where in natural units $16\pi G=1$ and $\omega_3$ is the volume of the 3-sphere. Also, $\mu_B$ is the electrostatic potential difference between the horizon and infinity. Since the constant value of the chemical potential outside the star is $m$, the mass of the fermionic species, therefore we use the same notation here also. Similarly we use $\mu_B$ to denote the constant part of the gauge field as it ultimately turns out to be the boundary chemical potential.

Now it is expected that outside the neutron star our solutions should reduce to the black hole solution. Therefore, we shall obtain a solution inside the neutron star and then patch up our solution with this black hole

[5] which is the relativistic version of the Navier-Stokes equation.

solution outside. Thus we start with a boundary condition at the origin (which may be thought of as the centre of the star) and make a choice of the time coordinate inside the star such that at the boundary the first derivative of the field strengths match. In order to determine the consistent boundary conditions at the origin we solve the equations about $r = 0$ and find that,

$$\begin{aligned}
A(r) &= A_0 + \frac{1}{180}r^2\left(-\frac{A_0m^5}{8\pi^2} + \frac{15A_0m^4\mu_0}{32\pi^2} - \right. \\
&\qquad\qquad \left. \frac{5A_0m^2\mu_0^3}{8\pi^2} + \frac{9A_0\mu_0^5}{32\pi^2} + 180A_0\right) + O(r^3), \\
B(r) &= 1 + \frac{1}{90}r^2\left(\frac{m^5}{16\pi^2} - \frac{5m^2\mu_0^3}{32\pi^2} + \frac{3\mu_0^5}{32\pi^2} - 90\right) + O(r^3), \\
\mu(r) &= \mu_0 + \frac{r^2}{92160\pi^2A_0}(32A_0m^5\mu_0 - 120A_0m^4\mu_0^2 + 160A_0m^2\mu_0^4 - 72A_0\mu_0^6 \\
&\quad - 46080\pi^2A_0\mu_0 + 135m^4q^2 - 270m^2q^2\mu_0^2 + 135q^2\mu_0^4) + O(r^3), \\
h(r) &= \mu_B - \frac{qr^2\left(m^2-\mu_0^2\right)^2}{1024\pi^2} + O(r^3),
\end{aligned} \tag{5.2.14}$$

solve the equations (5.2.10),(5.2.11) and (5.2.12) upto $O(r^2)$. Here $A_0$ and $\mu_0$ are the values of $A(r)$ and $\mu(r)$ at the origin. These are the parameters of our problem and we have to choose values for these parameters which serve as initial values of our differential equations. Again $m$ and $q$ are the mass and charge of a single species of fermion. The most striking thing to note about this solution is that the value of $B(r)$ at the origin is fixed to be unity. We do not have the freedom to choose this value on independent grounds. Also the parameter $q$ in (5.2.14) yield the charge of the black hole as $Q = \frac{2\sqrt{3}\omega_3}{8\pi G}q$ [21].

#### 5.2.2.1 Numerical Solution of the equations

We proceed to solve these equations numerically in the following way. At first we fix the value of the chemical potential at the origin to be $\mu_0$. Then we fix the value of $A_0$ to be unity and then fix a scale for the time coordinate in the patch inside the star so as to meet the boundary conditions $A(r) = 1/B(r)$ at the radius of the star ($R$). The radius of the star is obtained from the value of $r$ where the density $\rho(r)$ goes to zero or the chemical potential $\mu(r)$ goes to $m$ as can be easily checked from the equations (5.2.5) and (5.2.13). Further from the value of $A(R)$ (which is the same as $1/B(R)$), together with the matching condition for the Electric field at $r = R$, we determine the mass

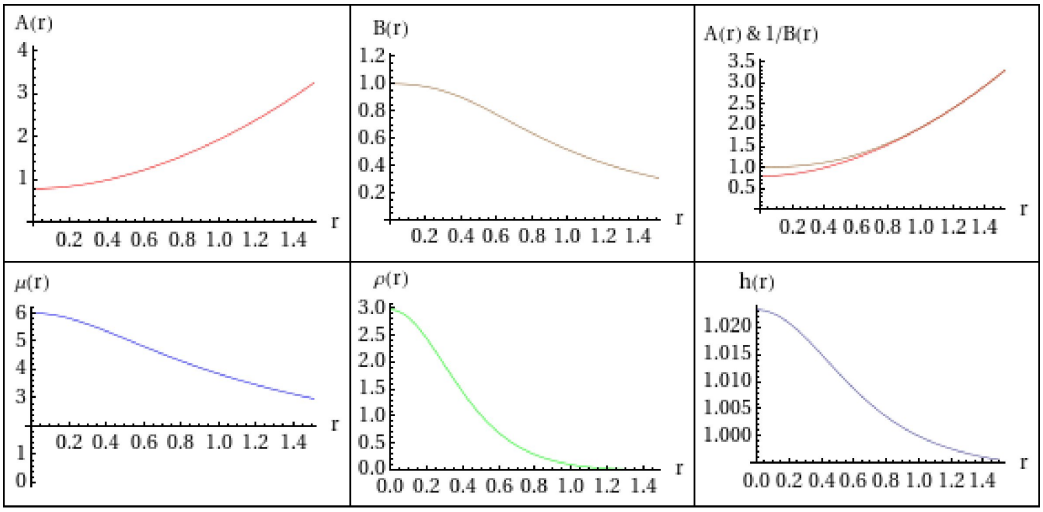


**Figure 5.1:** Solution of various functions inside the star. The values of the parameters are $m = 3$, $q = 1$ and $\mu_0 = 6$. We have shown the plots upto r=1.48 which is the critical radius of the star.

and charge of the black hole solution with which we patch up outside the neutron star. Note that in this procedure, matching of the first derivative of $A(r)$ (which is the gravitational field strength in a rough sense) at $r = R$ is automatic. As a part of our choice of units we take the $AdS$ radius to be unity.

In fig:5.1, we present the solution when the parameters $m = 3$, $q = 1$ and $\mu_0 = 6$. This corresponds to the core density of 2.97. The Mass of the star is 0.073 and the charge of the star is 0.0083 [6].The radius of the star is 1.48. Note that the density function $\rho(r)$ goes to zero at the edge of the star. Also the values of $A(r)$ and $1/B(r)$ match at the end of the star.

#### 5.2.2.2 A class of Neutron stars

Now we can vary the value of the chemical potential at the origin to obtain a large class of neutron stars. This amounts to obtaining neutron stars for various values of core density. Further under a variation of the core density (which varies form 0 to $\infty$) we can make a plot of the mass and radius of the star (see fig:5.2). In this plot we find there exists a maximum value of

[6]These values of the charge and mass should not be directly compared with the mass and charge of a single fermion since in this case we should also consider the Newton's constant which we have not included in the present analysis.

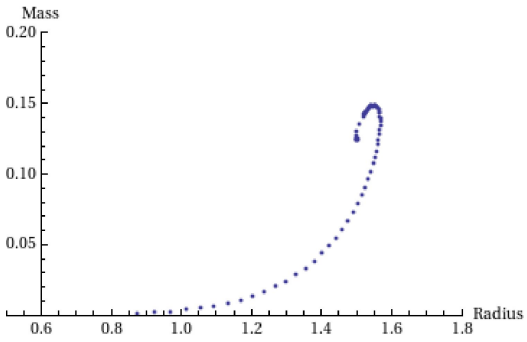


**Figure 5.2:** Plot for Mass vs the radius of the neutron star as the core density is varied. Here also we have taken $m = 3$ and $q = 1$.

mass for the star sometimes termed as critical mass of the star. [7] Further the solution ceases to exist at a particular value of the mass and radius. This is the signature of a critical behavior and occurs when the density at the origin approaches infinity. At this critical point the neutron star is expected to start collapsing into a black hole.

In a similar way, we can obtain a plot for the mass vs charge of the star (see fig:5.3). In this plot we see that for a given value of charge two solutions exist corresponding to two different masses. Presumably the one with more mass is the stable one, the other being unstable.

We again remind the readers of the intriguing fact that working in "global AdS" we have $S^3$ as spatial section thus providing a scale in the field theory, which is the radius say $R$ of $S^3$. There is yet another scale in the problem, the chemical potential $\mu$. The related phase transition from the star to a black hole occurs due to the competition between the two scales. In particular at the critical point of phase transition one would get $R_{S^3} \sim \frac{1}{\mu}$. So the very existence of $R_{S^3}$ is crucial for our purpose.

In recent years, all the various works [83; 80; 53; 54] on Fermi surfaces consider Minkowski space while considering the boundary field theory. This was important in order to have a well-defined momentum $k$. On a sphere $k$ is not a good quantum number, in particular if $R_{S^3} \sim \frac{1}{\mu}$ one might worry about whether the notion of a Fermi surface makes sense in the momentum space. The answer to this is, yes, indeed the notion can be justified. As we mentioned in Sec.5.2, that in our choice of units the charge and mass of the

[7] We can render a holographic interpretation to this critical mass, too. As found in [9] the limiting mass in the boundary CFT theory translates to a limiting conformal dimension of the composite operator made out of the fermionic primary fields which in the large N limit construct our model degenerate star.

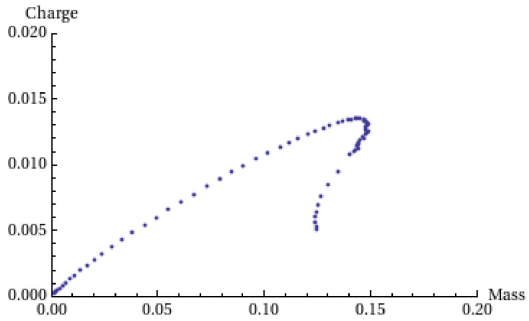


**Figure 5.3:** Plot for charge vs mass of the neutron star as the core density is varied. Here also we have taken $m = 3$ and $q = 1$

fermion are large, so that the boundary field theory fermions are locally in a flat space making sense of a Fermi momentum in approximate terms.

## 5.3 Holographic dual of the charged star

We now study the holographic description of this neutron star solution. By studying the dynamics of a probe fermion in this background one could get a hint at the boundary description of this charged neutron star.

### 5.3.1 Dirac Equation in Spherically symmetric space time

We first present the Dirac equations in spherically symmetric space times which we subsequently solve in our star background [84]. [8]

We have to incorporate the interaction of the probe fermion with the fermions forming the star. This we accomplish by considering a new gauge (different from the existing one) with only a non-zero time component being the chemical potential, due to the fermions forming the star. We justify this procedure in Appendix 5.5.

We consider the metric to be of the form (as in (5.2.1))

$$ds^2 = -A(r)dt^2 + B(r)dr^2 + r^2\left(d\theta^2 + \sin^2\theta d\phi^2 + \sin^2\phi\sin^2\theta d\lambda^2\right), \quad (5.3.15)$$

The natural choice of vielbein basis vectors are

$$e_{\tilde{t}}^{t} = \sqrt{A}; \quad e_{\tilde{r}}^{r} = \sqrt{B}; \quad e_{\tilde{\theta}}^{\theta} = r; \quad e_{\tilde{\phi}}^{\phi} = r\sin\theta; \quad e_{\tilde{\lambda}}^{\lambda} = r\sin\theta\sin\phi. \quad (5.3.16)$$

[8] One should pay attention to the fact that while the fermions are free in the bulk, they are not so on the boundary (i.e. they don't obey Dirac equation on the boundary) as the boundary theory is strongly coupled.

where $\{\tilde{t}, \tilde{r}, \tilde{\phi}, \tilde{\theta}, \tilde{\lambda}\}$ are the tangent space coordinates. Then the non zero components of the spin connection are

$$\begin{gathered}\omega_t^{\tilde{t},\tilde{r}} = -\frac{1}{2}\frac{A'(r)}{\sqrt{A\ B}}; \quad \omega_\theta^{\tilde{r},\tilde{\theta}} = \frac{1}{\sqrt{B}}; \\ \omega_\lambda^{\tilde{r},\tilde{\lambda}} = \frac{\sin\theta\sin\phi}{\sqrt{B}}; \quad \omega_\phi^{\tilde{r},\tilde{\phi}} = \frac{\sin\theta}{\sqrt{B}}; \\ \omega_\lambda^{\tilde{\theta},\tilde{\lambda}} = \cos\theta\sin\phi; \quad \omega_\lambda^{\tilde{\phi},\tilde{\lambda}} = \cos\phi; \quad \omega_\phi^{\tilde{\theta},\tilde{\phi}} = \cos\theta.\end{gathered} \tag{5.3.17}$$

Using the above equations the Dirac equation

$$(\not{D} - m)\psi = 0,$$

reduces to

$$\left(\Gamma^{\tilde{r}}\frac{1}{\sqrt{B}}\partial_r + \Gamma^{\tilde{t}}\frac{1}{\sqrt{A}}\nabla_t - \frac{1}{2}\frac{1}{\sqrt{B}}\left(\frac{A'(r)}{2A} + \frac{3}{r}\right)\Gamma^{\tilde{r}} + \frac{1}{r}\not{D}^{(S^3)} - m\right)\psi = 0. \tag{5.3.18}$$

where $\not{D}^{(S^3)}$ is the Dirac operator on the three sphere. The eigenvalues of this operator are [15]

$$\kappa = \pm i\left(\frac{3}{2} + n\right), \quad n \in \{0, 1, 2, \dots\}. \tag{5.3.19}$$

We shall denote the eigenfunction corresponding to these eigenvalues by $f_\kappa$. Also the $\nabla_t$ operator denote the gauge covariant derivative and contains both the gauge field and its time derivative. All the gamma matrices in (5.3.18) have a tangent space index and hence are flat space gamma matrices. Here we use the following basis for the gamma matrices.

$$\Gamma^{\tilde{r}} = \mathbb{I} \otimes (-\sigma_3); \quad \Gamma^{\tilde{t}} = \mathbb{I} \otimes (i\sigma_1); \quad \Gamma^{\tilde{i}} = \sigma^i \otimes \sigma_2. \tag{5.3.20}$$

where $\sigma^i$ are the ordinary Pauli matrices. Further we consider the following separation of variables

$$\psi = f_\kappa \begin{pmatrix} \phi_+ \\ \phi_- \end{pmatrix} e^{-i\omega t}. \tag{5.3.21}$$

where $\phi_\pm$ are the eigenvectors of $\Gamma^{\tilde{r}}$ with eigenvalues $\pm 1$. Using this separation of variables the Dirac equation (5.3.18) reduces to the following set of coupled first order equations

$$\begin{gathered}\left(\partial_r + \frac{1}{2}\left(\frac{A'(r)}{2\sqrt{A}} + \frac{3}{r}\right) + m\sqrt{B}\right)\phi_+ - \sqrt{B}\left(\frac{u(r)}{\sqrt{A}} - \frac{k}{r}\right)\phi_- = 0. \\ \left(\partial_r + \frac{1}{2}\left(\frac{A'(r)}{2\sqrt{A}} + \frac{3}{r}\right) - m\sqrt{B}\right)\phi_- + \sqrt{B}\left(\frac{u(r)}{\sqrt{A}} + \frac{k}{r}\right)\phi_+ = 0.\end{gathered} \tag{5.3.22}$$

where $k = i\kappa$, and $u(r) = \omega + \mu(r) - 3/2qh(r)$ [9].

### 5.3.2 The flow equation

In this subsection we will derive and analyze the so-called flow equation for the Dirac fermions in $AdS_5$. Using the set of equations 5.3.22, one can define the wave function at small $r$ to be of the form: (Note that $m$ is the fermionic mass, and it enters in the expansion)

$$\begin{aligned} \phi_- &= \alpha \left( r^{mL} + \dots \right) + \beta \left( r^{-(mL+1)} + \dots \right), \\ \phi_+ &= \gamma \left( r^{-mL} + \dots \right) + \delta \left( r^{(mL-1)} + \dots \right), \end{aligned} \tag{5.3.23}$$

Here $L$ is the $AdS$ radius that we have taken to be unity $L = 1$. The coefficients $\alpha$, $\beta$, $\gamma$ and $\delta$ are what the authors of [80] call A, B, C, D in their article and they are related with one another. The retarded Green function could be written as [83; 80]

$$G_R = \epsilon^{-2m} \lim_{\epsilon \to 0} \begin{pmatrix} \xi_+ & 0 \\ 0 & \xi_- \end{pmatrix} \Bigg|_{1/\epsilon} \tag{5.3.24}$$

where $\xi_-$ is defined as suitably defined ratio between $\phi_-$ and $\phi_+$.

$$\xi_- = -i \frac{\phi_-}{\phi_+} \tag{5.3.25}$$

From the system of equations, (5.3.22) the flow equation can be derived, dividing the second equation by $\phi_+$ and inserting into it the first one, finally yielding:

$$i\partial_r \xi_- - 2i\xi_- m\sqrt{B} - \xi_-^2 \sqrt{B} \left( \frac{u(r)}{\sqrt{A}} - \frac{k}{r} \right) + \sqrt{B} \left( \frac{u(r)}{\sqrt{A}} + \frac{k}{r} \right) = 0 \tag{5.3.26}$$

The numerical solution of this equation has some singularity problems in $r$, due to the choice of boundary conditions, thus preventing its use in the calculation of the correlator in the neutron star background. This issue needs further careful investigation.

#### 5.3.2.1 The initial conditions

Now we have to specify the boundary conditions for the equations (5.3.22). This is done by demanding regularity of the solution near the origin ($r = 0$).

[9] Note that the unconventional factor of 3/2 is present because here we are using a different normalization of charge.

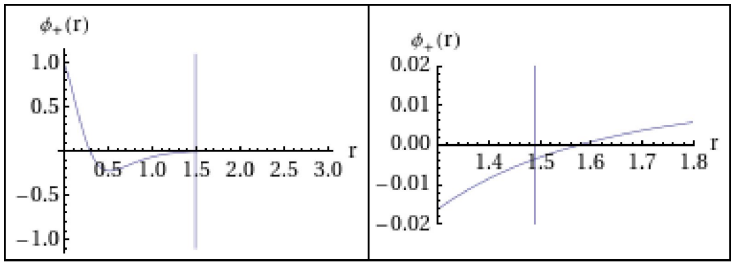


**Figure 5.4:** Plot of $\phi_+$ in the star background constructed in the previous section. The vertical line denotes the value of $r$ for the edge of the star. Here the values of the parameters are $m = 3$, $q = 1$, $\mu_B = 1$, $k = 3/2$, and $\omega = 3$. In the right image we focus on the edge where the first derivative of the function is continuous.

This regularity criterion in general depends on the value of $k$ once we fix the mass and charge of the fermion. The lowest positive value is $k = 3/2$, in which we will focus for our present purpose. In this case the regularity at the origin demands, that if $\phi_+$ is 1 at the origin then $\phi_-$ should be $-1$ i.e.

$$\phi_+(r = 0) = 1 \quad ; \quad \phi_-(r = 0) = -1$$

We shall use this boundary condition to solve the equations (5.3.22).

#### 5.3.2.2 Numerical solution of the Dirac equation

The solution of the probe fermion in the neutron star background is obtained numerically for $m = 3$, $q = 1$ and $k = 3/2$. It is shown in figs:5.4 & 5.5. Here we use the boundary conditions as discussed in §§5.3.2.1. We at first let the differential equation evolve to obtain a solution up to the end of the star and subsequently use the value of $\phi_\pm$ at this edge as the initial value for the subsequent evolution outside the star. The first derivative match of the solution in these two patches is automatic (see figs:5.4 & 5.5) and directly follows from the fact that all the functions that appear in the equations (5.3.22) are continuous at the edge of the star. One possible direction, one can take from here, is that, one might try to compute the boundary correlation function in the presence of the star and understand the behavior of the bulk Fermi surface in terms of the boundary correlators, taking the same route outlined in the formalism of [66]. A noteworthy point here, is that the only difference, we should care about, is that we need to evaluate the fermionic correlators in the neutron star background, whereas there exist large number

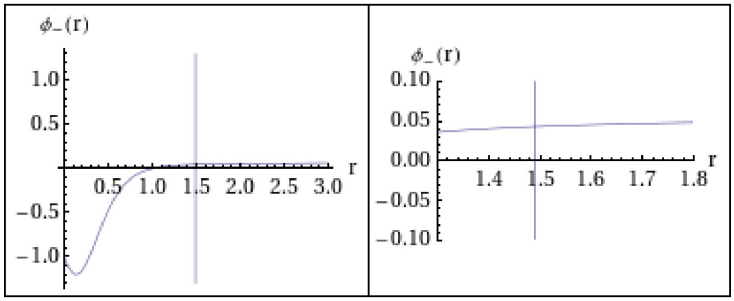


**Figure 5.5:** Plot of $\phi_-$ in the star background constructed in the previous section. Here the values of the parameters are also $m = 3$, $q = 1$, $\mu_B = 1$, $k = 3/2$, and $\omega = 3$. Again the first derivative of $\phi_-$ is continuous as can be seen from the plot on the left.

of literature doing the same computation in the background of a charged black hole (See for example [83; 95; 80; 56; 82].)

### 5.3.3 Kosevich-Lifshitz oscillations in $AdS_5$ neutron star

It has been shown recently in [54] that, the charged star shares some important features with the Fermi liquid. In particular, the presence of the Kosevich-Lifshitz oscillations [53] in magnetic field has been shown in the case of $AdS_4$ charged fermion star. As said in [54] the arguments used to demonstrate this feature could be generalized to higher dimensions, showing that even in $AdS_5$ Kosevich-Lifshitz oscillations are present, nevertheless the Luttinger theorem is violated. In order to calculate the magnetic susceptibility $\chi = -\frac{\partial^2\Omega}{\partial B^2}$ we can use the relation between the free energy and the total charge in the dual CFT as in [55; 54]:

$$\hat{\Omega} \propto \hat{Q} = \int_0^{r_s} \sqrt{g(s)} r^3 \sigma(r) dr \tag{5.3.27}$$

where in general the charge density is

$$\sigma = \int_m^{\mu} g(E)\nu(E)dE \tag{5.3.28}$$

and the density of states in the full theory is

$$g(E) = \beta E(E^2 - m^2 - \ell B) \tag{5.3.29}$$

The easiest way to generalize the argument as presented in [54] to the higher dimensional case is to add an extra dimension, i.e. by considering the

cylindrical-like metric

$$ds^2 = -f dt^2 + \frac{1}{f} dr^2 + r^2 d\omega_2 + dz^2 \tag{5.3.30}$$

and then the integral expressing the charge density is generalized in $AdS_5$ just by adding an integration over $p_z$

$$\sigma = \frac{\beta B}{2} \int_{-\infty}^{\infty} dp_z \sum_l \int_{-\infty}^{\infty} dp \sum_l \frac{1}{1 + e^{\frac{E(l,p,p_z)-\mu}{T}}} \tag{5.3.31}$$

The energy, as in the $AdS_4$ case, is

$$E(l, p, p_z) = \sqrt{p^2 + p_z^2 + \ell B_{loc}} \tag{5.3.32}$$

The local physical quantities are related to the dual field theory quantities as [54]:

$$\begin{aligned} B_{loc} &\propto \frac{1}{r^2} \hat{B} \\ T_{loc} &= \frac{\hat{T}}{\sqrt{g_{tt}}} \end{aligned} \tag{5.3.33}$$

In the following calculation we will drop out this subscript, and restore the correct dependence on physical quantities back to position at a later point. The Poisson resummation over Landau levels gives

$$\sigma = \frac{\beta B}{2} \sum_k \int_0^{\infty} dl \int_{-\infty}^{\infty} dp_z \int_{-\infty}^{\infty} dp \sum_l \frac{1}{1 + e^{\frac{E(l,p,p_z)-\mu}{T}}} \tag{5.3.34}$$

Now expanding the Fermi distribution in terms of Matsubara frequencies and transforming the integral over $\ell$ into an integral over energies the integral (5.3.34) becomes

$$\begin{aligned} \sigma = -\frac{\beta T}{2} \sum_{k,n} \int_{-\infty}^{\infty} dp_z \int_{-\infty}^{\infty} dp\, e^{-\pi i k (p^2 + p_z^2 + m^2)/B} \times \\ \times \int_{\sqrt{p^2+p_z^2+m^2}}^{\infty} dE E \frac{e^{\pi i k E^2/B}}{E - \mu(1 + i\frac{T}{\mu} 2\pi(n + \frac{1}{2}))} \end{aligned} \tag{5.3.35}$$

This integral could be performed rotating the integration path so that the exponential in the numerator becomes real and decreasing, i.e. considering the rotation of the energy as $E \to E e^{i\pi/4}$ if $k > 0$ or $E \to E e^{-i\pi/4}$ if $k < 0$, and remembering that the lower integration limit is set to $\sqrt{p^2 + p_z^2 + m^2}$. In

this analytical continuation one has to take into account the role of the poles given by Matsubara frequencies. These poles contribute only if $p^2 + p_z^2 \leq \mu^2 - m^2$ and in addition $n + 1/2 > 0$ if $k > 0$ and $n + 1/2 < 0$ if $k < 0$. The contribution of the poles is the one giving the oscillatory part of the charge density $\sigma_{osc}$, and thus it' s the only one we will consider next, hence through the Residue theorem the $\sigma_{osc}$ is

$$\sigma_{osc} = 2\pi\beta T\mu \ \mathrm{Im} \sum_{k,n>0} e^{i\pi k(\mu^2-m^2)/B} e^{-4\pi^2 k\left(n-\frac{1}{2}\right)T\mu/B} \iint_D dp_z dp \, e^{-i\pi k(p^2+p_z^2)/B} \tag{5.3.36}$$

while the last integration is made in the region $D$, being the circle of radius $\sqrt{\mu^2 - m^2}$ in the plane $(p, p_z)$. This expression could be inserted in (5.3.27), thus obtaining the oscillating part of the free energy

$$\hat{\Omega}_{osc} \propto \hat{Q}_{osc} = 2\pi\beta T\mu \ \mathrm{Im} \sum_{k,n>0} \int_0^{r_S} dr r^3 \sqrt{g(r)} e^{i\pi k(\mu^2-m^2)/B} e^{-4\pi^2 k\left(n-\frac{1}{2}\right)T\mu/B} \times \\ \times \iint_D dp_z dp \, e^{-i\pi k(p^2+p_z^2)/B} \tag{5.3.37}$$

Since $\mu \gg B$, a saddle point approximation could be done. The $r$ dependence of the fast oscillating exponential is

$$e^{i\pi k(\mu^2-m^2)/B} = \exp i\pi k \left(\frac{h^2}{f} - m^2\right) \frac{r^2}{\hat{B}} = \exp ik \frac{A(r)}{\hat{B}} \tag{5.3.38}$$

With this approximation the integral (5.3.27) becomes

$$\hat{Q}_{osc} = 2\pi\beta \ \mathrm{Im} \sum_{k,n>0} r^* \sqrt{g(r^*)} \frac{m^* e^{i\pi/4} \sqrt{\hat{B}}}{\sqrt{A''(r^*)}} e^{i\pi k \frac{A(r^*)}{\hat{B}}} e^{-4\pi^2 k\left(n-\frac{1}{2}\right)m^* T/B} \times \\ \times \iint_D dp_z dp \, e^{-i\pi k(p^2+p_z^2)/B} \tag{5.3.39}$$

where, as usual, $r^*$ is the value of the radius where the argument of the exponential has an extremum. The last integration could be done passing to circular coordinates in the $(p, p_z)$ plane inserting the radial coordinate $\rho = \sqrt{p^2 + p_z^2}$ as

$$\iint_D dp_z dp \, e^{-i\pi k(p^2+p_z^2)/B} = \int_0^b \rho d\rho e^{-i\pi k\rho^2/B} = e^{-i\frac{b^2\pi}{2B}} \frac{\sin \frac{\pi b^2}{2B}}{\pi} \tag{5.3.40}$$

where $b = \sqrt{\mu^2 - m^2}$ has been defined. The oscillatory part of the total charge is then obtained introducing this result in (5.3.39). The summation over the index $n$ could be done as usual, giving an hyperbolic sine, moreover the sum over $k$ could be suppressed considering only the term $k = 1$, since the other terms are negligible. In the end after all dusts get settled the oscillating free energy is

$$\begin{aligned}\hat{\Omega} \propto \hat{Q}_{osc} &= 2\pi\beta \ \mathrm{Im}\left[\frac{1}{r^*}\sqrt{g(r^*)}\frac{m^*\hat{B}^{3/2}}{\sqrt{A''(r^*)}}e^{i\pi\frac{A(r^*)}{\hat{B}}}e^{-i\frac{b^2\pi}{2\hat{B}}}\frac{\sin\frac{\pi b^2}{2\hat{B}}}{\pi}\sum_{n>0}e^{-4\pi^2\left(n-\frac{1}{2}\right)m^*T/B}\right] = \\ &= F(r^*)\frac{\hat{B}^{\frac{5}{2}}}{\sqrt{A''(r^*)}}\frac{2\pi m^*T/B}{\sinh 2\pi m^*T/B}\mathrm{Im}\left[e^{i\pi/4}e^{i\pi\frac{A(r^*)}{\hat{B}}}e^{-i\frac{A(r^*)\pi}{2B}}\right]\sin\frac{\pi A(r^*)}{2B} = \\ &= F(r^*)\frac{\hat{B}^{\frac{5}{2}}}{\sqrt{A''(r^*)}}\frac{2\pi m^*T/B}{\sinh 2\pi m^*T/B}\left[\frac{\sqrt{2}}{2} - \cos\left(\frac{\pi A(r^*)}{B} - \frac{\pi}{4}\right)\right]\end{aligned} \tag{5.3.41}$$

The function $F(r^*)$ contains all the factors coming from the integration over the radial coordinates, like $\sqrt{g(r^*)}$ and the numerical prefactors. As can be seen, the expression found agrees with the standard result for three dimensional systems, apart from an additional and unimportant offset of the oscillations. In particular the usual scaling dimension with the magnetic field is found, i.e. $\hat{\Omega} \propto B^{5/2}$ [3] and the same frequency dependence of oscillations on the extremal section of the Fermi volume is observed.

## 5.4 Discussions

In a nutshell the findings of our paper is as follows: We built, using numerical means, a charged neutron star in the $AdS_5$ and analyzed in detail the related gravitational collapse to form a black hole. We depicted the critical behavior of the degenerate star with few plots and then solved the Dirac equation in the spherically symmetric star geometry. We wrote down a flow equation governing the dynamics of fermions constructing the charged neutron star in $AdS_5$. We encountered few problems while computing the boundary correlation function in the presence of the star, we list the difficulties that arise in finding the fermionic correlator in the star background. In a sense, according to [25; 9], it is an open question to find a reliable realization of the degenerate star using AdS/CFT duality and find a CFT interpretation of the OV limit [104] in the context of collapse phenomena. Here we note that, if one computes the retarded Green function 5.3.24 in the charged $AdS_5$ extremal

RN Black Hole background then, according to [80],

$$k_F \approx k_F(0) \exp(-\sigma m L) \tag{5.4.42}$$

i.e. one observes that the Fermi momentum fall off exponentially from the value it takes at zero fermion mass with $k_F(0) \simeq 0.8155$ and $\sigma \simeq 0.80$ for $AdS_5$ geometry, clearly indicating a violation of Luttinger's theorem and hence proving a non-Fermi liquid behavior in the black hole phase. This initially prompted us to make a conclusion that one possible holographic interpretation one could dub to this collapse process is that when a neutron star collapse to form a black hole, seeing from a boundary point of view one finds a second order phase transition from an ideal degenerate Fermi gas to a non-Fermi liquid. Recently in a paper [54] the authors have found that the Kosevich-Lifshitz oscillations still persist in the charged neutron star phase. In the same article the authors also explain how to reconcile the violation of Luttinger theorem in the case of the charged fermion star and the existence of the KL oscillation and the argument is still true in our $AdS_5$ case : only fermions in the spherical shell of radius $r^*$ contribute to the oscillations, and thus it' s not possible to reconstruct the whole Fermi volume from the analysis of oscillations. From the boundary field theory point of view this means that not all the degrees of freedom are taken into account through quantum oscillations, and this results in the violation of Luttinger theorem. Reproducing the calculations done in [54] in our $AdS_5$ charged star, we have found again the appearance of the KL oscillations due to magnetic field consistent with the standard results for three dimensional systems (see [3]). After all these, it is still not clear how to realize a holographic dual of the $AdS_5$ star, although it seems to us that both the star and the black hole are non-Fermi liquid states of matter.

Finally, despite trying to give a concrete holographic picture of this underlying phenomena we tried to rethink from a different perspective, all the existing results on this subject and did a coherent study of all of them reaching a conclusion that this elusive phenomena still require further studies.

## 5.5 The zero temperature and finite chemical potential two point function in flat space

In our analysis above we have used the crucial fact that the effect of finite chemical potential at zero temperature is captured by introducing a gauge field whose time component is the chemical potential (all other components being zero). In this section we shall try to justify this statement by considering fermions in flat space with a constant potential. We shall do this by

considering the two point function of the fermions. At first we shall view, the introduction of the chemical potential, as a redefinition of the vacuum state of theory of free fermions. Them from there we shall demonstrate that the two point function computed in this new vacuum state is the same as that computed for the case where the chemical potential is introduced through the time component of the gauge field. The later method more elegant and easy to generalize. In fact, we have used this above in more complicated settings where the chemical potential has a spatial variation. Therefore, in order to be certain, [10] we present an analysis of the situation in this simple setting and verify the equivalence of the two methods.

### 5.5.1 The free Fermi sea: The operator calculation

In this subsection we consider free massive fermions in flat space with the fermions being filled upto the fermi level with fermi momentum $k_F$. Thus the chemical potential [11] of the system is non-zero and is given by

$$\mu = \sqrt{k_F^2 + m^2},$$

with $m$ being the mass of the fermion. We consider the system to be at zero temperature. We will be interested to calculate the Feynman propagator or the time ordered two point correlator or this system. We shall perform this through an operator calculation in which the two point function is the expectation value of a product of two field operators in a state. This state is the one in which all the single particle states upto the Fermi momentum is filled up.

We consider free fermions in flat space with the system being described by the Dirac Lagrangian [111] This theory is a quadratic theory and can be solved exactly. The fields $\psi$ and $\bar{\psi}$ can be expanded in terms of the creation

[10] This fact is certainly true and is very well known for finite temperature. In case of finite temperature the chemical potential can be introduced but putting a twisted boundary condition for the fermion (instead of a mere anti-periodic one) along the compactified time circle. It is very well known that such twist can be undone by a gauge field whose time component is the chemical potential. This implies that the chemical potential can also introduced through such a gauge field without putting the twist. What we verify here is that it this fact continues to hold even at zero temperature.

[11] Here we shall define the chemical potential to be the energy required to add one more particle at the fermi momentum

and annihilation operators as follows

$$\psi(x) = \int \frac{d^3p}{(2\pi)^3}\frac{1}{\sqrt{2E_p}}\sum_s \left(a_p^s u^s(p)\exp\left(-ip.x\right) + b_p^{s\dagger}v^s(p)\exp\left(ip.x\right)\right),$$
$$\bar{\psi(x)} = \int \frac{d^3p}{(2\pi)^3}\frac{1}{\sqrt{2E_p}}\sum_s \left(a_p^{s\dagger}\bar{u}^s(p)\exp\left(ip.x\right) + b_p^{s}\bar{v}^s(p)\exp\left(-ip.x\right)\right). \tag{5.5.43}$$

Now we shall incorporate the presence of a finite chemical potential by constructing a state in which the fermions are filled upto the energy equal to the chemical potential, characterized by the fermi momentum. Let us denote the state in which the fermions are filled upto the fermi level by $|k_F\rangle$ such that,

$$|k_F\rangle = \prod_p^{k_F}\sqrt{2E_p}a_p^{s\dagger}|0\rangle. \tag{5.5.44}$$

Now for the time ordered correlation function we are required to calculate the quantities $\langle k_F|\psi(x)\bar{\psi}(y)|k_F\rangle$ and $\langle k_F|\bar{\psi}(y)\psi(x)|k_F\rangle$. These quantities evaluate to

$$\begin{aligned}
\langle k_F|\psi(x)\bar{\psi}(y)|k_F\rangle &= \int_{k_F}^{\infty}\frac{d^3p}{(2\pi)^3}\frac{1}{2E_p}(\not{p}+m)\exp\left(-p.(x-y)\right),\\
\langle k_F|\bar{\psi}(y)\psi(x)|k_F\rangle &= \int_{k_F}^{\infty}\frac{d^3p}{(2\pi)^3}\frac{1}{2E_p}(\not{p}-m)\exp\left(-p.(y-x)\right)\\
&\quad+\int_0^{k_F}\frac{d^3p}{(2\pi)^3}\left((\not{p}+m)\exp\left(-p.(x-y)\right)\right.\\
&\qquad\left.+(\not{p}-m)\exp\left(-p.(y-x)\right)\right).
\end{aligned} \tag{5.5.45}$$

Now the time-ordered two point correlation function is given by

$$S_F(x-y) = \begin{cases} \langle k_F|\psi(x)\bar{\psi}(y)|k_F\rangle, \text{ for } x_0 > y_0, \text{ (close the contour below)},\\ -\langle k_F|\bar{\psi}(y)\psi(x)|k_F\rangle, \text{ for } y_0 > x_0, \text{ (close the contour above)}. \end{cases} \tag{5.5.46}$$

Now the above two point function can be captured in the contour integral

$$S_F(x-y) = \int\frac{d^4p}{(2\pi)^4}\frac{i\left(\not{p}+m\right)}{p^2-m^2}\exp -ip.(x-y). \tag{5.5.47}$$

where the contour for $p_0$ is chosen as shown in fig:5.6. Nevertheless, the same answer can be obtained with the usual contour prescription (the dotted red

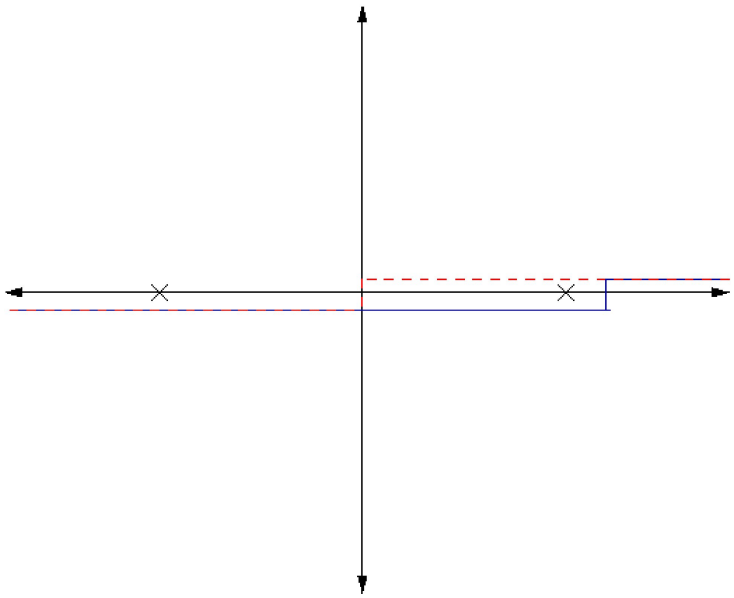

**Figure 5.6:** The contour prescriptions. The blue line is the new contour prescription in the presence of a finite constant chemical potential. The red dotted line represents the usual contour prescription.

line in fig:5.6) if we include a real shift of $\mu$ in $p_0$. Therefore it is convenient to define the shifted variable,

$$\tilde{p}_0 = p_0 - \mu$$

and make this substitution in (5.5.46). Then in terms of this shifted variable $\tilde{p}_0$ the contour prescription is the usual one. Now in terms of this shifted variables, the effect of $\mu$ is completely captured is we introduce a gauge field whose time component is $\mu$. This is true if we consider the eigenvalues of the $\partial_t$ operator to be $\tilde{p}_0$, instead of $p_0$. This justifies our use chemical potential as the time component of the gauge field.

# Chapter 6

# Solid States systems as Gravitational waves antennas

## Introduction

The formulation of elasticity in general relativity is analyzed, following the lines of Carter & Quintana [17]. As a first point, the description of the kinematics of a continuum medium requires some attention, and it will be analyzed in the first section together with the difference between the Lagrangian and the Eulerian framework. In the second section then the equation ruling the dynamics of an elastic medium will be derived, perturbation theory and possible effects on graphene monolayer are analyzed. In the last part of the chapter it will be analyzed the effect of gravitational waves in 3D TI, showing that the rotation of Dirac matrices is the main perturbation introduced by gravitational waves.

## 6.1 Kinematics

The richness of general relativity basically relies on the treatment of space and time at the same level, with the possibility of mixing them in whatsoever way is desired (or needed). At once, this also implies that the concept of space and time coordinates looses its meaning, considering that in the general case coordinates are not defined globally. Though extremely powerful, great drawback comes in the treatment of realistic systems in general relativity: the Newtonian concept of "body" as a finite region of space occupied by an ensemble of particles being subject to time-evolution, indeed, needs space and time to be clearly distinguishable. In space-time, i.e. a 4- dimensional pseudo-Riemannian Lorentzian manifold $(\mathcal{V}_4, g_{\mu\nu})$, dynamics of an ensemble

of particles is described by a collection of events making up an open submanifold $\mathcal{M} \subset \mathcal{V}_4$. To extract the physical meaning of its evolution, i.e. the time-like evolution of each particle of the medium, a reference manifold $\mathcal{B}$ is introduced, distinguished from $\mathcal{V}_4$, whose points are the idealized particle of the medium. The relationship between events $x^\mu \in \mathcal{V}_4$ and points $X \in \mathcal{B}$ is carried out through the *projection* map $\mathcal{P}$ from space-time to the abstract body $\mathcal{B}$

$$\mathcal{P} : x \in \mathcal{M} \to X \in \mathcal{B}. \tag{6.1.1}$$

This map projects a time-like curve, i.e. a curve in space-time whose tangent vector obeys the normalization condition $u_\mu u^\mu = -1$, to a point in $\mathcal{B}$ thus associating to each point of the idealizecd body its evolution in space-time. This is better said affirming that through the image through $\mathcal{P}^{-1}$ of a point $X \in \mathcal{B}$ is a time-like curve in $\mathcal{M}$. The projection $\mathcal{P}$ is also smooth, in the sense that it associates open neighborhoods in $\mathcal{B}$ to open neighborhoods in space-like surfaces in $\mathcal{M}$, i.e. given a point $x^\mu$ in a given space-like submanifold contained in $\mathcal{M}$ has a neighborhood $\mathcal{U}$ for which the projection $\mathcal{P} : \mathcal{U} \to \mathcal{B}$ is a differentiable embedding. The body $\mathcal{B}$ in general is a differential manifold but not necessarily a Riemmanian one, since there is not a metric intrinsically defined in it. A particular case in which on the contrary it is possible to define a metric in the body will be analyzed later in the paragraph.

Among all the possible coordinations of $\mathcal{M}$ the *co-moving coordinates* $x^a$ are the closest ones to the intuitive evolution of a continuum medium, and they will be used in all the following calculation. The projection of a given point $x^a (a = 1, 2, 3, 0)$[1] in these coordinates is $\mathcal{P} = X(x^1, x^2, x^3)$, where $X$ is a fixed coordination in $\mathcal{B}$. In addition, in a *properly* co-moving system of coordinates $x^0 \equiv \tau$ measures the proper time of the particle in the medium, i.e. $ds^2 > 0$ if $d\tau = 0$ and $ds^2 = -d\tau^2$ when $dx^1 = dx^2 = dx^3 = 0$. Note that the projection is necessary to define such a system of coordinates.

Both the coordinates $x^a$ and $(X^a, \tau)$ can be used to specify the state of the continuum.The description made using the space time coordinates is called *Eulerian*, while the description carried out through the reference body coordinates is called *Lagrangian* [116]. Note that the Lagrangian description requires the flow field $u^a$ to be given.

The definition of the flow vector $u^a$ given by $\mathcal{P}$ implies the definition of the symmetric tensor $\gamma_{ab}$

$$\gamma_{ab} = g_{ab} + u_a u_b \tag{6.1.2}$$

[1]Latin indexes $a, b, ...$ will be always used to indicate co-moving coordinates. Greek indexes $\alpha, \beta, ...$ will be used to label coordinates in the idealized body. The Greek indexes $\mu, \nu...$ are reserved to general coordinates in $\mathcal{V}_4$, and not used in the following.

having null contraction with $u^a$, i.e. $\gamma_{ab}u^b = 0$, and thus called *orthogonal projection tensor*. The tensor $\gamma_{ab}$ acts like an effective metric for u-orthogonal tensor fields, i.e. tensor fields having null contraction with the velocity $u^a$ and this makes clear its physical meaning: it determines the the distances between neighboring point in their rest frame, playing the role of the left Cauchy tensor [131] in classical theory, and it thus describes the *state of strain* of the system.
The projection map $\mathcal{P}$ induces a canonical isomorphism between the algebra of tensors defined in $\mathcal{B}$, also called material tensors, and the sub-algebra of u-orthogonal tensors in $T(\mathcal{V}_4) \equiv \otimes_i^j T_i^j(\mathcal{V}_4)$. This canonical isomorphism can be extended from tensors to tensor fields in the case of materially constant fields, i.e. tensor fields in space time whose projection through $\mathcal{P}$ is independent of the point in the world line. All the formulas in the following will be expressed in terms of space-time tensors, and only those containing materially constant fields will be subject to an unambiguous interpretation in terms of material tensors.
In all the treatment of material tensorial fields raised and lowered indexes are distinguished, since in general there is not an intrinsically defined metric on $\mathcal{B}$, untill the projection tensor $\gamma_{ab}$ is materially constant in itself (in this case the body is called *rigid*. This is equivalent to the definition given by Born and discussed in [130]). In other words, the metric needed to raise and lower indexes of tensors defined on the body $\mathcal{B}$ is the strain state of the body that is the output of the theory. In general the metric induced on $\mathcal{B}$ through the projection of $\gamma_{ab}$ will be not canonically defined, since it would depend on reparametrizations of $\tau$ and thus only when $\gamma_{ab}$ is constant respect to proper time $\tau$ the linear relation between covariant and contravariant tensors is well established. A general u-orthogonal tensor, on the other hand, will be projected into a material tensor depending on time, this projection being not canonical, in the sense specified previously. For such a field a notion of derivation along the world line, the *convected derivative*, is defined. In particular, the convected differential corresponds to the transport along the world line of an infinitesimal amount $d\tau$

$$\mathcal{P}(dT(x)) = d\mathcal{P}(T)(X, \tau) \tag{6.1.3}$$

where $d\mathcal{P}(T)(X, \tau)$ is the variation at a fixed point $X = \mathcal{P}(x)$ of the tensor $\mathcal{P}(T(x))$ due to an infinitesimal variation $d\tau$. The coefficient of the differential $d\tau$ defines the *convected derivative*

$$[T]^*(x) = \frac{d}{d\tau}T(x). \tag{6.1.4}$$

The convected derivative of a u-orthogonal field is zero if and only if it is a material constant field. In co-moving coordinates a material constant field

has constant components, i.e. independent of $\tau$. In other words, a material constant field is subject to parallel transport along the world lines, i.e. they are Lie transported by the flow field $u^a$. This identification of convected derivative can be extended to all tensor fields, giving an operational meaning to the definition above

$$[\ ]^* = \mathcal{L}_u. \tag{6.1.5}$$

Among all the tensor fields, the convected derivative of the strain tensor will play an important role for the following discussion. From (6.1.5) it follows that

$$[\gamma_{ab}]^* = \mathcal{L}_u \gamma_{ab} = 2(u_{(a;b)} + \dot{u}_{(a} u_{b)}) \equiv 2\theta_{ab}. \tag{6.1.6}$$

where $\theta_{ab}$ is the strain rate, and it is part of the decomposition of the covariant derivative of the flow field

$$u_{a;b} = \theta_{ab} + \omega_{ab} - \dot{u}_a u_b. \tag{6.1.7}$$

above the antisymmetric rotation tensor $\omega_{ab}$ has been introduced. The strain rate tensor can be further reduced introducing the trace free orthogonal tensor $\sigma_{ab}$, the shearing rate tensor

$$\theta_{ab} = \sigma_{ab} + \frac{1}{3}\theta\gamma_{ab} \tag{6.1.8}$$

here the trace of the strain rate tensor (also called *expansion rate*) $\theta = \theta^a_a \equiv \gamma^{ab} u_{a;b}$ has been introduced. The convected derivative of $\gamma^{ab}$ follows from (6.1.6) and the obvious equality $[\gamma_a{}^b]^* = 0$

$$\left[\gamma^{ab}\right]^* = -2\theta^{ab} \tag{6.1.9}$$

$$[\gamma_{ab}]^* = 2\theta^{ab} \tag{6.1.10}$$

As an important example of constant material field it will be analyzed the density tensor field $n_{abc}$. This tensor represents a canonical measure, possibly the only one in the general case, in the body $\mathcal{B}$ and it allows to define the density of particles per unit volume

$$dN = n_{abc} dX^a \wedge dX^b \wedge dX^c \tag{6.1.11}$$

The corresponding tensor in space time $n_{abc}$ is u-orthogonal $n_{abc}u^a = 0$ and its contraction with the space-volume density $n_{abc}\epsilon^{abc}$ derived from the Levi-Civita symbol defined in $\mathcal{V}_4$ will give the expression of the density of particles $n$ in the real space time. The space-volume is defined as $\epsilon_{abc} = \epsilon_{abcd}u^d$, and thus is u-orthogonal too. The convected derivative of the space-volume form comes from the $\tau$ derivative of $u^d$

$$[\epsilon^{abc}]^* = -\theta\epsilon_{abc} \tag{6.1.12}$$

and thus it determines the convected derivative of $n$, assumed that by definition the tensor $n_{abc}$ is materially constant, i.e. $[n_{abc}]^* = 0$,

$$[n]^* = -\theta n \tag{6.1.13}$$

Now that kinematics of a continuum medium and tensor fields has been established, in the following section the basic notions of elasticity will be defined.

## 6.2 Theory of Perfect Elasticity

Before using the machinery of the previous section to write the equations ruling the dynamics of a generic elastic continuum medium, the definition of such a medium will be given. A perfectly elastic material gives a symmetric contribution $T_{ab}$ to the energy momentum tensor respecting some additional conditions:

- there is no material energy transport relative to the local rest frames of the medium, i.e. the flow vector $u^a$ is an eigenvector of $T_{ab}$,
- the force $f^a$ due to the interaction of the medium with other fields, e.g. the electromagnetic field, respects the general conservation rule $T^{ab}{}_{;b} = f^a$,

From the first condition it follows that the energy momentum tensor $T_{ab}$ can be written as

$$T_{ab} = \rho u_a u_b + p_{ab} \tag{6.2.14}$$

where $\rho$ is the energy density and the symmetric tensor $p^{ab}$, called pressure tensor or negative stress tensor, is u-orthogonal. The reversibility of the evolution of a perfectly elastic body requires that $\rho$ and $p_{ab}$ are well defined functions of the strain $\gamma_{ab}$. This means that the projection of these quantities through $\mathcal{P}$ in their material correspondent depends only on the components of the projection of the strain tensor $\mathcal{P}(\gamma_{ab})$. As a counter-example, the stress energy tensor of a viscoelastic material will depend on $\mathcal{P}(\gamma_{ab})$ and its convected derivatives. As in the non general relativistic case, the dynamics of the system is contained in the energy momentum conservation law, holding by the second hypothesis given above (index lowered and raised respect to this definition so to have a final result consistent with [17])

$$\nabla^b T_{ab} = \gamma^{bc} \nabla_c T_{ab} = f_a. \tag{6.2.15}$$

Following the assumptions above, the energy-momentum tensor is function of the strain tensor $\gamma_{ab}$ through the seven functions $\rho$, $p_{ab}$. Since, as seen from

its definition (6.1.2), the strain tensor is completely determined once that the flow vector $u^a$ is known than the unknowns of eq. (6.2.15) are really the three independent components of the vector $u^a$. Projecting (6.2.15) on the space-platform through the contraction with the strain tensor, it is possible to write the three equations that solve the problem completely. Indeed, by virtue of (6.2.14) the covariant derivative of $T_{ab}$ explicitly is

$$\gamma^{bc}\nabla_c T_{ab} = \gamma^{bc}\left[\dot{\rho}u_a + \rho\dot{u}_a + \rho u_a\theta + (u_a\nabla_e u_d + \gamma_{ad}\dot{u}_e)p^{de}\right]. \tag{6.2.16}$$

Inserting this explicit form in (6.2.15) and contracting with $\gamma^{ef}$ gives three independent equation of motion

$$(\rho\gamma^{fe} + p^{fe})\dot{u}_e = f^f - \gamma^c{}_e\gamma^f{}_d\nabla_c p^{de} \tag{6.2.17}$$

these equations are enough to find the value of the three independent components of the flow vector $u^a$, once that the constitutive equations that specify the dependence of the stress tensor on $\gamma_{ab}$ are given. However another equation is obtained from (6.2.15) contracting it with the flow vector

$$\dot{\rho} = -\rho\theta - p^{ab}\theta_{ab}. \tag{6.2.18}$$

The presence of this equation is quite disturbing at a first glance, since it makes the system over-complete. Since it is a relation between the density $\rho$ and the stress tensor it will be proved, instead, that this equation greatly simplifies the constitutive equations. Indeed, the satisfaction of (6.2.18) is necessary and enough to completely determine the seven unknown functions in the energy momentum tensor $\rho, p^{ab}$. Eq. (6.2.18) written in term of convected differentials is

$$d\rho + \frac{1}{2}(\rho\gamma^{ab} + p^{ab})d\gamma_{ab} = 0 \tag{6.2.19}$$

and from this equation is possible to write the components of the stress tensor as a well defined function of the strain tensor $\gamma_{ab}$

$$p^{ab} = -2\frac{\partial\rho}{\partial\gamma_{ab}} - \rho\gamma^{ab}. \tag{6.2.20}$$

Thus, once specified the only free function $\rho$ in terms of the strain tensor, the energy-momentum tensor $T_{ab}$ is completely determined. The density $\rho$ can also be expressed in terms of the mass per particle $m$, $\rho = nm$. Eq. (6.2.20) expressed through derivatives of $m$ becomes, by virtue of equation (6.1.13)

$$p^{ab} = -2n\frac{\partial m}{\partial\gamma_{ab}} \tag{6.2.21}$$

To express the compatibility conditions when the 6 independent components of the strain tensor are given it is necessary to introduce the elasticity tensor $E^{abcd}$

$$E^{abcd} = -2\frac{\partial p^{ab}}{\partial \gamma_{cd}} - p^{ab}\gamma^{cd} \tag{6.2.22}$$

and by eq. (6.2.21), if the mass per particle is given it becomes

$$E^{abcd} = 4n\frac{\partial^2 m}{\partial \gamma_{ab}\partial \gamma_{cd}} \tag{6.2.23}$$

From eqs. (6.2.22) and (6.2.23) it follows that the elasticity tensor has only 21 independent components. If the equation of state is given specifying the functions $p_{ab}(\gamma_{ef})$ the symmetry condition for the corresponding tensor $E_{abcd}$ is the necessary and sufficient condition for the existence of the density function $\rho$ (or $m$). These conditions are the equivalent in general relativity of the Saint Venant condition. Since the strain tensor here contains information about both the metric $g_{ab}$ and the dynamics through the flow vector $u^a$, then the Elasticity tensor contains information about the curvature of the continuum system coming from both space-time and from the dynamics of the system. It follows that the known form of Saint Venant condition is a particular case in which the effective curvature is null, since there is no curvature in Minkowski space-time and in linear elasticity the strain do not produce any additional curvature. In this case, in addition, the vanishing effective curvature makes possible to define the strain tensor as a function of derivatives of the displacement vector [116; 78].
Untill now, equation written are for the most general case. In the following section the linearized case of an Hookean elastic body will be analyzed, making connection with the liner elasticity as expressed in Landau.

## 6.3 Linear Elasticity

The linear approximation of elasticity as formulated above is obtained expanding the constitutive equation $m(\gamma_{ab})$ up to the first order in the components of the strain tensor. The expansion is made around a reference configuration of the continuum where the elastic energy is minimized, i.e. the unstrained configuration. The strain tensor of this configuration will be indicated with $\kappa_{ab}$, considered as a material constant u-orthogonal tensor. To express the difference in the strain state in the dynamical evolution of the system from the unstrained configuration the Lagrangian strain tensor $e_{ab}$ is introduced

$$e_{ab} = \frac{1}{2}(\gamma_{ab} - \kappa_{ab}). \tag{6.3.24}$$

From eq. (6.1.10) it follows that the evolution of the Lagrangian strain tensor is given by

$$[e_{ab}]^* = \theta_{ab} \tag{6.3.25}$$

The mass per particle in the linear approximation is given by a quadratic form of the covariant components of the strain tensor

$$m = m_0 + K^{abcd} e_{ab} e_{cd} \tag{6.3.26}$$

where the tensor $K^{abcd}$ has the same symmetry properties of the elasticity tensor, and the link between these two is better specified using eq. (6.2.23)

$$E^{abcd} = nK^{abcd}. \tag{6.3.27}$$

Applying eq. (6.2.21) the pressure tensor is written simply in terms of the elasticity tensor in the linear approximation

$$p^{ab} = -E^{abcd} e_{cd}. \tag{6.3.28}$$

The isotropic case is the simplest one, where the tensor $K^{abcd}$ is given in function of rotational invariant combinations of the inverse of the reference strain configuration

$$K^{abcd} = \lambda(\kappa^{-1})^{ab}(\kappa^{-1})^{cd} + \mu[(\kappa^{-1})^{ac}(\kappa^{-1})^{db} + (\kappa^{-1})^{ad}(\kappa^{-1})^{cb}] \tag{6.3.29}$$

The coefficients $\lambda$ and $\mu$ are the Lamé coefficients, and are supposed to be materially constant i.e. with null convected derivative. This tensor is the analogous of the non-general relativistic case that could be found in literature [122]. To establish the connection with the usual formulation of linear elasticity a particular case will be considered: the reference strain will be taken delta-like $\kappa_{ab} = \delta_{ab}$. This is equivalent to say that in the reference configuration the body is in Minkowski metric, and it is a good starting point for a perturbative study of the effects of metric on an elastic body. Using this particular Ansatz the mass $m$ in (6.3.26) is written as

$$m - m_0 = \lambda e^2 + 2\mu e^{ab} e_{ab} = \left(\lambda + \frac{2}{3}\mu\right) e^2 + 2\mu r^{ab} r_{ab} \tag{6.3.30}$$

whrere $r_{ab} = e_{ab} - e/3\delta_{ab}$ and $e$ is the trace of the Lagrangian strain tensor $e = e^a{}_a$. This is exactly the form of the elastic free energy for the linear elasticity derived in Landau-Lifshitz. The pertubative approach to continuum mechanics in general relativity poses an important problem. In principle the state of strain of a continuum can change both due to a continuos displacements in its space-coordinates $x^a \to x^a + \Delta x^a(x^b)$ or due to a local

change of the metric $g_{ab} \rightarrow g_{ab} + \delta g_{ab}$. A displacement can always be "gauged away" in a change in the metric through a change of coordinates, thus a fully-consistent perturbation theory can be based only on perturbation to the metric. However, it is often convenient to keep fixed the coordinates, for example for symmetry reasons, and thus a suitable perturbation theory should keep these two form of perturbations. A fully consistent perturbation theory is built in [19; 16; 18; 27] and references therein, and it will be the subject of the following section.

## 6.4 Perturbative approach to elastodynamics in curved space time

The viewpoint exposed in the previous section about the dynamics of a continuum system is mathematically satisfactory but physically unclear. The intuitive description of the dynamics of an elastic body is based on the calculation of the displacement of point of the body from their unstressed equilibrium positions. In the general relativistic description the concept of displacement vector is lacking up to now, but this absence is innate in the basic setting of the problem. A possible simple definition of displacement vector could use the reference body $\mathcal{B}$: supposing the definition of a global coordinate system in the body, a displacement could be defined trivially as $X^\alpha \rightarrow X^\alpha + \Delta X^\alpha$. This variation produces a shift in the world lines through the inverse mapping $\mathcal{P}^{-1}(\mathcal{B})$: $x^\alpha \rightarrow x^{'a} = x^a + \xi^a(x^b)$. Unfortunately, this shift is in principle indistinguishable from a variation of the metric, since the coordinate $x^{'a}$ can be used to describe space-time by applying the change of coordinates on the metric

$$g'_{ab} = \frac{\partial x^c}{\partial x'^a} \frac{\partial x^d}{\partial x'^b} g_{cd}. \tag{6.4.31}$$

From this discussion it is clear that a coordinate system must be fixed in space-time in order to define displacement in the intuitive way. In this way, displacements and variation of the metric appear as separate perturbations for an elastic body. This is equivalent to what is implicitly done in ordinary elastodynamics, since the displacement is define with respect to an inertial frame of reference, where Minkowski flat metric is defined. From now on, the system of coordinates in space-time will be indicated as $x^a$. The variations in physical quantities can now be defined in the two coordinates systems: the variations defined in the co-moving system of coordinates will be named *Lagrangian variations* and indicated with $\Delta$, while the variations defined in the fixed space-time coordinates will be indicated as *Eulerian variations* and

identified with $\delta$. By definition, Lie derivative connects these two different descriptions

$$\Delta - \delta = \mathcal{L}_\xi \tag{6.4.32}$$

since it is the difference between a tensorial field (the variation in this case) parallel transported (Lagrangian variation) and the tensorial field itself (Eulerian variation). As an example, from (6.4.32) it is possible to write the Lagrangian variation of the metric when a displacement $\xi^a$ is defined, known its Eulerian variation $\delta g_{ab} = h_{ab}$

$$\Delta g_{ab} = h_{ab} + 2\xi_{(a;b)} \tag{6.4.33}$$

It is possible to apply these definition to the problem of defining the dynamics of displacements of an elastic body, by considering the Lagrangian variation of the equation of elasticity (6.2.17) in the form

$$\rho \dot{u}^a + \gamma^a{}_c p^{cb}{}_{;b} = 0 \tag{6.4.34}$$

In order to write the Lagrangian variation of this equation, the variation of the different tensorial fields are needed [18]. The variation of the density $\rho$ is

$$\Delta\rho = -\frac{1}{2}\rho y^{cd}\Delta_{cd} \tag{6.4.35}$$

and the variation of the pressure is

$$\Delta p^{ab} = -\frac{1}{2}\left(E^{abcd} + p^{ab}\gamma^{cd} - \frac{4}{c^2}p^{c(a}u^{b)}u^d\right)\Delta cd \tag{6.4.36}$$

where

$$y^{cd} = \gamma^{cd} + \frac{1}{\rho c^2}p^{cd}. \tag{6.4.37}$$

Using these formulas the Lagrangian variation of eq. (6.2.17) becomes

$$\begin{aligned}(A^{ab}{}_c{}^d - \rho y^a{}_c u^b u^d)\Delta\Gamma^c{}_{bd} = &-\gamma^a{}_c E^{cebd}{}_{;e}\epsilon_{bd} + \\ &+\frac{1}{c^2}\left(p^{ab}\dot{u}^d - \frac{1}{2}\dot{u}^a p^{bd} - 2A^{a(b}{}_c{}^{e)}v^c{}_e u^d + \rho y^a{}_c \dot{u}^c u^b u^d\right)\Delta_{bd}\end{aligned} \tag{6.4.38}$$

where the Lagrangian variation of the connection coefficient is

$$\Delta\Gamma^c{}_{bd} = \xi^c_{;(b;d)} + h^c{}_{(b;d)} - \frac{1}{2}h_{bd}{}^c - \xi^e R^c{}_{(bd)e}. \tag{6.4.39}$$

Eq. (6.4.38) greatly simplifies when small perturbation of the metric are considered, acting on a weak gravitational field [18; 16]

$$\gamma^a{}_c u^b u^d (\xi^c{}_{b;d} + h^c{}_{b;d} - \frac{1}{2} h_{bd}{}^{;c}) = \rho^{-1} \left[ E^{abcd} \left( \xi_{c;d} + \frac{1}{2} h_{cd} \right) \right]_{;b} \tag{6.4.40}$$

This equation can be found adding the perturbation [27]

$$\mathcal{L}' = -\frac{1}{2} h_{ab} T^{ab} \tag{6.4.41}$$

to the lagrangian of a continuous medium. The simplest case that can be considered is a gravitational wave interacting with an elastic medium in flat space time. The covariant derivatives in this case are replaced with ordinary derivatives, and the Hilbert gauge for the perturbation to the metric $h_{ab}$

$$h_a{}^b{}_{;b} = \frac{1}{2} h_b{}^b{}_{;a} \tag{6.4.42}$$

makes the terms depending on $h_{ab}$ in the left side of (6.4.40) to drop out, living the simple equation [27]

$$\partial_t (\rho \partial_t \xi^a) = \partial_b \left[ E^{abcd} \left( \xi^{c,d} - \frac{1}{2} h^{cd} \right) \right]. \tag{6.4.43}$$

It follows that an isotropic medium, whose elasticity tensor is given in (6.3.29), couples with geometry only through the inhomogeneities of the medium. In general, this inhomogeneity is given by the boundary of the solid body with vacuum [27; 137]. A brief example on the use of eq. (6.4.40) is given in the next subsection.

### 6.4.1 Axially symmetric perturbation of a membrane

In this subsection it will be analyzed the case of an axial symmetric change of coordinates added to flat space time

$$x^a \to x^a + f(r) \delta^{a3} \tag{6.4.44}$$

where $r = \sqrt{x^2 + y^2}$. The function $f(r)$ is supposed to have a compact support, i.e. $f(r) \to 0$ for $r \to \infty$, and $f'(0) = 0$. The metric in the coordinates $(t, r, \theta, z')$ is

$$g_{ab} = \begin{pmatrix} -1 & 0 & 0 & 0 \\ 0 & 1 + (f'(r))^2 & 0 & -f'(r) \\ 0 & 0 & r^2 & 0 \\ 0 & -f'(r) & 0 & 1 \end{pmatrix} \tag{6.4.45}$$

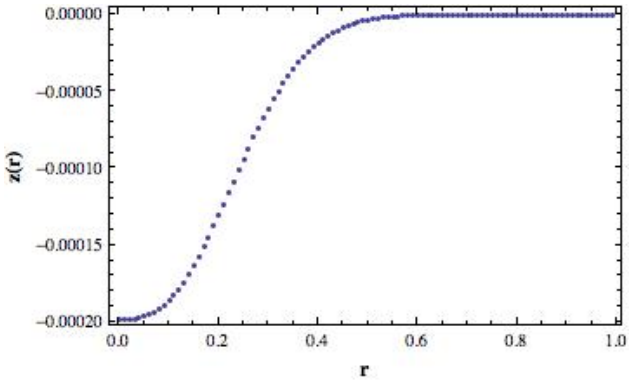


**Figure 6.1:** Radial deformation of a membrane in an gaussian axial symmetric perturbation, with parameters $a = 0.1$, $b = 0.01$ in arbitrary units.

In the case of a membrane the out-of-plane and in-plane deformations can be decoupled [78]. For the out-of-plane deformations, only the displacement $\xi_z(x, y)$ is considered to be different from zero. With this assumption, and considering the radial symmetry of the problem, eq. (6.4.40) becomes

$$\xi_z''(r) = -f''(r) \Rightarrow \xi_z(r) = -f(r) \tag{6.4.46}$$

with the boundary conditions $\xi_z \to 0$ for $r \to \infty$ and $\xi_z'(0) = 0$. For the in-plane deformation the equation reduces again to a very simple form

$$\partial_r \xi_r = \frac{1}{2}(f'(r))^2 \tag{6.4.47}$$

The solution to this equation in the case of a gaussian perturbation $f(r) = ae^{-x^2/b^2}$ is plotted in fig.6.1. Thus, from eq. (6.4.46) the observer in coordinates $x'^a$ sees the membrane curved in the $z$ direction following the profile of the perturbation $f(r)$ and contracted with radial symmetry in a neighborhood of the origin.

## 6.5 Interaction of gravitational waves with monolayer graphene

In this section the existence and the corresponding magnitude of the scattering of gravitational waves on graphene will be analyzed. As a first step, the efficiency of energy transfer from gravitational waves to graphene monolayer will be calculated. In his article Dyson makes estimations of the energy transfer in the scattering of gravitational waves with the surface of Earth,

considered as flat. Considering a gravitational incident with angle $\theta$ with the inward normal $k = (\omega/c)(\sin\theta, 0, \cos\theta)$, the perturbation to the metric given by the gravitational wave is

$$h_{ij} = aR_jR_ke^{i(k_ix^i-\omega t)} \tag{6.5.48}$$

where $a$ is a dimensionless parameter that fixes the amplitude of gravitational waves and for a circularly polarized wave the vector $R_i$ is

$$R_i = \frac{1}{\sqrt{2}}(\cos\theta, i, -\sin\theta). \tag{6.5.49}$$

The displacement vector $y^j$ is calculated using the boundary conditions, through the consideration that velocity both the longitudinal and transverse modes is much smaller than the velocity of light $c_t < c_l \ll c$

$$y^i = \frac{a}{2}\frac{c_t}{\omega}\sin\theta\left(\cos\theta, i, -\frac{c_t}{c_l}\sin\theta\right). \tag{6.5.50}$$

The energy per unit surface and unit time of the gravitational wave transformed in elastic energy of the Earth is

$$Q = \frac{1}{2}\rho\omega^2[c_t(|y^1|^2 + |y^2|^2) + c_l|y^3|^2]. \tag{6.5.51}$$

The total flux of energy per unit time carried by the gravitational wave is [77]

$$F = \frac{c^3\omega^2a^2}{64\pi G}|\cos\theta| \tag{6.5.52}$$

The efficiency of the transfer $\epsilon$ is defined as the ratio between $Q$ and $F$

$$\epsilon \propto \left(\frac{8\pi G\rho}{\omega^2}\right)\left(\frac{c_t}{c}\right)^3 \tag{6.5.53}$$

Dyson is interested in the $1Hz$ band of gravitational waves, and his estimations of physical effects proceeds as follows: two factor enter this estimation, the mass density and the velocity of transverse waves. Using the values $\rho = 5.5g/cm^3$ and $c_t \approx 4.5\times10^5 cm/s$ Dyson estimates $8\pi G\rho \approx 5\times10^{-6}sec^{-2}$, and the ratio between the transverse velocity and the velocity of light is about $1.5 \times 10^{-5}$, giving an efficiency in the case of Earth $\epsilon \approx 10^{-21}$. A first estimation for the effects on graphene could be done using the corresponding values for bulk graphite [11; 4] $\rho = 2.23g/cm^3$, $c_t = 1.38 \times 10^6 cm/s$, giving $8\pi G\rho = 3.7\times10^{-6}s^{-2}$ and $c_t/c \approx 10^{-5}$, giving an estimation for the efficiency $\epsilon \approx 3.6 \times 10^{-19}$. This estimation is made for the $1Hz$ band, as in the case of

Dyson's calculation, and it shows that bulk graphite is 2 order of magnitudes more efficient than Earth to reveal gravitational waves. If the $1GHz$ band is considered, the presence of the $\omega^{-2}$ factor in (6.5.53) reduces drastically the efficiency to the value $\epsilon \approx 10^{-37}$.
A finer estimation could be done using the mass density and the transverse velocity for monolayer graphene. Due to dimensionality ($\rho \sim M/L^2$ and not $M/L^3$) eq. (6.5.51) cannot be used for an estimation of the elastic energy flux. An estimation done in the same spirit of Dyson can be performed as follows: the energy flux per unit time can be calculated dividing the power generated by elastic forces inside the graphene monolayer for the area of the monolayer itself. Given the displacement $y^i$ in graphene, the power of elastic forces $P$ can be roughly estimated as

$$P = F|\dot{y}| = k|y||\dot{y}| = M\omega^2|y||\dot{y}|.$$

Dividing by the area of the sample and considering that $\dot{y} \approx \omega y$ and eq. (6.5.50) the flux of elastic energy for a graphene monolayer $Q_g$ is

$$Q_g = \rho\omega^3|y|^2 = \frac{a^2}{4}\rho\omega v_s^2. \tag{6.5.54}$$

where $v_s$ is the sound velocity. By using (6.5.52) for the energy flux of gravitational waves, the efficiency for graphene evaluates as

$$\epsilon_g \propto \frac{16\pi G\rho}{\omega v_s}\left(\frac{v_s}{c}\right)^3 \tag{6.5.55}$$

In the case of graphene, the mass density is [63] $\rho = 7.6\times10^{-8}g/cm^2$, and the sound velocity [140] is $v_s \approx 8Km/s$. With these values of the parameters, the dimensionless quantity $16\pi G\rho/v_s\omega$ has the value

$$\frac{16\pi G\rho}{\omega v_s} \approx \frac{3\times10^{-20}}{\omega}. \tag{6.5.56}$$

Thus, in the case of the gigahertz band this quantity evaluates as $3\times10^{-29}$. The ratio between the velocity of sound and the velocity of light is about $2.6\times10^{-5}$, giving a value for the efficiency in the gigahertz window $\epsilon(\omega = 1GHz) \approx 10^{-42}$. In the $1Hz$ this values reaches the value $\epsilon(\omega = 1Hz) \approx 10^{-33}$.
From (6.5.52) it can be estimated the value of the magnitude of the gravitational waves $a$, and thus the order of magnitude of the displacements (6.5.50). Indeed, for a black body the flux is $F = 2\times10^{-5}erg/cm^2s$, and

thus $a\omega = 3 \times 10^{-21} Hz$. For a normally incident wave $y = av_s/2\omega$, that could then be evaluated explicitly by virtue of the preceding considerations

$$y = 1.5 \times 10^{-21} Hz \left(\frac{v_s}{\omega^2}\right) \tag{6.5.57}$$

In the case of graphene in the gigahertz band of gravitational waves this displacement is of the order of $1.5 \times 10^{-33} cm$. In conclusion, in the case of a membrane the efficiency $\epsilon \sim \omega^{-1}$, and thus in principle at high frequency it reacts better than a 3D solid, but this gain is overwhelmed by the small mass density. It also follows from the value of the frequency windows interesting to this study that the average displacement generated by a gravitational wave is 16 orders of magnitude smaller than what is expected for Earth, following the estimations found in litterature.

## 6.6 Graphene as a gravitational wave antenna through the interaction with electromagnetic field

In this section the case of gravitational waves will be considered. When the metric is of the form $g_{\mu\nu} = g^0_{\mu\nu} + h_{\mu\nu}$ the Einstein equations are simply

$$R_{\mu\nu} = \Box h_{\mu\nu} = 0 \tag{6.6.58}$$

where $\Box = \nabla^\mu \nabla_\mu$. In the following the symmetric traceless gauge will be used in which the perturbation $h_{\mu\nu}$ satisfies the gauge conditions

$$\partial_\mu h^\mu_\nu = 0, \quad h^\mu_\mu = 0. \tag{6.6.59}$$

The explicit form of $h_{\mu\nu}$ satisfying these conditions is

$$h_{\mu\nu} = \begin{pmatrix} 0 & 0 & 0 & 0 \\ 0 & h_+ & h_\times & 0 \\ 0 & h_\times & -h_+ & 0 \\ 0 & 0 & 0 & 0 \end{pmatrix}, \tag{6.6.60}$$

where both $h_+$ and $h_\times$ are functions of $kz - \omega t$. From eq. (6.6.59) it follows that the determinant of the metric is unchanged, since $g = g_0 + h^\mu_\mu \equiv g_0$, where $g_0$ is the determinant of the unperturbed metric. Tensorial indexes are lowered and raised with the unperturbed metric $g^0_{\mu\nu}$. In this section it will be assumed that $g^0_{\mu\nu} = \eta_{\mu\nu}$, i.e. the unperturbed metric is the Minkowski one.

As shown in the preceding section, the coupling of graphene with gravitational waves could be taken as negligible. This can be thought as advantage, and not necessarily as a drawback. If graphene is made to interact with another physical field that is better coupled to geometry of space-time, then it's possible to use the knowledge trasport properties in graphene to highlight this interaction. The first candidate as a possible interacting field is the electromagnetic field. The coupling of electromagnetic field with geometry is one the most studied subjects in general relativity, and the basics elements needed to carry out our analysis can be found in standard manuals [96]. More sophisticated studies can be found in both classical literature [128] and more recent developments [132], but this treatment based on co-moving coordinates will not be used here, since at this stage we are interested in the effects of a small curvature perturbing Minkowski space-time. The field tensor $F_{\mu\nu}$ satisfies the Maxwell equations

$$F_{\mu\nu;\lambda} + F_{\mu\lambda;\nu} + F_{\lambda\nu;\mu} = 0 \tag{6.6.61}$$

$${}^{*}F^{\mu\nu}{}_{;\nu} = *j^{\mu}. \tag{6.6.62}$$

The Maxwell equations are unperturbed by space-time geometry in the case of gravitational waves. Indeed, the field tensor by definition is

$$F_{\mu\nu} = \nabla_{\mu}A_{\nu} - \nabla_{\nu}A_{\mu} = \partial_{\mu}A_{\nu} - \partial_{\nu}A_{\mu} \tag{6.6.63}$$

where the last equality is justified by the symmetry of Christoffel symbols $\Gamma^{\lambda}_{\mu\nu} = \Gamma^{\lambda}_{\nu\mu}$. Eq. (6.6.62) written explicitly is

$$\frac{1}{\sqrt{-g}}\partial_{\mu}\sqrt{-g}F^{\mu\nu} = j^{\nu} \tag{6.6.64}$$

Since the determinant of the metric is unchanged by the perturbation $h_{\mu\nu}$, then the Maxwell equations are the same as in flat space-time. The corrections to the covariant components of the vector potential $A^{\mu}$ are then null too, but this is not the case for the contravariant ones $A_{\mu}$, that obeys to the equation

$$\Box A_{\mu} = R^{\nu}{}_{\mu}A_{\nu} \tag{6.6.65}$$

where the d' Alembert operator in curved space time is $\Box = g^{\mu\nu}\nabla_{\nu}\nabla_{\mu}$. Considering that for a contravariant vector field, the covariant differentiation is $\nabla_{\mu}A_{\lambda} = \partial_{\mu} - \Gamma^{\xi}_{\mu\lambda}A_{\xi}$, the wave equation reads explicitly

$$\frac{1}{\sqrt{-g}}\partial_{\mu}\sqrt{-g}g^{\mu\eta}\nabla_{\eta}A_{\lambda} - g^{\mu\nu}\Gamma^{\eta}_{\nu\lambda}\nabla_{\mu}A_{\eta} = R^{\xi}{}_{\lambda}A_{\xi} \tag{6.6.66}$$

This equation greatly simplifies in the case of weak gravitational fields. Due to eq. (6.6.58) left side of (6.6.66) is zero and then taking only first order terms in (6.6.66) the wave equation become

$$\Box A_\lambda + h^{\mu\eta}\partial_\mu\partial_\eta A_\lambda + \eta^{\mu\eta}\partial_\mu\Gamma^\xi_{\eta\lambda}A_\xi = 0. \tag{6.6.67}$$

It can be demonstrated that the third term on the right-hand side is null, since

$$\eta^{\mu\eta}\partial_\mu\Gamma^\xi_{\eta\lambda} = \frac{1}{2}\eta^{\mu\eta}\eta^{\xi\sigma}[\partial_\mu\partial_\lambda h_{\sigma\eta} + \partial_\eta\partial_\mu h_{\sigma\lambda} - \partial_\mu\partial_\sigma h_{\eta\lambda}] \tag{6.6.68}$$

Due to eq. (6.6.58), (6.6.59) this term then is zero, leaving the equation

$$\Box A_\lambda + h^{\mu\eta}\partial_\mu\partial_\eta A_\lambda = 0. \tag{6.6.69}$$

where $\Box = \partial^\mu\partial_\mu$.

## 6.7 Graphite as a gravitational wave detector

From Eq.(6.5.53) it is seen that graphite could be a good candidate to detect gravitational waves, since it has a better efficiency than e.g. Earth. In this section a mechanical resonator made of a cylindrical bar of radius $R$ and with length $L$ of graphite will be studied. As a first step, the finite section of the bar will be neglected, later the correction to the eigenfrequencies due finite radius $R$ will be analyzed. If the radius is $R \ll L$ the length of the resonator is fixed imposing that the resonance frequency of the bar should be close to that of the gravitational wave we are interested in, i.e. 1 GHz. The eigenfrequencies of a bar with both the ends free are [78]

$$\omega_n = \pi\frac{v_s}{L}n \tag{6.7.70}$$

and, in the case of a bar, the velocity of sound is $v_s = \sqrt{E/\rho}$, where $E$ is the Young modulus and $\rho$ is the density. In the case of graphite $\rho = 1.79 \times 10^3 Kg/m^3$ and $E = 10\ Gpa$, and the request of an eigenfrequency $\omega_n \approx 1\ GHz$ gives a length of the order $L = 1\mu m$. In the following only the lowest mode $n = 1$ will be considered, and its frequency denoted with $\omega_0$. Let's treat the resonator as a spring that oscillates with frequency $\omega$ having the mass of the resonator $m = \rho V$ sticked at its ends. Defining with $\xi$ the deformation of the spring, its equation of motion is

$$\ddot{\xi} + \frac{\dot{\xi}}{\tau_0} + \omega_0^2\xi = \gamma \tag{6.7.71}$$

$\tau_0$ is the damping time for the mode, that takes into account internal dissipation processes of the material, and $\gamma$ is the acceleration produced by the gravitational waves. Here I will consider the case of a monochromatic wave, with $h_+$ polarization traveling along the $z$-axis

$$h_{\mu\nu} = h_+ \sigma_z e^{i(\omega t - kz)}. \tag{6.7.72}$$

In the following the resonator will be posed in the $xy$ plane, with generic orientation. The components of the acceleration $\vec{\gamma}$ are

$$\begin{aligned} \gamma_x &= -R_{x,0,j,0}\hat{x}^j = -\frac{1}{2}\omega^2 h_+ e^{i\omega t}\hat{x} \\ \gamma_x &= -R_{y,0,j,0}\hat{x}^j = \frac{1}{2}\omega^2 h_+ e^{i\omega t}\hat{y} \end{aligned} \tag{6.7.73}$$

and its projection along the oscillator direction is

$$\gamma = -\frac{1}{2}\omega^2 h_+ e^{i\omega t} L \sin^2\theta \cos 2\phi. \tag{6.7.74}$$

With this perturbation (6.7.71) has the following general solution

$$\xi = \frac{\frac{1}{2}\omega^2 h_+ L \sin^2\theta \cos 2\phi}{\omega^2 - \omega_0^2 + i\omega/\tau_0} e^{i\omega t}. \tag{6.7.75}$$

When $\omega$ is close to the resonance, i.e. $|\omega - \omega_0| \ll \omega_0$, the formula above simplies as

$$\xi = \frac{\frac{1}{4}\omega_0 h_+ L \sin^2\theta \cos 2\phi}{|\omega| - \omega_0 + i\ sign(\omega)/\tau_0} e^{i\omega t}. \tag{6.7.76}$$

The energy of the resonator, when exited by the gravitational radiation then is $E_{el} = 2 \cdot (1/2)\omega_0^2 \xi^2$. Assuming that the dumping due to internal processes is much bigger than that produced by the emission of gravitational waves from the resonator, the cross section of this idealized resonator can be calculated making the ratio between this elastic energy and the flux of energy of gravitational waves

$$E_{GW} = T^{0z} = \frac{1}{32\pi}\omega^2 h_+^2. \tag{6.7.77}$$

The resulting cross-section $\sigma(\omega)$ is

$$\sigma(\omega) = \frac{2\pi M L^2 (\omega_0^2/\tau_0) \sin^4\theta \cos 2\phi}{(|\omega| - \omega_0)^2 + (1/2\tau_0)^2} \tag{6.7.78}$$

It's easy at this point to introduce the effect of unpolarized incoming gravitational radiation. Indeed, the other polarization $h_\times$ will have the same

contribution but for a factor $\sin^2 2\phi$ instead of the cosine. Thus, the cross section for unpolarized radiation $\langle\sigma\rangle$, obtained through an average over the direction of the incoming wave and the detector is

$$\langle\sigma(\omega)\rangle = \frac{8\pi}{15}\frac{ML^2(\omega_0^2/\tau_0)}{(|\omega|-\omega_0)^2+(1/2\tau_0)^2} \tag{6.7.79}$$

The maximum value of this quantity is $\langle\sigma(\omega_0)\rangle \equiv \langle\sigma\rangle_{max}$

$$\langle\sigma\rangle_{max} = \frac{8\pi}{15}8\pi ML^2(\omega_0^2\tau_0) \tag{6.7.80}$$

This value can be expressed in a more suggestive way introducing the Schwarzchild radius $r_g = 4mg/c^2$

$$\frac{\langle\sigma\rangle_{max}}{(2L)^2} = \frac{4\pi^2}{15}\frac{r_g}{\lambda_0}(\omega_0\tau_0). \tag{6.7.81}$$

This quantity for a graphite bar of $1\mu\ m$ length is quite small: $r_g = 8\times 10^{-45}m$, $\lambda_0 \approx 10^{-1}m$. The product $Q = \omega_0\tau_0$ is the energy dissipated per radian of oscillation, and it depends on the internal dissipation of the material. Following Weber it will be taken equal to $10^5$, giving finally $\langle\sigma\rangle_{max}/(2L)^2 \approx 5\times 10^{-39}$.
In general, the radiation hitting the detector will not be monochromatic, as in the case considered until now. When the frequency window is bigger than the width of the resonance of the detector the meaningful quantity is not the cross section $\sigma(\omega)$ but its integral over frequencies, often called "integral over the resonance"

$$\int_{-\infty}^{\infty}\sigma(\omega)\frac{d\omega}{2\pi} \tag{6.7.82}$$

The integral over the resonance of equation (6.7.79) can be expressed in a similar fashion of (6.7.81)

$$\frac{1}{(2L)^2}\int_{-\infty}^{\infty}\sigma(\omega)\frac{d\omega}{2\pi} = \frac{2\pi^2}{15}\frac{r_g}{\lambda_0}\omega_0 \approx 10^{-34} \tag{6.7.83}$$

This quantity also has the advantage of being independent of the internal dissipation. All the above formulae have been derived simplifying the detector as a spring, but a more refined estimation of the cross section can be done by using a symmetric shape for the bar, i.e. cylindrical

### 6.7.1 Vibrating bar as a detector

In this subsection with radius $R$ and length $L$ will be used as a detector for gravitational waves [105; 117; 96]. Given the complete set $\vec{U}_n$ of eigenvectors

for each eigenmode of the bar the general displacement $\vec{\xi}$ is

$$\vec{\xi} = \sum_n B_n(t)\vec{U}_n \tag{6.7.84}$$

and the equation of motion for the coefficients $B_n(t)$ takes into account the coupling with the driving force coming from gravitational wave with Riemann tensor $R^{\alpha}_{\beta\gamma\delta}$

$$\ddot{B} + \frac{\dot{B}_n}{\tau_n} + \omega_n^2 B_n = -c^2 R_{i0j0} \int d^3x \;\; U_n^i x^j. \tag{6.7.85}$$

In the following the components of the variation of the moment of inertia will be indicated with $U^{ij}$

$$U^{ij} = \int d^3x \;\; U_n^i x^j. \tag{6.7.86}$$

When the mode parameter $\alpha_n$

$$\alpha_n = \frac{n\pi R}{L} \tag{6.7.87}$$

is less than unity then the finite cylinder can be approximated with an infinite one (Pochammer Chree approximation) and the cross section can be calculated up to the second order in $\alpha_n$ in a similar way of that of a spring [105]. In the following the dimensionless variables $\rho$ and $\zeta$ will be used

$$\begin{aligned} \rho &= r/R \\ \zeta &= z/R. \end{aligned} \tag{6.7.88}$$

The eigenfrequencies of the bar up to the second order in $\alpha_n$ are

$$\omega_n = \frac{\alpha_n}{R} v_s \sqrt{1 - \frac{1}{2}\sigma^2 \alpha_n^2} \tag{6.7.89}$$

where $\sigma$ is the Poisson ratio and the corresponding mode at the same order has components

$$\begin{aligned} U_n^{\rho} &= A_n \sigma \alpha_n \sin(\alpha_n \zeta) \\ U_n^{\theta} &= 0 \\ U_n^{\zeta} &= A_n \left(1 - \frac{\sigma}{2}\alpha_n^2 \rho^2\right) \cos(\alpha_n \zeta) \end{aligned} \tag{6.7.90}$$

where $A_n$ is the normalization costant for the $n$th mode

$$A_n = \sqrt{\frac{2}{V}} \left[1 + \frac{\sigma(1-\sigma)}{4}\alpha_n^2\right] \tag{6.7.91}$$

and $V$ is the volume of the bar. With this definition the quantities (6.7.86) up to the order $o(\alpha_n^2)$ are

$$U_n^{ij} = \sqrt{2V}\frac{L}{(n\pi)^2}[(-1)^n - 1]\begin{pmatrix} -(\sigma/4)\alpha_n^2 & 0 & 0 \\ 0 & -(\sigma/4)\alpha_n^2 & 0 \\ 0 & 0 & 1-(\sigma^2/4)\alpha_n^2 \end{pmatrix}. \tag{6.7.92}$$

From this expression it follows that only the odd modes, i.e. when $n = 2m+1$, there is a coupling between the eigenmodes of the bar and the gravitational radiation. The Riemann tensor for unpolarized radiation incident at an angle $\theta_i$ from the detector axis is

$$R_{i0j0} = \begin{pmatrix} -R_+\cos^2\theta_i & R_\times\cos\theta_i & R_+\cos\theta_i\sin\theta_i \\ R_\times\cos\theta_i & R_+ & -R_\times\sin\theta_i \\ R_+\cos\theta_i & -R_\times\sin\theta_i & -R_+\sin^2\theta_i \end{pmatrix} \tag{6.7.93}$$

The driving term in (6.7.85) then is

$$-c^2 R_{i0j0}U_n^{ij} = -c^2 R_+(U_n^{22} - U_n^{33})\sin^2\theta_i \tag{6.7.94}$$

The energy adsorbed by the $n$-th mode then is

$$\begin{aligned} E_n &= -c^2\rho(U_n^{22} - U_n^{33})\sin^2\theta_i \int_{-\infty}^{\infty} dt\dot{B}(t)R_+(t) = \\ &= c^4\rho(U_n^{22} - U_n^{33})^2\sin^4\theta_i \int_{-\infty}^{\infty} d\omega \frac{1}{\tau_n}\frac{\omega^2|R_+(\omega)|^2}{(\omega^2-\omega_n^2)^2 + \frac{\omega^2}{\tau_n^2}} = \\ &= \int_{-\infty}^{\infty} d\omega\sigma_n(\omega)F(\omega) \end{aligned} \tag{6.7.95}$$

where the flux of the incoming wave is

$$F(\omega) = \frac{c^7}{4\pi G}\frac{|R_+(\omega)|^2}{\omega^2} \tag{6.7.96}$$

and the expression of the cross section $\sigma_n(\omega)$ is

$$\sigma_n(\omega) = \frac{4\pi G}{c^4}\rho(U_n^{22} - U_n^{33})^2\sin^4\theta_i\frac{1}{\tau_n}\frac{\omega^4}{(\omega^2-\omega_n^2)^2 + \frac{\omega^2}{\tau_n^2}}. \tag{6.7.97}$$

The integral over the frequencies of this cross section would be divergent, unless the approximation of having the resonance frequency close to the incoming wave one. This ultraviolet divergence is not physical since the adsorbed

energy has a cut-off coming from the flux $F(\omega)$. This consideration leads to the definition of the integral over the resonance

$$\int_{-\infty}^{\infty}\sigma_n(\omega)d\omega=\frac{1}{F(\omega_n)}\int_{-\infty}^{\infty}\sigma_n(\omega)F(\omega)d\omega=\frac{8}{\pi}\frac{M}{n^2}\frac{G}{c}\left(\frac{v_s}{c}\right)^2\sin^4\theta_i\left[1+\frac{\sigma(1-2\sigma)}{2}\alpha_n^2\right] \tag{6.7.98}$$

This cross section goes like $n^{-2}$, i.e. the first mode has the biggest cross section. Moreover, it goes like $(v_s/c)^2$ and not as $(v_s/c)^3$ as in the Dyson case, thus having a better efficiency. In addition it has not been obtained in the close-to-resonance approximation, thus in principle the resonator can have a general dimension, not fixed requesting that the resonance frequency has to be close to that of the incoming gravitational waves. The only approximation done is that the dimension of the resonance has to be much smaller than one wave-length, otherwise the driving force them in the equation for the coefficient $B(t)$ (6.7.85) has to be corrected adding higher order terms in $x^j$.

## 6.8 Interaction of gravitational waves with a 3D TI

In the previous sections the mechanical effects of gravitational waves on 2D and 3D systems has been discussed, showing that these effects are negligible due to the magnitude of gravitational waves and the frequency windows that is interesting to discriminate between different cosmological theories. In this section the coupling of Dirac fermions with a gravitational wave traveling along the $z$-direction is discussed, and a comparison with mechanical effects will be done. In order to write the tetrads it's useful to introduce the mixing angle $\varphi$ and the total amplitude of the gravitational wave $h=\sqrt{h_+^2+h_\times^2}$ so that the two polarizations $h_+$ and $h_\times$ are

$$\begin{aligned}h_+&=h(t,z)\sin\varphi\\h_\times&=h(t,z)\cos\varphi\end{aligned} \tag{6.8.99}$$

Using this convention the tetrads $e^a{}_\mu$ connecting the local Lorentzian frame with the general coordinates $x^\mu$, i.e. such that $\eta_{ab}e^a{}_\mu e^b{}_\nu=g_{\mu\nu}$ (with $g_{\mu\nu}=\eta_{\mu\nu}+h_{\mu\nu}$ and $h_{\mu\nu}$ in (6.6.60) for the gravitational waves), then are

$$e^a{}_\mu=\begin{pmatrix}1 & 0 & 0 & 0\\ 0 & -\frac{\sqrt{(1-\sin\varphi)(1-h(t,z))}}{\sqrt{2}} & \frac{\sqrt{(\sin\varphi+1)(h(t,z)+1)}}{\sqrt{2}} & 0\\ 0 & \frac{\sqrt{(1+\sin\varphi)(1-h(t,z))}}{\sqrt{2}} & \frac{(\sec\varphi-\tan\varphi)\sqrt{(\sin\varphi+1)(h(t,z)+1)}}{\sqrt{2}} & 0\\ 0 & 0 & 0 & 1\end{pmatrix} \tag{6.8.100}$$

where the latin index is the row one, and the latin one is the column index. The inverse tetrads are

$$e_a{}^{\mu} = \begin{pmatrix} 1 & 0 & 0 & 0 \\ 0 & -\frac{1-\sin\varphi}{\sqrt{2}\sqrt{(1-\sin\varphi)(1-h(t,z))}} & \frac{\cos\varphi}{\sqrt{2}\sqrt{(1-\sin\varphi)(1-h(t,z))}} & 0 \\ 0 & \frac{\sqrt{\sin\varphi+1}}{\sqrt{2}\sqrt{h(t,z)+1}} & \frac{\cos\varphi}{\sqrt{2}\sqrt{(\sin\varphi+1)(h(t,z)+1)}} & 0 \\ 0 & 0 & 0 & 1 \end{pmatrix} \tag{6.8.101}$$

In the following I will focus on 3D topological insulators, whose Hamiltonian is

$$H = -i\gamma^a \partial_a + \beta M \tag{6.8.102}$$

where the matrices $\gamma^a = \sigma_a \otimes \sigma_x$, $(a = 1, 2, 3)$ and $i\beta = i\mathbb{I} \otimes \sigma_z$ (here the $\sigma_a$ are the Pauli matrices and $\mathbb{I}$ is the identity in 2 dimensions) play the role of Dirac matrices, i.e. they satisfy the Clifford algebra. The spin connection (2.1.19) calculated starting from (6.8.100) and (6.8.101) is in general quite complicated. So, instead of proposing the form of $\Omega_\mu$ for whatsoever value of the mixing angle $\varphi$, I'll discuss the spin connection up to the linear order in the amplitude of the gravitational waves whose modulus is $h(t, z) = a \sin\omega t \sin kz$ for the two polarization i.e. the two limits $\varphi \to 0$ and $\varphi \to \pi/2$. For a +-polarized gravitational wave the components of the spin connection are

$$\begin{aligned} \Gamma_0 &= 0 \\ \Gamma_x &= \frac{i}{2}\left[\Sigma_{0y}\partial_t h + \Sigma_{yz}\partial_z h\right] \\ \Gamma_y &= -\frac{i}{2}\left[\Sigma_{0x}\partial_t h + \Sigma_{xz}\partial_z h\right] \\ \Gamma_z &= 0. \end{aligned} \tag{6.8.103}$$

The spin connection for the ×-polarized wave, instead, is

$$\begin{aligned} \Gamma_0 &= \Gamma_z = 0 \\ \Gamma_x &= \frac{i}{2\sqrt{2}}[(\Sigma_{0x} + \Sigma_{0y})\partial_t h + (\Sigma_{xz} + \Sigma_{yz})\partial_t h] \\ \Gamma_y &= \frac{i}{2\sqrt{2}}[(-\Sigma_{0x} + \Sigma_{0y})\partial_t h + (-\Sigma_{xz} + \Sigma_{yz})\partial_t h] \end{aligned} \tag{6.8.104}$$

The spin connections (6.8.103) and (6.8.104) are related by a $\pi/4$ rotation. However, the spin connection gives a second order contribution in the Dirac

equation. Indeed, even $\Gamma_\mu$ has a first order contribution the total perturbation introduced in the Dirac equation $\gamma^a e_a{}^\mu \Gamma_\mu$ is of order $h^2$. The only first order perturbation introduced by gravitational waves in the Dirac equation then is the rotation of the Dirac matrices.

# Appendices

# Appendix A

# Mathematical Basic Instruments

In this appendix it is done a resume of mathematical instruments used in the main text. The main aim of this appendix is to contain the mathematical pre-requisites necessary to understand the Chern class, without the ambition to be an exhaustive exposition of the mathematics presented. Thus, starting from basic notions of differential geometry, the appendix will cover the theory of fiber bundles and principal bundles, that is at the base of the definition of topological invariants. The exposition will follow the lines of [100].

## A.1 Preliminaries: Basic Differential Geometry

Let be $f : M \to N$, where $M$ and $N$ are differential manifold. The function $f$ induces a map between the tangent spaces of $M$ e $N$, called differential of $f$ and a map between the cotangent spaces of the two manifolds, called pullback or codifferential of $f$. Let $\gamma : \mathbb{R} \to M$ be a curve in M and $X$ a tangent vector to this curve in the point $p$. The differential $f_*$ di $f$ is defined as the map associating to the vector $X$ in $p$the vector $Y$ tangent to the image of $\gamma(t)$ through $f$ in the point $f(p)$. Given the coordinates $x^\mu$ in the patch containing $p$ and $y^\alpha$ the coordinated of the patch containing $f(p)$, the components of the vector $Y$ are

$$Y^\alpha = \frac{\partial y^\alpha}{\partial x^\mu} X^\mu$$

Let $\omega$ be a 1-form defined in $f(p)$. The codifferential $f^*$ of $f$ associates the 1-forma $\omega'$ acting on $X$ as $\omega$ acts on the differential of $X$, i.e the vector $Y$ above, and its components are

$$\omega'_\mu = \frac{\partial y^\alpha}{\partial x^\mu} \omega_\alpha$$

The formal definition of codifferential of the application $f$ is

$$f^*\omega(X) = \omega(f_*X)$$

In the following Lie groups will be used, and it is useful to summarize some of their characteristics. A Lie group $G$ is a differential manifold where it has been introduced a group structure so that

- the multiplication $\cdot : G \times G \to G$ is differentiable,
- the association of the inverse of each element is differentiable.

The right traslation $R_a$ and the left one $L_a$ are defined as

$$R_a g = ga, \quad L_a g = ag$$

The tangent space in the identity of the Lie group $G$ $T_eG$ is isomorphical to the left invariant fields, i.e those fields defined in $G$ so that

$$L_{a*}X\Big|_g = X\Big|_{ag}$$

The set of the left invariant fields, endowed with the Lie parenthesis $[\ ,\ ] : \chi(M) \times \chi(M) \to \chi(M)$

$$[X, Y]^\nu = X^\mu \partial_\mu Y^\nu - Y^\mu \partial_\mu Y^\nu$$

is denoted with $\mathfrak{g}$ and named Lie algebra.

### A.1.1 Differential forms and De Rham cohomology

Let $M$ be a differential manifold and $T_pM$ its tangent space in the point $p \in M$. A 1-form (or covector) $\omega$ is defined as a linear application from the tangent space to the field of the real numbers

$$\omega : T_pM \to \mathbb{R}$$

The set of 1-forms is the vector space $T_p^*M$, and it is defined as the dual space of $T_pM$. An basis in $T_p^*M$ is made up of the applications $dx^\mu$ (also named $\theta^\mu$), defined as the application that associates to the vector $X \in T_pM$ its $\mu$-th component

$$dx^\mu(X) = X^\mu$$

The $r$-forms are defined as the antysimmetrical linear and real-valued applications in $\underbrace{T_pM \times T_pM \times \ldots T_pM}_{r\ volte}$. The set of $r$-forms is indicated as $\Lambda_p^r(M)$

and a basis in this space is defined starting from the outer products of the basis 1-form in $T_p^*M$

$$dx^{\mu_1} \wedge dx^{\mu_2} \wedge \ldots dx^{\mu_r} = \sum_P \sigma(P) dx^{\mu_{P(1)}} \otimes dx^{\mu_{P(2)}} \otimes \ldots \otimes dx^{\mu_{P(r)}}.$$

The outer product has the following properties

- $dx^{\mu_1} \wedge dx^{\mu_2} \wedge \ldots dx^{\mu_r} = 0$ if an index is repeated;
- $dx^{\mu_1} \wedge dx^{\mu_2} \wedge \ldots dx^{\mu_r} = \sigma(P) dx^{\mu_{P(1)}} \wedge dx^{\mu_{P(2)}} \wedge \ldots dx^{\mu_{P(r)}}$
- the outer product is linear in each of its arguments.

A generic $r$-form $\omega$ is then a linear combination of the basis $r$-form

$$\omega = \frac{1}{r!} \omega_{\mu_1 \ldots \mu_r} dx^{\mu_1} \wedge dx^{\mu_2} \wedge \ldots dx^{\mu_r}$$

The components $\omega_{\mu_1 \ldots \mu_r}$ are completely antysimmetric in the indexes. The dimension of $\Lambda_p^r(M)$ is $\binom{m}{r}$, where $m$ is the dimension of the differential manifold $M$. The outer derivative $d_r$ is an appilcation from $\Lambda_p^r(M)$ to $\Lambda_p^{r+1}(M)$

$$d_r : \Lambda_p^r(M) \to \Lambda_p^{r+1}(M)$$

defined as

$$d_r \omega = \frac{1}{r!} \left( \frac{\partial}{\partial x^\nu} \omega_{\mu_1 \ldots \mu_r} \right) dx^\nu \wedge dx^{\mu_1} \wedge dx^{\mu_2} \wedge \ldots dx^{\mu_r}$$

Note that $d_{r+1} d_r \equiv d^2$ is a null operator. The space $\Lambda_p^0(M)$ is defined as the space of the functions defined in the manifold $M$. Consider the case $M = \mathbb{R}^3$ and $f$ a function defined in $M$. The outer derivative $f$ is a 1-form whose components coincide with the derivatives of $f$, i.e. the differential of the function

$$df = \partial_\mu f dx^\mu$$

The outer derivative of a 1-form $\omega_1$ is the curl

$$d\omega_1 = (\partial_x \omega_y - \partial_y \omega_x)\, dx \wedge dy + (\partial_y \omega_z - \partial_y \omega_z)\, dy \wedge dz + (\partial_x \omega_z - \partial_x \omega_z)\, dz \wedge dx$$

In the case of a 2-form $\omega_2$, $d\omega_2$ is the divergence

$$d\omega_2 = (\partial_x \omega_{yz} + \partial_z \omega_{xy} + \partial_y \omega_{zx}) dx \wedge dy \wedge dz$$

This considerations cover all the orders of $r$-form in $\mathbb{R}^3$, since there are not $r$-forms with $r > 3$. An $r$-form $\omega$ is said to be closed if $d_r\omega = 0$ and exact if it exists an $r-1$-form $\eta$ so that $d_{r-1}\eta = \omega$. The set of the closed $r$-forms is indicated as $Z^r(M)$ while the set of the exact ones with $B^r(M)$. Since $d^2 = 0$ then $B^r \subset Z^r$. It is possible to define an equivalence relation between the closed differential form: $\eta \equiv \omega$ if they differ for an exact form, i.e. $\omega = \eta + d\psi$. The quotient space respect to this relation is the *r-th de Rham cohomology group* $H^r(M)$

$$H^r(M) = Z^r(M)/B^r(M).$$

Cohomology groups are relevant in the discussion about Chern classes: these, indeed, are equivalence classes between closed forms i.e. elements of $H^r(M)$.

## A.2 Fiber Bundles: Definitions

A fiber bundle is defined as the set $(E, \pi, M, F, G)$ where

- E is a differential manifold said *total space*,
- F is a differential manifold named fiber or typical fiber,
- G is a Lie group, named structure group, acting on the left in F,
- $\pi$ is a surjective application $\pi : E \to M$, such that the image of a point in M through its inverse $\pi^{-1}(p) = F_p \cong F$ is the fiber in$p$.

Let $\{U_i\}$ be an open covering in M, endowed with a diffeomorfism $\phi_i : U_i \times F \to \pi^{-1}(U_i)$ such that $\pi \circ \phi_i(p, f) = p$. The application $\phi_i$ is said local trivialization. Note that by definition trivialization does not mix fibers, i.e. fixed $p \in M$ and varying $f \in F$ the image of the application $\phi_i(p, f) = \phi_{i,p}(f)$ is the fiber in $p$. In the intersection of two patches $U_i \cap U_j$ it is defined an application $t_{ij} = \phi_{i,p}^{-1} \circ \phi_{j,p} : F \to F$, the *transition function*, is an element of the structure group. Trivializations are then linked by a biunivocal application

$$\phi_j(p, f) = \phi_i(p, t_{ij}(p)f)$$

. Given $u \in \pi^{-1}(U_i \cup U_j)$ so that $\pi(u) = p$, through the inverse of the trivializations are associated two different elements of $F$

$$\phi_{i,p}^{-1}(u) = f_i, \quad \phi_{j,p}^{-1}(u) = f_j$$

The elements $f_i$ e $f_j$ are linked through $t_{ij}$, $f_i = t_{i,j}(p)f_j$. The properties of the transition functions, defined so that the patches in the covering are

linked in a consistent way, are

$$\begin{aligned} t_{ii} &= \mathbb{I} \\ t_{ij} &= t_{ji}^{-1} \\ t_{ik} &= t_{ij} \circ t_{jk}. \end{aligned} \tag{A.2.1}$$

When all the transition functions coincide with the identity the fiber bundle is defined as trivial and it is nothing but the product $M \times F$. It is possible to define different trivializations in the same patch, the difference between them will always be in the element associated by the inverse to a given element of the bundle. These elements are linked in a way similar to the transition functions through the functions $g_i = \phi_{i,p}^{-1} \circ \tilde{\phi}_{i,p}$. The functions $g_i$ also define the transformation rule for the transition function

$$\tilde{t}_{ij} = \tilde{\phi}_{i,p}^{-1} \circ \tilde{\phi}_{j,p} = g_i^{-1} \circ t_{ij} \circ g_j.$$

The section $s : M \to E$ is an application such that $\pi \circ s = \mathbb{I}_M$. The image of a point $p \in M$ through $s$ is then an element in $F_p$. The set of the section defined in the bundle is indicated with $\Gamma(M, F)$.

### A.2.1 Principal Bundles

A principal bundle is a fiber bundle where the fiber coincides with the strucutre group

$$(E, \pi, M, G, G) \equiv P(M, G).$$

In principal bundles is defined the right action of the group $G$ on the fiber. GIven a local trivialization $\phi_i : U_i \times F \to \pi^{-1}(U_i)$ it associates to an element $u \in \pi^{-1}(U_i)$ the couple $(p, g_i)$. The right action is then defined as $\phi_{i,p}^{-1}(ua) = (p, g_i a)$. The right action so defined is independent of the trivialization. Indeed,

$$ua = \phi_j(p, g_j a) = \phi_j(p, t_{ji} g_i a) = \phi_i(p, g_i a).$$

Given a section in a principal bundle it is possible to define a local canonical trivialization, defined as

$$s_i(p) = \phi(p, e).$$

All the other elements in the fiber are obtained through the right action of the group. Starting from a principal bundle it is possible to define bundles with different fibers. Let $F$ be a differential manifold on witch the structure group acts on the left. An element in the associated fiber $(E, \pi_E, M, G, F, P)$ is defined through the couple

$$(u, v) \in P \times F$$

The action of the group $G$ on $P \times F$ is defined through the right action of the group on the pricipal bundle $P$

$$g \rightarrow (ug, g^{-1}v)$$

The projection on the associated bundle is defined through the projection on the principal bundle, i.e. $\pi_E(u, v) \equiv \pi(u)$.

# Appendix B

# Kubo Formula

In this appendix the basics of linear response theory [76; 98] are revised. Before the work of Kubo, the most common technique used to calculate non-equilibrium quantities, such as response functions, was the kinetic equation for the molecular distribution function. Such an equation is in itself an approximation and it has been proved to hold only after strictly (and often not satisfied) conditions on the interaction. The Kubo formula, based on fluctuation-dissipation approach, allows to overcome all these difficulties.

## B.1 Linear Response theory

Given a many body Hamiltonian $H$, the density matrix $\rho$ in Scrödinger picture obeys the Liouville equation

$$i\hbar\frac{d\rho}{dt} = [H, \rho] \tag{B.1.1}$$

and the expectation value of an observable $B$ is

$$B(t) = \mathrm{Tr}\{\rho(t)B\}. \tag{B.1.2}$$

When $H$ is of the form

$$H = H_0 + V(t) \tag{B.1.3}$$

the density matrix can be decomposed as

$$\rho(t) = \rho_0 + \Delta\rho \tag{B.1.4}$$

where $\rho_0$ is the density matrix for the unperturbed Hamiltonian in the grand-canonical ensemble

$$\rho_0 = \zeta^{-1}\exp\{-\beta(H_0 - \nu N)\}, \quad \text{with} \quad \zeta = \mathrm{Tr}\exp\{-\beta(H_0 - \mu N)\}.$$

In the formula $\mu$ is the chemical potential and $N$ is the number operator. Putting (B.1.4) in (B.1.1), and equation for $\Delta\rho$ at the linear order is derived, which in interaction picture is

$$i\hbar\frac{d}{dt}\Delta\rho_I = [V_I(t), \rho_0]. \tag{B.1.5}$$

In the hypothesis that the perturbation $V(t)$ is turned on adiabatically in the past, the equation for $\Delta\rho$ has to be solved with the boundary condition

$$\lim_{t\to-\infty} \Delta\rho = 0. \tag{B.1.6}$$

The solution of (B.1.5) then is

$$\Delta\rho(t) = -\frac{i}{\hbar}\int_{-\infty}^{t} dt'[V_I(t'), \rho_0]. \tag{B.1.7}$$

Let's consider now the case of an observable $B$ having null expectation value in the unperturbed system, i.e. $\mathrm{Tr}\{\rho(t)B\} = 0$. The expectation value of $B$ in the perturbed system then is

$$B(t) = -\frac{i}{\hbar}\int_{-\infty}^{t} dt'\mathrm{Tr}\{[V_I(t'), \rho_0]B_I(t)\} = \frac{i}{\hbar}\int_{-\infty}^{t} dt'\mathrm{Tr}\{\rho_0[V_I(t'), B_I(t)]\}, \tag{B.1.8}$$

where in the last equality the ciclic property of the trace has been used. Taking a perturbation of the type

$$V(t) = AF(t), \quad \text{with} \quad F(t) = e^{i(\omega+i\eta)t} \tag{B.1.9}$$

Eq. (B.1.8) becomes

$$B(t) = \int_{-\infty}^{t} dt'\phi_{BA}(t-t')F(t') \tag{B.1.10}$$

where it has been introduced the response function, i.e. the Green function of the operators $A$ and $B$

$$\phi_{BA} = \frac{i}{\hbar}\mathrm{Tr}\{\rho_0[A, B_I(t)]\}\theta(t), \tag{B.1.11}$$

$\theta(t)$ being the step function. Following Kubo [76] the response function can be usefully expressed as

$$\phi_{BA}(t) = \int_0^{\beta} d\lambda\mathrm{Tr}\{\rho_0\dot{A}(-i\hbar\lambda)B(t)\}\theta(t). \tag{B.1.12}$$

## B.2 Electrical conductivity

In this section the formalism exposed previously will be used to calculate the electrical conductivity, making connection with the formulas in Ch. 1. Consider a system made up of $N$ electrons subject to an electric field

$$V(t) = e\sum_{i=1}^{N} \mathbf{x}_i \cdot \mathbf{E}(t). \tag{B.2.13}$$

The response function (B.1.12) then reads

$$\phi_{B\nu} = e\theta(t)\int_0^\beta d\lambda \mathrm{Tr}\{\rho_0 J_\nu(-i\hbar\lambda)B(t)\} \tag{B.2.14}$$

where it has been used the definition of current $J_\nu = \sum_{i=1}^{N} \dot{x}_i^\mu$. The response to the applied field is obtained choosing $B$ as the current density

$$J_\nu = -eJ_\nu(\mathbf{r}) = -\frac{e}{2}\sum_{i=1}^{N} v_i^\nu \delta(\mathbf{r}-\mathbf{r}_i) + \delta(\mathbf{r}-\mathbf{r}_i)v_i^\nu \tag{B.2.15}$$

so that the response function is the electrical conductivity which explicitly is

$$\phi_{B\nu} \equiv \sigma_{\mu\nu} = -e^2\theta(t)\int_0^\beta d\lambda\ \mathrm{Tr}\{\rho_0 J_\nu(-i\hbar\lambda)J_\mu(\mathbf{r},t)\} \tag{B.2.16}$$

The sample averaged conductivity invoked in Ch. 1 then is

$$\sigma_{\mu\nu}(t) = \frac{1}{A}\int d\mathbf{r}\sigma_{\mu\nu}(\mathbf{r},t) \tag{B.2.17}$$

where $A$ is the size of the system.

# Appendix C

# Green function in the free case

In this appendix a review of the spectral representation of the Green's function is given, leading to the formalism used in Ch. (2) to analyze the case of the edge dislocation in graphene.

## C.1 The spectral representation

The Green's function of the operator $L(z)$ is defined through the equation

$$[\omega - L(z)]G(\mathbf{r}, \mathbf{r}\,', \omega) = \delta(\mathbf{r} - \mathbf{r}\,') \tag{C.1.1}$$

The spectral representation for the Green's function [31] in general is

$$G(\mathbf{r}, \mathbf{r}\,', \omega) = \int dc\, \frac{\Psi_c(\mathbf{r})\Psi_c^\dagger(\mathbf{r}\,')}{\omega - \lambda_c} \tag{C.1.2}$$

where $c$ is the label for the continuous spectrum $\lambda_c$ of the operator $L(z)$ and the discrete spectrum of this operator is supposed to be absent. I am here interested in analyzing the case of Dirac equation in 2+1 dimensions, i.e. $L = -i\gamma^a\partial_a$ with the following choice for the Dirac matrices

$$\begin{aligned} \gamma^0 &= -i\sigma_z \\ \gamma^1 &= \sigma_y \\ \gamma^2 &= -\sigma_x \end{aligned} \tag{C.1.3}$$

and $\sigma_i$ is the $i$-th Pauli matrix as usual. The equation for the Green's function in the domain of frequencies then is

$$[E + i\sigma \cdot \nabla]G(\mathbf{r}, \mathbf{r}\,', \omega) = i\sigma_z\delta(\mathbf{r} - \mathbf{r}\,') \tag{C.1.4}$$

Considering the decomposition of a plane wave in angular momentum eigenfunctions

$$\Psi = \frac{1}{\sqrt{2}} \sum_m i^m \begin{pmatrix} J_m(kr) \\ isJ_{m+1}(kr)e^{i\theta} \end{pmatrix} e^{im(\theta-\theta_k)} \tag{C.1.5}$$

The Green function of an edge dislocation analyzed in term of angular momentum eigenfunctions is

$$\begin{aligned} G\left(\vec{r},\vec{r}\,',\omega\right) &= i \int pdp \sum_{m,s} \frac{e^{im(\theta_r-\theta_{r'})}}{\omega - sp} \times \\ &\times \frac{1}{2} \begin{pmatrix} J_m(pr)\, J_m(pr') & -is\, J_m(pr)\, J_{m+1}(pr')\, e^{-i\theta_{r'}} \\ -is\, J_{m+1}(pr) J_m(pr')\, e^{i\theta_r} & -J_{m+1}(pr)\, J_{m+1}(pr')\, e^{i(\theta_r-\theta_{r'})} \end{pmatrix} = \\ &= \frac{i}{2\pi\hbar^2 v_F^2} \sum_m \int_{-\infty}^{\infty} EdE\, \frac{e^{im(\theta_r-\theta_{r'})}}{\omega - E} \times \\ &\times \frac{1}{2} \begin{pmatrix} J_m(x)\, J_m(x') & -is\, J_m(x)\, J_{m+1}(x')\, e^{-i\theta_{r'}} \\ -is\, J_{m+1}(x) J_m(x')\, e^{i\theta_r} & -J_{m+1}(x)\, J_{m+1}(x')\, e^{i(\theta_r-\theta_{r'})} \end{pmatrix} \end{aligned} \tag{C.1.6}$$

where the dimensionless variables $x = |E|r/\hbar v_F$ and $x' = |E|r'/\hbar v_F$ have been introduced as in Chapter 2, and it has been taken into account that the Bessel functions of integer order are real functions. The integration path in the complex $E$ plane is shown in fig. C.1. The contribution from the circumference at infinity is null, as in the case of Fermi liquids [134]. Only the contribution from the pole at $\omega$ then remains. The series in (C.1.6) can

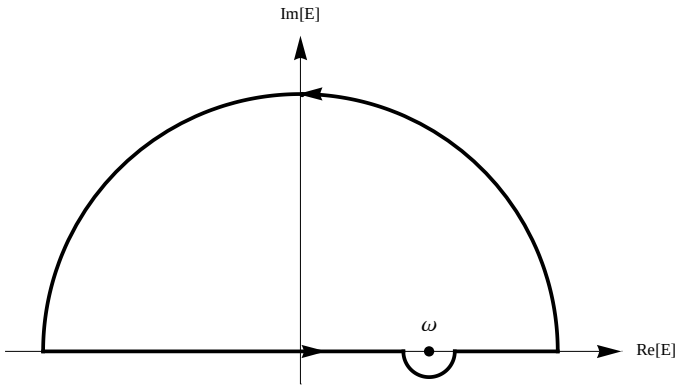


**Figure C.1:** Integration circuit in the complex $E$ plane in (C.1.6).

be summed with the help of Graf's theorem [2]

$$\begin{aligned}
\sum_m e^{im(\theta_r-\theta_{r'})} J_m(\omega r)\, J_m(\omega r') &= J_0(\omega\rho) \\
\sum_m e^{im(\theta_r-\theta_{r'})} J_m(\omega r)\, J_{m+1}(\omega r')\, e^{-i\theta_{r'}} &= iJ_1(\omega\rho)e^{-i\frac{\theta'+\theta}{2}} \\
\sum_m e^{im(\theta_r-\theta_{r'})} J_{m+1}(\omega r)\, J_m(\omega r')\, e^{i\theta_r} &= iJ_1(\omega\rho)e^{i\frac{\theta'+\theta}{2}} \\
\sum_m e^{i(m+1)(\theta_r-\theta_{r'})} J_{m+1}(\omega r)\, J_{m+1}(\omega r) &= J_0(\omega\rho)
\end{aligned} \tag{C.1.7}$$

So that a closed form for the Green function is ($\rho(\omega)$ is the density of states at $\omega$)

$$G\left(\vec{r},\vec{r}\,',\omega\right) = \rho(\omega)\,\frac{1}{2}\begin{pmatrix} J_0(\omega\rho) & J_1(\omega\rho)e^{-i\frac{\theta'+\theta}{2}} \\ J_1(\omega\rho)e^{i\frac{\theta'+\theta}{2}} & -J_0(\omega\rho) \end{pmatrix} \tag{C.1.8}$$

# Bibliography


[1] The carbon fullerenes admit a continuum description in terms of two Dirac equations on the surface of a sphere[42]. Lattice effects, such as scattering between the two equations, lead to corrections which scale as $(a/R)^2$, where $a$ is the lattice spacing, see[46]. We do not find terms of similar magnitude at the surface of a topological insulator.

[2] M. Abramowitz and I.A. Stegun. *Handbook of Mathematical Functions: With Formulas, Graphs, and Mathematical Tables*. Applied mathematics series. Dover Publications, 1965.

[3] A. A. Abrikosov. *Fundamentals of the Theory of Metals*. North Holland.

[4] I.I. Al-Qasir and North Carolina State University. *Thermal Neutron Scattering in Graphite*. North Carolina State University, 2007.

[5] P.S. Alsing, J. Evans, and K.K. Nandi. *Gen.Rel.Grav.*, 33:1459, 2001.

[6] Alexander Altland and Martin R. Zirnbauer. Nonstandard symmetry classes in mesoscopic normal-superconducting hybrid structures. *Phys. Rev. B*, 55:1142–1161, Jan 1997.

[7] T. Ando. *J.Phys. Soc. Japan*, 75:074716, 2006.

[8] T. Ando, T. Nakanishi, and R. Saito. *J. Phys. Soc. Japan*, 67:2857, 1998.

[9] X. Arsiwalla, J. de Boer, K. Papadodimas, and E. Verlinde. Degenerate stars and gravitational collapse in AdS/CFT. *Journal of High Energy Physics*, 1:144, January 2011.

[10] B. A. Bernevig and S.-C. Zhang. Quantum spin hall effect. *Phys. Rev. Lett.*, 96:106802, 2006.

[11] O. L. Blakslee, D. G. Proctor, E. J. Seldin, G. B. Spence, and T. Weng. Elastic constants of compressionâĂŘannealed pyrolytic graphite. *Journal of Applied Physics*, 41(8):3373–3382, 1970.

[12] L. Brey and J. J. Palacios. *Phys. Rev. B*, 77:041403, 2008.

[13] T. J. I'A. Bromwich. On the influence of gravity on elastic waves, and, in particular on the vibrations of an elastic globe. *Proceedings of the London Mathematical Society*, s1-30(1):98–165, 1898.

[14] A. A. Burkov, M. D. Hook, and Leon Balents. Topological nodal semimetals. *Phys. Rev. B*, 84:235126, Dec 2011.

[15] R. Camporesi and A. Higuchi. On the eigenfunctions of the Dirac operator on spheres and real hyperbolic spaces. *Journal of Geometry and Physics*, 20:1–18, September 1996.

[16] B. Carter. Interaction of gravitational waves with an elastic solid medium. 1982.

[17] B. Carter and H. Quintana. Foundations of general relativistic high-pressure elasticity theory. *Proceedings of the Royal Society of London. A. Mathematical and Physical Sciences*, 331(1584):57–83, 1972.

[18] B. Carter and H. Quintana. Gravitational and acoustic waves in an elastic medium. *Phys. Rev. D*, 16:2928–2938, Nov 1977.

[19] Brandon Carter. Elastic perturbation theory in general relativity and a variation principle for a rotating solid star. *Communications in Mathematical Physics*, 30:261–286, 1973. 10.1007/BF01645505.

[20] A. H. Castro Neto, F. Guinea, N. M. R. Peres, K. S. Novoselov, and A. K. Geim. The electronic properties of graphene. *Rev. Mod. Phys.*, 81:109, 2009.

[21] A. Chamblin, R. Emparan, C. V. Johnson, and R. C. Myers. Charged AdS black holes and catastrophic holography. *Phys. Rev D*, 60(6):064018, September 1999.

[22] A. Cortijo and M. A. H. Vozmediano. Effects of topological defects and local curvature on the electronic properties of planar graphene. *Nucl. Phys. B*, 763:293, 2007.

[23] Alberto Cortijo, Adolfo G. Grushin, and Maria A. H. Vozmediano. Topological insulating phases in mono and bilayer graphene. 2010.

[24] J. P. Dahlhaus, C.-Y. Hou, A. R. Akhmerov, and C. W. J. Beenakker. Geodesic scattering by surface deformations of a topological insulator. *Phys. Rev. B*, 82(8):085312, Aug 2010.

[25] J. de Boer, K. Papadodimas, and E. Verlinde. Holographic neutron stars. *Journal of High Energy Physics*, 10:20, October 2010.

[26] Fernando de Juan, Alberto Cortijo, and María A. H. Vozmediano. Charge inhomogeneities due to smooth ripples in graphene sheets. *Phys. Rev. B*, 76(16):165409, Oct 2007.

[27] F. J. Dyson. Seismic Response of the Earth to a Gravitational Wave in the 1-Hz Band. *The Astrophysical Journal*, 156:529, May 1969.

[28] Freeman J. Dyson. Statistical theory of the energy levels of complex systems. i. *Journal of Mathematical Physics*, 3(1):140–156, 1962.

[29] Freeman J. Dyson. Statistical theory of the energy levels of complex systems. ii. *Journal of Mathematical Physics*, 3(1):157–165, 1962.

[30] Freeman J. Dyson. Statistical theory of the energy levels of complex systems. iii. *Journal of Mathematical Physics*, 3(1):166–175, 1962.

[31] Eleftherios N. Economou. *Green's Functions in Quantum Physics*. Springer, 2006.

[32] R. Egger, A. Zazunov, and A. Levy Yeyati. Helical luttinger liquid in topological insulator nanowires. *Phys. Rev. Lett.*, 105(13):136403, Sep 2010.

[33] Vladimir I. Fal'ko, K. Kechedzhi, E. McCann, B.L. Altshuler, H. Suzuura, and T. Ando. *Solid State Communications*, 143:33 – 38, 2007.

[34] Xiao-Yong Feng, Wei-Qiang Chen, Jin-Hua Gao, Qiang-Hua Wang, and Fu-Chun Zhang. Anderson impurity in a helical metal. *Phys. Rev. B*, 81(23):235411, Jun 2010.

[35] L. Fu and C. L. Kane. Topological insulators with inversion symmetry. *Phys. Rev. B*, 76:045302, 2007.

[36] L. Fu, C. L. Kane, and E. J. Mele. Topological insulators in three dimensions. *Phys. Rev. Lett.*, 98:106803, 2007.

[37] Liang Fu and C. L. Kane. Time reversal polarization and a $z2$ adiabatic spin pump. *Phys. Rev. B*, 74(19):195312, Nov 2006.

[38] A. K. Geim. *Science*, 324:1530–1534, 2009.

[39] A.K. Geim and K.S.Novoselov. *Nat. Mater.*, 6:183, 2007.

[40] Sébastien Giraud and Reinhold Egger. Electron-phonon scattering in topological insulators. *Phys. Rev. B*, 83:245322, Jun 2011.

[41] J. González, F. Guinea, and J. Herrero. Propagating, evanescent, and localized states in carbon nanotube–graphene junctions. *Phys. Rev. B*, 79:165434, Apr 2009.

[42] J. González, F. Guinea, and M. A. H. Vozmediano. Continuum approximation to fullerene molecules. *Phys. Rev. Lett.*, 69:172, 1992.

[43] D.L. Greenaway and G. Harbeke. Band structure of bismuth telluride, bismuth selenide and their respective alloys. *Journal of Physics and Chemistry of Solids*, 26(10):1585 – 1604, 1965.

[44] F. Guinea. *J Low Temp. Phys.*, 153:359, 2008.

[45] F. Guinea. Models of electron transport in single layer graphene. *J Low Temp Phys*, 153:359, 2008.

[46] F. Guinea, J. González, and M. A. H. Vozmediano. Electronic interactions in fullerene spheres. *Phys. Rev. B*, 47(24):16576–16581, Jun 1993.

[47] F. Guinea, M. I. Katsnelson, and A. K. Geim. *Nat.Phys.*, 6:30, 2010.

[48] F. Guinea and Tony Low. Band structure and gaps of triangular graphene superlattices. *Philosophical Transactions of the Royal Society A: Mathematical, Physical and Engineering Sciences*, 368(1932):5391–5402, 2010.

[49] C. R. Hagen. Aharonov-bohm scattering amplitude. *Phys. Rev. D*, 41:2015–2017, Mar 1990.

[50] C. R. Hagen. Aharonov-bohm scattering of particles with spin. *Phys. Rev. Lett.*, 64:503–506, Jan 1990.

[51] F. D. M. Haldane. Model for a quantum hall effect without landau levels: Condensed-matter realization of the parity anomaly. *Phys. Rev. Lett.*, 61:2015, 1988.

[52] S. A. Hartnoll. Quantum Critical Dynamics from Black Holes. *ArXiv e-prints*, September 2009.

[53] S. A. Hartnoll and D. M. Hofman. Generalized Lifshitz-Kosevich scaling at quantum criticality from the holographic correspondence. *Phys. Rev B*, 81(15):155125, April 2010.

[54] S. A. Hartnoll, D. M. Hofman, and A. Tavanfar. Holographically smeared Fermi surface: Quantum oscillations and Luttinger count in electron stars. *EPL (Europhysics Letters)*, 95:31002, August 2011.

[55] S. A. Hartnoll and A. Tavanfar. Electron stars for holographic metallic criticality. *Phys. Rev D*, 83(4):046003, February 2011.

[56] Sean Hartnoll, Joseph Polchinski, Eva Silverstein, and David Tong. Towards strange metallic holography. *Journal of High Energy Physics*, 2010(4):1–54, 2010-04-01.

[57] Sean A Hartnoll. Lectures on holographic methods for condensed matter physics. *Classical and Quantum Gravity*, 26(22):224002, 2009.

[58] M. Z. Hasan and C. L. Kane. Topological insulators. *Rev. Mod. Phys.*, 82:3045, 2010.

[59] I. F. Herbut, V. Juricic, and O. Vafek. *Phys. Rev. Lett.*, 100:046403, 2008.

[60] Hiroshi and Ezawa. Phonons in a half space. *Annals of Physics*, 67(2):438 – 460, 1971.

[61] Bao-Ling Huang and Massoud Kaviany. *Ab initio* and molecular dynamics predictions for electron and phonon transport in bismuth telluride. *Phys. Rev. B*, 77:125209, Mar 2008.

[62] Bao-Ling Huang and Massoud Kaviany. *Ab initio* and molecular dynamics predictions for electron and phonon transport in bismuth telluride. *Phys. Rev. B*, 77:125209, Mar 2008.

[63] E. Hwang. Acoustic phonon scattering limited carrier mobility in two-dimensional extrinsic graphene. *Physical Review B*, 77(11), 2008.

[64] E. W. Hwang, S. Adam, and S. Das Sarma. *Phys.Rev. Lett.*, 98:186806, 2007.

[65] Rok Žitko. Quantum impurity on the surface of a topological insulator. *Phys. Rev. B*, 81(24):241414, Jun 2010.

[66] N. Iqbal and H. Liu. Real-time response in AdS/CFT with application to spinors. *Fortschritte der Physik*, 57:367–384, June 2009.

[67] C. L. Kane and E. J. Mele. *Phys. Rev. Lett.*, 78:1932, 1997.

[68] C. L. Kane and E. J. Mele. Quantum spin hall effect in graphene. *Phys. Rev. Lett.*, 95:226801, 2005.

[69] C. L. Kane and E. J. Mele. Z2 topological order and the quantum spin hall effect. *Phys. Rev. Lett.*, 95:146802, 2005.

[70] M. I. Katsnelson, F. Guinea, and A. K. Geim. *Phys.Rev. B*, 79:195426, 2009.

[71] M.I. Katsnelson and A.K. Geim. *Philos. Trans. R. Soc. A*, 366:195, 2008.

[72] Hagen Kleinert. *Gauge Fields in Condensed Matter Physics*. World Scientific Pub Co Inc, 1987.

[73] Mahito Kohmoto. Topological invariant and the quantization of the hall conductance. *Annals of Physics*, 160(2):343 – 354, 1985.

[74] D. Kolesnikov and V. Osipov. *JETP Lett.*, 87:419, 2008.

[75] M. Konig, S. Wiedmann, C. Brune, A. Roth, H. Buhmann, L. W. Molenkamp, X.-L. Qi, and S.-C. Zhang. Quantum spin hall insulator state in hgte quantum wells. *Science*, 318:766, 2007.

[76] Ryogo Kubo. Statistical-mechanical theory of irreversible processes. i. general theory and simple applications to magnetic and conduction problems. *Journal of the Physical Society of Japan*, 12(6):570–586, 1957.

[77] L. Landau and E. M. Lifshitz. *The Classical Theory of Fields*. Addison-Wesley Publishing Co., 1962.

[78] L. D. Landau and E. M. Lifshitz. *Theory of Elasticity*. Pergamon Press, 1975.

[79] L.D. Landau and L.M. Lifshitz. *Quantum Mechanics Non-Relativistic Theory*. Butterworth-Heinemann, 1981.

[80] F. Larsen and G. van Anders. Holographic Non-Fermi Liquids and the Luttinger Theorem. *ArXiv e-prints*, June 2010.

[81] D.-H. Lee. The surface states of topological insulators - dirac fermion in curved two dimensional spaces. *Phys. Rev. Lett.*, 103:196804, 2009.

[82] S.-S. Lee. Non-Fermi liquid from a charged black hole: A critical Fermi ball. *Phys. Rev D*, 79(8):086006, April 2009.

[83] H. Liu, J. McGreevy, and D. Vegh. Non-Fermi liquids from holography. *Phys. Rev D*, 83(6):065029, March 2011.

[84] A. Lopez-Ortega. The Dirac equation in D-dimensional spherically symmetric spacetimes. *ArXiv e-prints*, June 2009.

[85] Augustus E. H. Love. *A treatise on the mathematical theory of elasticity.* Dover, 2011.

[86] G.Y. Lyubarskii. *The Application of Group Theory.* 1960.

[87] G. D. Mahan. *Many-particle Physics.* Plenum Press, 1990.

[88] J.L. Mañes. *Phys.Rev. B*, 76:045430, 2007.

[89] E. McCann and V. I. Fal'ko. Symmetry of boundary conditions of the dirac equation for electrons in carbon nanotubes. *J. Phys.: Condens. Matter*, 16:2371, 2004.

[90] J. McGreevy. Holographic duality with a view toward many-body physics. *ArXiv e-prints*, September 2009.

[91] A. Mesaros, D. Sadri, and J. Zaanen. *arxiv:0909.2703*, 2009.

[92] A. Mesaros, D. Sadri, and J. Zaanen. Berry phase of dislocations in graphene and valley conserving decoherence. *Phys. Rev. B*, 79:155111, Apr 2009.

[93] Jannik C. Meyer, A. K. Geim, M. I. Katsnelson, K. S. Novoselov, T. J. Booth, and S. Roth. *Nature*, 446:60–63, 2007.

[94] G. Miele and P. Vitale. *Nuc. Phys. B*, 494:365, 1997.

[95] Koenraad Schalm Mihailo Čubrović, Jan Zaanen. String theory, quantum phase transitions, and the emergent fermi liquid. *Science*, 325(5939):439–444, July 2009.

[96] C.W. Misner, K.S. Thorne, and J.A. Wheeler. *Gravitation.* W. H. Freeman, 1973.

[97] J. E. Moore and L. Balents. Topological invariants of time-reversal-invariant band structures. *Phys. Rev. B*, 121306:75, 2007.

[98] Giuseppe Morandi. *Quantum Hall Effect.* Bibliopolis, 1988.

[99] W. Mück and K. S. Viswanathan. Conformal field theory correlators from classical field theory on anti–de sitter space: Vector and spinor fields. *Phys. Rev. D*, 58:106006, Oct 1998.

[100] M. Nakahara. *Geometry, Topology and Physics.* Adam Hilger, 1990.

[101] H. B. Nielsen and M. Ninomiya. Absence of neutrinos on a lattice : (i). proof by homotopy theory. *Nuclear Physics B*, 185:20, 1981.

[102] K. Nomura and A. H. MacDonald. *Phys. Rev. Lett.*, 98:076602, 2007.

[103] K. S. Novoselov, A. K. Geim andS. V. Morozov, D. Jiang, M. I. Katsnelson, I. V. Grigorieva, S. V. Dubonos, and A. A. Firsov. *Nature*, 438:197, 2005.

[104] J. R. Oppenheimer and G. M. Volkoff. On massive neutron cores. *Phys. Rev.*, 55:374–381, Feb 1939.

[105] Ho Paik and Robert V. Wagoner. Calculation of the absorption cross section of a cylindrical gravitational-wave antenna. *Physical Review D*, 13(10):2694–2699, 1976.

[106] Z.-H. Pan, A. V. Fedorov, D. Gardner, Y. S. Lee, S. Chu, and T. Valla. Measurement of an exceptionally weak electron-phonon coupling on the surface of the topological insulator $bi_2se_3$ using angle-resolved photoemission spectroscopy. *Phys. Rev. Lett.*, 108:187001, May 2012.

[107] V. Parente, P. Lucignano, P. Vitale, A. Tagliacozzo, and F. Guinea. Spin connection and boundary states in a topological insulator. *Phys. Rev. B*, 83:075424, Feb 2011.

[108] Cheol-Hwan Park, Li Yang, Young-Woo Son, Marvin L. Cohen, and Steven G. Louie. New generation of massless dirac fermions in graphene under external periodic potentials. *Phys. Rev. Lett.*, 101:126804, Sep 2008.

[109] V. M. Pereira, J. Nilsson, and A. H. Castro Neto. *Phys. Rev. Lett.*, 99:166802, 2007.

[110] V.M. Pereira, A.H. Castro Neto, and N.M.R. Peres. *Phys. Rev. B*, 80:045401, 2009.

[111] M. E. Peskin and D. V.Schroeder. *An Introduction to Quantum Field Theory.* Addison - Wesley Advanced Book Program.

[112] R. E. Prange. Quantized hall resistance and the measurement of the fine-structure constant. *Phys. Rev. B*, 23(9):4802–4805, May 1981.

[113] Jose Pujol. *Elastic Wave Propagation and Generation in Seismology.* Cambridge, 2003.

[114] Xiao-Liang Qi and Shou-Cheng Zhang. Topological insulators and superconductors. *Rev. Mod. Phys.*, 83:1057–1110, Oct 2011.

[115] Y. Ran, Y. Zhang, and A. Vishwanath. One-dimensional topologically protected modes in topological insulators with lattice dislocations. *Nature Phys.*, 5:298, 2009.

[116] A Romano. *Continuum Mechanics Using Mathematica.* Springer, 2006.

[117] R. Ruffini and J.A. Wheeler. *Relativistic Cosmology and Space Platforms.* European Space Research Organization, 1970.

[118] S. Sachdev. Condensed matter and AdS/CFT. *ArXiv e-prints*, February 2010.

[119] Wen-Yu Shan, Hai-Zhou Lu, and Shun-Qing Shen. Effective continuous model for surface states and thin films of three dimensional topological insulators. *New Journal of Physics*, 12:043048, 2010.

[120] A. V. Shytov, M. I. Katsnelson, and L. S. Levitov. *Phys. Rev. Lett.*, 99:236801, 2007.

[121] Yuri M. Sirenko, K. W. Kim, and Michael A. Stroscio. Near-surface electrons and acoustic phonons: Energy and momentum relaxation. *Phys. Rev. B*, 56:15770–15781, Dec 1997.

[122] D. E. Soper. *Classical Field Theory.* New York Wiley, 1976.

[123] L. Stodolsky. *Gen Rel. Grav.*, 11:391, 1979.

[124] T. Suzuura, H. Ando. *Phys. Rev. B*, 65:235412, 2002.

[125] J. C. Y. Teo, L. Fu, and C. L. Kane. Surface states and topological invariants in three-dimensional topological insulators: Application to bi1-xsbx. *Phys. Rev. B*, 78:045426, 2008.

[126] Jeffrey C. Y. Teo and C. L. Kane. Majorana fermions and non-abelian statistics in three dimensions. *Phys. Rev. Lett.*, 104(4):046401, Jan 2010.

[127] Jeffrey C. Y. Teo and C. L. Kane. Topological defects and gapless modes in insulators and superconductors. *Phys. Rev. B*, 82(11):115120, Sep 2010.

[128] D. Thorne, K. S.; MacDonald. Electrodynamics in curved spacetime - 3+1 formulation. *Monthly Notices of the Royal Astronomical Society*, 198:339, 1982.

[129] D. J. Thouless, M. Kohmoto, M. P. Nightingale, and M. den Nijs. Quantized hall conductance in a two-dimensional periodic potential. *Phys. Rev. Lett.*, 49(6):405–408, Aug 1982.

[130] A. Trautman. *Lecture in theoretical Physics*. Brandeis Summer School, 1964.

[131] C. Truesdell and W. Noll. *The non-linear field theories of mechanics*. Springer, 2004.

[132] Christos G Tsagas. Electromagnetic fields in curved spacetimes. *Classical and Quantum Gravity*, 22(2):393, 2005.

[133] R. Levin V. Sandomirsky, A. V. Butenko and Y. Schlesinger. Electric-field-effect thermoelectrics. *Journal of Applied Physics*, 90(5):2370–2379, 2001.

[134] C. M. Varma. Non-fermi-liquid states and pairing instability of a general model of copper oxide metals. *Phys. Rev. B*, 55:14554–14580, Jun 1997.

[135] M. A. H. Vozmediano, F. de Juan, and A. Cortijo. *phys. Rev. B*, 76:165409, 2007.

[136] G. N. Watson. *A treatise on the theory of Bessel functions*. 1922.

[137] J. Weber. Detection and generation of gravitational waves. *Physical Review*, 117(1):306–313, 1960.

[138] T. O. Wehling, A. V. Balatsky, A. M. Tsvelik, M. I. Katnelson, and A. I. Lichtenstein. *Europhys. Lett.*, 84:017003, 2008.

[139] Hermann Weyl. Elektron und gravitation i. *Zeitshrift Physik*, 56:330–352, 1929.

[140] B Wunsch, T Stauber, F Sols, and F Guinea. Dynamical polarization of graphene at finite doping. *New Journal of Physics*, 8(12):318, 2006.

[141] Y. Xia, D. Qian, D. Hsieh, L. Wray, A. Pal, H. Lin, A. Bansil, D. Grauer, Y. S. Hor, R. J. Cava, and M. Z. Hasan. Observation of a large-gap topological-insulator class with a single dirac cone on the surface. *Nat Phys*, 5(6):398–402, 06 2009.

[142] C. Xu and J. E. Moore. Stability of the quantum spin hall effect: Effects of interactions, disorder, and z2 topology. *Phys. Rev. B*, 76:045322, 2006.

[143] D. Xu, I. Skachko, A. Barker, and E. Y. Andrei. *Nature Nano*, 3:491–495, 2008.

[144] Matthew Yankowitz, Jiamin Xue, Daniel Cormode, Javier D. Sanchez-Yamagishi, K. Watanabe, T. Taniguchi, Pablo Jarillo-Herrero, Philippe Jacquod, and Brian J. LeRoy. Emergence of superlattice dirac points in graphene on hexagonal boron nitride. *Nat Phys*, 8(5):382–386, 05 2012.

[145] J. Zak. Berry's phase for energy bands in solids. *Phys. Rev. Lett.*, 62:2747–2750, Jun 1989.

[146] Haijun Zhang, Chao-Xing Liu, Xiao-Liang Qi, Xi Dai, Zhong Fang, and Shou-Cheng Zhang. Topological insulators in bi2se3, bi2te3 and sb2te3 with a single dirac cone on the surface. *Nature Phys.*, 5:438, 2009.

[147] Y. Zhang, Y.W. Tan, H. L. Stormer, and P. Kim. *Nature*, 438:201, 2005.

[148] Yi Zhang, Ying Ran, and Ashvin Vishwanath. Topological insulators in three dimensions from spontaneous symmetry breaking. *Phys. Rev. B*, 79(24):245331, Jun 2009.

[149] Xuetao Zhu, L. Santos, C. Howard, R. Sankar, F. C. Chou, C. Chamon, and M. El-Batanouny. Electron-phonon coupling on the surface of the

topological insulator $bi_2se_3$ determined from surface-phonon dispersion measurements. *Phys. Rev. Lett.*, 108:185501, May 2012.

[150] Xuetao Zhu, L. Santos, R. Sankar, S. Chikara, C. . Howard, F. C. Chou, C. Chamon, and M. El-Batanouny. Interaction of phonons and dirac fermions on the surface of $bi_2se_3$: A strong kohn anomaly. *Phys. Rev. Lett.*, 107:186102, Oct 2011.